SOIL PATTERN RECOGNITION IN A SOUTH AUSTRALIAN SUBCATCHMENT

by

INAKWU OMINYI AKOTS ODEH

B.Sc. Hon. (Ibadan, Nigeria), M.Sc.(Samaru-Zaria, Nigeria)

Department of Soil Science

Waite Agricultural Research Institute

The University of Adelaide

Australia

Thesis submitted to The University of Adelaide

in fulfillment of the requirements for

the degree of Doctor of Philosophy

November 1990

TABLE OF CONTENTS

CHAPTER 3

DESIGN OF OPTIMAL SAMPLING SCHEMES BY GEOSTATISTICAL METHODS 30

CHAPTER 4

SOIL CLASSIFICATION WITH FUZZY-C-MEANS: SOIL-LANDFORM INTERRELATIONSHIPS AND OPTIMAL SAMPLING STRATEGIES 61

CHAPTER 7

LIST OF FIGURES

LIST OF PLATES

LIST OF TABLES

ABSTRACT

A geostatistical approach to spatial modelling of soil properties, in which sample semivariograms for the properties were used to design optimal sampling schemes, highlighted the difficulty of selecting a sampling scheme that provided a satisfactory compromise for all the properties used. This is because spatial changes in soil properties do not coincide. In order to redress this limitation of the geostatistical approach, a continuum approach to soil classification was adopted. This involved the use of the fuzzy-c-means (FCM) algorithm that is based on the theory of fuzzy sets, to quantify pedons into intragrade and extragrade classes by minimization of the objective functional for the most "precise" classification. Classification was validated by the mathematically heuristic methods.

The resulting fuzzy classes, which incorporated both the spatially dependent and the spatially independent variables into matrices of class membership coefficients, showed spatial continuity and contiguity that were associated with local variations in slope features and lithology. The semivariograms, estimated from the vectors of membership values, provided for a more realistic sampling strategy that took into account the association of soil changes with landform and lithology.

The problem of atypical pedons or extragrade members was solved by a modified Picard iteration which is embedded in the main FCM algorithm, thus optimally assigning atypical pedons into the extragrade class. However, the degree of fuzziness, denoted by fuzziness exponent, ϕ, was either determined by intuitive notions and/or by using a derivative of the objective functional the maximum of which indicated optimal fuzziness.

To elucidate the cause of soil variation, a multivariate approach was used. Hypothesizing that landform was the major factor influencing soil patterns in the study area, landform (point) attributes of gradient, profile convexity, plan convexity, aspect, upslope area and upslope distance were estimated by a nine-parameter quartic equation. The attributes were correlated with soil variables using canonical ordination analyses that assumed different models. Standard redundancy analysis (RDA), following data

transformation, was the most robust among the methods used. The results of RDA indicated that gradient angle, plan convexity and profile convexity accounted for much of the spatial changes of most of the soil properties measured for the study area. The soil-landform interactions were interpreted in terms of process-response subsystems. The significance of this outcome is that land unit delineation to define sampling pattern should prove to be a useful first step, prior to field soil survey work, by improving sampling efficiency and reducing classification errors.

Finally, the ultimate product of spatial modelling is the soil map. By implementation of an optimal sampling scheme in relation to the conspicuous changes in landform and lithology, isarithmic maps of fuzzy membership values were produced from kriged estimates. Composite maps, produced by summation of the membership values for the c + 1 classes resulting from each of the data sets, show the complexity of, and the spatial overlapping nature of, the fuzzy classes. Composite maps, produced by a maximum set-theoretic operator, show the core areas of the various fuzzy soil classes and the inter-core areas as the transition zones. Thus the soil continuum was realistically illustrated. The significance and relevance of fuzzy analysis and spatial modelling to geographical information systems are highlighted.

STATEMENT

This thesis contains no material which has been accepted for the award of any other degree or diploma in any university. To the best of my knowledge and belief, this thesis contains no material previously published or written by another person, except where due reference is made in the text.

I consent to this thesis being made available for loan and photocopying.

November 1990

Inakwu Ominyi Akots Odeh

ACKNOWLEDGEMENTS

I am very grateful to Dr. D. J. Chittleborough who introduced me to quantitative pedology. His guidance and stimulating discussions at the various stages of this work are gratefully acknowledged. I am also extremely grateful to Associate Professor A. B. McBratney of the School of Crop and Soil Science, University of Sydney, for giving me the initial impetus to delve into Soil Geostatistics and Fuzzy Sets Theory, and for his advice throughout this project. I sincerely thank all the staff members of the Department of Soil Science for their assistance, in particular J. Denholm, for his help with the field survey and sampling.

I am also thankful to the followings: Drs. A. W. Ward and W. T. Ward (formerly of the CSIRO Division of Soils, Brisbane), for their assistance with the Fuzzy-c-means program (FCME or FKME); Dr. C. J. F. Ter Braak for his useful suggestions on the use of his program, CANOCO; Dr. L. W. Zevenbergen for supplying his program for derivation of the landform attributes; and to Ms Nancy Cheng of School of Crop and Soil Science, University of Sydney, for typing chapter 7. I am also grateful to the following organizations: the South Australian Department of Lands for providing the resources for photogrammetric analysis of the aerial photographs covering the study area; CSIRO Division of Soils for making their facilities available for the initial data analysis. To the farmers, Mr. & Mrs. D. M./J. L. Driver and Mr. and Mrs D. Kievitt all of Forreston, I give my thanks for making their farmlands available for this project.

This work was accomplished through the financial support giving by the Australian International Development Assistance Bureau (AIDAB), the executor of the Commonwealth Scholarship awards of which I am onc of the beneficiaries; for this I am grateful to the Australian Government. I also thank the Agricultural University, Makurdi Nigeria, for granting me study leave.

Finally, I am exceedingly grateful to my wife, Ugwoma, for her continuous support, understanding and encouragement.

To my daughters: ***Echa and Ahiegwu***

CHAPTER 1

GENERAL INTRODUCTION

"There are few subjects upon which it is more difficult to make an accurate, and at the same time intelligible report, than upon soil. The difficulty arises partly from the nature of the subject and partly from the vagueness of the terms used in speaking of soils" :- Chamberlin (1883).

1.1 Introduction

Soil science has evolved through this century progressing from the philosophical tenets of Dokuchaev's era during the latter part of the 19th century to the now heralded quantitative methods that have been developed within the last four decades or so. These quantitative methods have been based on scholarly or scientific investigations using deterministic[1] concepts and equations which have commonly been proven valid in other fields, particularly chemistry, biochemistry, physics and other physical sciences. These methods have also been designed to answer questions associated with the initial development, subsequent management and continuing conservation of our land resources. Some of these deterministic analyses, which are based on Fisherian theory (Fisher, 1954) and involved the imposition of some specific field designs and treatments to remove the effect of soil and other environmental variation, have been quite successful. However, leaving this success behind us, a new type of soil science is evolving which recognizes the importance of understanding the complexity of soil variation that will enhance the quantification and formulation of alternative management practices. We must strive for greater success and take advantage of our added knowledge of spatial (and temporal) soil variability in order to enhance our research efforts, even when subjecting experimental sites to predetermined treatments (Nielsen, 1987).

---

[1] A deterministic process has an outcome that can be predicted with absolute certainty upon replication of the observations defining the process- it is in this sense a non-random process.

Within the last decade or so, the theory of regionalized variables (Matheron, 1965) has been applied successfully in soil studies. The theory, when applied, is generally termed geostatistics. It takes into account the structured and random components of spatially distributed variables and provides us with quantitative techniques for both description and optimal, unbiased estimation of soil variables at unvisited sites. Thus the application of this theory involves stochastic analyses (in contrast to the purely deterministic approach) in which mixtures of deterministic and random processes are modelled. The utilization of these methods has opened new vistas in soil science. When the soil is considered in terms of a space-time continuum, a more realistic concept is manifested (Nielsen, 1987). The methods which have emerged from the theory of regionalized variables that are useful in soil science are spatial dependence analysis (Burgess and Webster,1980a; Yost *et al.* 1982; Webster, 1985; Trangmar *et al.*, 1985), kriging and its various forms- ordinary, simple, lognormal, universal and disjunctive kriging (McBratney *et al.*, 1981; Burgess and Webster, 1980a & b; Trangmar *et al.*, 1985) and co-kriging (McBratney and Webster, 1983).

Kriging and co- kriging respectively utilize sample semivariograms and co-semivariograms (in preference to autocorrelograms and co-correlograms) for optimal interpolation of regionalized variables. Both of these methods are considered to be unbiased in the sense that they give exact interpolation, i.e., estimated value is identical to observed value when kriged (or co-kriged) site coincides with an observed site. A number of studies have suggested that kriging is worth the effort although, it has been criticized because of too many data required. In a recent work on spatial prediction of soil pH, Laslett *et al.* (1987) compared kriging with several spatial prediction methods and concluded that kriging, and to a less extent Laplacian smoothing splines, were the most reliable predictors. It was also recommended that where short range variability contributes significantly to estimation variance, observations for spatial interpolation should include many close pairs of samples thereby reducing estimation error. A similar study by Voltz and Webster (1990) also found that kriging performed better as a predictor than both cubic splines and the conventional classification in a situation where soil boundaries were found to be gradual. In a contrasting region where soil boundaries were abrupt, classification out-performed kriging and splines,

especially when predictions were made within the sharp boundaries. They recommended that a combined classification and kriging approach whereby within-class kriging is preceded by classification is most suitable for regions where soil variation is gradual with fuzzy boundaries. Prior to this work, Stein *et al.* (1989b) who, recognizing the importance of landform on soil variation, delineated the land into more uniform units before embarking on sampling for kriging. Their results indicated that while global kriging was successfully used initially, within-class kriging was still better. Whether land classification should be done prior to sampling for spatial interpolation of soil (properties) is dependent on the variability of terrain and the desired level of precision of output.

Co-kriging is particularly advantageous in that interdependence of variables can be used to enhance the estimation of either of the variables for unobserved locations (McBratney and Webster, 1983; Trangmar *et al.*, 1985), although there is the practical problem of analysing many soil variables simultaneously. To alleviate this problem, some authors (e.g. McBratney and Webster, 1981a) used the multivariate methods to transform their data before embarking on spatial analyses. Others have directly used multivariate methods of principal component analysis and reciprocal averaging for elucidation of spatial interactions of soil, vegetation and climate (Burrough *et al.*, 1977), and the methods of principal component analysis for cluster analysis (e.g. Norris, 1970). These multivariate methods are essentially analogous to basic linear regression or discrimination. In which case, those situations where a non-linear structure exists, which some authors claim (DeGruijter and McBratney, 1988) is the rule rather than exception in pedology, are poorly represented.

In conventional soil survey, soil profiles are described and analyzed. Then the profiles are allocated to classes using an existing soil classification system (usually hierarchical). This exercise is usually preceded by delineation of the land into presumed "uniform" units based on topographic and other environmental variables or aerial photo interpretation. The land units, now termed mapping units, and defined by their modal profiles, are referenced to taxonomic units in a soil classification by some diagnostic characteristics. These characteristic soil features are described by a legend which in turn describes the critical properties of the soil class units within the mapping units. The critical properties are viewed

as surrogates of unmeasured properties with which they are assumed to be correlated. It is then assumed that soil spatial variation and variations of soil features within the mapping units are minimal. In a recent study in the Lower Macquarie Valley New South Wales (Australia), McKenzie and Macleod (1989) showed that the normally used morphological surrogates were poor predictors of the agronomically important properties, thus confirming the earlier findings of some workers (e.g. Webster and Butler, 1976) that morphological variables have low correlations with other soil variables that are relevant to land use.

The usual assumption by pedologists, and indeed other agricultural scientists that deal with soil, that existing soil classification systems could be used to group soil profiles with similar agricultural potential has been described as erroneous (Webster, 1977b; Butler, 1980). In Australia, there are three national soil classification systems (which are discussed in chapter 2) that are used in addition to the Soil Taxonomy (Soil Survey Staff, 1975) and the FAO classification (FAO, 1974). Such general classification schemes produce groupings that hardly correspond to the local soil conditions. The consequence of this is that the natural groupings that exist in a locality may be split by imposition of an extraneous classification. Thus the reliable prediction of soil variables, both surrogates and non-surrogates, are hampered. McKenzie and Austin (1989) confirmed this in their study of utility of "Factual key" (Northcote, 1960) and Soil Taxonomy in the Lower Macquarie Valley. These two systems proved to be poor predictors of many relevant soil variables in comparison to classes generated from numerical classification specific to local conditions.

Before retrospective studies on soil survey quality were undertaken, most systematic soil maps produced by conventional methods were estimated to contain no more than 15 % impurities within such mapping units. This has since been proved otherwise (Beckett and Webster, 1971; Burrough, 1987). There is the need, therefore, to find some suitable means of recognizing soil patterns in terms of a continuum and realistically identify the presence of atypical pedons within the mapping units.

1.2 Soil Pattern Recognition

Soil pattern recognition is the central theme of the work presented here. It is, therefore, pertinent to define what the term "pattern recognition" entails. Simply put, the term "pattern recognition" entails "search for structure in data" (Bezdek, 1981). The main elements in this definition are search, structure and data. A set of data, X, describing objects drawn from a "population" or any physical process, can be either qualitative or quantitative or both. Faced with such data, the next line of action should be to search for the data patterns. The line of action may be dictated by the purpose for which the data is to be organized. Whatever is the purpose, either we use crisp classes to provide some simple understanding of the complex situation represented by the data or we directly use one of the complex and realistic models provided that the complexity is understandable (Dale *et at.*, 1989). If the processes generating the variation is known (and we can use some deterministic models to reveal this) we can use such information to aid us in organizing our data.

The search for data patterns varies from the traditionally subjective assessment in which the structure or "signal" (and "noise") (Burrough, 1986) is recognized by "eyeball" techniques and/or intuitive allocation of individuals into groups or units on the basis of relationships of the individuals to some external factors (as done in conventional soil survey methods), to quantitative or statistical pattern recognition techniques (e.g. numerical taxonomy). If the data carry information about processes generating them (and most pattern recognition techniques are deemed to make such an assumption), then structure represents the manner in which the data can be organized such that relationships between variables in the process can be identified (Bezdek, 1981). The data, the method of search and the model used will determine the recognized structure. This invariably means that the amount and type of information pertaining to the processes generating the data pattern (structure) is dependent on the model used. The question is: what specific quantitative techniques are used for pattern recognition in soil science? The techniques are collectively termed numerical classification and/or cluster analysis. In the future, these techniques will probably form the core of soil information transfer.

In classical numerical methods, classification is differentiated from cluster analysis. Whereas classification involves procedures used to discover association between subclasses (substructures) in a population, cluster analysis seeks interactions between subsets of a sample (Bezdek, 1981).

In soil science, classification "refers to the activity of dividing a set of objects into *disjoint* groups in such a way that objects in the same group are" more "similar to one another" (Gordon, 1987) than to objects in different groups. On the other hand, cluster analysis mostly refers to numerical methods (Webster, 1977b; DeGruijter, 1977) involving ordinations combined with geometrical representations of their results, and divisive systems and agglomerative systems (Burrough, 1986). In Bezdek's (1981) definition, classification entails searching for structure in an entire data space. This search can first be conducted using clustering in sample data, X, and then proceeding to classify rapidly (on the basis of recognized structure) the subsequent observations. In this work, classification and cluster analysis are used interchangeably, although there appears to be contradiction between the use of classification and the terms "assignment". Assignment involves allocation of an object into one of the known number of general classes (c) or "populations" of objects (Gordon, 1987). Pedologists, notwithstanding the fact that they have been informed of this distinction (e.g. Webster, 1977b) generally have not distinguished between classification and assignment in practice (Williams and Dale, 1965). The word classification is used for both tasks.

Natural soil classification systems, and indeed their numerical counterparts used by pedologists, are constrained to conform with discontinuous model of soil variation embedded in conventional soil survey methods. These classifications are composed of mutually exclusive classes with rigidly defined boundaries based on differentiating characteristics. If grouping of soil is to reflect the processes generating soil variation, then classification into crisp classes does not describe soil as it exists in the real world. An appropriate classification for the soil continuum is the one that recognizes the continuous nature of soil. Recently, DeGruijter and McBratney (1988) have proposed such a model of

soil classification. The model is based on the theory of fuzzy sets (Zadeh, 1965) which is a generalization of abstract set theory.

Soil pattern recognition cannot be complete without the elucidation of the underlying processes generating the patterns. This aspect concerns pedogenesis, a field of pedology that deals with soil formation (Buol *et al.*, 1973). As with traditional soil mapping, pedogenesis has been more deductive than quantitative in spite of the earlier work of Jenny (1941) which formulated functional relations of soil and the state factors. The functional approach makes use of the deterministic concept (as defined earlier) in which empirical functions are fitted to give mathematical description of the relation between a soil variable on the one hand, and a single soil-forming factor on the other. The soil-forming factors and their univariant solutions include: lithology- lithofunctions, topography- topofunctions, climate- climofunctions, biota- biofunctions and time- chronofunctions.

Jenny's (1941) concept has been criticized for a number of reasons, that: the state factors might vary simultaneously (Stephen, 1947); the biotic factor could be dependent on soil variables (Crocker, 1952); the equations are insoluble (Crowther, 1953); the concept is not process-oriented (Simonson, 1959). In spite of these criticisms, Jenny's equations have provided a vehicle for studying the relationships between the soil and the factors responsible for its formation and distribution pattern on the landscape. His concept formed the foundation of much work in pedology, particularly the application of topofunctions. Applications, using topofunctions, vary from single-curve fitting (e.g., Ruhe and Walker, 1968; Furley, 1971) to the multivariate approach (Webster, 1977a). The multivariate methods are particularly useful because the soil and most of the state factors are multivariate. With increased availability of powerful computers which have immensely improved our ability to process data, efforts should be directed towards using the multivariate approach to unravel the complexity of the soilscape.

Table 1.1 Types of quantitative models used for soil studies with examples and sources of uncertainty

Causality/ Uncertainty	Model: Deterministic	Stochastic	Non-statistical
Empirical	Generalized linear models, numerical taxonomy, Jenny's functional relations and (canonical) ordinations	Time series, spatial processes, temporal and spatial variations of soil properties	Fuzzy memberships
Mechanistic	Flow and diffusion of soil plasmic materials, profile and landscape development	?	?
Uncertainty	Imprecise measurement	Random processes	Vague description and continuum nature of soil

1.3 The Scope of this Work

Pedological studies have often been criticized, perhaps justifiably, for being qualitative in character. In response to these criticisms, quantitative models that have been developed within the last decade or so, are being used to describe, classify and study the spatial distribution pattern of soil as it occurs in the field. This quantitative approach enables us to make statements of high precision about soil and thereby allowing hypothesis testing.

Table 1.1 (adapted and modified from the Annual Report of CSIRO Division of Soils, 1986 p 13) gives a two-way classification of quantitative models which are being used for the study of soil phenomena. Until recently, most of the pedological models applied to soil pattern recognition were empirical (no or weak causality) and deterministic, because of the

complex nature of soil and the processes generating it, and our lack of understanding of this complexity. However, all that has changed as stochastic models have increasingly been used to describe the spatial (and temporal) variations of soil. To account for the continuous nature of spatial variation of soil, application of fuzzy membership models has recently begun (DeGruijter and McBratney, 1988; McBratney and DeGruijter, 1990). Additionally, mechanistic, deterministic models have a part to play in the study of soil-forming processes, especially, in conjunction with the models of landscape development. The future will decide the usefulness of mechanistic, stochastic models and mechanistic, fuzzy membership models (if any will ever emerge) in soil studies.

✓Three main types of quantitative methods are dealt with in the work presented here. First is the geostatistical approach for modelling spatial variations of soil properties. In regard to this approach, chapter 3 highlights the methods and the difficulties involved with applications in which many soil variables are employed. The second type covers the continuum approach to soil classification. This is dealt with mainly in chapter 4 which is a bold attempt to apply the generalized fuzzy-c-means (also known as ***fuzzy-k-means***) algorithms to soil classification. In chapter 5, the multivariate methods commonly used in ecological studies are applied to the study of soil-landform interrelationships. Thus chapter 5 constitutes the third main approach which meets the requirement of elucidating the *cause* of soil variation in the study area. Chapter 6 is complementary to chapter 4, thus completing the work of soil pattern recognition, i.e., making of soil maps that reflected the continuous nature of soil. Preceding all of these, however, is chapter 2 which gives general descriptions of the physical characteristics of the study area to which these approaches have been applied.

CHAPTER 2

PHYSICAL CHARACTERISTICS OF THE STUDY AREA

2.1 Location of the Study Area

The study area is located in a subcatchment near Forreston in the Mt Lofty Ranges, about 60 km north-east of Adelaide in South Australia. Geodetically, the subcatchment is at approximately 34° 48' N and 138° 54' E (Fig. 2.1) which is equivalent to the Australian National Grid Reference of 6148800mN, 308500mE and 6147800mN, 310100mE. Several factors were taken into consideration in selection of the study area:

1) that the area be relatively uniform in lithology to minimize the effect of parent material on soil formation and thereby facilitate the evaluation of soil-landform interaction;
2) that the area be geomorphologically (and geologically) stable within recent geologic times; this criterion was necessary to satisfy the requirement that soil development had not been interrupted by any catastrophic geomorphic event;
3) that the area be minimally disturbed by human interference in terms of cultivation for agricultural production, infrastructural construction (e.g. roads), etc.

These criteria were met to a considerable extent as the description of the physical characteristics of the study area will attest.

2.2 Geology

The subcatchment is within the Adelaide Geosyncline (Forbes and Preiss, 1987) which encompasses the present day Mt Lofty Ranges and Flinders Ranges (Fig. 2.2). The Geosyncline is a complex sedimentary basin in which there was accumulation of sediment

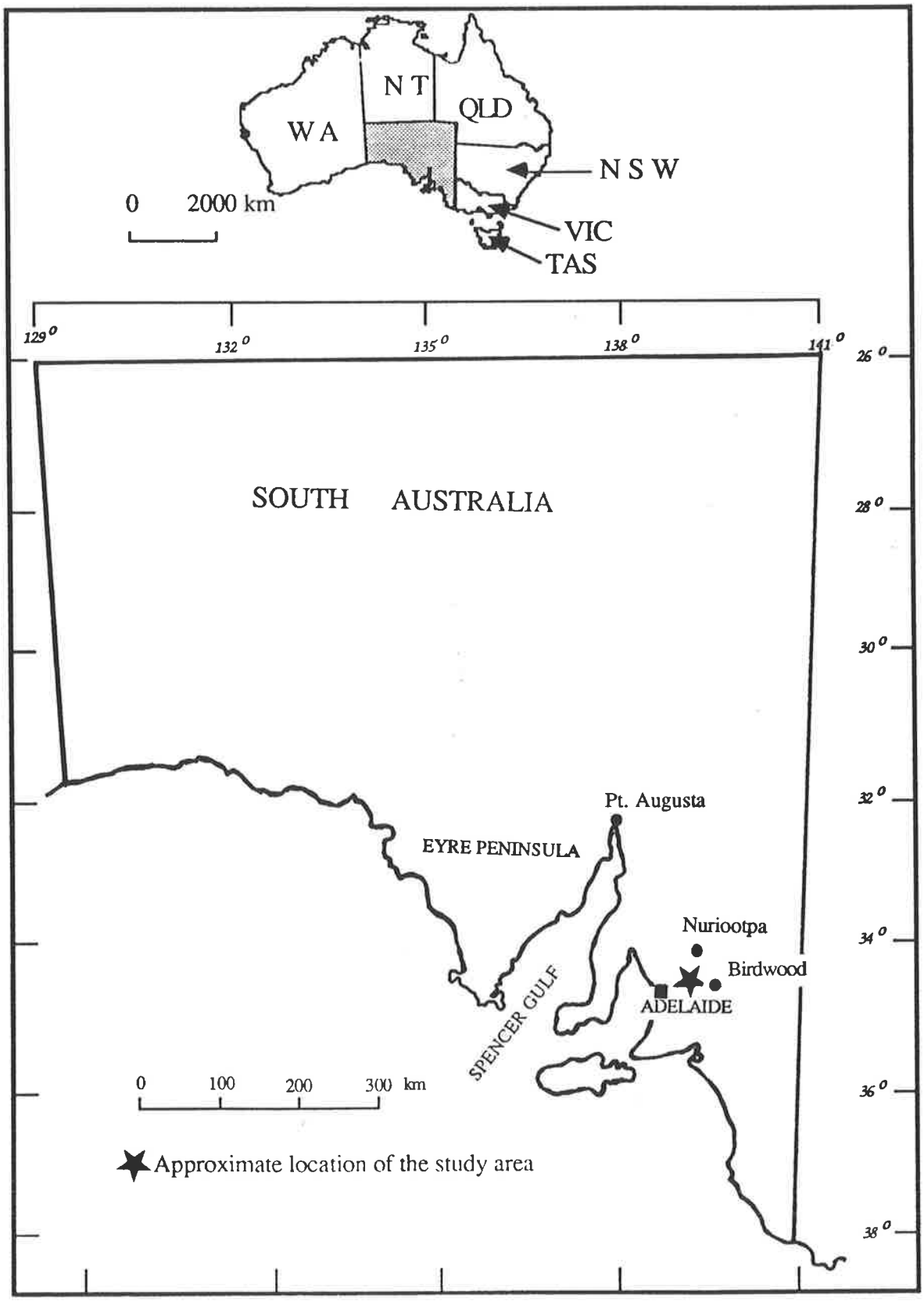

Fig. 2.1 Location of the study area.

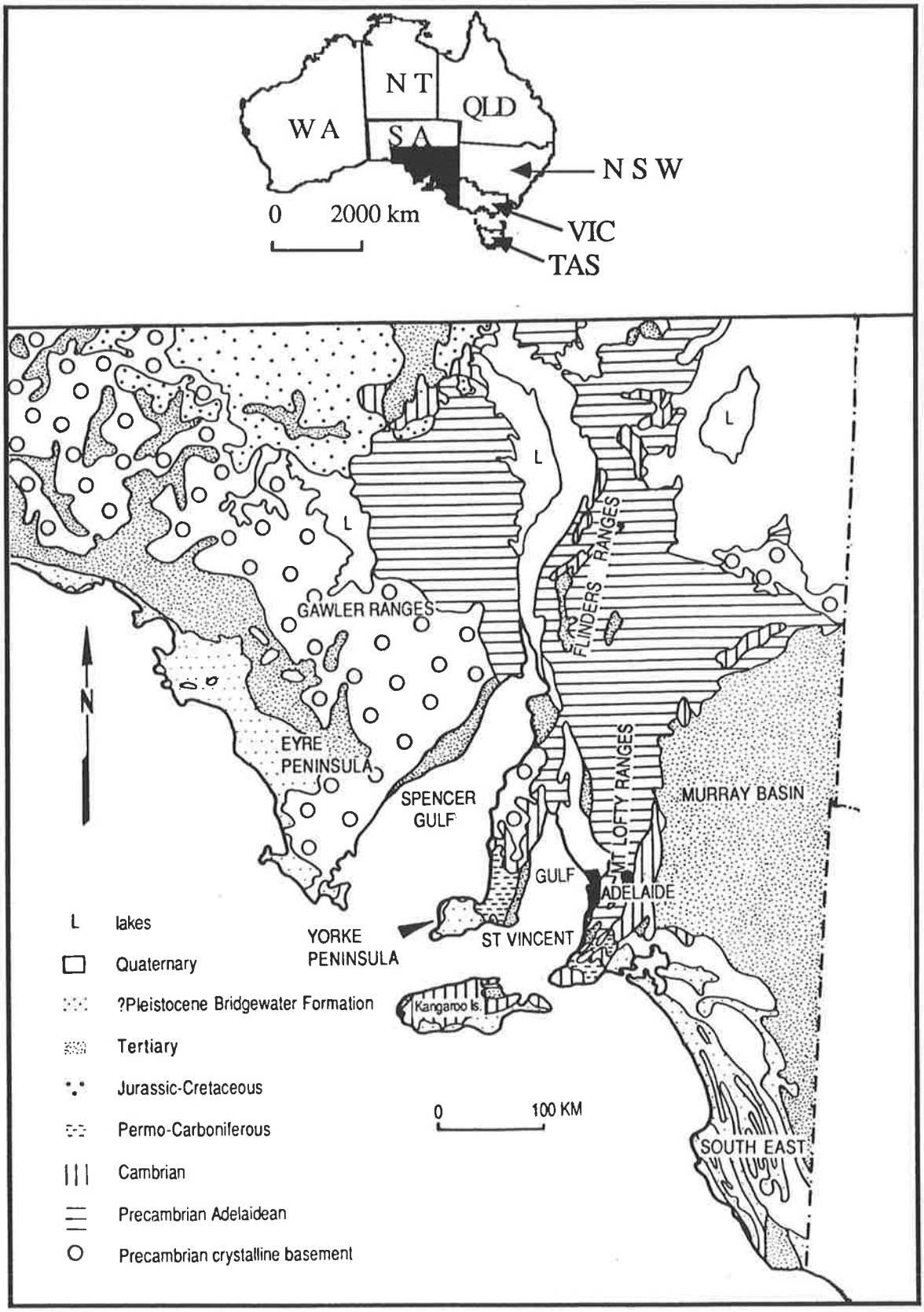

Fig. 2.2 Generalized geology of southern South Australia (modified from 1: 1000 000 geological map of S. Australia, S. Australia Dept. of Mines & Energy, 1980); ● = approximate location of the study area.

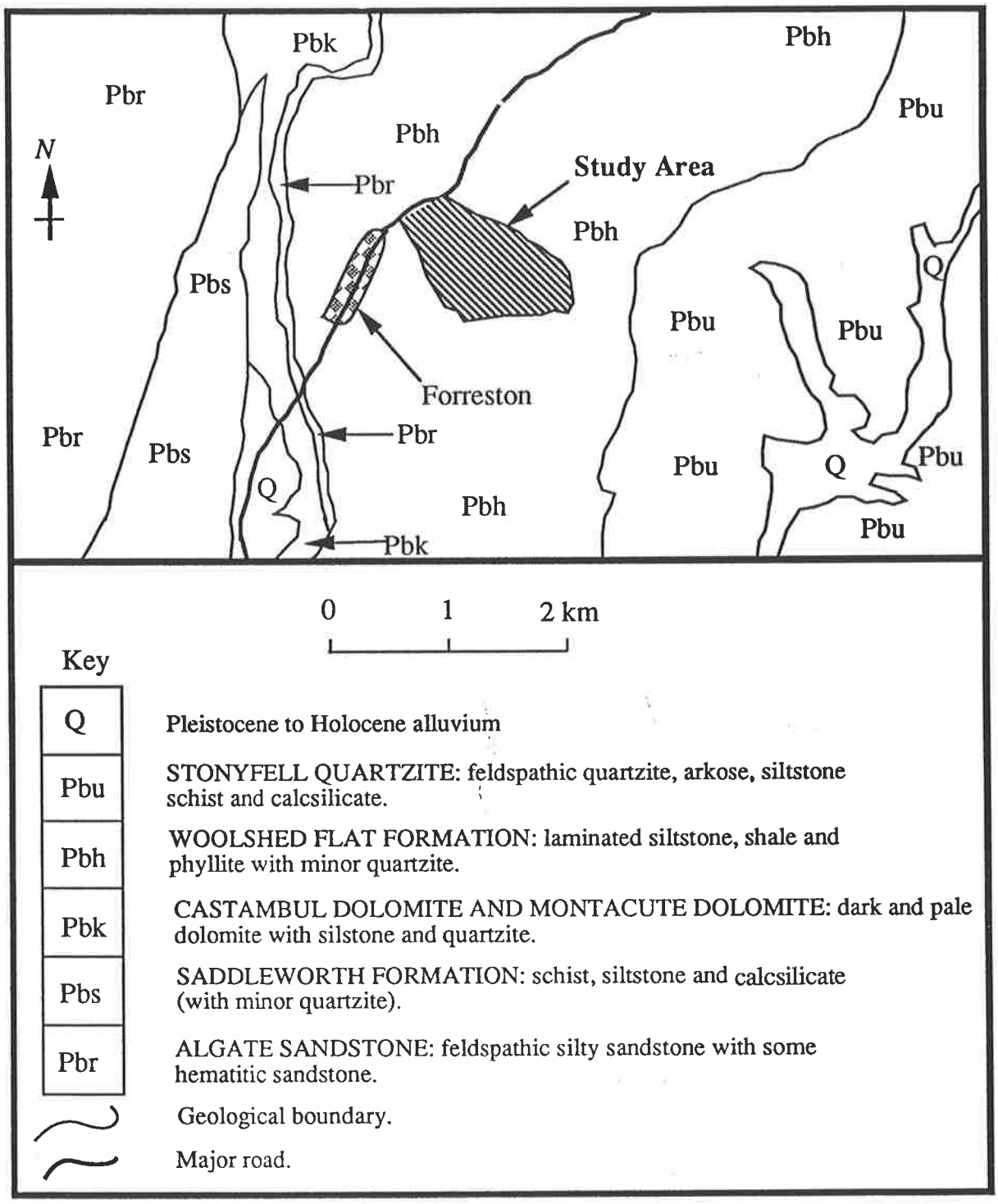

Fig. 2.3 Geology of the study area and its immediate surroundings (modified from 1: 50 000 geological map sheet 6628-II (Onkaparinga), S. Australian Dept. of Mines & Energy, 1979)

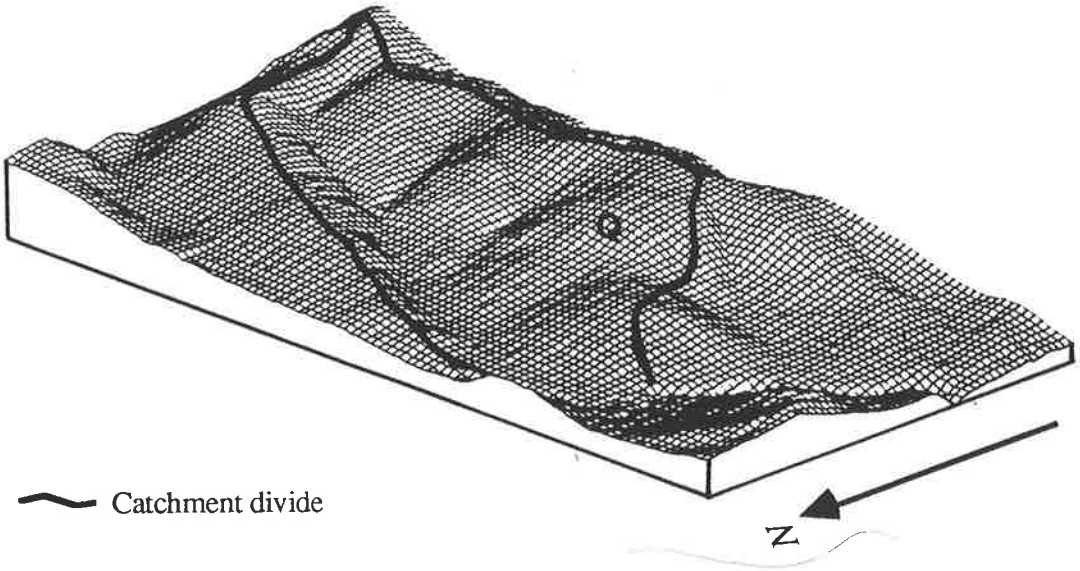

Fig. 2.4 Perspective block diagram of a digital elevation model computed from a 71 x 111 point altitude matrix of the study area; each grid cell is 20 x 20 m; the view is north-east at 5° from the horizontal; vertical exaggeration = 5.0

Plate 2.1 Phyllites and schists on a cut surface of a quarry located at the southern edge of the subcatchment.

that later became folded and metamorphosed.

A great part of Adelaide Geosyncline consists of Precambrian (Proterozoic) rocks termed the Adelaidean which, in the Mt Lofty region, range in age from 800-900 m.y. (million years) to 570 m.y. (Daily *et al.*, 1976). The Adelaidean rocks overly the crystalline basement which outcrops in some antisynclinal or upfolded areas and at the edges of the Flinders-Mt Lofty block. The immediate region surrounding the study area is underlain by some of the earliest Adelaidean Formations collectively termed the "Burra Group" (Forbes and Preiss, 1987) which consists of the Algate Sandstone, the Woolshed Flat Shale and its Balhannah Shale member, and the Stonyfell Quartzite (Fig. 2.3). Sedimentation of Burra Group commenced in the middle of Proterozoic (700-800 m.y.), with "a fluvial to marginal-marine clastic influx, followed by cycles of trangressive-regressive marginal-marine and lagoonal carbonates, basimal shales and deltaic sandstones" (Preiss, 1987). Specifically, the subcatchment is underlain by the Woolshed Flat Formation (Wilson, 1952) which includes shales, laminated siltstones, phyllites (Plate 2.1) and minor quartzites (S. Aust. Dept. of Mines and Energy, 1979). There are no dolomite and carbonate lenses between the sedimentary beds as found in the other sections of the Formation.

2.3 Geomorphology

There is a close link between the landscapes of the Flinders-Mt Lofty block and their geological history (Northcote, 1983). The oldest landform within the two Ranges is the lateritized summit high plain (Twidale, 1976) located at high elevations (300-400 m). Residuals, such as the Mt Lofty summit (727 m), rise above the general level of the plain. The age (and the origin) of the summit plain are still controversial. Whereas many geologists (e.g., Daily *et al.*, 1976) have regarded the summit carapace and surface to be of late Tertiary age, Twidale (1976) strongly adduced Mesozoic age. However, subsequent events that shaped the present landscape are more relevant and important to this study than the absolute age. The following account, largely taken from Twidale (1976) and Northcote

Plate 2.2 Perspective view of the study area (from Q on Fig. 2.4) looking eastwards

(1983), gives a general geomorphological history of the study area and its surrounding regions.

The Mesozoic (or Tertiary ?) summit plain was disrupted by pronounced fault lines which were established during the Palaeozoic orogeny. The orogenic movements caused the development of complex (but clearly defined) upland blocks inter-meshed with irregularly shaped grabens and depressions. Thus, much of the land to the west and east of the Flinders-Mt Lofty block, were submerged beneath the sea due to their subsidence in the Cretaceous period. In the early Tertiary, further subsidence allowed for innundation of all but the higher parts of the present Ranges. The Pleistocene witnessed another uplift during which the Flinders and Mt Lofty Ranges emerged as a large horst. The continuation of uplift of the block in the later Pleistocene was recurrent with sinking of the land to the west, and thus resulting in great north-south faults that produced the rift valleys now occupied by the present Spencer Gulf and Gulf St. Vincent.

During the long process of elevation, the various rivers and streams on the uplifted block were rejuvenated. These rivers and their tributaries undercut into the duricrust of the summit plain, thus causing mass wasting and denudation. Considered in general terms, the complex juxta-folded sedimentary and metasedimentary sequences were subjected to differential weathering and erosion so that the major depressions and the residual ridges display strong structural patterns. The structural control with a northerly trend is closely associated with geological patterns and the major faults.

The resulting contemporary landscape consists of rugged and high strike ridges of the Flinders Ranges to the north and the undulating tablelands and flat-topped crests in the Mt Lofty Ranges to the south extending south-westward to Kangaroo Island. The landform features of the study area are characterized by gently rolling hills bounded on both sides by relatively high ridges of the Stonyfell Quartzite to the east and the smooth rounded ridges of the Algate Sandstone to the west (Fig. 2.3). The terrain within the subcatchment itself comprises predominantly of round hills and spurs (Fig. 2.4; Plate 2.2) with slopes ranging from less than 1% on the lower slopes to just over 20% on the middle to upper slopes. The

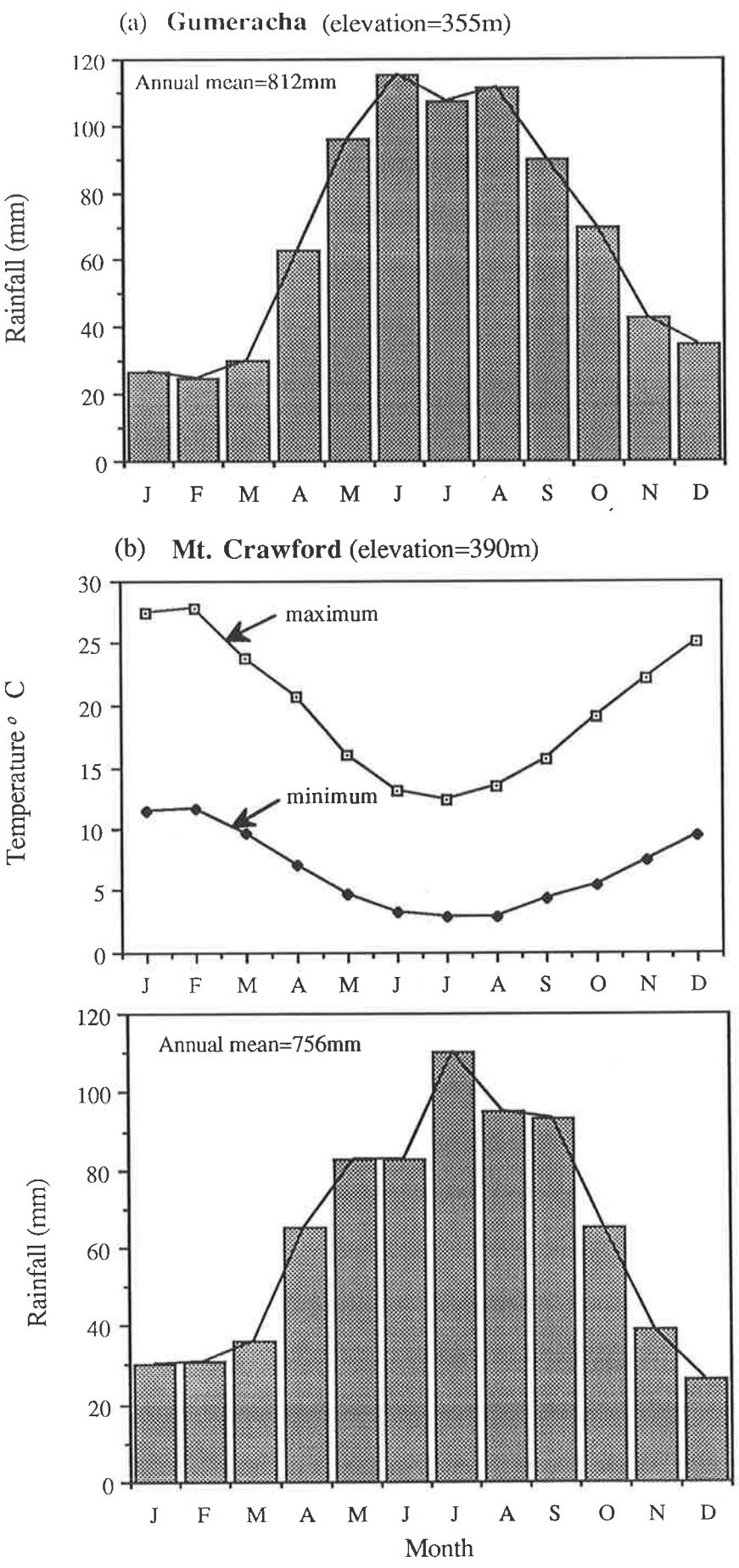

Fig. 2.5 Annual distribution of (a) rainfall for Gumeracha and (b) rainfall and, maximum and minimum temperatures for Mt. Crawford

highest point at the south eastern tip of the subcatchment is a spot height of 478 m above sea level. Relief is about 60 m. There is no conspicuous rock outcrop. Occasionally minor gully erosion (probably initiated by the farmers' activity) occurred but the farmers have stabilized the gully headward extension. The main creek that runs through the subcatchment in the south-east to north-west direction is of second order with three minor creeks forking southwards from the main.

2.4 Climate

Evidence has suggested that today's climate of southern Australia (and indeed the whole of Australia) is not largely different from climate of the Miocene times, i.e. 25 m.y (Barker, 1986). This is because Australia, since the Miocene, has been near its present latitudinal position following its northward movement from the Antarctica. The continent had then spanned the Tropic of Capricorn in the north and the cooler latitudes in the south. Thus climatic conditions that exist today are largely due to events that occurred 15-40 m.y. ago. However, during the same epoch, the sea penetrated well into the Murray Basin bringing maritime conditions to the inland (Beckmann, 1983).

The present latitudinal location of Australia provides for two main moisture bearing atmospheric systems which affect the climate of the continent: a tropical (monsoonal) system in the north; and a cooler polar system in the south. The latter system, in conjunction with a continental system, is responsible for seasonal variation of climate in southern Australia. The seasonal changes are characteristic of a Mediterranean-type climate with cool, wet winters, and warm to hot, dry summers- equivalent to Koppen's climatic class, Csb (Laut *et al.*, 1977). In the central Mt Lofty Ranges, mean annual rainfall varies from 500 mm in the lower plains to 1200 mm in the upland areas. Orographic effects caused by the upland areas account for larger amount of rainfall. Fig. 2.5(*a* and lower *b*) shows rainfall distribution in the two nearest recording stations to the study area. The nearest of the two stations, Gumeracha, is at an elevation of about 355 m above sea level and 3 km south-west of the study area. The second station is at Mt. Crawford which is about 10 km north-east of the

subcatchment and 290 m in elevation. Rainfall distribution shows a marked similarity between the two stations as Fig. 2.5(*a* and lower *b*) shows. The wetter months are April to October inclusive at the two stations. Even though Gumeracha is at a lower elevation, its annual mean rainfall (812 mm) is slightly higher than that for Mt. Crawford (756 mm). This is because the polar moisture-bearing winds that bring rainfall to the region are mostly southerly, and therefore rainfall decreases northward through areas of the same longitudinal swath. Mean annual evaporation for the central Mt Lofty subregion is between 1800 mm and 1900 mm.

Temperatures vary from cold to cool in winter and from cool to hot in summer. At Mt. Crawford, the hottest month is February with a mean maximum temperature of 27.9 °C and a mean minimum of 11.6 °C (Fig. 2.5 upper *b*). The coolest month is July, when the mean maximum falls to 12.3 °C and the mean minimum to 3.0 °C. The seasonal range of maximum mean temperature is 16.3 °C and of minimum is 9.3 °C, which are considered to be high. Elevation is the most important factor affecting temperature, especially the minimum (Maschmedt, 1987). This is particularly so in winter when topographic influences cold air movements. Frost incidence is determined by these air movements and is more frequent in the valleys than on the hilltops. Mt. Crawford has a considerably high incidence of frost- about 59 annually.

Annual cycles of relative humidities are the inverse of temperature variations. The highest relative humidities are recorded during winter months, June-July, when the air temperatures are in their lowest levels. During the winter periods, values as high as 80% at 0900 hours were recorded for stations in the upland areas of the Mt Lofty Ranges (Laut *et al.*, 1977).

Surface wind patterns, as recorded in Mt. Crawford station, indicated that January winds from southerly and easterly are the most frequent. In winter, especially in July, winds from the westerly and northerly predominate. Such patterns of winds in the Mt Lofty region differ from those of the lowland areas (e.g. Adelaide plain) in that in the latter areas, a strong south-westerly component is present in the afternoons for most of the year (Laut *et al.*, 1977).

Plate 2.3 Remnants of native vegetation on the eastern slopes of the subcatchment; mainly *Eucalyptus leucoxylon* and *E. obliqua*

2.5 Vegetation and Land Use

Little is known of the pre-European vegetation of the Mt Lofty region. However, a broad reconstruction of the natural vegetation has been accomplished based on evidence from records, sketches, and paintings kept by the explorers and the early settlers, and from the remnants of the native vegetation (Barker,1986). Generally, native vegetation could have reflected the broader regional climate. The Mt Lofty region constitutes a large portion of the 4 % of South Australia, which on the average, receives more than 500 mm annual rainfall. It is pertinent to state here that South Australia is the driest of all Australian states (75 % of the state receives less than 200 mm annual rainfall). The obvious consequence of this general aridity is that only about 3% of the state, including the Mt Lofty Ranges which receives annual rainfall of about 600 mm or more, was wooded (Barker, 1986). In the Mt Lofty Ranges, especially the central subregion where the study area is located, open forest was the dominant formation (Laut *et al.*, 1977; Barker, 1986). Species composing this formation were mainly blue gum (*Eucalyptus leucoxylon*), messmate stingybark (*E. oblqua*), brown stingybark (*E. baxteri*) and the cup gum (*E. cosmophylla*). The then existing (pre-European) forest formation represented the remnants of an extensive forest in the southern belt of the Australian continent that existed during the Tertiary. The forest had contracted due to increased aridity in the Pleistocene and Holocene epochs when the ocean had receded from the Murray Basin (Laut *et al.*, 1977).

Little of the original open forest once covering the region remains today as extensive clearing for agricultural production has taken place since European settlement. In the study area, only a few stands of Eucalyptus (*E. leucoxylon* and *E. obliqua*) remain on the eastern slopes of the subcatchment (Plate 2.3).

The study area is within the intensive grazing zone north-east of Adelaide. An investigation into land titles of sections of land within and adjacent to the study area indicated that a number of land sections (the northern and the eastern portions of the subcatchment) were first leased out in 1923. The remaining land sections were first leased out in the mid-

thirties. Until as recently as 1983, no land use other than pastoral production was recorded except for the lower slopes adjacent to the main creek (north-west of the subcatchment) that had been used for market gardening since 1964. It was only in 1983 and 1984 that much of the other parts of the study area was used for vegetable production. Since then (until the time of writing), the area has only been used for cattle and sheep grazing with limited surface loosening of soil for pasture production.

2.6 Soil

2.6.1 Previous work and historical development

The earliest inventory of the soil of the region started with the exploratory work of Prescott (1931) which marked the beginning of modern soil science in Australia. This work culminated in the publication of a soil map at a scale of 1: 20 million which was based on broad relations of soils with vegetation and climate. The map showed the Mt Lofty region as being dominated by red-brown earths (*Rhodoxeralfs* or *Palexeralfs*). A little over a decade later, Prescott (1944) revised the 1931 map and published a second map at a scale of 1: 10 million. This map essentially showed two soil groups in the Mt Lofty region: podzols (*Haplorthod*) in the upland areas and red-brown earths on the plains. This was followed by Stephen's (1961) re-compilation of a soil map of Australia at a scale of 1: 5 million which indicated three main soil landscapes in the Adelaide region: lateritic podzolic soils (*Palexeralfs* or *Plinthoxeralfs*) on the tablelands of the Fleurieu peninsula; podzolic soils in the central Mt Lofty subregion and red-brown earths on the plains. A further modification of Stephen's map was accomplished by Stace *et al.* (1968) in which the number of groups were reduced but given more definitive characteristics, although the same soil groups as indicated on Stephen's map were shown to be present in the Adelaide region.

A "factual key" approach to soil description and classification (Northcote, 1960), developed concurrently with Stephen's work, culminated in the publication of the "Atlas of Australian Soils" at a scale of 1: 2 million. This map, the most popular among Australian

Table 2.1 Dominant soil profiles of the study area and their properties according to Northcote (1976), and their probable classification in the Soil Taxonomy and the World Soil Map (Moore *et al.*, 1983).

Factual Key	#1GSG	Soil Taxonomy	World Soil Map	Landscape position	#2 PM	Morphology	
						A	B
Dy3.22	Yellow podzolic soils	*Palexeralf* *Rhodoxeralf*	Albic Luvisol	mid-slopes	Quarzite-rich	hardsetting	mottled yellow clay
Dr2.22	Non-calcic brown soils	*Rhodoxeralf*	Chromic Luvisol	upper and mid- slopes	Phyllite, slates & shales	hardsetting	red pedal clay
Uc6.11	Lithosol soils	*Xerorthent*	Eutric Regosol	steep slopes	Coarse-grained Quartz-rich	A1 pedal	–
Dy5.43	Solodic soils	*Natrixeralf*	Solodic Planosol	lower slopes	Coarse-grained alluvium	sandy	mottled yellow clay

#1 GSG = Great Soil Group of Stace *et al.*, (1968)
#2 PM = parent material

Table 2.2 Dominant soil profiles of the study area and their properties according to Maschmedt (1987), and their probable classification in the Soil Taxonomy and the World Soil Map (Moore *et al.*, 1983).

Factual Key	#1 GSG	Soil Taxonomy	World Soil Map	Landscape position	#2Occurrence	#3PM	Morphology	
							A	B
Dr3.22	Red-brown podzolic soils	*Rhodoxeralf* *Palexeralf*	Chromic Luvisol	upper & mid- slopes	extensive	Quartz-rich	A1 apedal	mottled yellow
Dr2.22	Red podzolic soils	*Palexeralf*	Chromic Luvisol	upper & mid- slopes	common	Phyllite, slate	hardsetting	red, pedal clay
Dy2.41	Yellow podzolic soils	*Haploxeralf*	Orthic Luvisol	mid-slopes	limited	medium-fine sandstone	hardsetting	yellow clay
Dy3.61	Lateriric podzolic soils	*Plinthoxeralf* *Palexeralf*	Plinthic Luvisol	crests & slopes	minor	lateritized phyllite slate & sandstone	hardsetting	mottled yellow clay
Dy3.42	Yellow-brown podzolic soils	*Haploxeralf*	Orthic Acrisol	lower slopes	extensive	deeply weathered phyllite & slate	hardsetting	mottled yellow clay
Dy3.41	Yellow podzolic soils	*Haploxeralf*	Orthic Acrisol	lower slopes	limited	deeply weathered phyllite & slate	hardsetting	mottled yellow clay

#1 GSG = Great Soil Group (Stace *et al.*, 1968)
#2 Occurrence = very extensive (60-90 %), extensive (30-60 %), common (20-30 %), limited (10-20 %), and minor (0-10 %)
#3 PM = parent material

pedologists and other soil scientists, also includes the classification into Great Soil Groups by Stace *et al.* (1968). Thus in Australia, two indigenously developed classification systems are being used in addition to two others that are more international: the Soil Taxonomy (Soil Survey Staff, 1975) and classification on the World Soil Map (FAO, 1974).

The "Atlas of Australian Soils" showed compound soil landscapes in the Adelaide region that constitute over 20 Principal Profile Forms (PPFs), with those of Uniform Primary Form (U) occurring mainly on the coastal plains, and those of Duplex Primary Form (D) in the hills and valleys of the Mt Lofty Ranges (Northcote, 1976). Specific to the study area, the dominant soil forms as indicated on the Atlas are shown in Table 2.1. Their equivalent classification in the Soil Taxonomy and the World Soil Map (Moore *et al.*, 1983) are also shown.

The most recent and detailed soil inventory covering the study area was in the form of a reconnaissance map produced at a scale of 1: 50 000 (Maschmedt, 1987). Only two broad soil groups (Stace *et al.*, 1968) were identified in the study area: moderately deep to deep yellow podzolic soils; and the shallow red-brown podzolic soils. Their equivalent PPFs and classification in the Soil Taxonomy and in the World Soil Map are also shown in Table 2.2. It contrasts and contradicts what appeared on the "Atlas of Australian Soils" which epitomizes the high level of generalization in Northcote's (1960) work.

2.6.2 Soil genesis

Soil development in the Mt Lofty region is linked with its landscape history (Northcote, 1983). It is therefore clear that the present soilscapes (and the various landforms) in the region resulted largely from the basic regional geology and weathering processes that have taken place during more recent geologic times. Whereas the continents in the northern hemisphere were covered by extensive icesheets during the Pleistocene period, Australia had not experienced any major glaciation since the Paleozoic period. Thus in Australia, soil (and product of weathering) was not stripped and mixed as happened in northern Europe and

North America during the Pleistocene glaciation (Twidale, 1976). Instead the Australian land mass had been exposed to weathering since Mesozoic times, and therefore allowed soil development on the exposed surfaces which were later subjected to erosion. This sequence of events accounts for the wide range of soil groups that exist in the Mt Lofty region as weathering and erosion processes that had occurred on the land surfaces had also revealed a large variety of local parent materials (Northcote, 1976).

At the regional level, lithology and to a lesser extent climate, appear to be the dominant factors affecting soil development and distribution patterns in the Mt Lofty Ranges (Maschmedt, 1987). Generally, the southern part of the Ranges has been geomorphologically more stable and therefore consists of extensive laterite-capped tablelands in comparison with the central Mt Lofty subregion which consists of dissected ridges and depressions with lateritic material preserved only on the ridge crests (Northcote, 1976). The lateritic tablelands and the ridge crests are the remnants of the summit high plain that is of Mesozoic age (Twidale, 1976). The uplift of the Flinders-Mt Lofty block during the Pleistocene caused extensive erosion and consequently stripped the older weathering products and thus exhumed the underlying weathered materials. The exposed materials then became available for renewed weathering and soil formation (Stephen, 1946). The soil on the land surfaces below the ridge crests in the central Mt Lofty subregion (the study area is on some of these surfaces) was formed in this manner (Northcote, 1976).

Considered at the local scale, the characteristics of soil formed on such exhumed surfaces are much more influenced by topographic variables than other factors (Maud, 1973), even though local variation in lithology may be important in some situations. In spite of the close relationships between soil and topography, no clear analysis has been carried out for the region especially at the local level.

As shown in Tables 2.1 and 2.2, duplex soils predominate in the study area. Duplex soils, defined as mineral soils "with a texture contrast of one and a half texture groups or greater between the A and B horizons" (Northcote, 1960), are characterized by sandy or loamy A horizon overlying abruptly a more clayey B horizon. The term "textural groups", as used in this defnition, refers to the textural classes as determined by "feel" method in the

field. A number of hypotheses have been proposed to account for the pedogenetic processes responsible for formation of these soils, viz: 1) translocation of fine material (especially fine clay) from surface horizon (Stace *et al.*, 1968; Chittleborough and Oades, 1980; Chittleborough *et al.*, 1984); 2) differential weathering and leaching of primary and secondary minerals in the surface and the subsurface horizons (Brewer, 1955); and 3) *in situ* weathering of material in the B horizon to clay with concomitant destruction of clay in the A horizon (Oertel, 1974). If the theory of soilscape evolution as described above is accepted, then a combination of all the three processes is more plausible. However, the relative importance of each of these processes would depend on the local conditions, particularly lithology, topography and suitability of the medium for chemical and mechanical breakdown of materials. It could be that the clay in the A horizon was destroyed by chemical dissolution and/or, depending on the steepness of the local slope, mechanically removed by illuvial processes down the profile into the B horizon or by geomorphological processes down slope into the main drainage system. The pre-existing sedimentary layering is another possible explanation for texture contrast of duplex soils (Sleeman, 1975).

CHAPTER 3

DESIGN OF OPTIMAL SAMPLING SCHEMES BY GEOSTATISTICAL METHODS

3.1 Introduction

Traditionally, soil survey and soil classification have been the most practical approaches to separation and grouping of different soil types within the landscape. They rely on the surveyors' intuition to create classes and locate soil boundaries on the assumption that there are strong relations between soil type and the environment. These subjective methods have attracted the critical interest of a number of authors (Beckett and Webster, 1971; Burgess *et al.*, 1981; McBratney *et al.*, 1981; Burgess and Webster, 1984).

3.1.1 Methods of soil inventory

The classical method

The classical method, (as traditional or conventional soil survey is called-e.g.Burgess *et al.*, 1981; Trangmar *et al.*, 1985; Webster, 1985), implies that soil classes are discrete with abrupt boundaries. Thus the predicted value of a soil attribute at any unsampled location is the value for the typical pedon or mean value for the mapping unit. The precision of any prediction is therefore dependent on the homogeneity of the mapping units and hence on the within-unit variance (Trangmar *et al.*, 1985). Usually there is no independent quality control or verification of precision other than the assumption of strong relations between soil type and the environment. The classical approach does not account for the spatially-dependent component of the variability within the mapping unit (Burgess and Webster, 1980; McBratney and Webster, 1981a),

especially for intensive surveys of small areas and featureless areas with no obvious changes in soil boundaries.

The classical method usually involves incorporation of some exotic classification system (Butler, 1980) which may not be relevant to the objective of the survey or the area being surveyed. Moreover, many classification systems make use of only few diagnostic properties, especially those that can easily be measured. As Dudal (1986) noted, these properties may not necessarily be the most important from the viewpoint of land utilization.

The emerging methods

Because of the uncertainty inherent in the classical method, a number of workers have proposed new approaches aimed at providing known precision for, and improving the quality of, soil maps. Burgess and Webster (1984) used the gamma function to describe the probability distribution of soil boundary spacings in order to improve the siting of soil boundaries in the field. However, most classifications for specific purposes may require more information than the field-observed soil variables that this method suggests. In addition, the mathematics involved may not be attractive to pedologists, most of whom are not familiar with the intricate computations that are needed to be done quickly in the field, although this could be programmed for field computers.

The geostatistical approach based on the theory of regionalized variables (Matheron, 1965) have been applied extensively in soil studies (Burgess and Webster, 1980; McBratney *et al.*, 1981; Burgess *et al.*, 1981; Trangmar *et al.*, 1985). This approach involves a prior knowledge of the semivariogram which may be determined by transect sampling during the initial stage of survey. The semivariogram is needed to estimate the error variance of interpolation for any sampling scheme to be used in the main stage of survey. This approach is optimal because the sparsest sampling intensity that can achieve a desired precision could be derived for a given soil attribute.

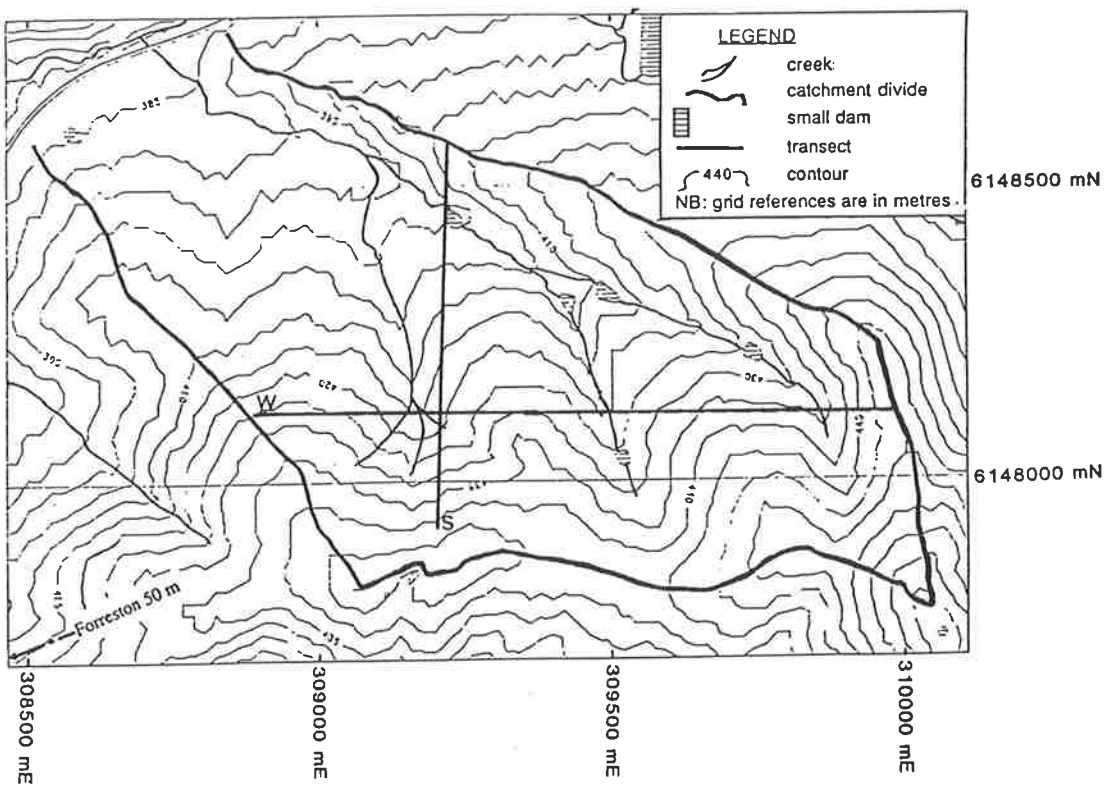

Fig. 3.1 A contour map of the study area showing the transects.

3.1.2 The main objectives

The main objectives of the work described in this chapter were to:

1) determine the spatial structures of soil properties with the aim of designing optimal sampling schemes for the study area;
2) highlight the difficulties involved in a purely geostatistical approach to achieve the first objective.

3.2 Transect Survey and Laboratory procedures

3.2.1 The study area

Detailed description of the study area is contained in chapter 2.

3.2.2 Transect survey

For the purpose of this investigation, the line-transect technique was used as it was considered more suitable for the study of spatial variation of soil in a small area (McBratney and Webster, 1981a). To ensure an accurate geodetic reference, a laser theodolite was used to lay two transects, orthogonal to each other, in the west-east and south-north directions. The directions were chosen to transect the most obvious variability in the landscape and hence reveal any related soil anisotropy (Fig. 3.1). In order to ensure that sampling reflected both the local and general soil variation, paired sampling was adopted, with each pair containing points 2 m apart and adjacent pairs 8 m apart (Fig. 3.2). The laser theodolite was also used to locate sampling points with reference to some neighbouring spot heights to ensure geodetic accuracy of about 0.3m.

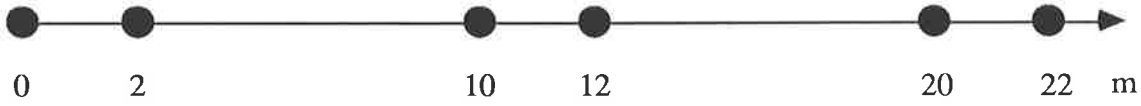

Fig. 3.2 Layout of sampling scheme along a transect; the symbol, ●, is a sampling point.

Table 3.1 The soil variables

Variable*[1]	Unit of measurement	Type	Transformation
Soil colour (main and mottle)	Munsell notations	semi-numerical	CIELab*[2]
Structural features			
a) Grade	rating (0-5)	ordinal	nil
b) Type	shape of aggregates	nominal	fuzzy coding*[3]
Consistence (plasticity, and stickiness)	rating (0-5)	ordinal	nil
Consistence (strength)	rating (1-7)	ordinal	nil
Cutan abundance	rating (0-5)	ordinal	nil
Mottle abundance	rating (0-5)	ordinal	nil
Particle-size fractions	%	numerical	nil
Organic carbon	%	numerical	nil
Electrical conductivity	S m^{-1}	numerical	nil
pH	pH unit	numerical	nil

*[1]Each variable was determined for both topsoil and subsoil; mottle abundance and cutan abundance were determined for subsoil and parent material.
*[2]Munsell notations were transformed to CIE (Commission International d'Eclairage) coordinates of L, a and b; the quantity L is the lightness of colour comparable to the Munsell value; the coordinates a and b are related to chroma in terms of $(a^2 + b^2)^{0.5}$ and hue in terms of the ratio a/b (CIE, 1978).
*[3]Fuzzy coding allows for partial values between and including 0 and 1 (see Table 3.2).

Undisturbed 50 mm soil cores to bedrock were taken at each point for the determination of key physical, chemical and morphological properties. Throughout this chapter and subsequent chapters, the west-east and north-south transects are simply

referred to as W-E transect and S-N transect respectively. A total of 247 cores were initially taken with 100 on transect-S and 147 on transect-W. All symbols that include W or S or their lower case subscripts describe conditions or quantities associated with transect-W or transect-S.

3.2.3 Morphology description

The samples were taken to the laboratory and key morphological characteristics (see Table 3.1) of the major horizons, topsoil (0-20 cm) and subsoil (40-60 cm), were determined in accordance with the modified system of McDonald *et al.* (1984). Depth of dark-stained topsoil, depth to mottles, depth to maximum clay, depth of solum and depth to bedrock were also measured for each pedon. The main and mottle colours were obtained by comparing with the Munsell colour chart under standard illumination (Pendleton and Nickerson, 1951; Melville and Atkinson, 1985).

Table 3.2 Fuzzy coding of structural type

Type	Horizontality	Verticality	Flatness	Accomodation
Platy	1.0	0.1	1.0	1.0
Lenticular	1.0	0.3	0.3	1.0
Prismatic	0.2	1.0	1.0	1.0
Columnar	0.2	1.0	0.9	0.9
Angular blocky	1.0	1.0	1.0	1.0
Subangular blocky	0.7	0.7	0.5	0.5
Granular	0.2	0.2	0.0	0.1
Massive	0.0	0.0	0.0	1.0
Single grain	0.0	0.0	0.0	0.0

Quantification of ordinal morphological variables

Some of the ordinal variables that are the morphological parameters were coded and/or transformed as shown in Tables 3.1 and 3.2. The Munsell notations were transformed into CIELAB coordinates (CIE, 1978) to give some uniformity of scale. The fuzzy coding of structural features as shown in Table 3.2 is a reflection of vagueness of soil structural description as contained in McDonald *et al.* (1984) and in many other soil survey manuals.

3.2.4 Laboratory procedures

Particle-size analysis

The subsamples were first air-dried, ground with a rubber pestle, and the gravel fraction obtained by sieving with a 2 mm sieve. A further subsample of 25 g or 40 g, depending on the approximate clay content as perceived by the"feel" method, was disaggregated in water with an ultrasonic probe for 15 minutes. Organic material was then removed by pre-treatment of the sample with 30 % hydrogen peroxide. The few samples that contained carbonate were pre-treated with 10 % hydrochloric acid to remove the carbonate. Dispersion was achieved by agitating the pre-treated sample on a mechanical stirrer for 10 minutes using 5 % hexametaphosphate as dispersing agent. The sample was transfered quantitatively into sedimentation cylinder and made up to 1 L with deionized water. The main particle-size fractions (sand, silt and clay) were determined using the hydrometer method (Gee and Bauder, 1986).

Soil pH and electrical conductivity

The pH was determined in a 1:5 soil-water suspension (McLean, 1982). A 1: 5 soil-water suspension was prepared by adding 50 mL of air-equilibrated deionized water to 10g of air-dry soil and mechanically shaken end-over-end for 1 hour at 25 ^{o}C. After allowing the suspension to settle for 1 hour, the pH of the supernatant was measured

while stirring gently, using a pH meter and combination electrode calibrated at pH 7.0 and 4.0. The pH was recorded on an air-dry basis.

The electrical conductivity (Ec) of the supernatant was also determined using a calibrated conductivity cell and meter (Rhoades, 1982). The record was expressed on an air-dry basis, corrected to 25 ^{o}C, in mS m^{-1} unit.

Organic carbon

Organic carbon (Oc) content was obtained by the dry combustion method using a Leco CR-12 resistance furnace (Merry and Spouncer, 1988). A 1.5 g or 2.5 g of soil sample (depending on the presumed Oc content; the lower the Oc the higher the amount of sample required for accurate Oc determination) was heated in the furnace in a stream of oxygen at 1200 ^{o}C. The few samples containing carbonate were pre-treated with 10 % hydrochloric acid to remove the carbonate. The percent Oc was calculated directly from the quantity of CO_2 produced after calibration using $CaCO_3$ (12 % C) and 3 soil samples of known Oc content.

3.3 Spatial Analysis and Discussion

3.3.1 The regionalized variable theory

The theory of regionalized variables (Matheron, 1965; 1971) provides the basis for estimating semivariogram of a soil property. The theory is also the basis for interpolation of soil properties by kriging and also to planning of a rational soil sampling scheme for mapping soil types (Oliver, 1987). Theoretically, it is defined as follows: given that $Z(x)$ denotes the value of a soil property at a point x, and $Z(x + \boldsymbol{h})$ the value at a point $(x + \boldsymbol{h})$, $Z(x)$ can be modelled by a random function that satisfies the conditions for the *intrinsic hypothesis* (Journel and Huijbregts, 1978; McBratney and Webster,1981a) that are less demanding than the *second-order stationarity* . The two

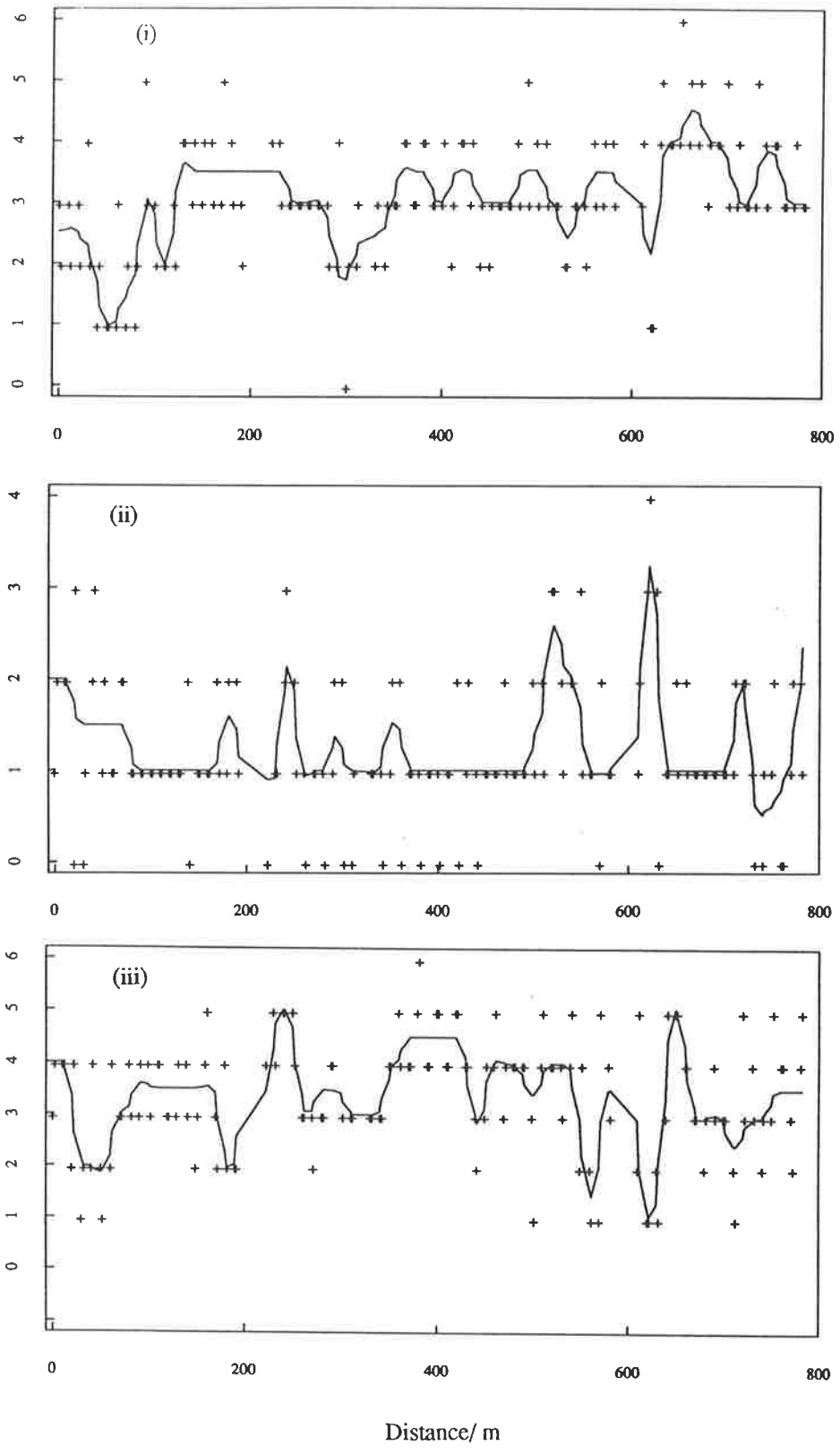

Fig. 3.3(a) Plots of the values of some selected ordinal variables versus distance along transect-W: (i) topsoil structural grade, (ii) subsoil structural grade and (iii) parent material cutan abundance.

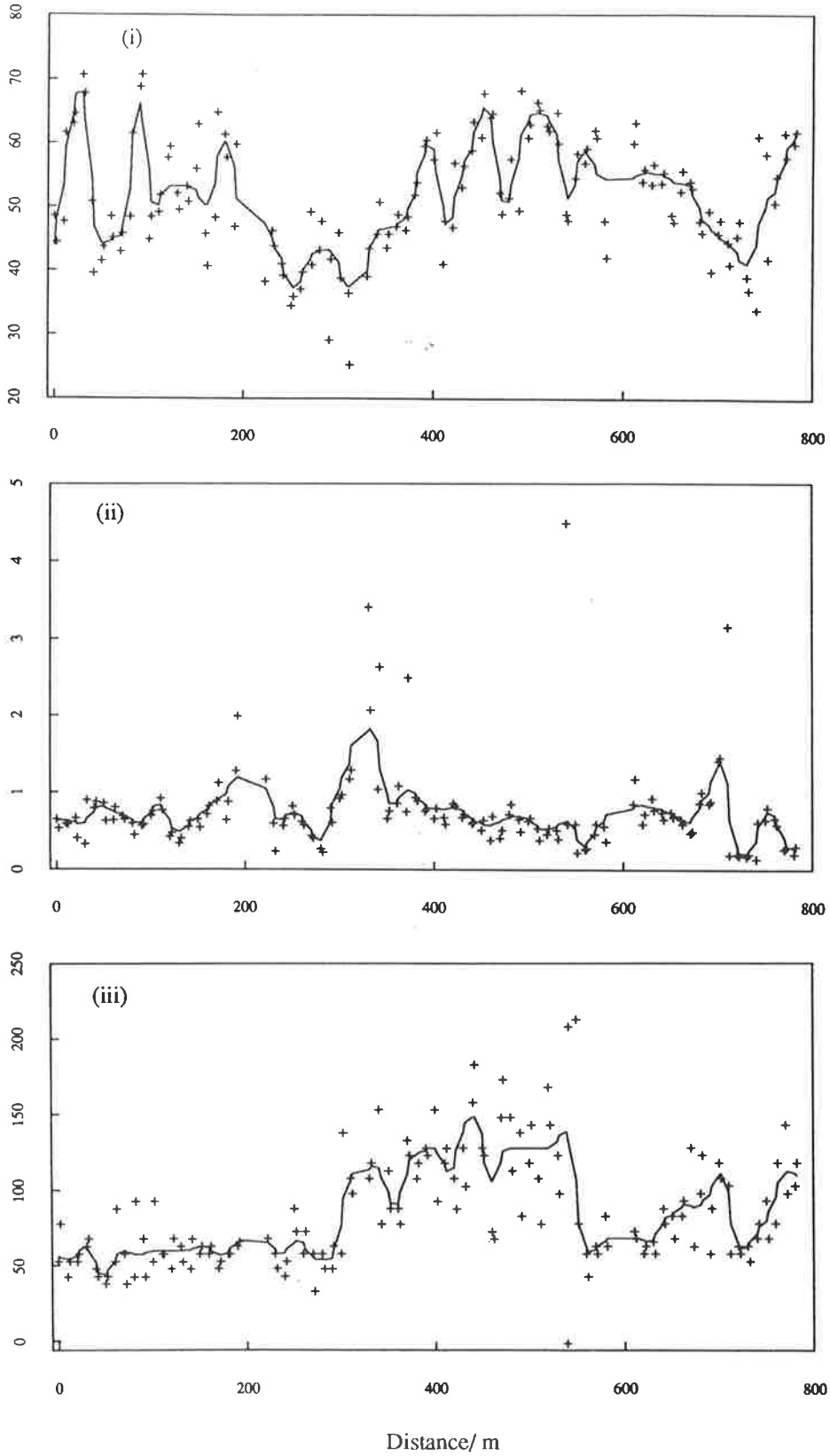

Fig. 3.3(b) Plots of the values of some selected numerical variables versus distance along transect-W: (i) topsoil % sand, (ii) % subsoil Oc and (iii) subsoil Ec (mS m^{-1}).

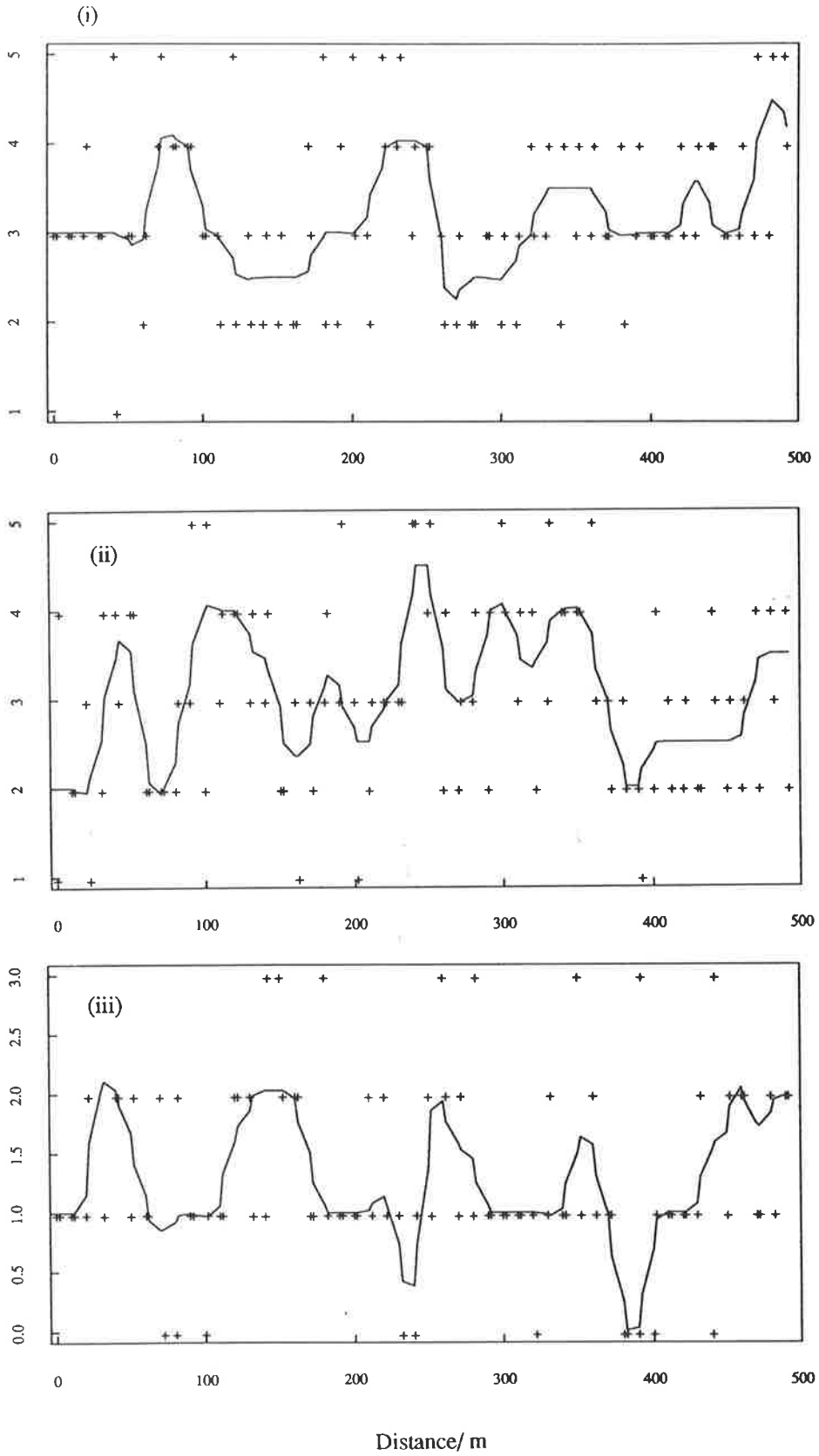

Fig. 3.4(a) Plots of the values of some selected ordinal variables versus distance along transect-S: (i) topsoil structural grade, (ii) subsoil structural grade and (iii) parent material cutan abundance.

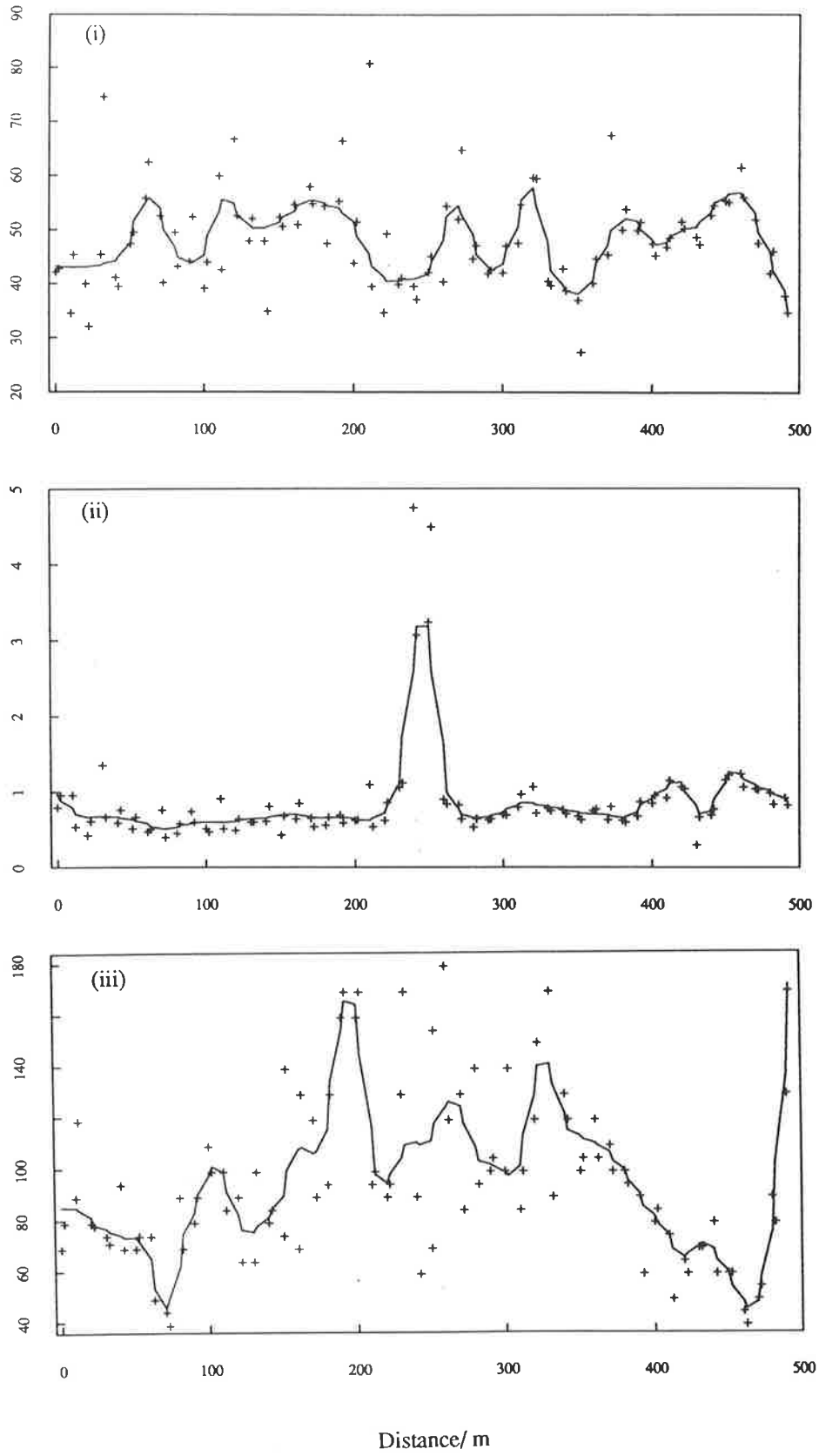

Fig. 3.4(b) Plots of the values of some selected numerical variables versus distance along transect-S: (i) topsoil % sand, (ii) % subsoil Oc and (iii) and subsoil Ec (mS m^{-1}).

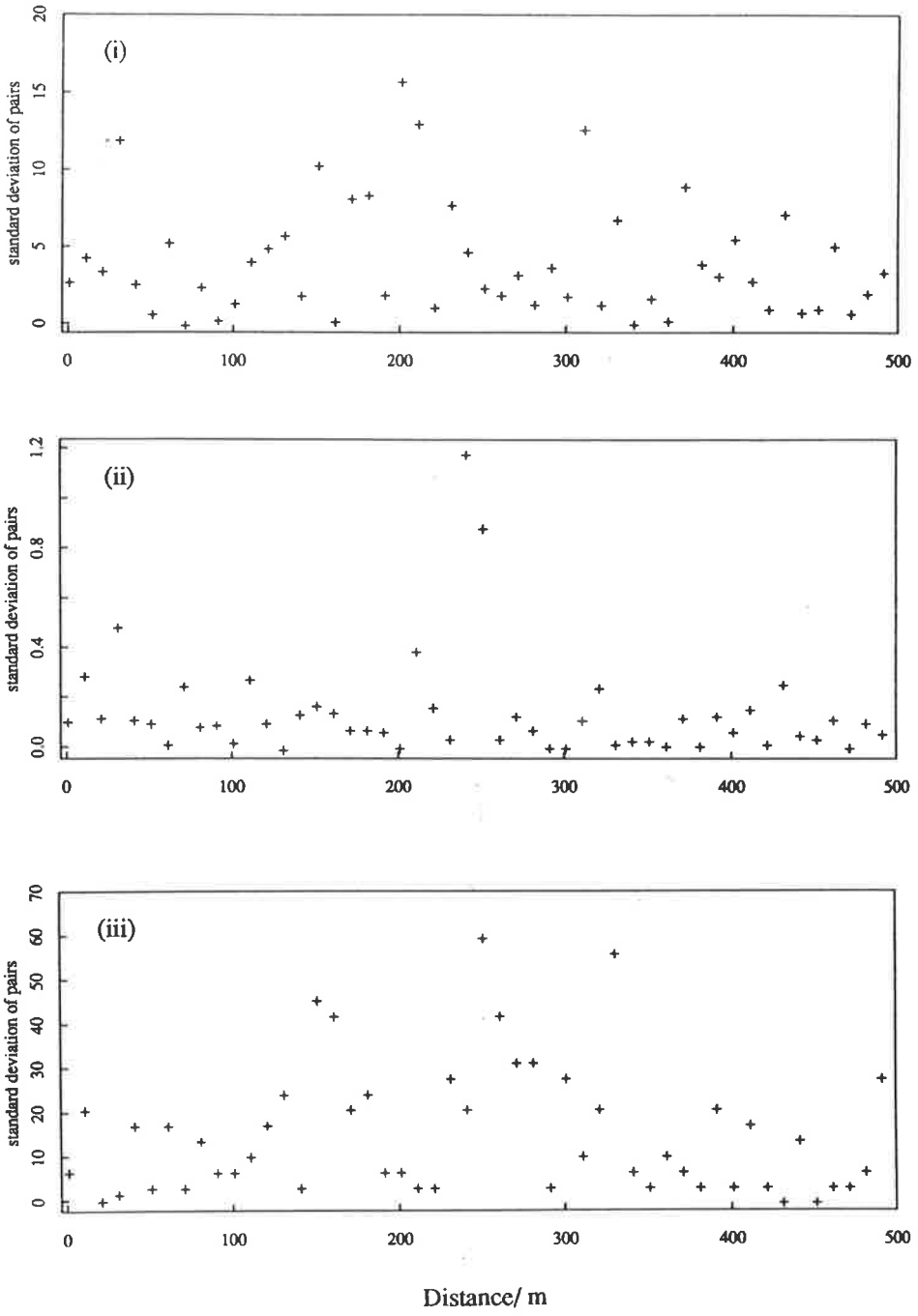

Fig. 3.5(a) Plots of standard deviation of pairs versus distance along transect-W for (i) topsoil % gravel, (ii) subsoil % Oc and (iii) subsoil Ec (mS m^{-1}).

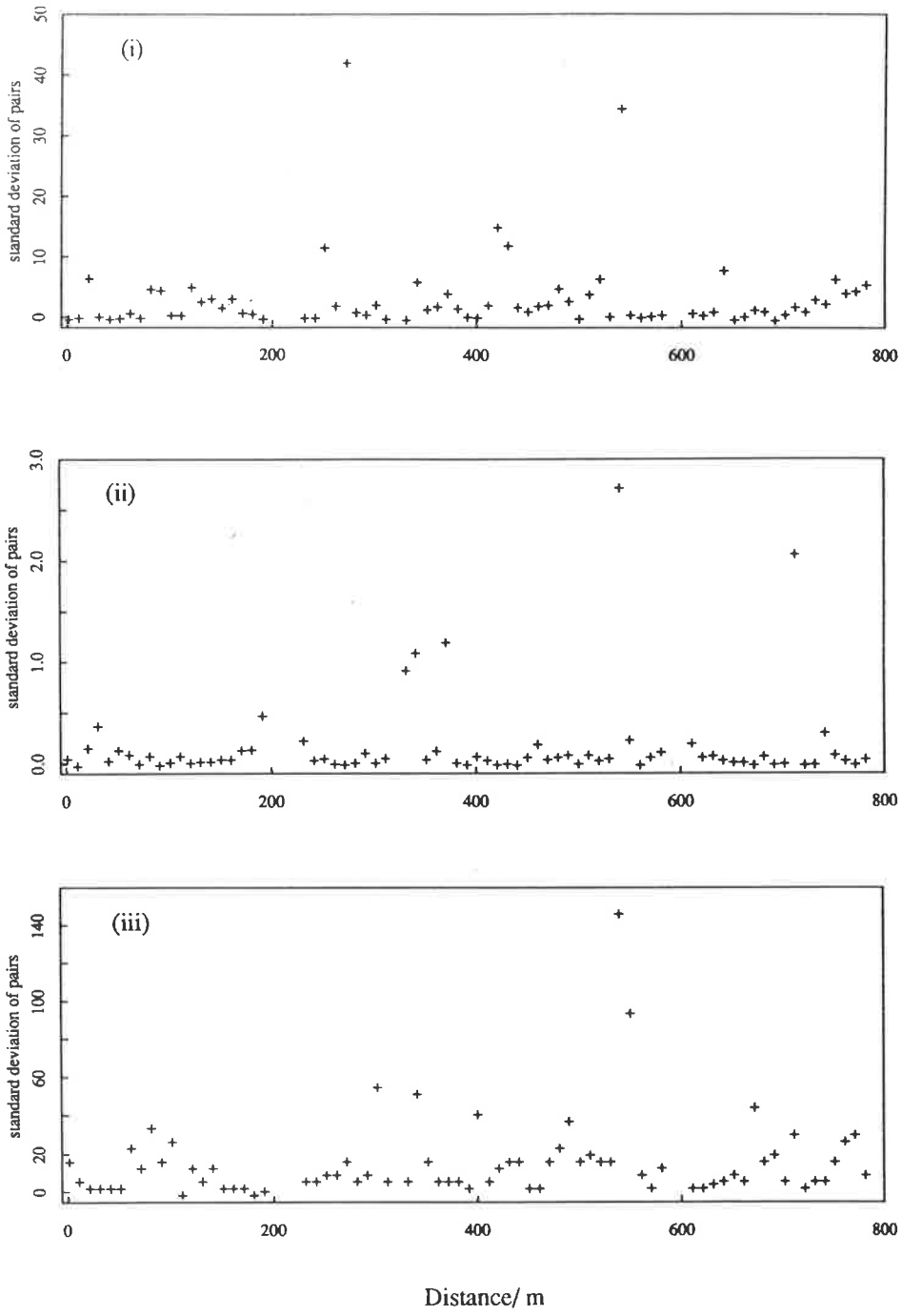

Fig. 3.5(b) Plots of standard deviation of pairs versus distance along transect-S for (i) topsoil % gravel, (ii) subsoil % Oc and (iii) subsoil Ec (mS m^{-1}).

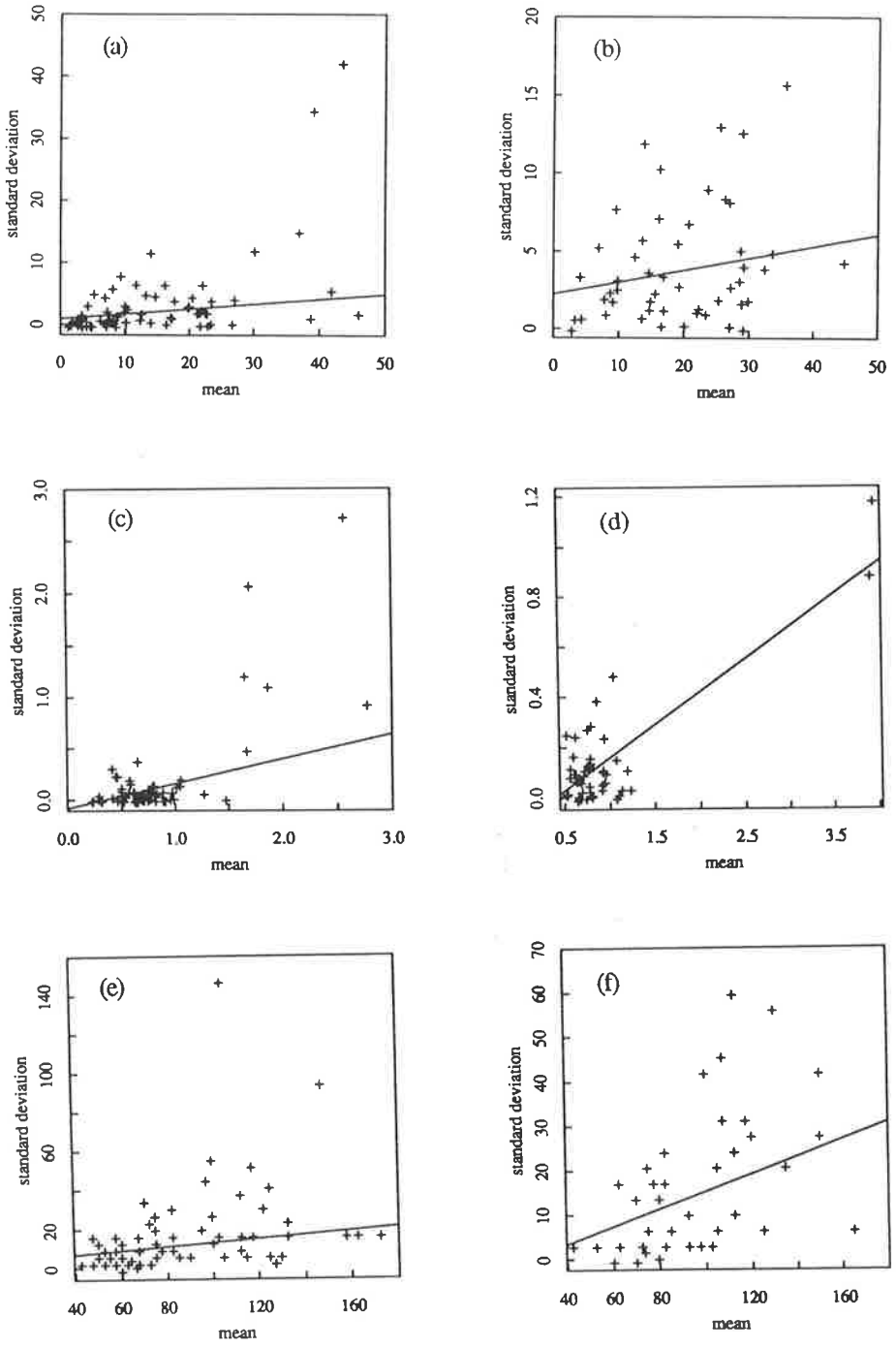

Fig. 3.6 Standard deviation-mean plots of (a) topsoil % gravel along transect-W, (b) topsoil % gravel along transect -S, (c) subsoil % Oc along transect-W, (d) subsoil % Oc along transect-S, (e) subsoil Ec (mS m^{-1}) along transect-W and (f) subsoil Ec (mS m^{-1}) along transect-S.

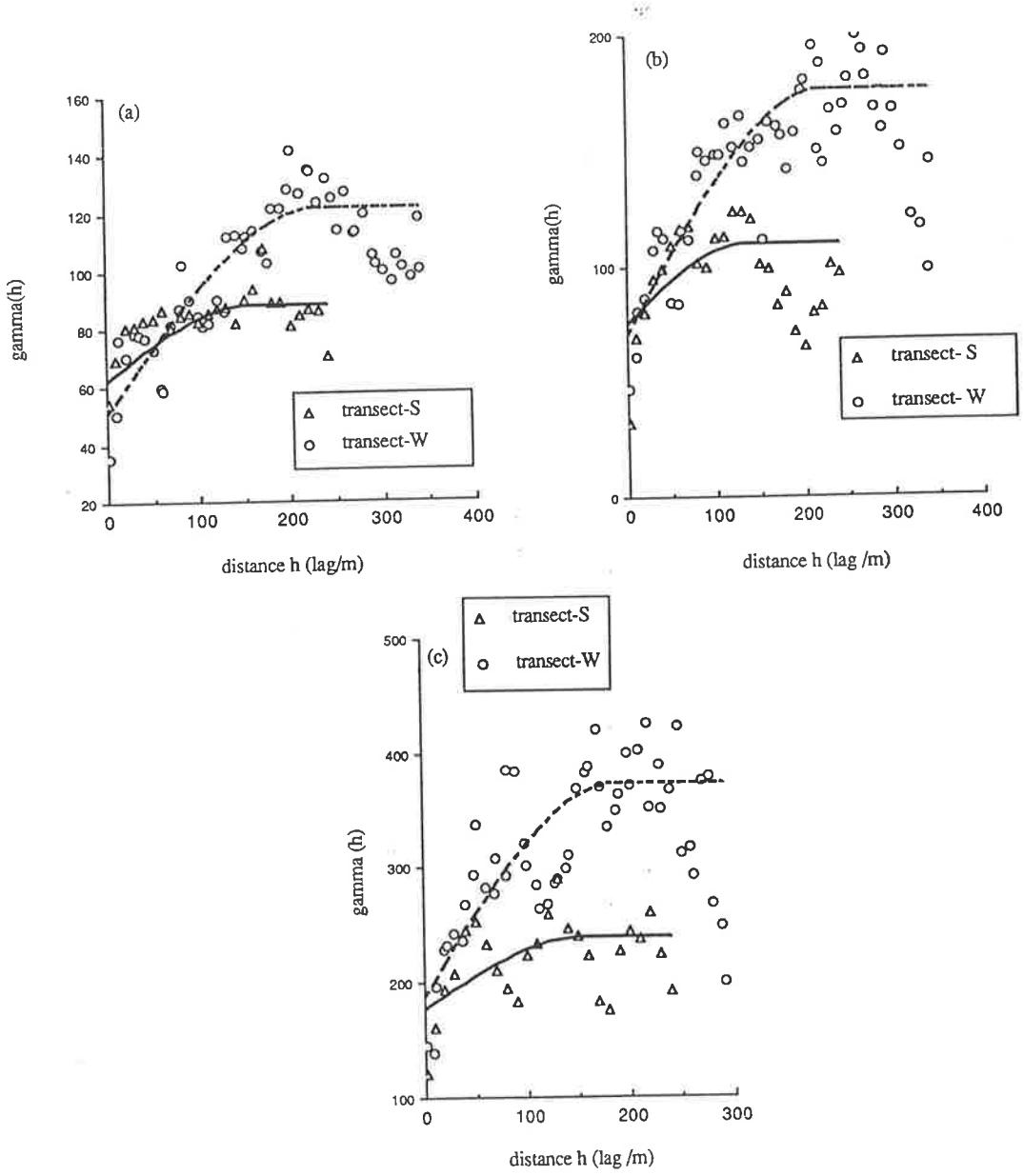

Fig. 3.7 Sample and model semivariograms showing anisotropic variation in (a) topsoil sand, (b) topsoil gravel and (c) subsoil clay; the gamma (h) is in $(\%)^2$.

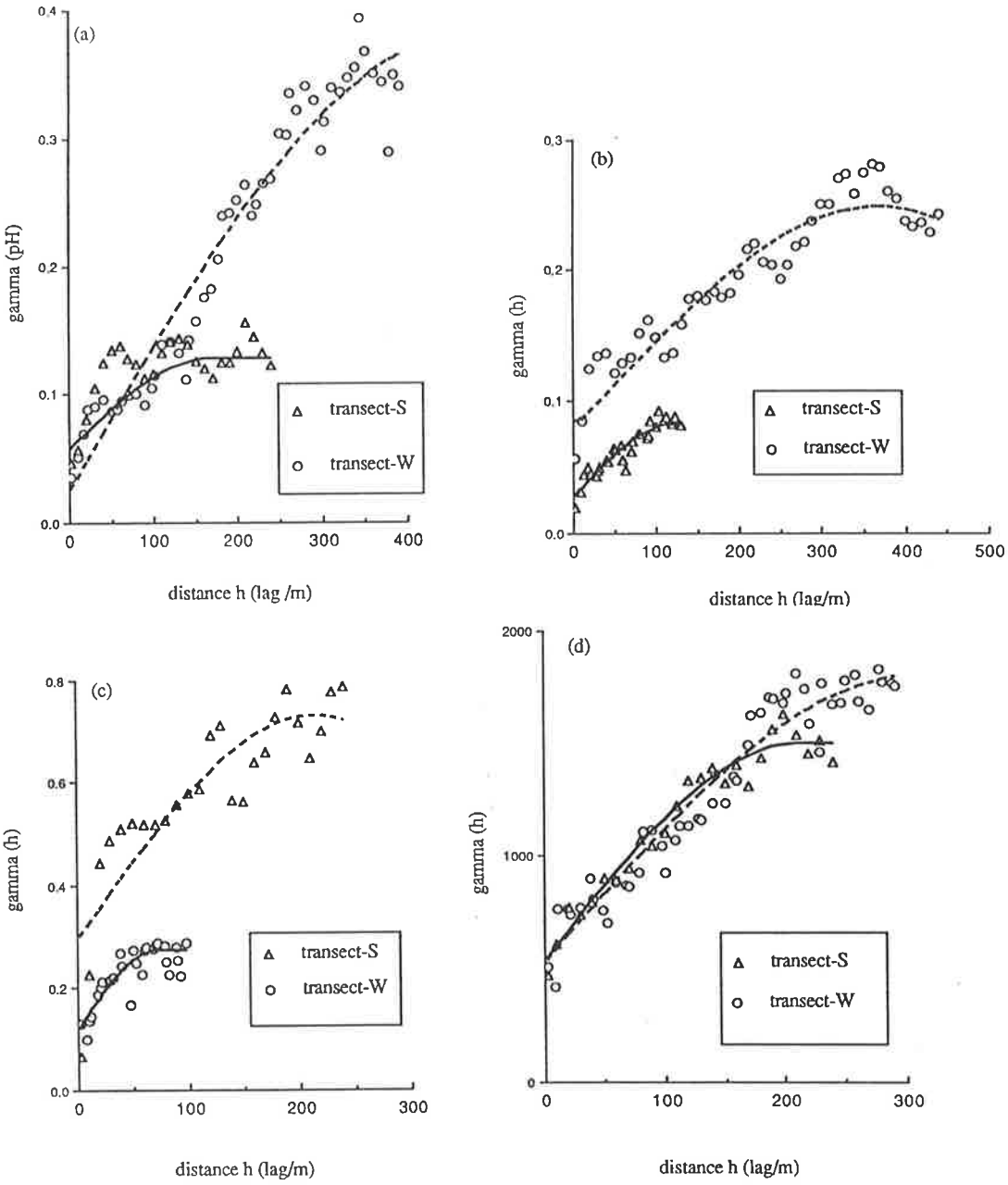

Fig. 3.8 Sample and model semivariograms showing anisotropic variation in (a) topsoil pH, (b) subsoil pH, (c) subsoil organic carbon content (%) and (d) subsoil electrical conductivity (mS m^{-1}); the gamma (h) for the soil attributes is in units of measurement squared.

conditions for the *intrinsic hypothesis* (Matheron, 1971) are expressed in terms of differences, $Z(x + \boldsymbol{h}) - Z(x)$, of the regionalized variable:

1) $E\{Z(x + \boldsymbol{h}) - Z(x)\} = 0$ for any x and $\boldsymbol{h}$ which means that the expectation of any $Z(x)$ is constant;
2) $\gamma(\boldsymbol{h}) = (1/2)E\{[Z(x) - Z(x + \boldsymbol{h})]^2\}$ for any x and $\boldsymbol{h}$, which defines the semivariance value, $\gamma(\boldsymbol{h})$, and states that the variance of the difference depends only on the lag vector **h**.

Based on the expression in condition (2) of the *intrinsic hypothesis,* semivariances for the continuously variable soil properties were estimated by

$$\gamma(\boldsymbol{h}) = \frac{1}{2(n-\boldsymbol{h})} \sum_{i=1}^{n-h} [z(x_i) - z(x_i + \boldsymbol{h})]^2 \qquad (3.1)$$

where $(x_1, x_2, \ldots, x_n)$ constitute n sampling locations along the transect.

3.3.2 Data exploration

For a start, the values of some of the ordinal and semi-continuous and continuous soil variables were plotted along the two transects on the basis of 4 point moving average. This was to aid in visualizing the coherency of spatial variation of the soil parameters along each of the transects. Figs 3.3(a and b) and 3.4(a and b) show the plots for some selected soil variables which illustrate clearly the difference between the purely numerical variables and the ordinal variables. The continuous (numeric) soil variables exhibit a more systematic spatial variation than the ordinal variables.

Homogeneity of variance

Homogeneity of variances of the continuous variables was checked by plotting their standard deviation of pairs against distance along the transects and standard deviation versus means. Figs. 3.5 and 3.6 illustrate the results of selected the variables. Evidently, the standard deviation of some of these variables either increases or decreases with increase in their means, indicating non-stationarity of variance (Fig 3.6). The same observations were made from the plots of standard deviation of pairs (note that paired sampling was adopted as shown in Fig. 3.2) versus distance along the transects (Fig. 3.5 (a and b)). While some standard deviation remains fairly constant for some variables (e.g. subsoil Oc on transect-S), it is quite scattered for some others (e.g. subsoil Ec along transect-W) meaning non-stationarity.

The continuous variables that exhibit non-stationarity were, therefore, log-transformed before embarking on spatial analysis. Such transformation compressed the effect of larger values and spread out the scale of the smaller ones, so that a nearly normal distribution was produced. Those variables that did not show much departure from the assumptions of the *intrinsic hypothesis* needed not be transformed as the short-range variability was the most important.

3.3.3 Sample semivariograms

The semivariances calculated using equation (3.1) can be plotted against the lag, **h**; the plotted curve or the function defining it is the semivariogram (Webster, 1985). The semivariogram derived for a given soil property can further be modelled using one of the safe or non-risky functions that are positive semi-definite (Journel and Huijbregts, 1978). The commonly used models in soil studies include

1) Linear model defined by

$\gamma(h) = C_0 + bh$ for $h > 0$

$\gamma(0) = 0,$

where C_0 is the nugget variance and b is the slope of the linear function;

2) The spherical model,

$$\gamma(h) = C_0 + C(3h / 2a - h^3 / 2a^3) \qquad \text{for } 0 < h \leq a$$

$$\gamma(h) = C_0 + C \qquad \text{for } h > a$$

$$\gamma(0) = 0, \qquad (3.2)$$

where a is the range and $C_0 + C$ constitutes the sill, the C denotes the spatially dependent component of the semivariogram, and the

3) Exponential model,

$$\gamma(h) = C_0 + C[1 - exp(-h/a)] \qquad \text{for } 0 < h \leq a$$

$$\gamma(0) = 0,$$

with a, C_0 and $C_0 + C$ having the same meanings as defined above.

The linear model is an unbounded type, i. e., it is without sill at the spatial range of analysis. The spherical and exponential models are transitive type with sill. The latter two models are extensively used in soil studies as they seem to define the form of experimental semivariograms well (Burgess *et al.*, 1981; Burrough, 1986). After a preliminary trial with the two non-linear models, the spherical model was found to be more attractive as it defined the sample semivariograms quite tightly. Figs. 3.7 and 3.8 show the sample and model semivariograms for selected soil variables in the two directions.

3.3.4 Soil anisotropy

The sample semivariogram model for a soil attribute in any given direction describes isotropic variation. As shown in Figs. 3.7 and 3.8, variation is not the same in the two directions, that is, the soil variation is anisotropic. This is less so for the sample semivariogram of subsoil Ec (Fig. 3.8a). However, a number of anisotropic features are apparent. Each of the soil variables has different nugget variance in the two directions. Secondly, the gradient of the first few lags of a sample semivariogram is also different for the two directions. Thirdly, all the soil variables depict different sills in the two

directions, a feature normally referred to as zonal anisotropy (Trangmar *et al.*, 1985). It was therefore necessary that a model of anisotropy be enunciated that took account of all the above features. Taking the original sample semivariograms as

$$\gamma_w(h) = C_{0w} + C_w \quad \text{for transect-W and}$$
$$\gamma_s(h) = C_{0s} + C_s \quad \text{for transect-S,} \tag{3.3}$$

the following transformations were carried out:

the nugget variances for a given attribute were averaged as

$$\hat{C}_0 = \frac{C_{0w} + C_{0s}}{2}, \tag{3.4}$$

then the spatially dependent component was derived as

$$C'_w = \gamma_w(h) - \hat{C}_0 \text{ and}$$
$$C'_s = \gamma_s(h) - \hat{C}_0, \tag{3.5}$$

and in accordance with McBratney and Webster (1986), the gradients of the first few lags of the semivariograms were calculated as

$$b_w = 3C'_w / 2a_w \quad \text{for transect-W and}$$
$$b_s = 3C'_s / 2a_s. \quad \text{for transect-S} \tag{3.6}$$

The anisotropic ratios for the soil variables were then derived by

$$R = b_w / b_s. \tag{3.7}$$

Table 3.3 Parameter values of isotropic and anisotropic semivariograms for some soil attributes (N denotes pure nugget variation, a is in m and Oc denotes organic carbon; the semivariances are in the units of measurement squared)

soil attribute	$\gamma_w(h)$	$\gamma_s(h)$	C_{0w}	C_{0s}	$\hat{C}_0$	C'_w	C'_s	a_w	a_s	R in W : S
Topsoil sand (%)	121.9	88.3	50.4	68.9	60.1	61.9	28.3	233	157	1.5 : 1
Topsoil grav. (%)	176.8	109.1	70.1	75.2	72.4	104.8	37.1	224	134	1.7 : 1
Topsoil silt (%)	38.8	22.1	28.5	22.1	25	13.8	N	220	N	-
Topsoil clay (%)	34.3	38.1	24.9	19.18	22	12.3	16.1	306	73	1 : 5.5
Topsoil Oc (%)	0.87	0.19	0.43	0.19	0.31	0.56	N	171	N	-
Topsoil Ec mSm^{-1}	2748	1403	1408	1403	1406	1345	N	65	N	-
Topsoil pH	0.36	0.14	0.02	0.04	0.03	0.33	0.11	407	170	1.2 : 1
Subsoil sand (%)	211.8	68.3	87.3	68.3	77	134.8	N	178	N	-
Subsoil silt (%)	46.1	26.8	32.5	26.8	30	13.6	N	277	N	-
Subsoil clay (%)	392.0	239.1	185.9	175.7	180	212.0	59.1	190	156	3 : 1
Subsoil Oc (%)	0.27	0.63	0.12	0.25	0.18	0.09	0.45	73	116	1 : 3.2
Subsoil Ec	1705	1500	525	529	527	1178	973	277	213	1 : 1.1
Subsoil pH	0.25	0.08	0.08	0.03	0.06	0.19	0.03	360	129	2.7 : 1

The results of the transformations for some of the particle-size fractions are shown in Table 3.3. Some of these particle-size fractions depict pure nugget variances in the S-direction, a feature which is interpreted as absence of any spatial dependence in the data at the scale of sampling (Oliver, 1987). Anisotropic variation is in evidence for some other soil variables (e.g. topsoil sand, topsoil gravel subsoil clay, etc). The anisotropic ratios indicate higher variation in the W-direction than S-direction except for the topsoil clay fraction and subsoil organic carbon. The former has an anisotropic ratio of 5.5 which is considered large for soil properties (Trangmar *et al.*, 1985; McBratney and Webster, 1986).

3.2.5 Design of optimal sampling scheme

The procedure described in McBratney *et al.* (1981) and Burgess *et al.* (1981) was used here to derive optimal sampling schemes for the study area. This involves the theory of kriging, a method of interpolating a given soil property, z , at an unsampled location x_0 by the equation

$$z^*(x_0) = \sum_{i=1}^{n} \lambda_i z(x_i) \tag{3.8}$$

where λ_i are the weights associated with the sampling points. The weights sum to unity, a condition which indicates unbiased estimation. The kriging variance, which is a measure of deviation of the estimated values from the actual values, is defined by

$$\begin{aligned} \sigma_e^2 &= E\{[z(x_0) - z^*(x_0)]^2\} \\ &= 2\sum_{i=1}^{n} \lambda_i (x_i, x_0) - \sum_{i=1}^{n} \sum_{j=1}^{n} \lambda_i \lambda_j \gamma(x_i, x_j), \end{aligned} \tag{3.9}$$

where $\gamma(x_0,x_i)$ is the semivariance between x_0 and x_i and $\gamma(x_i, x_j)$ is the semivariance

between x_i and x_j.. To minimize kriging variance, the Lagrange multiplier, ψ, is introduced so that the σ_e^2 which is for punctual kriging, becomes

$$\sigma_e^2 = \sum_{i=1}^{n} \lambda_i \gamma(x_i, x_0) + \psi \tag{3.10}$$

and the variance for block kriging is estimated by

$$\sigma_B^2 = \sum_{i=1}^{n} \lambda_i \gamma(x_i, B) + \psi_B - \sigma^2(B), \tag{3.11}$$

where $\gamma(x_i, B)$ is the mean semivariance between the point, x_i and the block B, and σ_B^2 is the within block semivariance. The semivariogram parameter values in Table 3.3 are based on the linear section of the spherical models fitted to the sample semivariograms, so that the model used for estimating the kriging variances is in the form

$$\gamma(h) = \hat{C}_0 + bh, \tag{3.12}$$

b being the gradient of the first few lags of the isotropic sample semivariogram, fitted by the spherical model, up to the sill at $h = a$. It was derived as in equation (3.6).

Burgess *et al.* (1981) and McBratney *et al.* (1981) have emphasized the merits of using regular grids in isarithmic mapping so that the design of sampling strategy in this work was considered in terms of rectangular grids. Using the semivariogram parameter values for particle-size fractions in Table 3.3, kriging variances were computed for points and block sizes of 10 x 10 m and 100 x 100 m respectively, by the OSSFIM program developed by McBratney and Webster (1981b). This was done by solving equations (3.10) and (3.11) using the model in equation (3.12) and a search radius of 2.00 and 50 nearest points. The computation of kriging variances was restricted to the particle-size variables only for ease of comparison. The results for some of the particle-

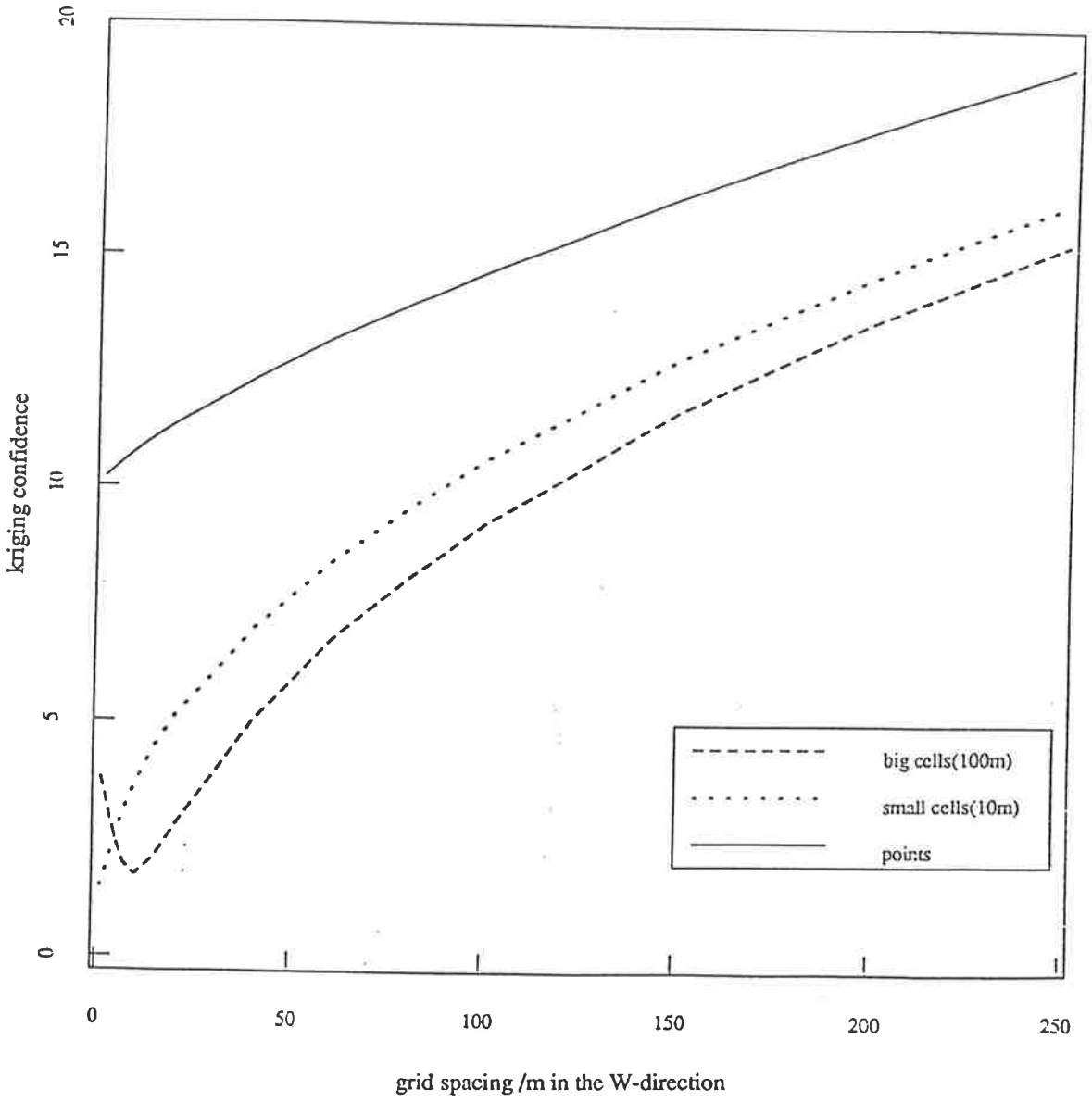

Fig. 3.9 Kriging confidence for punctual and block estimation of topsoil silt (%) as a function of grid spacing in transect-W direction.

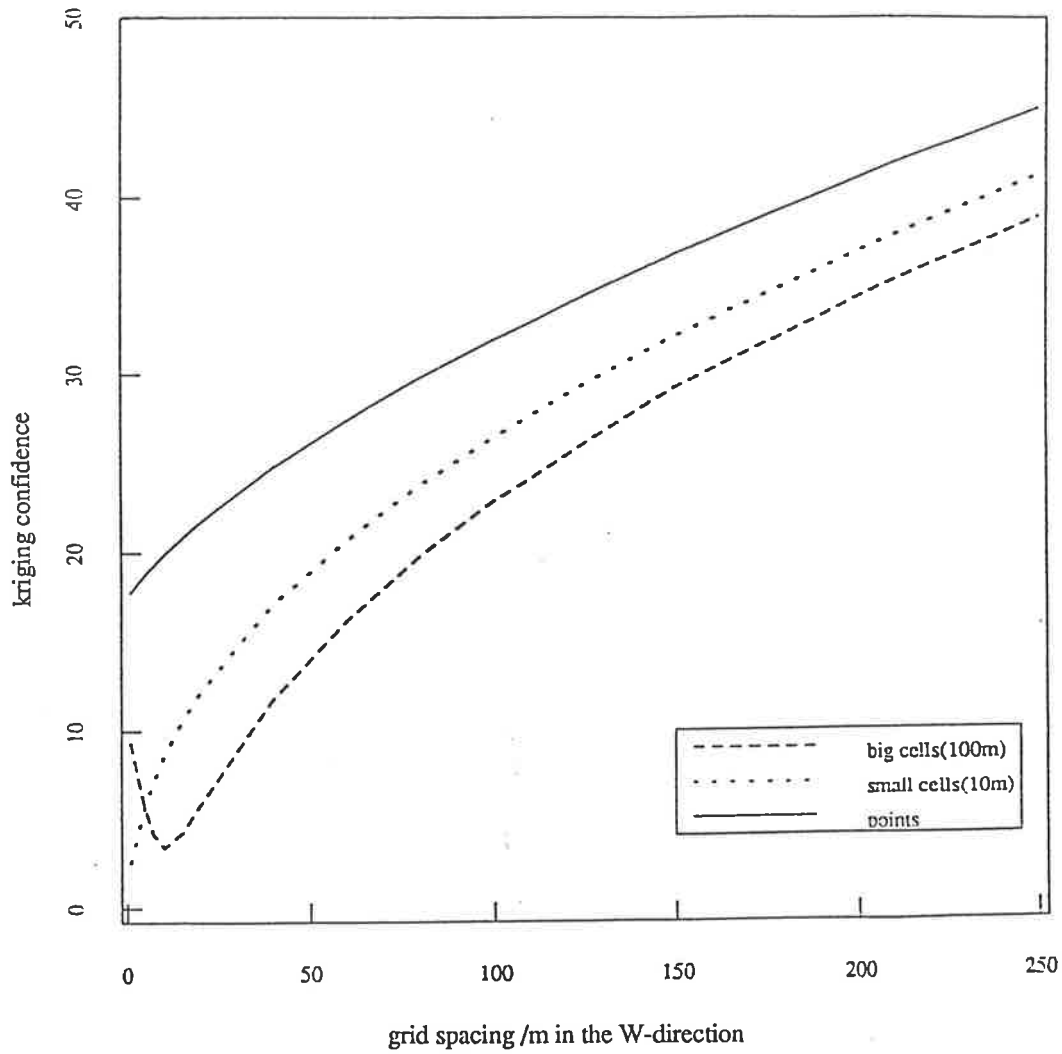

Fig. 3.10 Kriging confidence for punctual and block estimation of subsoil sand (%) as a function of grid spacing in transect-W direction.

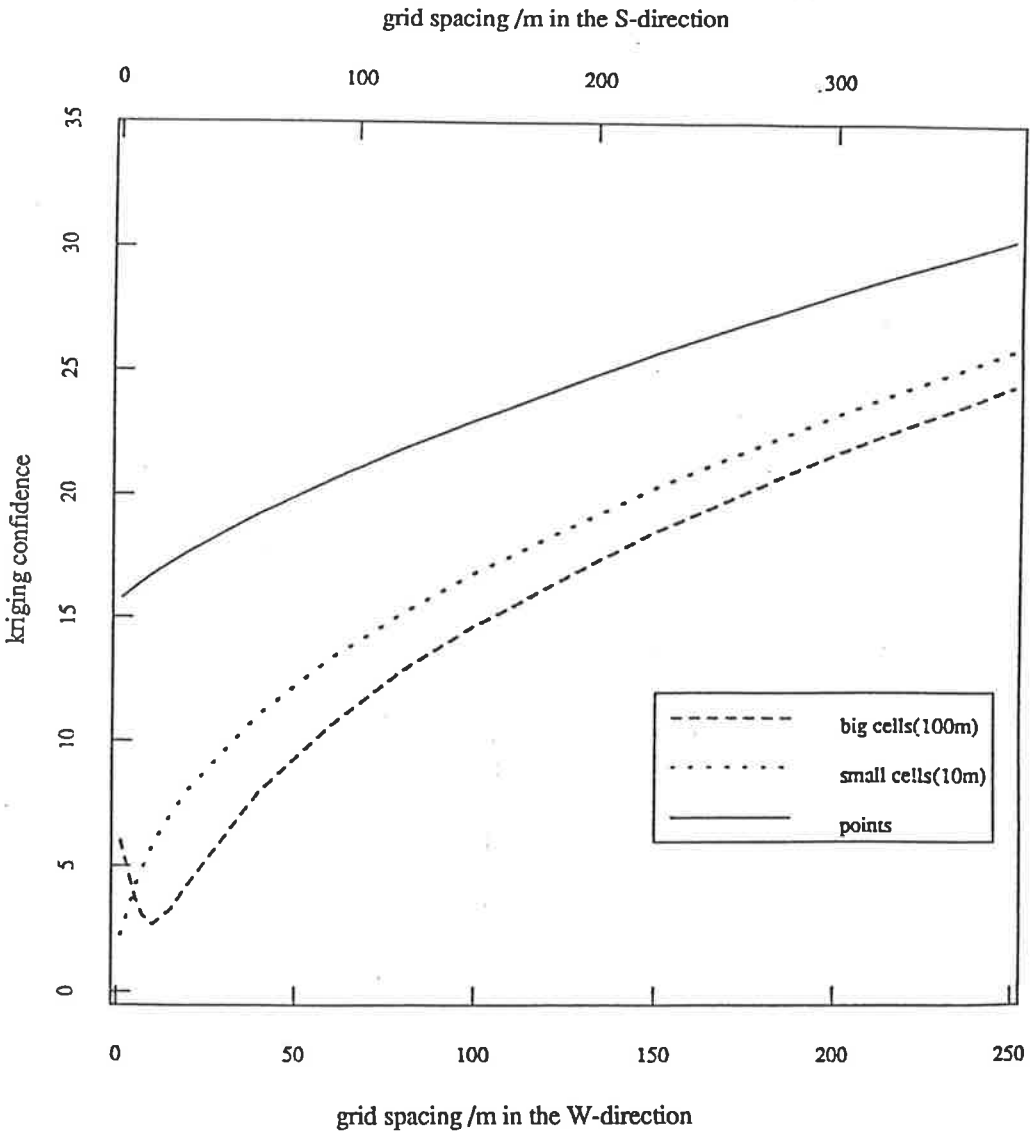

Fig. 3.11 Kriging confidence for punctual and block estimation of topsoil sand (%) as a function of grid spacing in transect-W and transect-S directions.

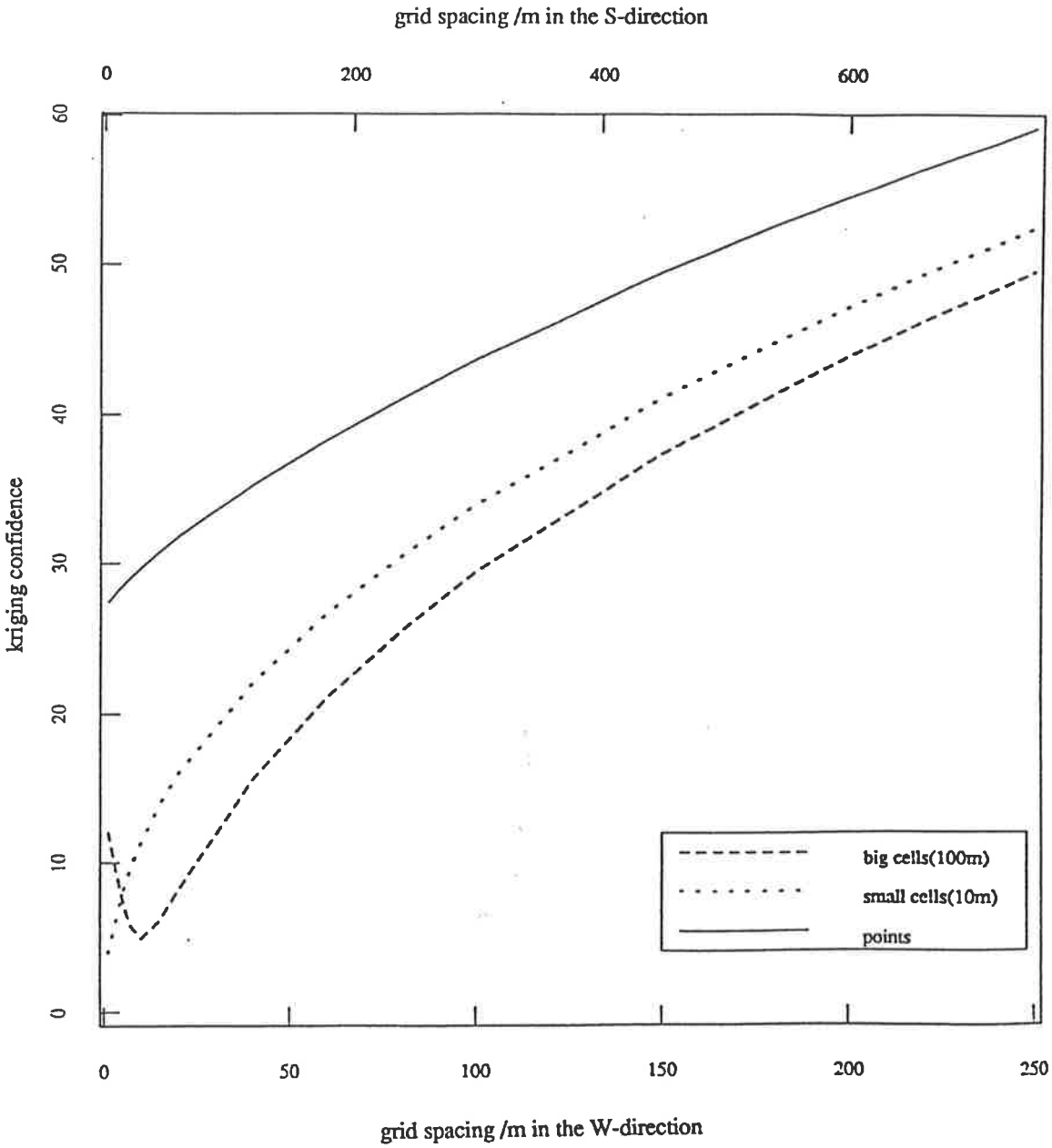

Fig. 3.12 Kriging confidence for punctual and block estimation of subsoil clay (%) as a function of grid spacing in transect-W and transect-S directions.

size data that depict variation in transect-W direction only are illustrated in Figs. 3.9 and 3.10. A confidence limit of 5 % (equivalent to error variance of 25 $(\%)^2$ of particle-size fraction) was chosen as reasonable because, as Burrough (1986, pp 158-159) reported, most conventional soil surveys at 1: 25,000 scale have within-class variances of between 10.6 and 41.9 $(\%)^2$ clay with an average variance of 39.9 $(\%)^2$. These estimates are unreliable; variances may be much higher, as estimates were based on few samples. Table 3.4 also gives the grid spacings in W-direction obtained for 10 x 10 m and 100 x 100 m cells at kriging confidence of 5 % for some particle-size fractions that show variation in W-direction only. A grid spacing at this error margin could not be obtained for point estimates, because the error due to nugget variance is much higher than 5 %. Soil variation in the S-direction is pure nugget for these properties as sampling was too sparse to gain any insight into the form of autocorrelation. One option is to sample at closer intervals to incorporate more of the local variation into the spatial autocorrelation. There may be no end to this. Another option is to ignore the spatially independent variables and determine the optimal density of sampling for those that are anisotropically variable with the spatial component in both directions. The unidirectional optimal density of sampling for those that show variation in one direction only can be incorporated later. The latter option was followed.

The form of anisotropy exhibited by some of the soil variables has been discussed previously, the results of which are given in Table 3.3. To obtain the optimal density of sampling for a given soil property, e.g. one of the particle-size fractions for the topsoil, the kriging variances were computed against the corresponding grid spacings using the isotropic semivariogram derived for the direction of maximum variation, in this case W-direction. The grid spacing in the S-direction was then obtained as the grid interval in the W-direction times R, the anisotropic ratio as derived in equation (3.7). Figs. 3.11 and 3.12 illustrate the kriging error (square root of variance) plotted against grid intervals in both directions for some particle-size fractions. Again, choosing 5 % of the particle-size fraction as a reasonable maximum error, optimal sampling intervals obtained for some of the particle-size variables show anisotropic variation as shown in Table 3.4. Once

again the kriging errors are much higher for point estimates than for either 10 x 10 m or 100 x 100 m cells due to the large nugget variances. Table 3.4 also shows that optimal grid spacings are quite variable for different soil particle-size fractions, even without considering other spatially variable soil properties. The problem is how to choose a grid spacing at a given error variance to satisfy the spatial variation of several soil properties? One solution is to obtain the optimal density for all the soil variables required for a given classification and select the sampling scheme for the attribute that shows the least spatial variation. In this case sampling at 4 x 12 m or 16 x 48 m to estimate means of subsoil clay over blocks of 10 x 10 m or 100 x 100 m respectively would be close enough to map most of the soil particle-size variables to achieve an error of ≤ 5 %.

Table 3.4 Grid spacings in transect-W and transect-S directions obtained for some soil particle-size data at an estimation error of 5% (equivalent to 25 $(\%)^2$ error variance) for 10 x 10 m and 100 x 100 m blocks

Soil attribute	Block-size (m)	Grid spacing (m)	
		transect-W	transect-S
Topsoil sand	10 x 10	8	12
	100 x 100	23	35
Topsoil gravel	10 x 10	5	9
	100 x 100	20	32
Topsoil silt	10 x 10	20	*N*
	100 x 100	40	*N*
Subsoil clay	10 x 10	4	12
	100 x 100	16	48
Subsoil sand	10 x 10	5	*N*
	100 x 100	17	*N*

This approach is by no means easy, especially if all the other variables are considered. In this work there are 48 variables (Table 3.1) of which 18 are continuous

and of purely numeric type that show spatial dependence. To obtain error variances with the corresponding grid spacings for all 18 variables before deciding on the optimal sampling scheme will be computationally very involved, expensive, and probably not worth the effort. Even if this is attainable there is the problem of how to combine all the isarithmic maps resulting from such an exercise to serve the purpose of mapping the soil. Moreover, the spatially independent variables should be considered when mapping soil because they are also important from the viewpoint of soil management.

3.5 Conclusion

Geostatistics offers the possibilty of quantifying the spatial variation of a soil property within the range of spatial dependence, and thus facilitates the design of optimal sampling scheme at the initial stage of the soil survey. However, this study has shown how difficult it is to reach an optimal density of sampling when several soil variables are involved. This is particularly so as soil parameters showed spatial variation at different scales (there are also soil variables that showed discrete variations, and these may need to be included). To alleviate this problem, a suitable means of reducing the number of soil variables to a manageable number that still show spatial coherence of soil as a whole has to be adopted. A method that can achieve this outcome is considered in chapter 4.

CHAPTER 4

SOIL CLASSIFICATION WITH FUZZY-C-MEANS: OPTIMAL SAMPLING STRATEGIES AND SOIL-LANDFORM INTERRELATIONSHIPS

4.1 Introduction

Classification is a means of data reduction whereby a complex system represented by some sets of data is made explicit. Almost all soil surveys are accompanied by some form of grouping, be it the so called 'natural' systems of classification or the technically interpretative form. To conform with the discontinuous soil variation model embedded in the traditional soil survey methods, these classifications are composed of mutually exclusive classes with rigidly defined boundaries based on the differentiating characteristics. Whereas many of these classifications are meant to reflect the processes generating soil variability in the observations, most of such underlying processes may not produce crisp groups but a continuum (DeGruijter and McBratney, 1988; Dale *et al.*, 1989). An appropriate classification for a continuum is not one that assigns entities into non-overlapping classes but rather one in which the continuous nature of the system being classified is recognized.

Moreover the natural classification, and indeed its numerical counterparts used by pedologists, are hierarchical: these are an easy escape to organizing a complex system such as soil. In practice, hierarchies are neither ideal nor universally applicable (Dale *et al.*, 1989). Additionally, soil has no genetics in the sense used in biology (Webb, 1954) where hierarchical classification and numerical taxonomy have been successfully applied. There is also the problem of the layered nature of soil profiles (Moore and Russell, 1976). The constitution of soil profiles are juxtaposed horizons which are often very different in composition and arrangement (Fitzpatrick, 1980). Hence, it is difficult to compare soil profiles using hierarchical grouping.

4.1.1 The need for continuous (fuzzy) soil classes

The fact that soil bodies do not always exhibit discontinuous variation calls for an alternative approach to soil classification and mapping. Classification into mutually exclusive classes with rigidly defined boundaries, i.e., "hard" classification, is particularly unsuitable for the soil continuum. Most existing systems of soil classification are of this type. The transitional nature of soil boundaries should be reflected in some way in the taxonomic space. Additionally, it is not axiomatic that a soil entity should fit perfectly into only one class. This, in fact, is undesirable for a continuous system such as soil.

Within the last two decades or so, application of numerical methods to soil studies have been to contruct better classification by cluster analysis (e.g., Webster, 1977b; DeGruijter, 1977). These methods in some sense attempted to optimize the resulting classification, given the available data. However, the resulting classifications are still confined to discontinuous systems, just as with the traditional methods of soil classification.

The application of numerical methods in other fields, e.g. in language research (Jones and Jackson, 1967) and in marketing research (Arabie *et al.*, 1981), has been to create classification systems with overlapping classes. These systems with overlapping classes allow multiple class memberships although any individual still does or does not belong to a given class, i.e., only the problem of intragrades has been solved. The classes are still discontinuous.

The methods of cluster analysis which have been applied to soil classifications are, to some extent, based on continuous models in that data can be represented in a continuous ways by reducing the original variables to a smaller number of new quantitative variables. The new variables are then used as axes in scatter diagrams which display the individual as points in a low dimensional space. This type of approach is termed ordination. Examples include principal component analysis and multidimensional scaling (Webster, 1977b; DeGruijter, 1977). The disadvantages are: that the results are interpreted in terms of discontinuous classes; that there is lack of spatial coherence of the resulting classes for them to be mapped (Burrough, 1986); and that data with non-linear structure (a condition which is

usual with soil) are poorly represented by ordination. A logical response to these limitations of ordination methods would be to define and use continuous (or fuzzy) class models that reflect both the geographic and taxonomic variations of soil, and which are more suitable to model non-linear structures than ordination. Note that the two phrases, *fuzzy classes* and *continuous classes* are used here interchangeably.

4.1.2 The application of fuzzy set theory to cluster analysis

The problem of dealing with inexactness and uncertainty is a part of the wider human experience. However, it was not until Zadeh (1965) introduced the theory of 'fuzzy sets' that a mathematically meaningful method of quantifying such imprecision and uncertainty in natural phenomena was enunciated. Fuzzy set theory, which is a generalization of abstract set theory, stems from imprecision and uncertainty: its chief characteristic is the grouping of individuals into classes that do not have sharply defined boundaries. Fuzzy sets are useful whenever we have to describe ambiguity, vagueness, and ambivalence in conceptual or mathematical models of empirical phenomena. Since such models do not realistically describe physical phenomena, the strictly binary approach in which an entity either belongs to a class or not at all, is not always adequate to describe systems in the real world (Kandel, 1986).

The first well-defined application of the theory of fuzzy sets to cluster analysis was made by Ruspini (1969). Later, Dunn (1974) and Bezdeck (1974) developed the fuzzy-c-means (FCM) algorithm (which is also known as fuzzy-k-means or FKM algorithm), that became a landmark in the theory of cluster analysis. Since then, there has been rapid development in the application of fuzzy-c-means in various fields (Bezdek, 1981; Bezdek *et al.*, 1981; McBratney and Moore, 1985). Its application in soil studies has only recently begun (DeGruijter and McBratney, 1988; Powell *et al.*, 1989). In fact fuzzy clustering, termed here as fuzzy classification, is probably more applicable to the soil continuum than to most other natural systems (e.g., climate and vegetation). This notion is reflected in Fridland's (1974) observations, quoted by Hole and Campbell (1985), that "the soil cover

may be regarded as a discrete-continuous formation that is physically continuous but geographically discrete", and "classificationally, it (the soil cover) is liable to be either continuous (with gradual transitions between soils, though closely related soil forms) or discrete (with sharp transitions between soils and very dissimilar neighbouring soils)". Fridland's ideas are consistent with the complexity associated with soil variation at all scales, the resultant uncertainty in soil mapping and spatial interpolation (Webster, 1985) and our inability to sample and measure physical objects precisely as they occur in the real world (Burrough, 1987).

4.1.3 Objectives

The objectives of this chapter are to:

1) examine the basic principle and the essential aspect of the algorithmic procedure and validity of fuzzy classification;
2) evaluate the potentials of using the FCM to improve the geostatistical methodology to soil survey and to solve the problem of unequal variation of soil properties posed to geostatistical soil survey method;
3) examine the spatial relationships between fuzzy soil classes and the major landform and geologic features as an aid to delineating soil class boundaries and thus to enable a more effective sampling strategy that will improve geostatistical prediction at the main stage of survey.

4.2 The Concept of Fuzzy (Continuous) Classes

Suppose a survey of n sites lists values of p soil variables. This constitutes a data matrix, X, of size $n \times p$ values and the hard partitioning of the data into c classes would produce an $n \times c$ matrix , M, of membership values. Given that $M = m_{ij}$, $m_{ij} = 1$ if an individual, i (e.g. a pedon), belongs to class j and $m_{ij} = 0$ otherwise. Three conditions ensure that classes are exclusive, jointly exhaustive and non-empty:

(1) $\sum_{j=1}^{c} m_{ij} = 1$ $\qquad 1 \leq i \leq n$

(2) $\sum_{i=1}^{n} m_{ij} > 0$ $\qquad 1 \leq j \leq c$

(3) $m_{ij} \in \{0,1\}$ $\qquad 1 \leq i \leq n; \quad 1 \leq j \leq c.$

Condition (1) indicates that the sum of memberships of an individual over all classes is unity. Condition (2) ensures that there must be at least one individual having some degree of belongingness to a given class, otherwise that class is empty, a situation which is undesirable. It is the condition (3) that is of utmost importance and makes the difference between crisp classes and fuzzy classes. It states that an individual either belong to a class or not at all. For fuzzy classes, condition (3) is relaxed so that class memberships are allowed to be partial and thus can take any value between and including 0 and 1. The condition (3) then becomes a fourth viz:

(4) $m_{ij} \in [0,1]$ $\qquad 1 \leq i \leq n; \quad 1 \leq j \leq c$

Fuzzy classification techniques involve operations that satisfy conditions (1), (2) and (4) and therefore are generalizations of hard classifications. The best known fuzzy classification is the FCM (Bezdek, 1974; 1981) which is a generalization of hard-c-means (HCM) (Hartigan, 1975). The HCM is defined by the objective functional:

$$J(M,c) = \sum_{i=1}^{n} \sum_{j=1}^{c} m_{ij}\, d^2(x_{iv}, C_{jv}), \tag{4.1}$$

where $C=(C_{jv})$ is a $c \times p$ matrix of class centroids with C_{jv} denoting the centroid of class j for variable v, $1 \leq v \leq p$; $x_{iv} = (x_{i1}, \ldots, x_{ip})$, is the data value at site i; $d^2(x_{iv}, C_{jv})$ is the squared distance between x_{iv} and C_{jv} according to the chosen distance which for simplicity

will, henceforth, be denoted by d_{ij}^2; $J(M,c)$ is the sum of square error as a function of each individual by the centre of its class.

In dealing with situations where there are not well-separated groups with hybrid points between two or more groups, Ruspini (1969) introduced the fuzzification of HCM functional (equation 4.1) to accommodate the intragrades as:

$$J_F(M,c) = \sum_{i=1}^{n} \sum_{j=1}^{c} m_{ij}^{\ 2}\, d_{ij}^2, \tag{4.2}$$

Later, Dunn (1974) and Bezdek (1974) generalized Ruspini's fuzzy functional (equation 4.2) as

$$J_G(M,c) = \sum_{i=1}^{n} \sum_{j=1}^{c} m_{ij}^{\phi}\, d_{ij}^2, \tag{4.3}$$

where ϕ is the fuzziness exponent that determines the degree of fuzziness of the solution. The fuzziness exponent is chosen so that $\phi \in [1, \infty\}$. Equation (4.2) (and indeed equation 4.3), which is termed FCM objective functional, is minimized to satisfy conditions (1), (2) and (4) as defined above. With $\phi > 1$, minimization of $J_G(M,c)$ is achieved by Lagrangian differentiation of equation (4.3) using a Picard iteration of the following equations:

$$m_{ij} = \frac{d_{ij}^{-2/(\phi-1)}}{\sum_{k=1}^{c} d_{ik}^{-2/(\phi-1)}}, \quad 1 \le i \le n;\ 1 \le j \le c, \tag{4.4}$$

$$\text{and} \quad c_j = \frac{\sum_{i=1}^{n} m_{ij}^{\phi} x_i}{\sum_{i=1}^{n} m_{ij}^{\phi}}, \quad 1 \leq 1 \leq j . \tag{4.5}$$

4.2.1 The FCM Algorithm

The FCM algorithm is in accordance with the procedure contained in McBratney and Moore (1985) following Bezdek (1981). The Picard iteration is embedded in the algorithm based on iterative minimization of $J(M,c)$ as follows

[1] Choose the number of classes, with $1 < c < n$.

[2] Choose fuzziness exponent ϕ, *with* $\phi > 1$.

[3] Choose a measure of distance in the variable space, $d^2(x_i, c_{jv})$.

[4] Choose a value for stopping criteria ε, *(usually* $\varepsilon = 0.001$*).*

[5] Initialize $\boldsymbol{M} = \boldsymbol{M}^{(0)}$ *i.e. with random membership values or memberships from a HCM clustering.*

[6] At iteration $\varphi = 1, 2, 3 \ldots\ldots$,: *(re)-calculate* $\boldsymbol{c} = \boldsymbol{c}^{(\varphi)}$ *using equation (4.5) and* $\boldsymbol{M}^{(\varphi-1)}$.

[7] Recalculate $\boldsymbol{M}^{(\varphi)}$ *using equation (4.4) and* $\boldsymbol{c}^{(\varphi)}$, *constraining* m_{ij} *to 0 if numerical overflow would occur as* $d_{ij}^2 \approx 0$.

[8] Stop on convergence, i.e. if $||\boldsymbol{M}^{(\varphi)} - \boldsymbol{M}^{(\varphi-1)}|| \leq \varepsilon$, *otherwise go to step [6].*

An application of this algorithm (written in FORTRAN) in geology has been reported by Bezdek *et al.* (1981) and an application to climatic classification is given by McBratney and Moore (1985).

4.2.2 Choice of distance dependent metric

The metric is needed to optimize the performance of the objective functionals (equation 4.3), by normalization of the d_{ij}^2 using some norm-induced inner product that is a positive-definite matrix. The frequently used metric is the Euclidean norm:

$$d_{ij}^2 = \sum_{j=1}^{c} (x_{iv} - c_{jv})^2 \qquad 1 \le v \le p$$
$$= (x_i - c_j)' (x_i - c_j). \tag{4.6}$$

The Euclidean norm gives equal weight to all measured variables and it is insensitive to statistically dependent variables (Bezdek, 1981; DeGruijter and McBratney, 1988). Geometrically, it would normally generate (hyper-)spherical balls and therefore is most suitable when classes in X have the general shape of spherical clouds. In soil system, such spherically-shaped classes are in the "laps of the Gods".

Another valuable metric which has rarely been used in cluster analysis is the diagonal norm which is induced by the $p \times p$ diagonal matrix:

$$A_D = \begin{bmatrix} (1/\sigma_1)^2 & 0 & \cdots & 0 \\ 0 & (1/\sigma_2)^2 & \cdots & 0 \\ \vdots & & & \\ 0 & 0 & \cdots & (1/\sigma_p)^2 \end{bmatrix} \tag{4.7}$$

Thus the diagonal norm is

$$d_{ij}^2 = (x_i - c_j)' A_D (x_i - c_j). \tag{4.8}$$

Like the Euclidean norm, the diagonal norm is insensitive to statistically dependent variables but would compensate for distortions in the assumed spherical shape caused by disparities in variances among the measured variables. A third alternative is the Mahalonobis' norm defined by

$$d_{ij}^2 = (x_i - c_j)' \Sigma^{-1} (x_i - c_j). \tag{4.9}$$

where Σ is the pooled within-classes variance-covariance matrix. The Mahalonobis' norm would compensate for distortions like the diagonal norm, and, additionally account for the statistically dependent measured variables.

Whether the diagonal norm or Mahalonobis' norm is used depends on the correlations among measured variables to be analysed. In this study, both norms were tried on the various combinations of soil variables in which the geometrical and statistical properties of the data determined the acceptability of the results.

4.2.3 Optimal number of classes

An optimal number of classes generated (by FCM algorithm) from a given data set, X, supposedly should reflect substructures or their weak form within X. However, for a system such as soil, it is unlikely that a wholly satisfactory number of classes that could be considered optimal could be found because it is not known if the samples are representative of all the possible entia in either a geographical or taxonomic context. Moreover, there may be more than one way to generate an optimal number of classes with each solution reflecting successive substructures within the major structure. Additionally, classes will be generated any way, whether they exist or not. This is a common problem to all numerical

classifications. In spite of these inherent problems associated with "cluster validity", many authors have devised mathematical functionals as a means of solving for optimal number of classes. Two of these functionals, which are used in this study, are discussed in details. They are fuzziness performance index *(F')* and normalized classification entropy *(H')*, which were found to be most useful when applied to artificial data by Roubens (1982). These criteria were used to evaluate the varying number of fuzzy climatic classes by McBratney and Moore (1985) and of fuzzy soil classes by Powell *et al.*, (1989).

F' is defined by

$$F' = \frac{1-(cF-1)}{F-1}, \tag{4.10}$$

where F is the functional

$$F(M,c) = \sum_{i=1}^{n} \sum_{j=1}^{c} (m_{ij})^2 / n. \tag{4.11}$$

Bezdeck (1981, pp 102-103) showed that the value of F is dependent on the entries of a $c \times c$ similarity matrix, $S(M) = MM^T/n$. Thus the jk^{th} entry of $S(M)$ is defined by

$$s_{jk} = \sum_{i=1}^{n} m_{ij} m_{ik} / n, \tag{4.12}$$

where s_{jk} defines a measure of similarity on pairs of fuzzy classes. In other words, it quantifies the extent to which m_j and m_k share memberships over n data points in X with the provisos that $j \neq k$ and $0 \leq s_{jk} < 1$. Substituting equation (4.12) into equation (4.11) however, will yield

$$F(M,c) = \frac{\sum_{j=1}^{c} s_{jj}}{\sum_{j=1}^{c} s_{jj} + 2 \sum_{i=k+1}^{c} \sum_{k=1}^{c-1} s_{jk}}. \qquad (4.13)$$

Equation (4.13) shows that as F maximizes, $s_{jk} = 0$, *i.e*, there is no membership sharing between any pair of fuzzy classes (meaning that fuzzy classes are relatively hard and are suggestive of distinct substructures). Here lies the paradox in the logic: that if X has distinct substructures in it, then FCM algorithm should produce relatively hard classes (M) as determined by F. Conversely, as F' is a derivative of F (constrained as $0 \leq F' \leq 1$) as shown in equation (4.10), minimization of F' indicates optimal number of fuzzy classes that best reflect some substructures in X. Thus $F' = 1$ corresponds to maximum fuzziness and $F' = 0$ to nonfuzzy.

The normalized classification entropy, H', is derived from the classification entropy,

$$H = H(M, c) = -\sum_{i=1}^{n} \sum_{j=1}^{c} m_{ij} \log_{\beta}(m_{ij})/n, \quad 0 < \beta < \infty \qquad (4.14)$$

in the form: $H' = H/\log_{\beta} c.$ (4.15)

The logic of H' is based on information-theoretic entropy first introduced by Shannon (1948). The entropy describes the certainty (or uncertainty) of fuzzy c-partition of events of sample space X. As fuzzy groups themselves portray uncertainty (Bezdek, 1981) it is appropriate to adopt the idea of information content in this context. Because $\sum_{j=1}^{c} m_{ij} = 1$, the partition entropy can be re-defined as

$$H = \sum_{i=1}^{n} h(m_i)/n, \qquad (4.16)$$

and the normalized classification entropy thus becomes

$$H' = \frac{\sum_{i=1}^{n} h(m_i)/n}{\log_\beta c.}, \tag{4.17}$$

where h is the Shannon's (1948) entropy as $h(\mathbf{p})$[#1] $\Leftarrow -\sum_{j=1}^{c} m_j \log_\beta(m_j)$; $h(m_i)$, therefore, is the amount of fuzzy information about the membership of x_i in c subclasses that is retained by the column m_i. If $M = [1/c]$, membership assignments are maximally uncertain with most of the fuzzy information retained. On the other hand, there is maximum certainty in hard-c-partitioning because little or no fuzzy information is retained by the hard classes. To validate the optimal number of fuzzy classes, one presumes that minimization of H (and hence H') is consistent with maximizing the amount of information about the substructures in X that is generated by the FCM algorithm.

The problems with using F' and H' are twofold. The first is that both F' and H' have the tendency of monotonicity and therefore lack appropriate bench-marks against which their values can be judged as "good". The second problem has to do with the rationale underlying the logical use of these functionals to validate clustering: that is heuristics in nature. However, if the FCM algorithm consistently identifies substructures within X for a given metric d, the centroids c_j, and the fuzziness exponent ϕ, it is quite appropriate to accept them as "good". It is on this basis that both F' and H' are used here.

[#1] The notation, $\Leftarrow$, means 'implied by'.

4.3 Fuzzy Classification of Soil for Optimal Sampling Schemes

4.3.1 The soil data

In chapter 3, it was shown how difficult it was to apply geostatistical approach to the design of optimal sampling scheme for a multivariate system such as soil. An alternative method that takes cognisance of unequal variation of various soil properties is desirable. One approach which has been used constitutes the multivariate techniques such as principal component analysis (McBratney and Webster, 1981a). However, these methods assume linear relationships among soil variables, a condition which is not often the case with soil properties (DeGruijter and McBratney, 1988). It is expected that fuzzy classification, which takes into account the continuous nature of the soil continuum, might be appropriate to model such non-linear structures especially if the non-linearity is caused by multimodality. The fuzzy classification techniques were, therefore, applied to the soil data described in chapter 3 to obtain fuzzy soil classes, the membership coefficients of which are used to design optimal sampling schemes for the study area. Because of time constraint, and the need to come up with a quick sampling scheme at the initial stage of this work, the FCM algorithm, which does not segregate the extragrading soil members and therefore appears to be non-robust, was used. The algorithm requires less computing time than the later version which will be discussed in section 4.4.

In applying the FCM classification algorithm to the soil data, ϕ values of 1.11, 1.15 and 1.50 were tried, each for a series of 2 to 10 classes using the whole soil data. The results for $\phi = 1.11$ were not sufficiently fuzzy enough to warrant using the FCM classification techniques, and those for $\phi = 1.50$ were too fuzzy for the data set. The results for $\phi = 1.15$ were more appropriate and therefore accepted for further analysis. Before further analysis however, the problem of "cluster validity" had to be solved. The criteria of F' and H', as described in subsection 4.2.3, were used. Fig. 4.1 shows that both F' and H' are minimal when number of classes, c , equals 7, even though the actual minimum for F' is c equals 2. Common sense criteria indicate that c equals 7 should be

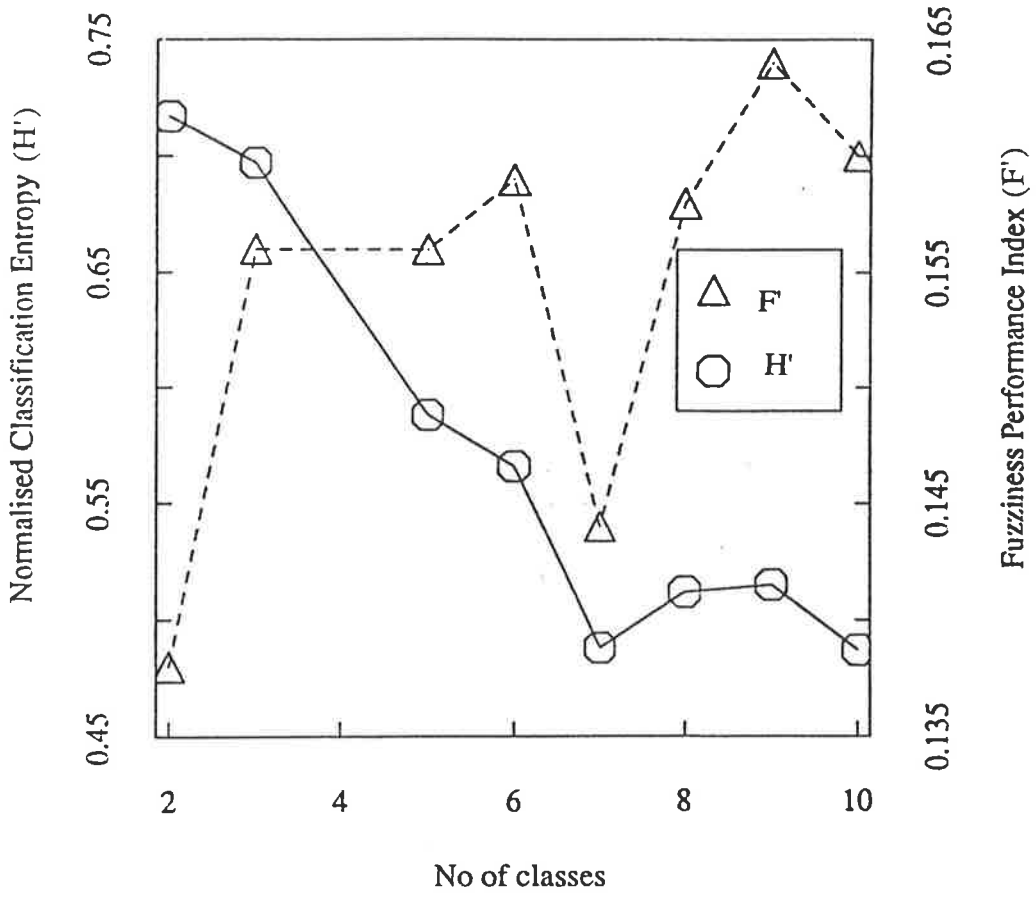

Fig. 4.1 Fuzziness performance index and normalized classification entropy against number of classes for whole soil data *(ϕ=1.15)*

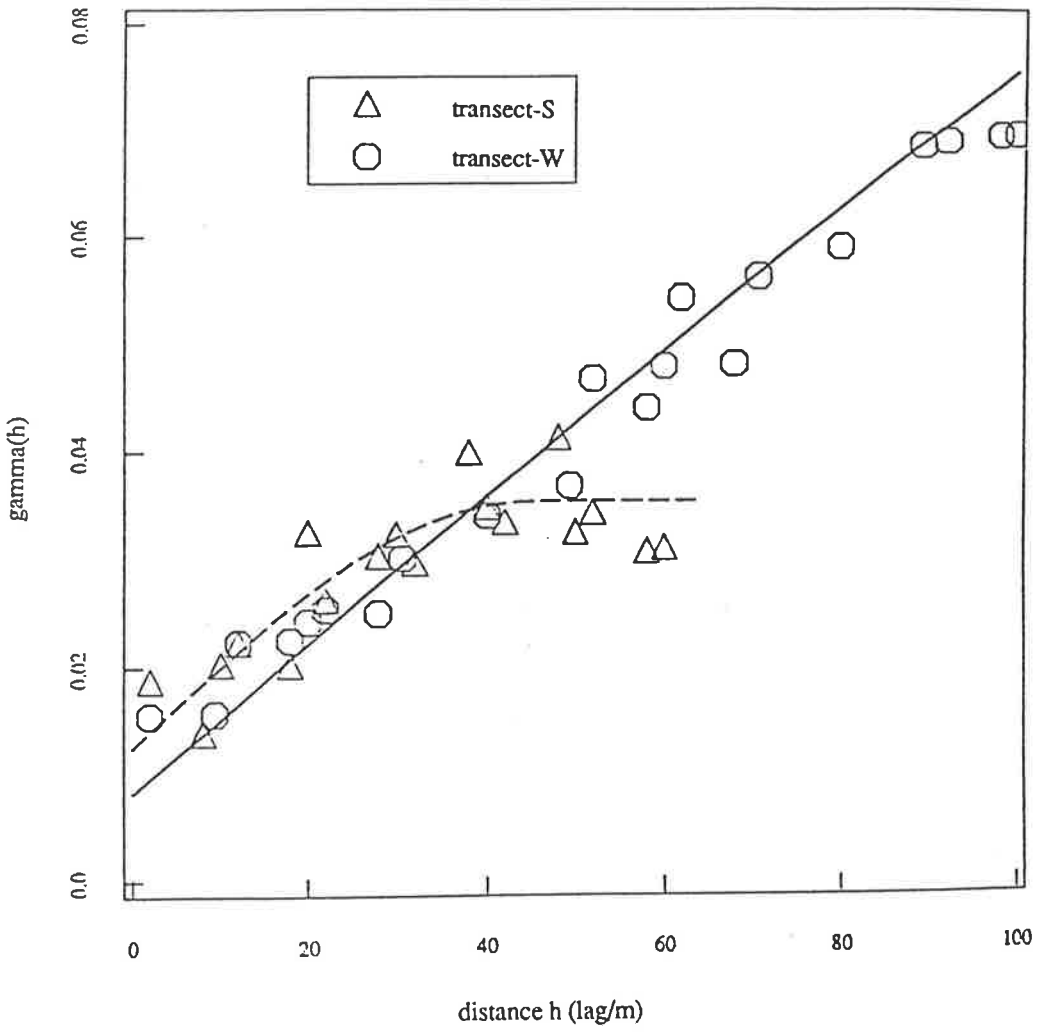

Fig. 4.2 Anisotropic semivariograms of fuzzy class membership coefficients for soil class B; the gamma(h) is in membership coefficient squared.

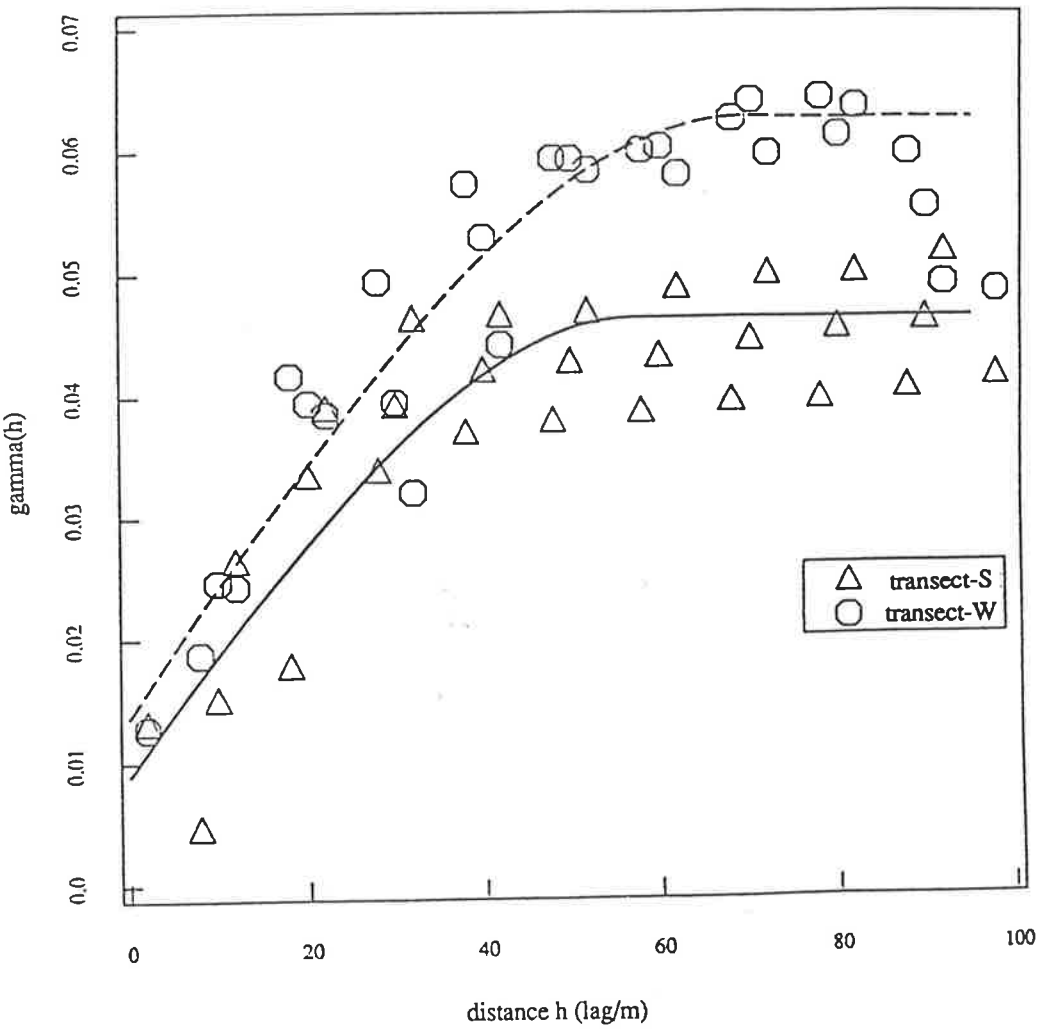

Fig. 4.3 Anisotropic semivariograms of fuzzy class membership coefficients for soil class G; the gamma(h) is in membership coefficient squared.

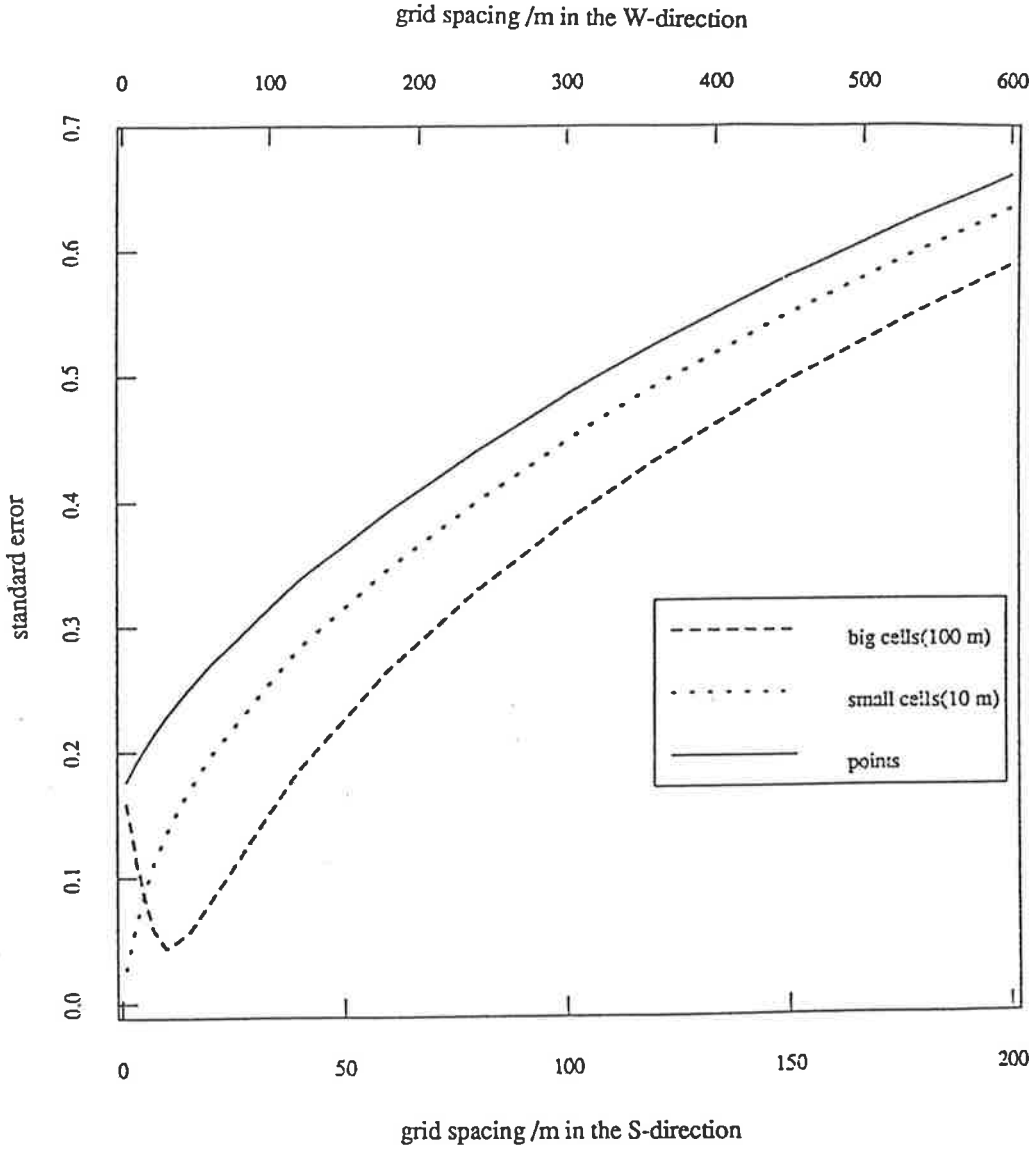

Fig. 4.4 Kriging error for punctual and block kriging of fuzzy class membership coefficients for soil class A as a function of grid spacings in transect-W and transect-S directions.

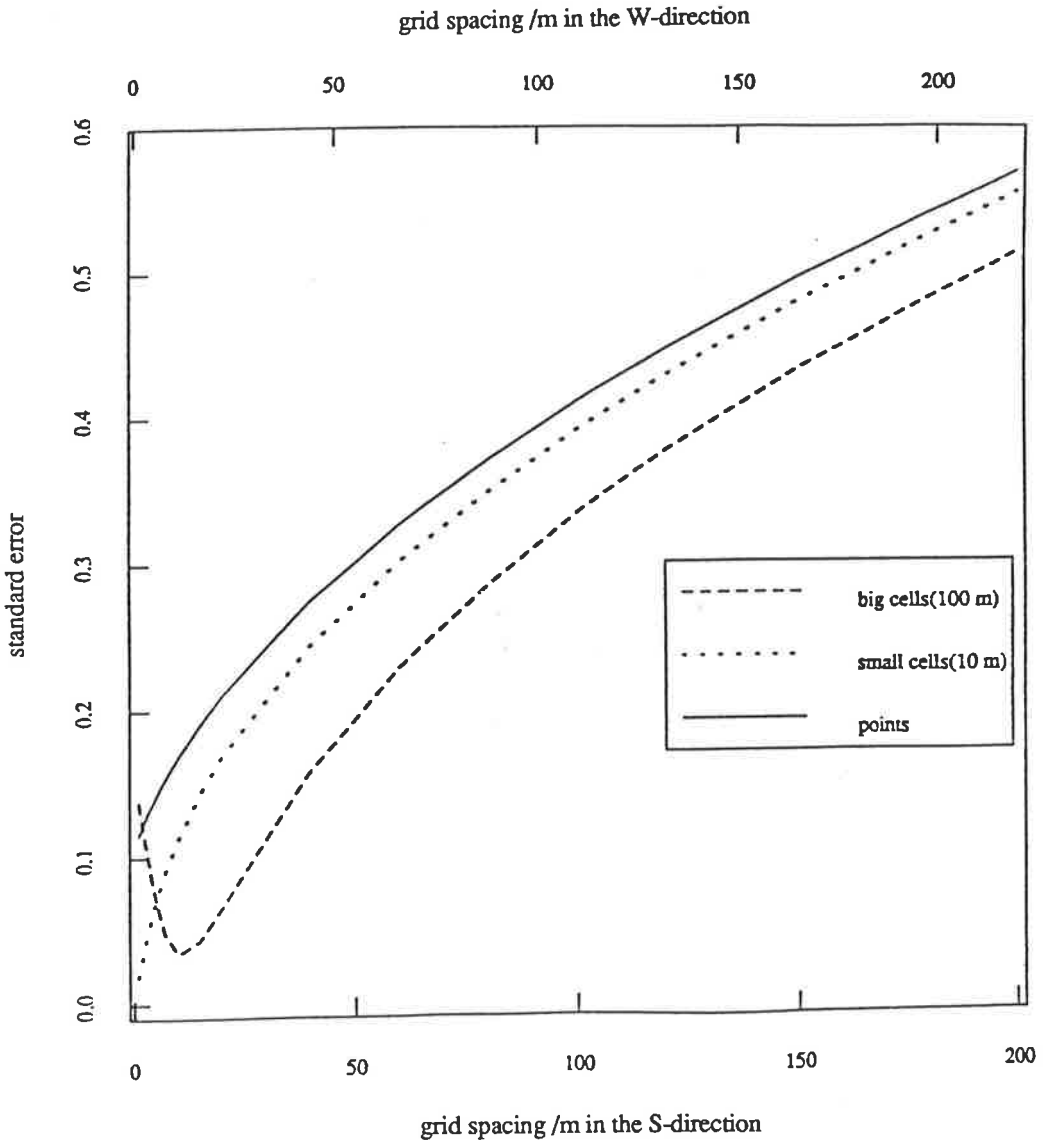

Fig. 4.5 Kriging error for punctual and block kriging of fuzzy class membership coefficients for soil class G as a function of grid spacings in transect-W and transect-S directions.

Table 4.1 The main features of the centroids for seven classes derive by J_G (ϕ=1.15) on the whole soil data.

Soil class	Main features of centroid
A	shallow (19 cm) topsoil of brown, slightly gravelly (15%) loam, moderately weak pedality (2.5) of granular structure, pH=7.0, overlying reddish brown heavy clay with common (15%) light olive brown mottles, moderate pedality (4) of angular blocky structure, pH=6.3; depth of solum=60 cm.
B	shallow (17 cm) topsoil of dark reddish brown, very gravelly (24%) loam, moderate pedality (3.5) of granular structure, pH=7.1, overlying yellowish red heavy clay with few (10%) reddish brown mottles, strong pedality (4) of angular blocky structure, pH=6.5; depth of solum=65 cm.
C	moderately deep (25 cm) topsoil of dark brown, slightly gravelly (15%) loam, moderate pedality (3.4) of granular structure, pH=6.9, overlying brown light medium clay with common (17%) dark reddish brown mottles, moderate pedality (3.1) of subangular blocky structure, pH=6.2; depth of solum=58 cm.
D	moderately deep (24 cm) topsoil of dark brown, slightly gravelly (17%) loam of moderate pedality (3.2) of subangular blocky structure, pH=7.1, overlying brown medium clay with few (5%) faint mottles, very weak pedality and massive , pH=6.2; depth of solum=57 cm.
E	shallow (18 cm) topsoil of dark reddish brown, very gravelly (30%) loamy sand , very weak pedality, loose and single-grained, pH=6.8, overlying reddish brown light medium clay with few (7%) yellowish brown mottles, moderately weak pedality (2) of subangular blocky structure, pH=6.1; depth of solum=48 cm.
F	shallow (19 cm) topsoil of dark brown, very slightly gravelly (9%) sandy loam, moderate pedality (2.7) of subangular blocky structure, pH=6.5, overlying yellowish brown heavy clay with common (16%) light olive brown mottles, moderate pedality (3.1) of subangular blocky structure, pH=6.2; depth of solum=58 cm.
G	very deep (35 cm) topsoil of very dark brown, very slightly gravelly (8%) loam, moderate pedality (3.2) of granular structure, pH=7.0, overlying dark brown loam with few (6%) yellowish brown mottles, moderate pedality (2.1) of subangular blocky structure, pH=6.5; depth of solum=86 cm.

Table 4.2 Parameter values of isotropic and anisotropic semivariograms for the soil classes (N denotes pure nugget variation and a is in m, the semivariances of soil classes are in membership coefficient squared).

Soil class	$\gamma_w(h)$	$\gamma_s(h)$	C_{0w}	C_{0s}	$\hat{C}_0$	C'_w	C'_s	a_w	a_s	R in W : S
A	0.0350	0.0575	0.0215	0.0335	0.0275	0.0075	0.0300	30	35	1 : 3.4
B	0.1314	0.0354	0.0083	0.0126	0.0105	0.1209	0.0249	309	45	1 : 1.4
C	0.0496	0.0353	0.0242	0.0228	0.0235	0.0236	0.0120	40	48	2.4 : 1
D	N	0.1154	0.0417	0.0573	0.0495	N	0.0659	-	30	-
E	N	N	0.0609	0.0286	0.0443	N	N	-	-	-
F	0.0686	N	0.0148	0.0101	0.0124	0.0562	N	50	-	-
G	0.0563	0.0463	0.0127	0.0090	0.0109	0.0454	0.0354	67	57	1.1 : 1

chosen for further analysis. The seven soil classes are arbitrarily labelled as class A, B, ..., G respectively. Table 4.1 gives a brief description of some soil class centroids.

4.3.2 Soil class membership semivariograms and optimal sampling strategy

The results of fuzzy-c-means classification as described above were in the form of a n x c class membership coefficients matrix $\boldsymbol{M}$, n being the total number of soil individuals (in this case pedons). There are 247 pedons sampled in this study with 100 on transect-S and 147 on transect-W. Taking a vector of membership coefficients of each fuzzy class, c_j, semivariances were estimated for each of the transect directions as described for the continuously variable soil attributes (see equation 3.1 in chapter 3, subsection 3.3.1). The sample semivariograms for some of the class membership coefficients were also fitted with the spherical model as per equation (3.2) in chapter 3. Some are illustrated in Figs. 4.2 and 4.3.

The class membership semivariograms of some classes show the same anisotopic features as for some of the soil variables described in chapter 3. Using the same reasoning and calculations contained in chapter 3, subsection 3.3.4 (equations 3.3-3.7), the semivariogram parameter values as presented in Table 4.2 were obtained. Like some of the particle-size variables, membership of a number of soil classes (classes A, B, and D) exhibit anisotropic variation with the maximum occurring instead in the S-direction. Variation of membership of class E is pure nugget in both directions indicating erratic occurrence across the landscape. This class is the shallow (solum depth is about 50 cm) variety described in Table 4.1. It occurs mainly on relatively steep slopes and slope breaks. Soil classes D and F appear to complement each other with the former predominantly occurring on transect-S and the latter on transect-W.

Using the form of model as contained in chapter 3 subsection 3.2.5- equation (3.12), the kriging variances and errors were also determined (with the OSSFIM program) for estimates on points and over blocks of 10 x 10 m and 100 x 100 m, with the corresponding grid spacings for all but soil class E. Some of the results are illustrated in Figs. 4.4 and

4.5. A kriging error of 0.1 of class membership was considered as a reasonable maximum for estimates over 1 *ha* (100 x 100 m block) and grid spacings for mapping the soil classes were obtained. The results are presented in Table 4.3.

Table 4.3 Grid spacings in transect-W and transect-S directions obtained for some soil classes at an estimation error of 0.1 of membership coefficient for 100 x 100 m block.

Soil class	Grid spacing (m)	
	transect-W	transect-S
A	47	23
B	42	29
C	27	66
D	*N*	21
F	23	*N*
G	31	33
Mean	34	34

As Table 4.3 shows, there are now six possible ways of optimally mapping the resulting soil classes in the study area. For example, if sampling was done at the interval of 23 m along transect-W and 21 m along transect -S as obtained for soil classes D and F respectively, it would suffice to block "krige" over 1 *ha* with an error margin of ≤ 0.1 of membership of all the classes listed in Table 4.3. There was room for modification, however. The sampling density can be optimized by relating soil occurrences to geologic and landform features as is done in the traditional survey method. This required some form of segmentation along the transects to elucidate boundary locations and spacings. This can be performed easily using the matrix of class membership coefficients and the method is described in the next section.

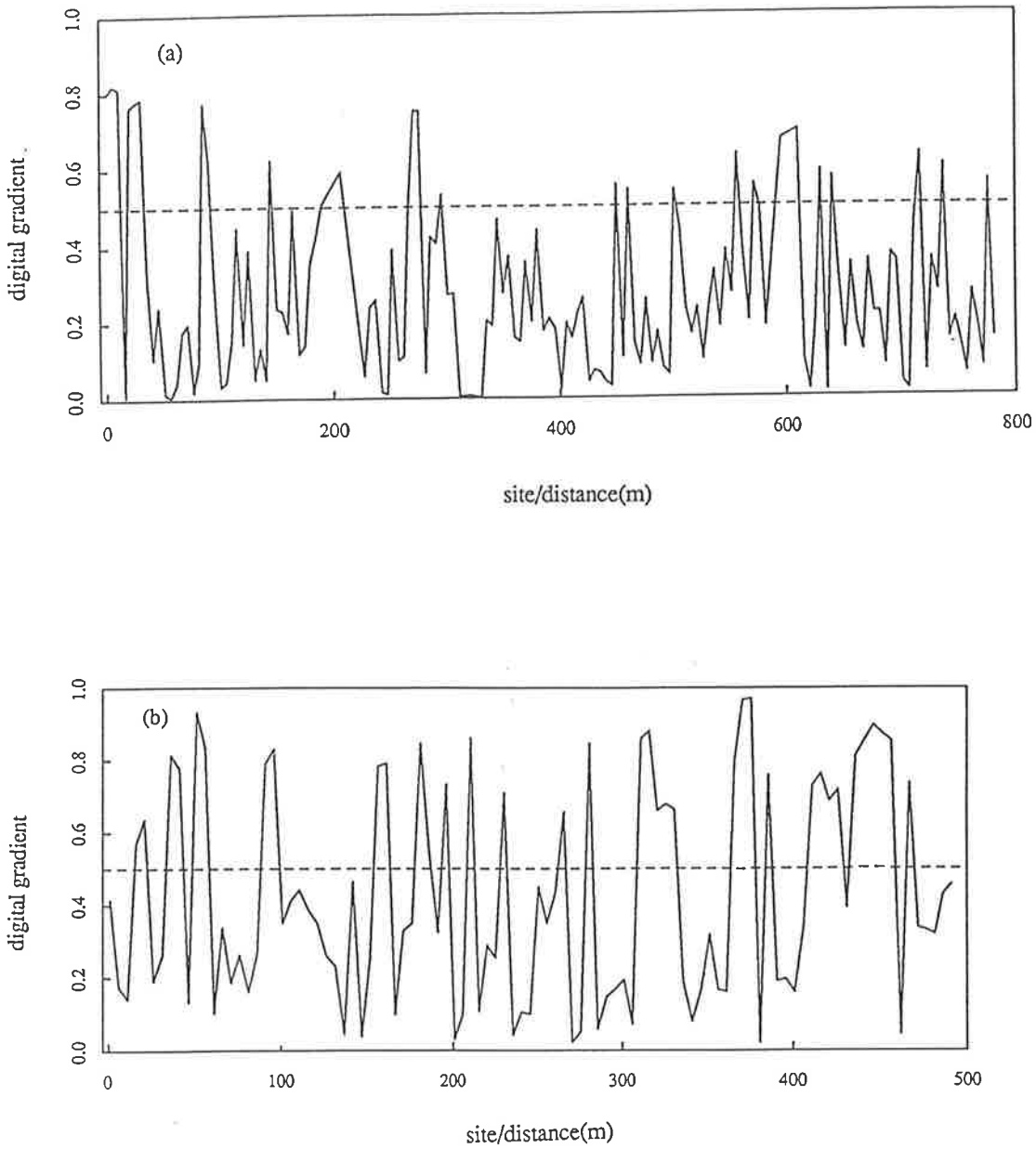

Fig 4.6 Digital gradient, g of soil classes along (a) transect-W and (b) transect-S as an indicator of segment boundaries.

4.3.3 Segmentation along transects

The sample semivariogram of membership of a given class merely indicates the spatial dependence and the range of variation along the transect. It does not indicate the physical locations of soil class boundaries and where each class predominates. Similarly, the sampling scheme obtained using the sample semivariogram only suggests optimal intensity of sampling and does not give information pertaining to boundary locations at this stage of survey. One approach is to proceed anyway and sample at the intervals suggested by the optimal sampling design using the sample semivariograms, and interpolate to produce isarithmic maps of soil class memberships. Boundaries can then be sought by overlaying of various isarithmic maps of membership of soil classes with boundary locations at certain cross-over values of membership coefficients (e.g. > 0.5 difference) between two points or areas. An alternative is further optimization of sampling density at the initial stage of survey. This can be achieved by some form of segmentation along transects and relating segment boundaries to some physical features that are predominant in the survey area. The latter option was preferred as this would further enhance sparser sampling intensity for the same level of precision.

With this in mind, the digital gradient segmentation procedure, an extension of the method described by Rosenfeld and Kak (1982) which has been used for soil study by Powell *et al.* (1991), was applied. The digital gradient is a measure of rate of change of membership between two sites on the transect. It is defined as

$$g_{x+0.5} = \left[\frac{\sum_{j=1}^{c} (m_{j,x} - m_{j,x+h})^2}{2} \right]^{0.5}$$

where m_j,x and $m_{j,x+1}$ are the memberships of class j at sites x and $x+h$ respectively, on the transect. Large values of g suggest points of sharp change and hence the soil (segment) boundaries and small values indicate points of stasis. Fig. 4.6 illustrates the digital gradient along the two transects. There are 15 and 17 prominent peaks above a value of $g = 0.5$ for

transect-W and transect-S respectively. The inter-peak distances were determined as an indication of segment lengths on each transect. Transect–W showed segment length in the range of 10 - 154 m with a mean of 44 m; while transect-S had a range of 10 - 65 m and a mean of 28 m. This was in agreement with the findings of the spatial analysis (see Table 4.3) which showed the spatial range varying from 30 to 309 m for transect-W and 30 to 57 m for transect-S.

To be useful for further optimization of the sampling strategy, the coincidence or otherwise of segment boundaries along the two transects with any conspicuous landform and geologic features in the field was sought. Up to 65% of the segment boundaries coincided with either slope breaks, ridge or spur crests, colluvio-alluvial contacts and some minor formation of quartz enrichment or quartzite within the main geologic formation of fine-grained phyllites and siltstones. Guided by these geomorphological and geologic features, it was envisaged that sampling would have to be at the intervals of 10 m, where these features are prominent, and 50 m where these features are virtually absent. These spacings are within the range of grid intervals given in Table 4.3 and have been adopted in the detailed sampling for interpolation of membership coefficients of the soil classes (Chapter 6).

4.4 A Generalized FCM: the Problem of Extragrade Members

Equation (4.3) literally solves the problem of intragrades, which represent the points and bridges between two classes, by giving intermediate memberships to these points. However, data points that are outliers, i.e. outside the classes and not in-between, are inadequately represented. This prompted Ohashi (1984) to propose a more robust version of FCM objective functional in which equation (4.3) is modified as

$$J_I(M,c) = \alpha \sum_{i=1}^{n} \sum_{j=1}^{c} m_{ij}^{\phi} d_{ij}^{2} + (1+\alpha) \sum_{j=1}^{c} m_{i*}, \qquad (4.18)$$

where m_{i*} denotes the membership to a fuzzy outlier class; α is a parameter that determines the mean value of m_{i*}. Ohashi's modification is aimed at accommodating the atypical entia in a special class. However, this does not solve the problem wholly because the memberships to this special class are spread across and over the taxonomic space and not as a hypersphere around the regular classes. This means that the method does not yield a good separation of the intragrade members from the extragrade members. It was not designed to do so. Intragrade memberships are supposed to be shared among the regular classes depending on the multivariate distances of the intragrades to the centroids of these classes.

The inadequacy of equation (4.18) to distinguish between intragrades and the extragrades provoked DeGruijter and McBratney (1988) to further modify Ohashi's (1984) objective functional. Their modification involves making the memberships to extragrade class to be inversely related to the distance to the class centroid such that

$$J_E(M,c) = \alpha \sum_{i=1}^{n} \sum_{j=1}^{c} m_{ij}^{\phi} d_{ij}^2 + (1+\alpha) \sum_{j=1}^{c} m_{i*} \sum_{j=1}^{c} d_{ij}^{-2}. \tag{4.19}$$

Thus if both m_{i*} and d_{ij}^2 are zero, then the contribution to the second term in equation (4.19) will also be zero. Minimization of $J_E(M,c)$ is achieved by heuristic Picard iteration of the following equations:

$$m_{ij} = \frac{d_{ij}^{-2/(\phi-1)}}{\sum_{k=1}^{c} d_{ik}^{-2/(\phi-1)} + \left\{ \frac{1-\alpha}{\alpha} \sum_{k=1}^{c} d_{ik}^{-2} \right\}^{-1/(\phi-1)}} \quad 1 \le i \le n;\ 1 \le j \le c, \tag{4.20}$$

$$m_{i*} = \frac{\left\{ \frac{1-\alpha}{\alpha} \sum_{k=1}^{c} d_{ik}^{2} \right\}^{-1/(\phi-1)}}{\sum_{k=1}^{c} d_{ik}^{-2/(\phi-1)} + \left\{ \frac{1-\alpha}{\alpha} \sum_{k=1}^{c} d_{ik}^{2} \right\}^{-1/(\phi-1)}} \quad 1 \le i \le n \tag{4.21}$$

and
$$c_j = \frac{\sum_{i=1}^{n} \{ m_{ij}^{\phi} - (1-\alpha)\alpha^{-1} d_{ij}^{-4} m_{i*}^{\phi} \} x_i}{\sum_{i=1}^{n} \{ m_{ij}^{\phi} - (1-\alpha)\alpha^{-1} d_{ij}^{-4} m_{i*}^{\phi} \}} \quad 1 \leq 1 \leq j. \tag{4.22}$$

The solutions to these equations are obtained through the iterative procedure of the FCM algorithm described in subsection (4.2.1) and which was accordingly modified.

The functional, $J_E(M,c)$ requires that the parameter α be chosen in order to determine the mean value of outlier memberships defined as

$$\bar{m}_{i*} = \frac{1}{n} \sum_{j=1}^{c} m_{i*}. \tag{4.23}$$

Since the $\bar{m}_{i*}$ is a function of α, *i.e.* $f(\alpha)$, the latter would have been estimated if $\bar{m}_{i*}$ is known but such information is not readily available. An alternative approach is to assign the mean number of classes as for the regular classes such that

$$\bar{m}_{i*} = 1/c+1. \tag{4.24}$$

This approach is the preferred starting point. However, as $\bar{m}_{i*}$ is not known *a priori*, it is quite appropriate to first find the root of $f(\alpha)$:

$$f(\alpha) = \frac{(\bar{m}_{i*}(\alpha)-1)}{(c+1)}. \tag{4.25}$$

To obtain the solution to equation (4.25), DeGruijter and McBratney (1988) suggested the use of Regula Falsi procedure involving repeated inverse linear interpolation between a negative and a positive value of $f(\alpha)$, and with Steffensen's convergence acceleration (Stoer and Bulirsch, 1980). This procedure is adopted here. A given iteration φ, thus contains two

Regular Falsi steps that yield two values as α' and α' respectively. The next accelerated step will, therefore, yield a value calculated as

$$\alpha^{(\varphi)} = \frac{\alpha'\alpha^{(\varphi-1)} - \alpha'^{2}}{\alpha' + \alpha^{(\varphi-1)} - 2\alpha'}. \tag{4.26}$$

A modified Picard iteration, nested within the main iteration of FCM algorithm, is used to solve equation (4.26) starting with $f(0) = {}^{-1}/(c+1)$ and $f(1) = {}^{c}/(c+1)$. The accelerated Regula Falsi iteration is continued until convergence is reached, i.e. when the root is determined to within 1% tolerance. The modified FCM algorithm is termed "fuzzy-c-means with extragrades (FCME) algorithm".

4.4.1 Application to the soil data

A FORTRAN program, FCME (or FKME), written by De Gruijter and McBratney (1988) and improved upon by Ward *et al.* (1990), was used for fuzzy classification of the soil data, and this time, using various combinations of soil variables. As required by FCME algorithm, certain parameters which include the distance measure (or metric), the range of classes to be generated, the fuzziness exponent (ϕ) and the stopping criterion (ε), need to be chosen. In the analyses the range of number of working classes was initially set as c = [2, 10], and the stopping criteria, ε, was assigned the value 0.001. The choice of the range of c was based on initial expectations, i.e. an approximate maximum number of structurally plausible classes were gauged from the data and from the results of application of the FCM algorithm to the data in subsection 4.3.1. Also the problems of "cluster validity" and the degree of fuzziness had to be solved. These problems were treated in a rather more subjective manner in subsection 4.3.1 but are treated here in more detail.

4.4.2 The degree of fuzziness

The degree of fuzziness is somewhat related to substructures within X and hence the optimal number of classes. In fact, fuzziness defines the extent to which the groups are compact and separated. Thus the validity functionals are in some degree a measure of fuzziness. However, with generalization of fuzzy objective functionals (Bezdek, 1974; Dunn, 1974), an appropriate value of ϕ, the fuzziness exponent, should be chosen to reflect the degree of fuzziness defined by substructures within X. This means that for a given value of ϕ, the validity functionals could be used as indicators of substructures in X. The question then is: which value of ϕ, for which the optimal number of classes in X has been determined by F' and H', is acceptable? An answer to this question entails some subjective element in the final judgements which nevertheless must be founded on a thorough expert knowledge of the data. The final judgements should be based on maintaining the balance between substructures and continuousness (McBratney and Moore, 1985).

In choosing ϕ, many workers have used the value of 2 (Bezdek, 1981; DeGruijter and McBratney, 1988). However, experience so far from the preliminary trials with the soil data and the reported work of Powell *et al.* (1989) suggests ϕ values ranging from 1.12 to 1.50. Based on this fact and setting c = [2, 10], three values of ϕ (i. e., 1.12, 1.30 and 1.50), were each tried on various combinations of soil variables viz: whole soil profile data including some morphological, physical and chemical variables; morphological data; textural variables constituted by particle-size fractions. The norms used were the Diagonal norm and Mahalanobis' norm, each of which were tried separately. The results and subsequent analysis arc discussed.

4.4.3 Optimal Combination of ϕ and c

At ϕ=1.12 , the FCME program "crashed" (indicated by program error) in the case of whole soil variables and morphological variables when both the diagonal and Mahalonobis' norms were tried. This was not the case with the particle-size data as will be discussed later. However, the probable reason for the program error was that the program attempted divisions by zero as $\phi \approx 1$ (see equations 4.20 and 4.21). Also at ϕ = 1.30 and 1.50, the membership values were even (i.e., $M = {}^{1}/_{c}$), and therefore are extremely fuzzy except for the extragrade classes. An attempt was made to rectify the situation by reducing the extragrade dependent exponent in equations (4.19) and (4.21) from 2.00 to 0.50, so that data points at some distance from a centroid of a given class would be given higher membership scores for that class than for the extragrade class. The results were not better than the previous ones. One reason for this stalemate is that some of the variables in the two data sets which have low variance caused the algorithm to minimize the distance dependent measure, d_{ij}, in equations (4.19-4.22). The use of the diagonal and Mahalonobis' norms should have rectified the deadlock because they transformed the data such that all the variables would have identical variance, although the consequence of this is an undue influence on the solutions by the low-variance properties. The suspicion was that the problem had more to do with choosing the right ϕ than any other reason. In chosing ϕ values of 1.13, 1.14, 1.15 and 1.20, the FCME algorithm was once again tried on the two data sets using c = [2, 10] for the whole soil data and c = [2, 8] for the morphological data, and only the diagonal norm. The diagonal norm was used because preliminary analysis suggested low correlations among most of the variables, although correlations were considerably high among textural variables. The extragrade dependent exponent was also reduced to 0.5.

Once again the FCME program "crashed" for the whole soil data at ϕ = 1.13 and 1.14 respectively. However, the structurally plausible fuzzy classes were identified at ϕ = 1.15 for the whole soil data and at ϕ = 1.13 for the morphological data. At higher value(s) of ϕ ,

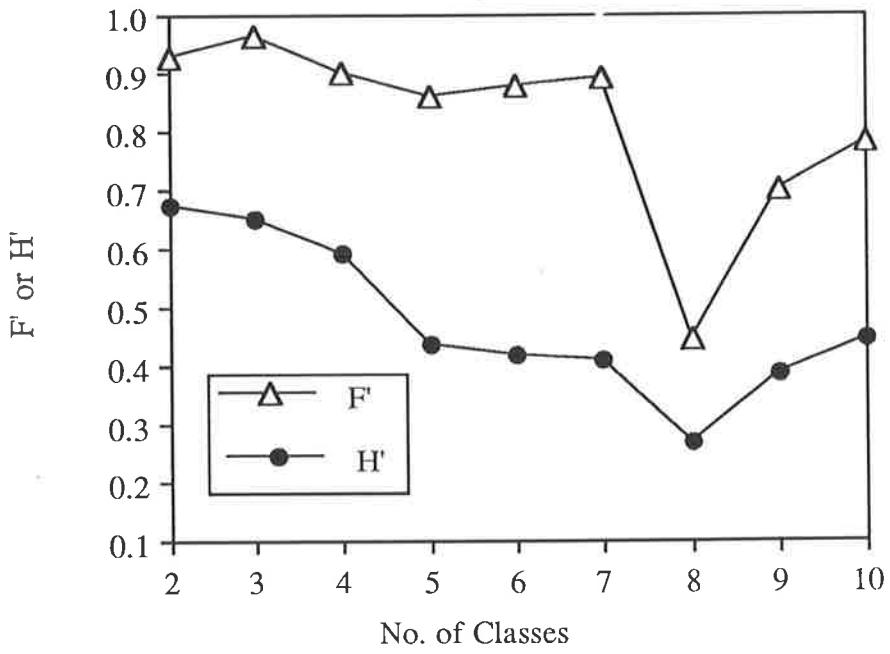

Fig 4.7 Fuzziness performance index (*F'*) and normalized classification entropy (*H'*) against number of classes for whole soil data (ϕ=*1.15*).

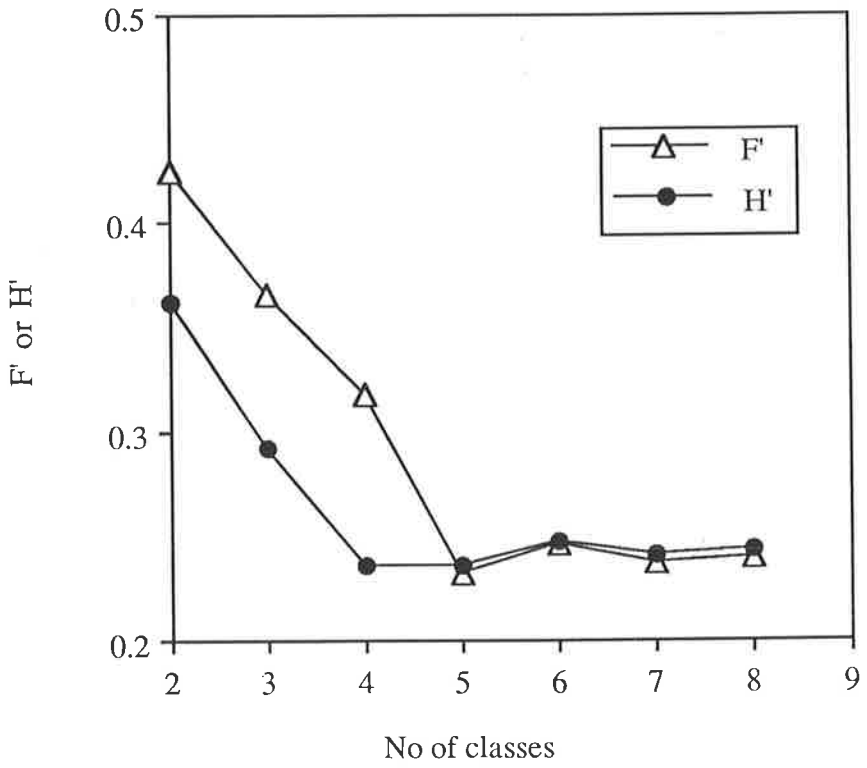

Fig 4.8 Fuzziness performance index (*F'*) and normalized classification entropy (*H'*) against number of classes for morphological data (ϕ=*1.13*).

class memberships obtained from either of the data sets were even (i.e., the memberships were extremely fuzzy with no identifiable substructures).

With the workable fuzziness exponents obtained for the two data sets, it now remained to determine the optimal number of classes that best reflected the natural substructures in each data set. This required the use of F' and H' criteria as described in subsection 4.2.3. Both F' and H' were obtained and plotted against the number of classes in Fig. 4.7 for whole soil data and Fig. 4.8 for the morphological data. Whereas in Fig. 4.7, both F' and H' are minimal at $c = 8$, in Fig. 4.8, F' and H' are minimal at $c = 6$. This means that the optimal combinations of ϕ and c are respectively 1.15 and 8 for the whole soil data, and 1.13 and 6 for the morphological data.

The results of fuzzy analysis on the textural data were different from those obtained for the whole soil and morphological data. All of the fuzziness exponents (i.e., $\phi = 1.12$, 1.30 and 1.50) which were initially tried on the textural data gave reasonable results from which the optimal number of classes could be obtained. This is because the particle-size variables are purely numeric with comparatively high variance and therefore did not pose minimization problems: nor did division by numerals close to zero (i.e, when $\phi \approx 1$) cause a problem. The only subsequent problem was how to determine the optimal combination of ϕ and c from several options of ϕ . This required the use of some form of quasi-mathematical procedure in combination with the criteria of F' and H', which is now described.

Bezdek (1981 pp 72-73) proved that the objective function value J_E, approaches zero as the ϕ value increases towards infinity. This means that J_E decreases monotonically with ϕ value on optimal pairs. Some authors (Bezdek, 1981) have assumed that the most valid number of classes in X is associated with an extremum of J_E or its derivative, such as a large change in slope or a large jump at (supposedly) optimal c. Differentiation of J_E with respect to ϕ, therefore, will yield

$$\frac{dJ_E}{d\phi} = \sum_{i=1}^{n} \sum_{j=1}^{c} m_{ij}^{\phi} \log(m_{ij}) d_{ij}^2$$

$$= \sum_{i=1}^{n} \sum_{j=1}^{c} [m_{ij} log(m_{ij})][m_{ij}^{(\phi-1)} d_{ij}^{2}]. \quad (4.27)$$

By obtaining $-\frac{dJ_E}{d\phi} c^{0.5}$, McBratney and Moore (1985) devised a measure of fuzziness in their analysis of two sets of climatic data. Their method involved the determination of J_E values for a series of ϕ and a range of c and then plotting curves of the derivative, $-\frac{dJ_E}{d\phi} c^{0.5}$ of optimal pairs against ϕ for each c. The best value of ϕ for a given c is at the maximum of the curve. The criterion used for choosing the optimal combination of c and ϕ is that the curve with the least maximum of $-\frac{dJ_E}{d\phi} c^{0.5}$ best indicates the natural groupings in the data set. This was also combined with the criteria of F' and H' as described previously. The limitation of this approach is the high computational effort and time required especially for a complex system such as soil. It is even more tedious when there are many soil variables involved in the analysis. To arrive at a reasonable optimal combination requires the derivation of the $-\frac{dJ_E}{d\phi} c^{0.5}$ curve for each of a number of c and a range of ϕ. An approach that minimized computation for fuzzy classification of particle-size data is described.

Using the criteria of F' and H', the optimal c was obtained for the lowest ϕ (1.12) and for the highest ϕ (1.50) that were initially tried on X (the particles-size data) based on Mahalonobis' entries. Note that Mahalonobis' norm was considered most suitable because of high correlations among soil particle-size fractions. The optimal c was found to be 5 for ϕ = 1.12 (Fig. 4.9) and 6 for ϕ = 1.50 (Fig. 4.10). Assuming that optimal c for ϕ values between 1.12 and 1.50 would not deviate much from 5 or 6 (using the criteria of F' and H', it was confirmed that optimal c = 6 for ϕ = 1.30 and the next best is c =5), there were now fewer options of optimal c (i.e., 5 or 6) from which optimal combination of c and ϕ could be validated. Which of these optimal c (5 or 6) is more amenable to the structure of the data and at what value of ϕ? This is where the derivative $-\frac{dJ_E}{d\phi} c^{0.5}$, as used by

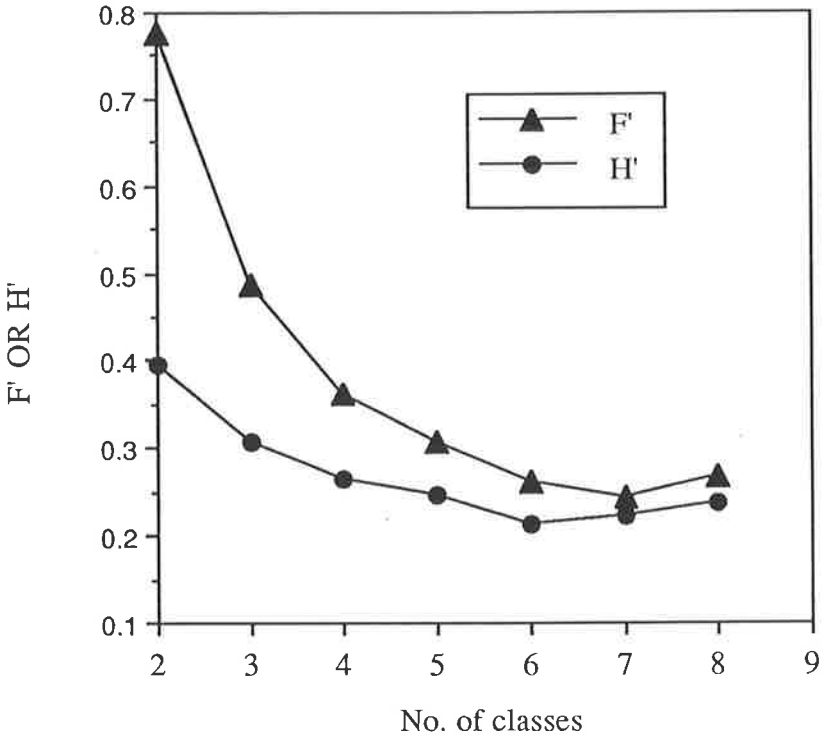

Fig 4.9 Fuzziness performance index (*F'*) and normalized classification entropy (*H'*) against number of classes for particle-size data (ϕ=*1.12*).

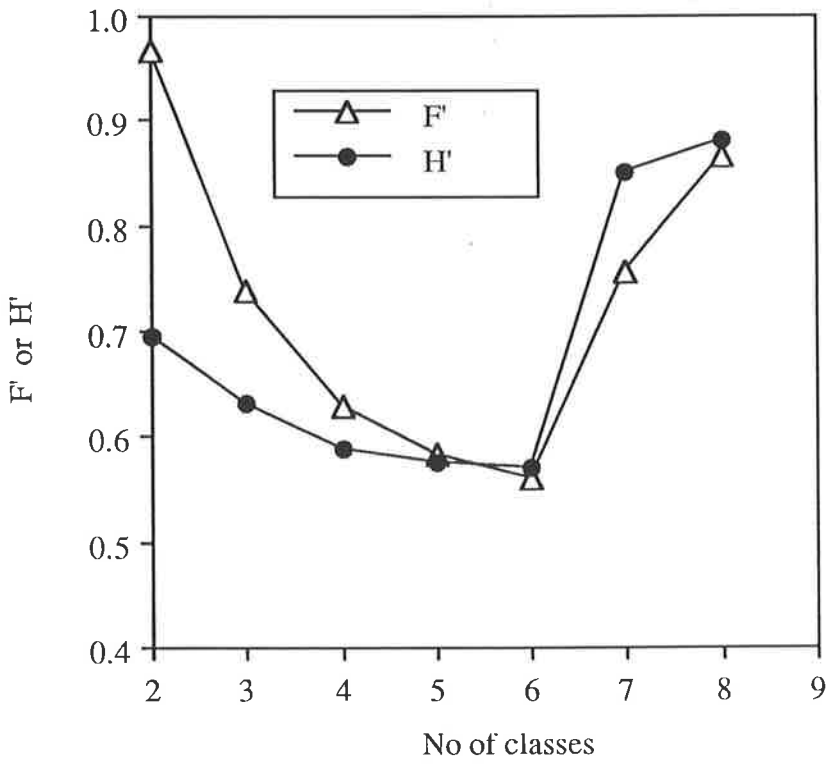

Fig 4.10 Fuzziness performance index (*F'*) and normalized classification entropy (*H'*) against number of classes for particle-size data (ϕ=*1.50*).

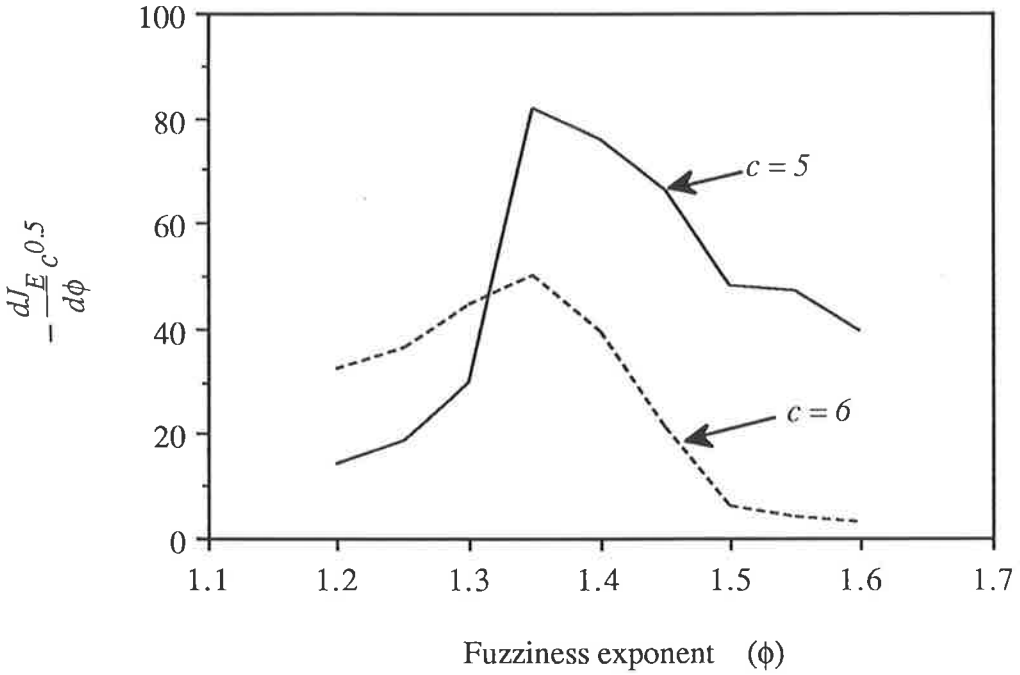

Fig. 4.11 Plot of $-\frac{dJ_E}{d\phi}c^{0.5}$ versus ϕ for five and six classes resulting from fuzzy classification of particle-size data

McBratney and Moore (1985), becomes useful. The optimized J_E values were computed for the fixed c =5 and c = 6 using a series of ϕ =[1.20, 1.60] at an increment of 0.05. The derivative $-\frac{dJ_E}{d\phi}c^{0.5}$, was obtained for each of the optimal c (5 or 6) and plotted against ϕ as illustrated graphically in Fig. 4.11. Evidently, the lowest maximum of the two $-\frac{dJ_E}{d\phi}c^{0.5}$ curves occurs at the curve of c = 6 and ϕ = 1.35. Thus 6 and 1.35 are the best optimal combination of c and ϕ which is suggestive of structure in the textural data. The F' and H' criteria as illustrated in Fig. 4.12 further confirm this.

4.4.4 The fuzzy soil classes

Having determined the optimal combination of ϕ and c for the various sets of soil variables, it was now relevant to examine the grouping resulting from the fuzzy processes. The fuzzy classification of a given data set, $\boldsymbol{X}$, would produce a $n \times c$ matrix, $\boldsymbol{M}$, of class

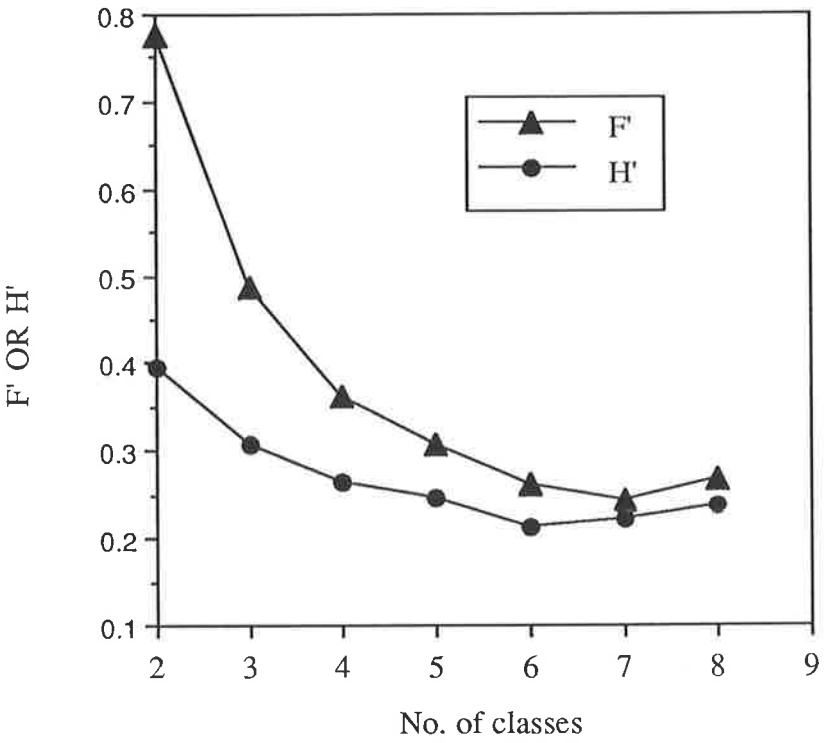

Fig 4.12 Fuzziness performance index (*F'*) and normalized classification entropy (*H'*) against number of classes for particle-size data (ϕ=*1.35*).

membership values, and a $c \times p$ matrix, $\boldsymbol{C}$, of class centroids. While the matrix, $\boldsymbol{M}$, is significant in terms of the degree of belongingness to all of the fuzzy classes, $\boldsymbol{C}$ gives the class means relative to which the membership values are weighted. The class centroids of a given fuzzy class are typical of that class. The individual membership value is, therefore, equivalent to the so called internal "purity" of a soil class defined by the degree to which a pedon sampled at random within a mapping unit matches the description of that soil class.

The extragrade class

The functional, J_E, was designed to cater for atypical pedons that do not belong to any (or have low memberships) of the usual classes optimally generated by FCME algorithm. The atypical pedons could be considered as part of the "impurity" that is interspersed within

Table 4.4 The main features of the centroids for eight classes derived by J_E ($\phi = 1.15$) on whole soil data (italicised clauses describe the relative landscape location and the parent material, if transported)

Class	Main features of centroid
Aw	moderately deep (20 cm) topsoil of dark brown, slightly gravelly (19 %) sandy loam, moderately pedality (3.2) of granular structure, pH = 7 .1; overlying reddish brown medium clay with common (14 %) yellowish brown mottles, moderately weak pedality (1) almost massive, pH = 6.3; depth of solum = 48 cm; *developed on colluvial material on slope breaks near creeks, slopes = 5-10 %.*
Bw	moderately deep (22 cm) topsoil of dark reddish brown, slightly gravelly (14%) loam, moderate pedality (3.4) of subangular blocky structure, pH = 7.1, overlying reddish brown clay loam with common (22 %) yellowish brown mottles, strong pedality (4) of angular blocky structure, pH = 6.5; depth of solum = 54 cm; *similar to Aw though contains less subsoil clay, also found on micro- (open) depressions on sideslopes, slopes = 1-10 %.*
Cw	shallow (18 cm) topsoil of yellowish brown, gravelly (17 %) loam, moderate pedality (3.2) of granular structure, pH = 6.9, overlying yellowish red heavy clay with common (13 %) reddish brown mottles, strong pedality (3.8) of angular blocky structure, pH = 6.4; depth of solum = 60 cm; *occurs on fairly steep slopes ≈ 15 %, and predominantly on the S-transect.*
Dw	shallow (16 cm) topsoil of dark brown, very gravelly (30 %) sandy loam, moderate pedality (3.4) of subangular blocky structure, pH = 7.2; overlying yellowish red heavy clay with few (8 %) faint mottles, strong pedality (4) of angular blocky structure, pH = 6.7; depth of solum = 59 cm; *occurs on spurs and crests and adjacent slopes (1-13 %).*
Ew	moderately deep (20 cm) topsoil of dark brown, very slightly gravelly (7 %) loam, moderately weak pedality (2.5) of subangular blocky structure, pH = 6.3; overlying brown heavy clay with common (17%) dark reddish brown mottles, moderate pedality (3) of subangular blocky structure, pH = 5.91; depth of solum = 78 cm; *occasional deep soils on sideslopes (5-15 %).*
Fw	very deep (32 cm) topsoil of very dark brown, very slightly gravelly (7 %) sandy loam, moderate pedality (2.7) of granular structure, pH = 7.2; overlying dark brown loam with few (7 %) yellowish brown mottles, moderate pedality (3.0) of subangular blocky structure, pH = 6.4; depth of solum = 87 cm; *imperfectly drained soils on the fringes of creeks- developed on alluvial material mixed with moderate amount of colluvium, slopes ≈ 1 %.*

Table 4.4 (continued)

Soil class	Main features of centroid
Gw	shallow (17 cm) topsoil of very dark reddish brown, slightly gravelly (16 %) loam, moderate pedality (3.3) of subangular blocky structure, pH = 7.1; overlying reddish brown heavy clay with common (14 %) yellowish brown mottles, moderate pedality (3.5) of angular blocky structure, pH = 7.1; depth of solum = 52 cm; *occurs side by side with and similar to Cw, though shallower and has more subsoil clay, slopes ≈ 15 %.*
Hw	moderately deep (24 cm) topsoil of dark brown, slightly gravelly (12 %)sandy loam, moderate pedality (3.5) of granular structure, pH = 6.8; overlying brown light medium clay with common (17%) dark reddish brown mottles, moderate pedality (3.4) of subangular blocky structure, pH = 6.8; depth of solum = 58 cm; *not common but occurs on crests, mainly on W-transect, slopes = 1-5 %.*

the map unit delineations, and therefore may complement the internal "purity" of mapping units referred to above.

By examining closely the original data and comparing the features values for pedons in the extragrade class (i.e. pedons with $m_{i*} > 0.5$) and their centroid values for the typical classes, it was established that the extragade pedons have extreme values for one or more of the measured features. For example, the pedons in the extragrade class resulting from fuzzy classification of the particle-size variables have either very low or very high values of one or more of the variables. The importance of the assignment into extragrade class (and indeed into typical classes) depends on whether the differences in the definitive features call for different management. It, however, shows the effectiveness of FCME algorithm in assigning pedons into plausible classes and differentiating the atypical pedons.

The class centroids

The descriptions of the main features of the class centroids resulting from fuzzy classification of the whole soil data are given in Table 4.4 and the class centroids for the

Table 4.5 Centroids of six fuzzy classes derived by J_E ($\phi = 1.35$) on particle-size fractions (italicised clauses describe the relative landscape location)

Class	Topsoil (%)				Subsoil (%)			Remark
	sand	silt	clay	gravel	sand	silt	clay	
At	43.29	26.77	29.94	13.05	22.11	15.59	62.31	slightly gravelly sandy clay loam over clay *-mainly on crests and near slope breaks, slopes = 5-10 %*
Bt	46.07	43.43	10.50	12.37	20.26	21.18	58.60	-slightly gravelly loam over clay *-on gentle slopes (1-5 %) at colluvio-alluvial junctions*
Ct	50.20	35.89	13.91	7.43	34.61	32.32	33.08	-loam over clay loam *-most texturally uniform, on gentle slopes adjacent to creeks*
Dt	53.20	35.36	11.44	30.70	32.52	19.09	48.27	-very gravelly sandy loam over clay loam *-coarse-textured, on steep slopes (> 15 %)*
Et	53.66	34.89	11.45	9.91	45.07	18.93	36.05	-sandy loam over sandy clay loam *-in association with C, also on sideslope micro- (open) depressions*
Ft	63.13	23.27	13.60	20.60	20.76	15.71	63.54	-moderately gravelly sandy loam over clay *-in association with A but coarser, predominantly on W-transect*

particle-size variables are shown in Table 4.5. In order to validate the membership values, the measured features of some pedons, x_i, with relatively high and low membership values, m_{ij}, in a class j, were compared with the centroids of the class. Table 4.6 shows the comparison for some particle-size variables of selected pedons. While the class centroids for a number of classes are not much different from corresponding values measured for pedons with high memberships in these classes, pedons with low memberships have feature values that are markedly different from the corresponding centroids. This confirms the cluster validity measures adopted.

Also in Table 4.5, the textural categories of the class centroids (Soil Survey Staff, 1975) indicates high efficiency in fuzzy partitioning of the particle-size data into meaningful groupings in the existing soil classification systems. Whereas some centroids values of some textural variables are not much different between some fuzzy classes, their allocation into different groups is justified by the differences in the centroid values of some other variables. This is consistent with the observations of Hole and Campbell (1985 p 104) that

Table 4.6 Comparison of centroids for some particle-size variables and their values for selected pedons with high and low memberships of a given class

Pedon No.	Class and membership	Particle-size variable, *F*	Pedon value of *F* (%)	Class centroid value of *F* (%)
4	E- 0.851	topsoil sand	60.11	53.66
7	E- 0.150	topsoil sand	71.11	53.66
28	C- 0.909	subsoil clay	38.91	33.08
77	C- 0.273	subsoil clay	53.28	33.08
42	A- 0.906	topsoil silt	27.93	26.78
40	A- 0.315	topsoil silt	14.58	26.78
103	B- 0.932	subsoil sand	14.57	20.26
170	B- 0.200	subsoil sand	12.42	20.26
223	D- 0.851	subsoil clay	53.59	48.27
226	D- 0.349	subsoil clay	42.11	48.27
87	F- 0.956	topsoil gravel	23.32	20.60
108	F- 0.043	topsoil gravel	1.94	20.60

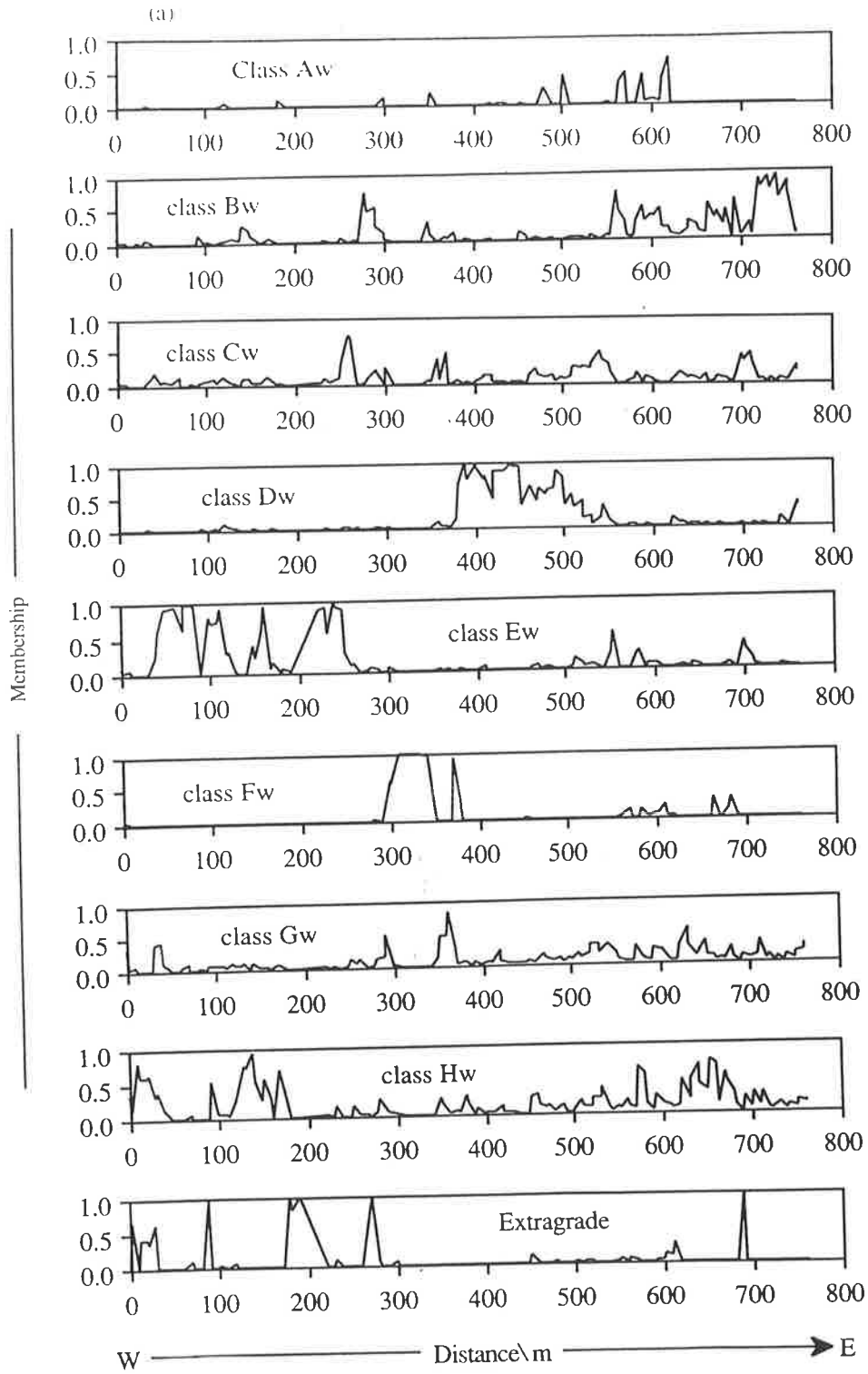

Fig. 4.13(a) Membership grades resulting from optimal (fuzzy) classification of whole soil data plotted along transect-W.

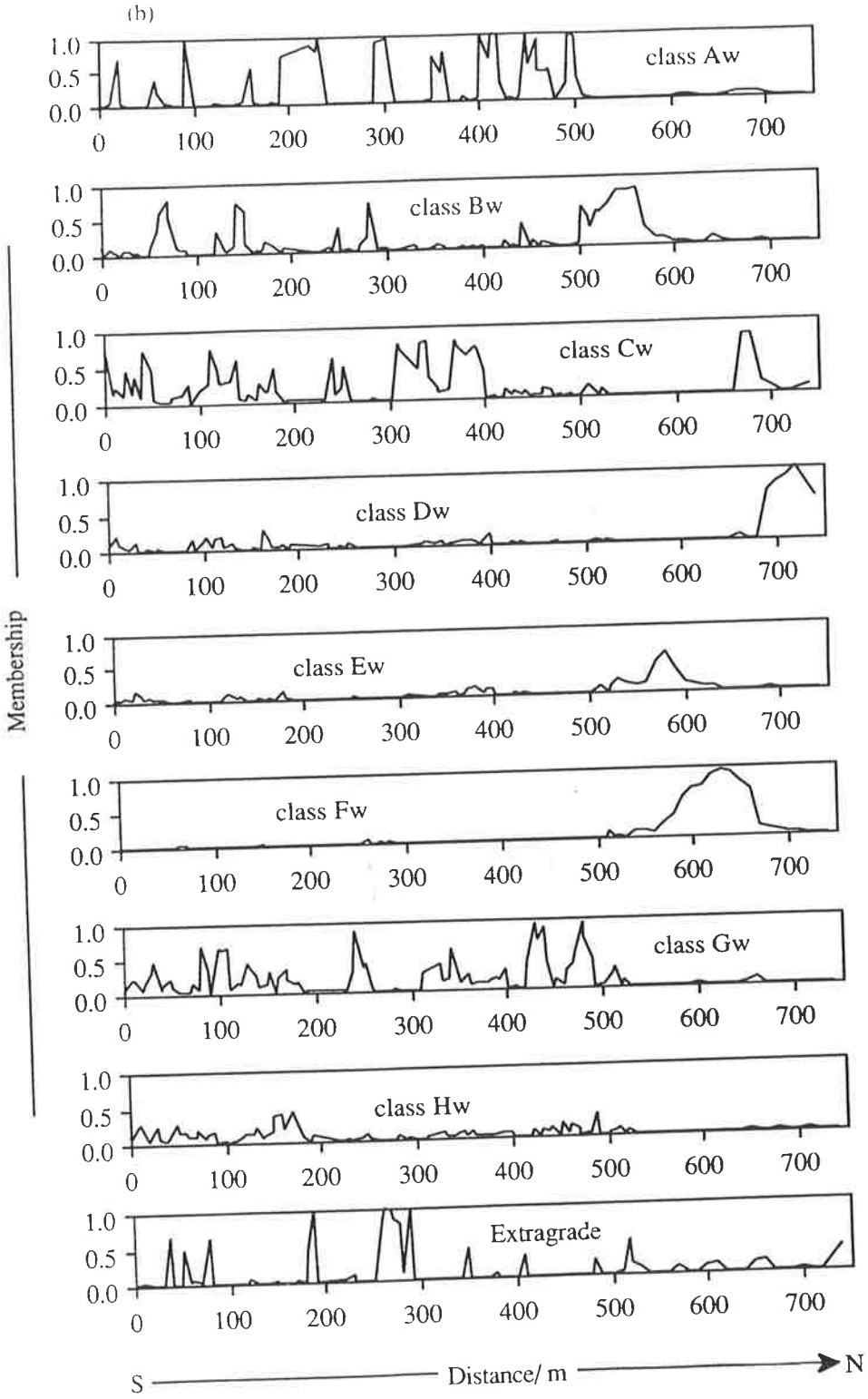

Fig. 4.13(b) Membership grades resulting from optimal (fuzzy) classification of whole soil data plotted along transect-S.

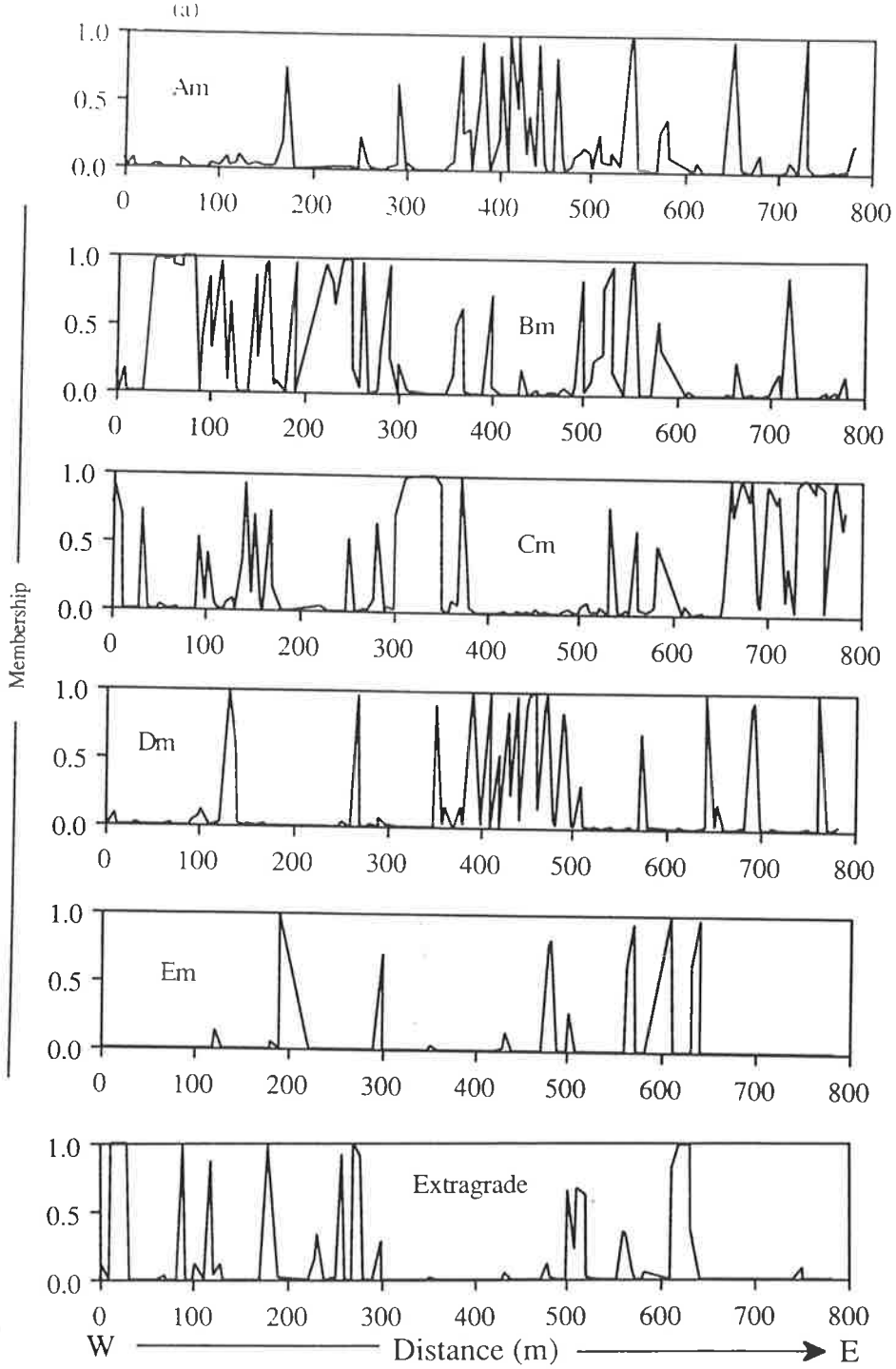

Fig. 4.14(a) Membership grades resulting from optimal (fuzzy) classification of morphological data plotted along transect-W.

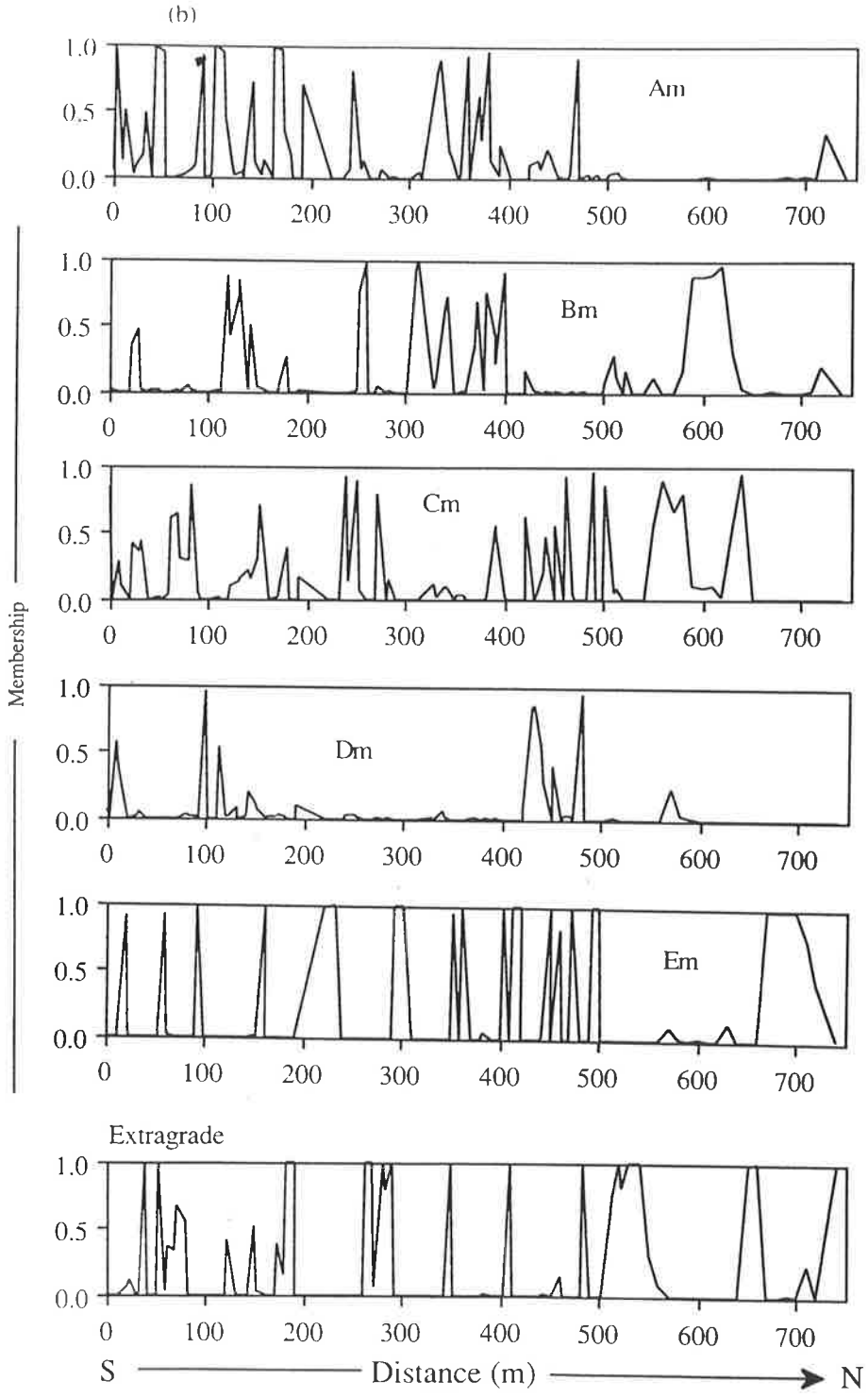

Fig. 4.14(b) Membership grades resulting from optimal (fuzzy) classification of morphological data plotted along transect-S.

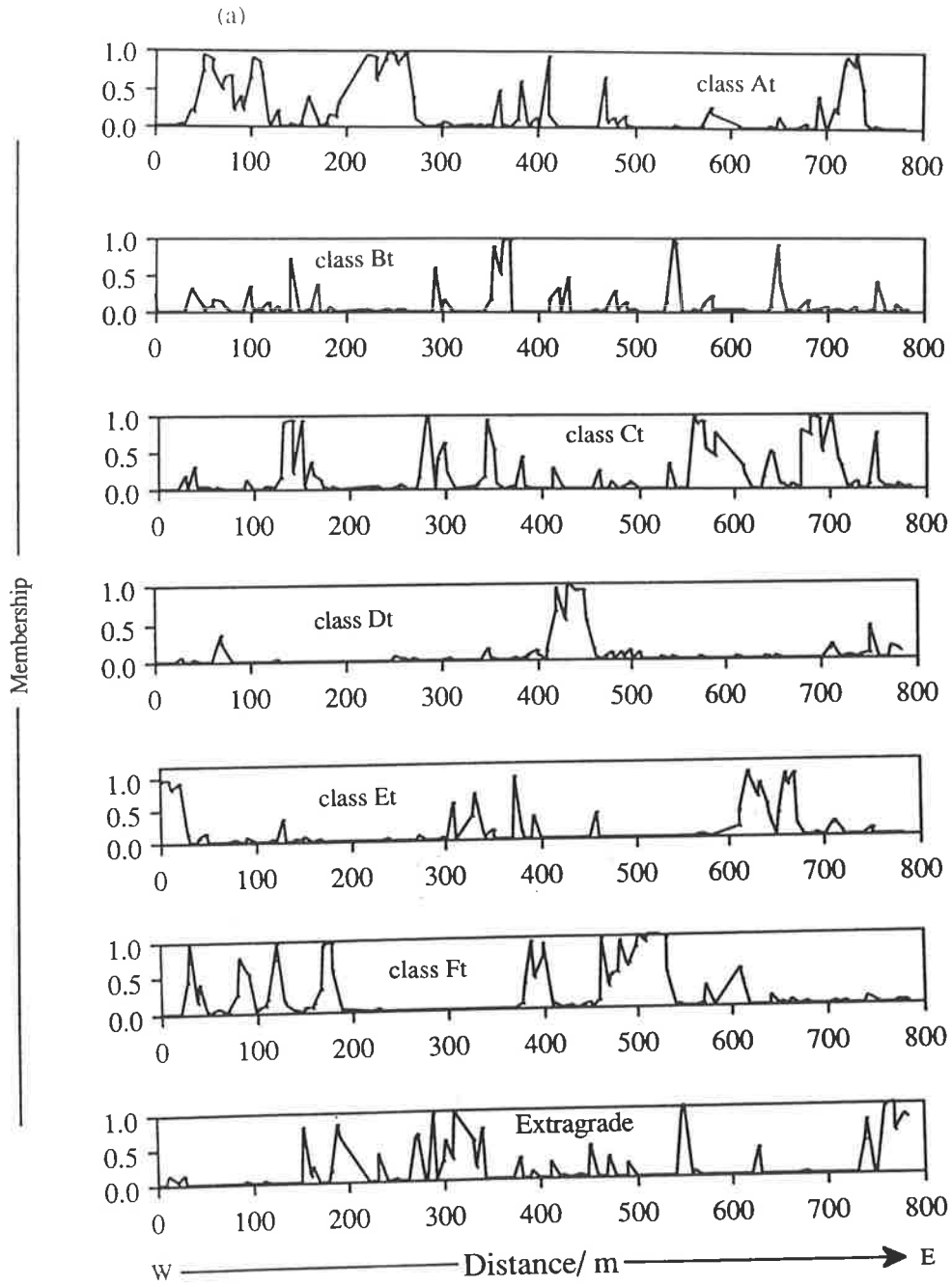

Fig. 4.15(a) Membership grades resulting from optimal (fuzzy) classification of particle-size data plotted along transect-W.

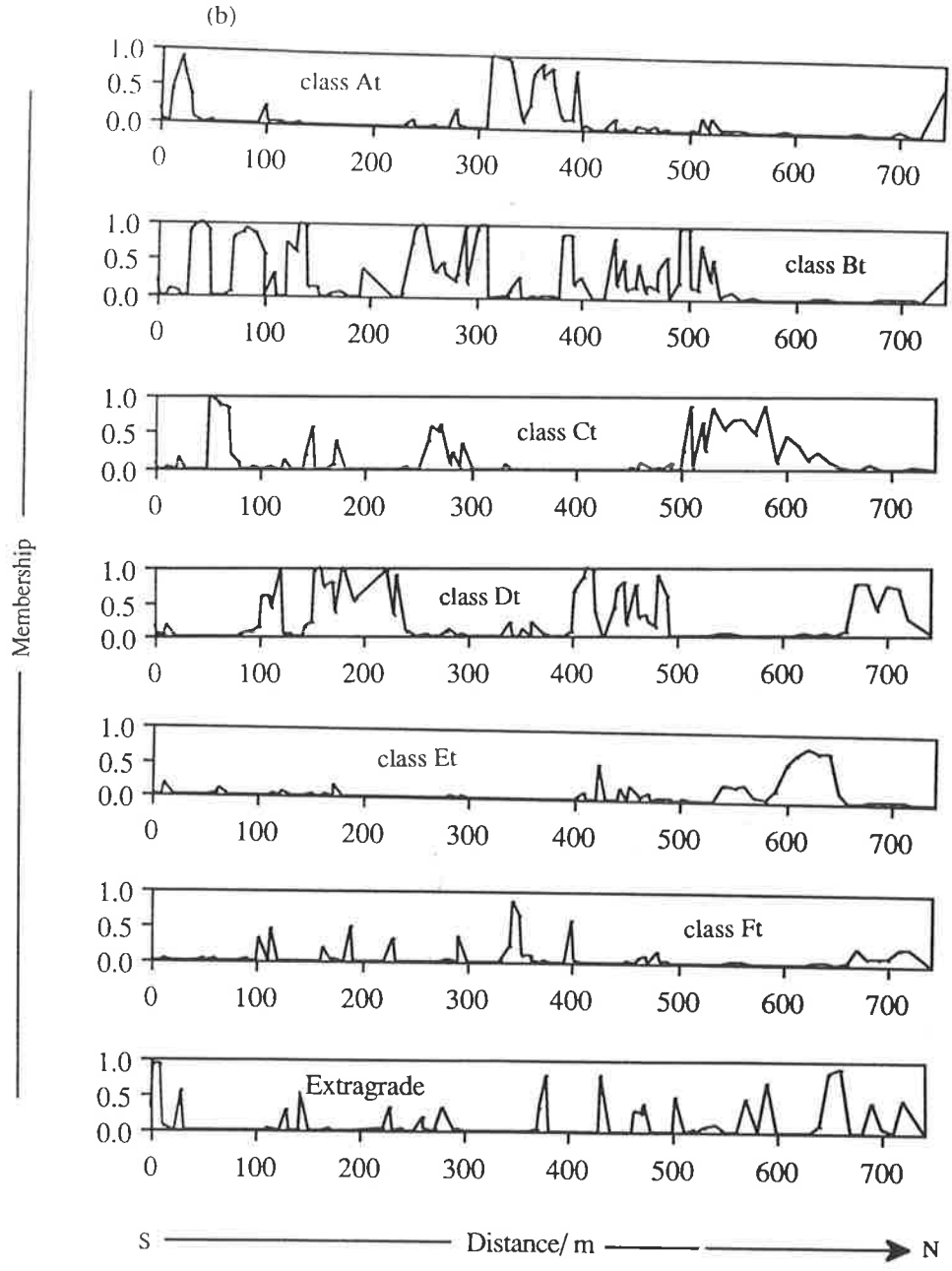

Fig. 4.15(b) Membership grades resulting from optimal (fuzzy) classification of particle-size data plotted along transect-S.

"... some soil properties ... change very abruptly across boundaries, while others display very gradual changes across the same boundaries". Although, this notion describes soil variation in the geographical context, the same can be extended to the taxonomic context. Moreover, there are some links between some classification systems and spatial continuity and contiguity of the resulting classes that may have been caused by some generating physical processes.

Spatial continuity and contiguity of fuzzy classes

A major limitation of cluster analyses which has been applied to soil data is the lack of spatial coherence of the resulting clusters (Burrough, 1986). It is, therefore, difficult to make physical interpretation of clusters obtained by these analyses. In fuzzy classification, there is reasonable contiguity and continuousness of fuzzy classes (Figs. 4.13 and 4.15). However, spatial continuousness of some classes is mainly short-ranged indicating more or less erratic local variation. This is particularly so for the fuzzy morphological classes as indicated by spiky projections in the graphical representations in Fig. 4.14. The discrete nature of variation in morphological features (*cp* the soil particle-size variables) probably caused this erratic behaviour. Generally, the local variation could be associated with changes in the parent material and landform features.

Relationships with landform

An important question that needs to be answered by classification of the data is whether they carry information about the processes generating them. If this is the case, then the structure, which represents the manner in which this information can be organized so that the relationships between variables in the data and the processes can be understood, should be identified. If the processes are known to be influenced by some external factor(s) that are easily observed and quantified, then the relationships between structure in the data and the factors can be useful for further rapid classification and mapping of the subsets of the data. This is a fundamental quest of all classification systems.

In the study area, the most apparent factor affecting soil distribution is the landform. The parent material (fine-grained phyllites and schists with occasional minor intrusions of quartz and quartzite) is essentially uniform across the landscape. Thus soil spatial variation is mostly due to lateral and vertical pedogenetic processes differentially caused by the effects of landform. Comparing Figs. 4.13 and 4.14 with Fig. 4.16, it is quite obvious that some fuzzy soil classes occur in association with certain landscape positions and slopes. The relative landscape positions and slopes associated with the various fuzzy classes are given in Table 4.4 for the whole soil data and in Table 4.5 for the particle-size variables. However, as the spatial continuity of fuzzy morphological classes is very erratic (Fig. 4.14), it is difficult to relate the morphological classes to landform features. This does not preclude some form of functional relation between morphology and landform.

Generally, the nature of soil variation appears to be related to the complexity of landscape processes of which slope features appear to be the most significant. The process-response outcome varies from one soil features to the other. This is why the nature of spatial continuity of fuzzy classes is dependent on the soil feature used for classification. The relationships of individual soil variables with landform is analyzed in chapter 5.

4.5 Conclusions

From this study the following conclusions are drawn:

1) Fuzzy classification takes into account the continuous nature of soil. Spatial variation in soil is usually gradual, and where boundaries exist, are fuzzy. Fuzzy classification techniques, therefore, are more realistic than the conventional approach.

2) The flexibility of fuzzy classification allows for any number of classes within the fuzzy c-partition space, $1 < c < n$ (if the soil is uniform or the number of classes is equal to the total number of pedons in an area, then classification would not be necessary), from which an optimal number of classes can be chosen by means of "cluster validity" functionals. An optimal number of classes thus chosen is regarded as a realization of some structural organization due to some physical processes.

3) The spatial continuity (and contiguity) of fuzzy soil classes allows for geographically more realistic representations of the fuzzy classes by geostatistical interpolation methods and mapping, than is done conventionally.

Finally, it should be pointed out that the approach used here for determining the balance between structure in the data and continuity of the resulting classes, i.e. the optimal combination of c and ϕ, is heuristic in nature. The obvious difficulty with this approach is that there is some degree of subjectivity in the final judgements. This should not be portrayed as bad: we should call on our intuitive skill to judge whether algorithmically suggested substructures for a given data set are reasonable or not. As Dale *et al.* (1989) suggested, to advance soil classification (and indeed soil science) requires the combination of imaginative hypothesis generation and testing, with inductive modelling. We must strive for greater success in this direction.

CHAPTER 5

ELUCIDATION OF SOIL-LANDFORM INTERRELATIONSHIPS BY CANONICAL ORDINATION ANALYSIS

5.1 Introduction

From the preliminary study and the results in chapter 4 that indicated spatial relationships between soil entities and the landform, it became clear that the most important factor affecting soil distribution patterns in the study area is landform, although local variation of parent rock is also a contributory factor. It, therefore, became apparent that a study that would improve our knowledge of soil distribution patterns in terms of correlations of a number of soil variables with landform, represented by its derivative attributes, should be carried out. This was the major aim of the study reported in this chapter.

5.1.1 Quantitative methods in pedology

Modern pedology is principally based on the idea that soil distribution on the landscape is as a result of processes caused by interactions between the factors of soil formation. Jenny (1941) first developed mathematical functions for soil-factor relations and since then many workers have made attempts to mathematically model the influence of factors of soil formation on soil development and distribution (Huggett, 1975; Yaalon, 1975). A large number of models have been devised to explain the influence of slope morphology on soil development and correlate slope parameters with soil variables. These models have been based on the premise that the vertical movement of material is far more important than movement tangential to the surface (Huggett, 1975). However, a two dimensional approach to the study of soil-landform relationships as in the concept of catena

(Milne, 1935) is only valid where across-slope, or plan, convexities (curvatures) does not exist. This is rarely the case, especially in fluvial landscapes where divergence and/or convergence of flowlines are caused by variation in profile and plan curvatures.

Three dimensional approach- from catchment subsytems to the drainage basin

The modern concept of soils widely held is one that considers soils as "dynamic natural three-dimensional bodies or landscapes, each having a lateral dimension on the earth's surface and depth delimited by that material beneath the soil *per se* which can be treated as parent material or not soil" (Soil Survey Staff, 1962). While the vertical sequum of properties (Buol *et al.*, 1973) from the soil surface to a depth where material is considered non-soil are mainly due to pedogenetic processes, the lateral sequum which is the succession of contiguous soil bodies may be due to either differential pedogenetic processes and/or geomorphological processes. Hence soil variation in three-dimensional context should be considered from the points or pedons through the subsytems of catchments to the broader drainage system. In this study the soil-landform interactions is considered within the framework of a subcatchment using the landform (point) attributes and the measured soil properties. The measurement of point attributes defining the land morphology is termed specific geomorphometry (Evans, 1980). The historical development of specific geomorphometric methods as related to soil-landform interactions is briefly discussed.

Aandahl (1948) was the first to recognize the influence of land-surface plan and profile curvatures on soil formation and distribution. However, it was Troeh (1964) who first developed a quantitative method of fitting a paraboloid of revolution to the landscape to estimate the gradient, profile and plan convexities and relate these to soil properties. His work indicated a strong correlation between land-surface form and some soil variables. This finding was interpreted in terms of the influence of land-surface configuration on the drainage status of soil. Since Troeh's work, other researchers have investigated the influence of land-surface curvatures on water movement and distribution (Anderson and Burt, 1978; O'Loughlin, 1981; Burt and Butcher, 1985), and on soil variability (Webster, 1977a).

Coincident with recent advances in soil science which have enabled us to quantify an increasing number of soil variables, is the need for an effective means of relating these variables to environmental attributes causal to soil variability. This is fundamental, not only to our understanding of soil genesis and distribution, but also to a more accurate prediction of soil at unvisited locations than is now possible by current methodology. In the case of the topographic factor, this is even more so as recent developments in remote sensing and photogrammetric techniques (Evans, 1980) have greatly improved our ability to produce accurate digital elevation models (DEMs). DEMs are useful for the determination of landform attributes (Evans, 1980; Zevenbergen and Thorne, 1987) important to soil development and distribution, even for unvisited points within the landscape. A known correlation between these attributes and the soil variables measured for carefully selected sample pedons could, therefore, improve the accuracy of interpolation of the soil variables at unsampled points. In recognizing this, Stein *et al.* (1988 a & b) adopted a procedure which incorporated stratification of land into more or less uniform units before embarking on sampling for geostatistical interpolation by kriging.

5.1.2 Multivariate approach to soil-landform studies

Generally, simple regression and multiple regression analyses have been the main analytical tools for soil-landform correlation studies (Ruhe and Walker, 1968; Furley, 1971; Burt and Butcher, 1985). However, these analytical techniques may not be suitable when large numbers of variables are involved. In such situations, other multivariate methods are recommended (Ross *et al.*, 1975). Intrinsic methods such as principal component analysis (PCA), involving a single set of soil data, have been applied for numerical classification of soils (Norris, 1970; Cipra *et al.*, 1970; Moore and Russell, 1976), an economical and effective survey procedure (Burrough and Webster, 1976), soil variation studies (McBratney and Webster, 1981), and indirectly for pedogenetic studies (Sondheim *et al.*, 1981). However, extrinsic methods which relate patterns in one set of variables (factors or predictors) to those in another set of variables (soils or outcomes) would, perhaps, improve

the predictive power of interpolation techniques and thus soil pattern recognition. If the relation between the two sets of variables is sufficiently strong, we may be able to predict directly the soil from its environment (Webster, 1977a).

Extrinsic methods such as linear discriminant analysis for soil pattern recognition (Webster and Burrough, 1974) and canonical correlation analysis (COR) for soil-environment interrelationships (Webster, 1977a) are all variants of the basic linear transformation. Another linear method, which has been applied in ecological studies but not yet tried in soil-environment research, is the redundancy analysis (RDA) . Although these linear methods may be successful, an alternative to the basic assumption that soil variables are systematically and monotonically related to environmental attributes has not been tested. Also used in the field of ecology but not yet tried in soil studies, are correspondence analysis (CA) and canonical correspondence analysis (CCA) which are based on the non-monotonic Gaussian (bell-shaped) species response models. CCA has been demonstrated to be more robust in extracting variation in species abundance in relation to the environment than linear models such as RDA and COR (Ter Braak, 1986) when the relations among species variables and environmental attributes are non-linear and unimodal . CCA highlights the main features of variation in a population in relation to the environment. Whereas CCA is a direct gradient analytical method in which the axes are chosen with respect to the environmental attributes, CA is an eigenvector ordination technique aimed at visualizing the pattern of distribution in a given set of data.

5.1.3 Objectives

The main objective of this chapter is to evaluate the relationships of soil variables with the landform, and also with some parent material-related attributes. Additionally, the aim is to investigate the robustness, and therefore the usefulness, of various ordination methods that assume different relational models of soil variables with landform attributes. Robustness, as used here, was equated with the efficiency of a model to extract variation of soil properties in relation to the environmental (landform) attributes even when the basic

assumptions of the model were violated. Specific aims are, therefore, to:

(1) determine the appropriateness of various ordination methods in the study of soil-landform interrelationships in a South Australian subcatchment at Forreston;

(2) evaluate the pedogenetic implications of ordination results as a tool to understanding the soil distribution pattern in the subcatchment.

In Chapter 4, it was established that there existed sytematic relationships of soil as a whole with landform in the study area. In this chapter, specific soil variables measured for points (or pedons) along the transects are correlated with specific geomorphometric attributes determined for corresponding points.

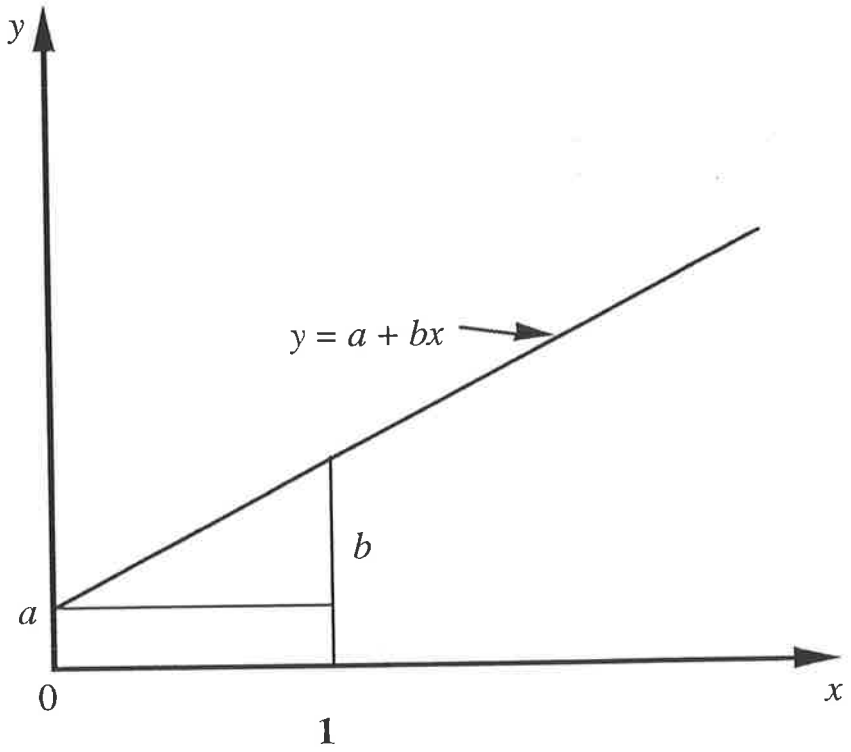

Fig. 5.1 A hypothetical linear model.

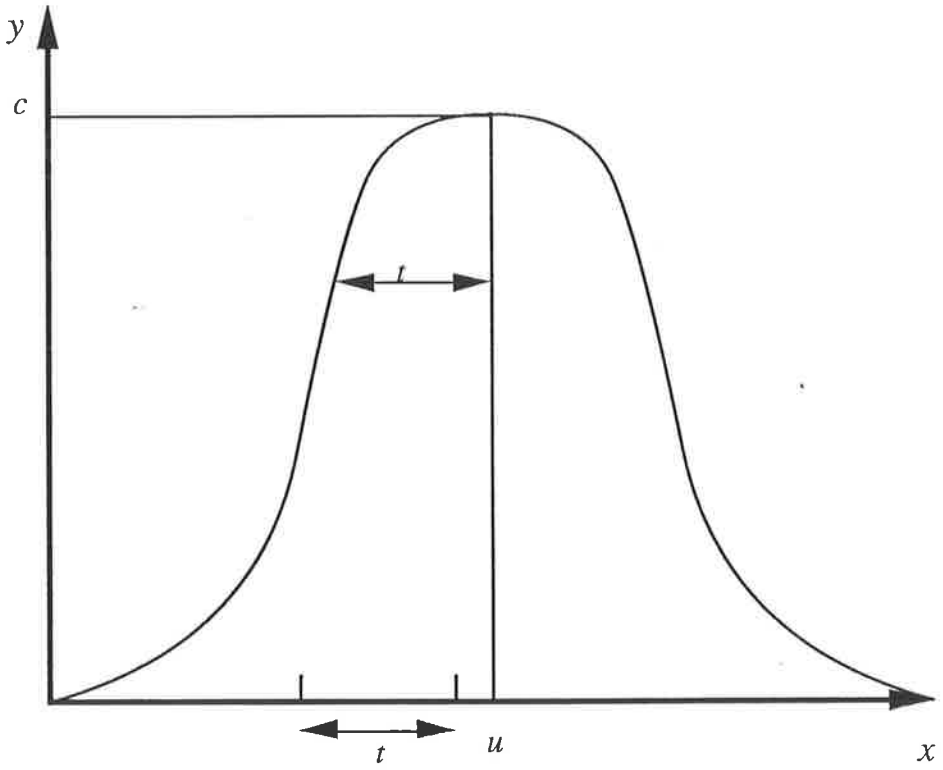

Fig. 5.2 A hypothetical unimodal model.

5.2 The Principles and Application of Canonical Ordination Analysis

Suppose for a survey with n sites (e.g. pedons) that m variables and q environmental attributes are determined. Let **Y** be the data matrix of the variables and **V** be the matrix of environmental attributes; y_{ik}, an element of **Y**, is the value of variable k at site i and v_{ij}, an element of **V**, is the value of environmental attribute j at site i. In the usual intrinsic methods of ordination (e.g. PCA) the aim would be to summarize the main gradient in the data by simple linear transformation similar to the basic linear regression model (Fig. 5.1) by iteratively computing the vector loading and the component scores using the equations:

$$\tilde{b}_k = \sum_{i=1}^{n} \frac{y_{ik}\, x_i}{s_x^{\,2}} \qquad (5.1)$$

and

$$\hat{x}_i = \sum_{i=1}^{m} \frac{y_{ik}\, b_k}{s_b^{\,2}} \qquad (5.2)$$

where b_k is the slope or vector loading and $\tilde{b}_k$ its estimate; x_i is the site score and $\hat{x}_i$ its estimate; $s_x^{\,2}$ and $s_b^{\,2}$ are the variance of x and b respectively (Ter Braak and Prentice, 1988).

However, in the procedure which assumes a Gaussian response curve (Fig. 5.2), an ordination axis is constructed such that the data will optimally fit a Gaussian response curve defined by the function:

$$E(y_{ik}) = c_k exp[-0.5(x_i - u_k)^2\, t_k^{-2}]$$

where $E(y_{ik})$ is the expected value of y_{ik} which has score x_i on the ordination axis; c_k is the maximum parameter for variable k; u_k is the optimum or the value of x for which the maximum is attained for variable k; and t_k is the level of tolerance for variable k.

In ecological studies ordination of species data using either linear or Gaussian models may be followed by an indirect gradient analysis (Ter Braak, 1986) in which the ordination axes are related to the environmental attributes. This is usually done by multiple regression analysis (Montgomery and Peck, 1982) of the site scores on the environmental attributes using the equation:

$$x_i = b_0 + \sum_{j=1}^{q} b_j\, v_{ij}$$

where b_0 is the intercept and the b_j are regression coefficients. Alternatively, a direct

gradient analysis in which the regression equation is incorporated into the ordination algorithm may be used to simultaneously carry out ordination and multiple regression of the resulting axes on the environmental attributes. The direct gradient analyses based on linear regression models are RDA and COR, and that which is based on a unimodal model is the CCA. RDA and COR are essentially the same, except, that in RDA the variable scores are the weighted sum of site scores, whereas COR involves estimating the variable parameters by multiple regression of the site scores on the variables (Ter Braak, 1987; Ter Braak and Prentice, 1988).

For CCA estimation of the parameter values of c_k, u_k and t_k by non-linear least squares regression or linear maximum likelihood methods (as would be required for the classical Gaussian model) requires heavy computation. A robust and computationally simpler procedure is weighted averaging which need not conform to the stringent assumptions of the Gaussian model (Ter Braak, 1985). The transition formulae that link Gaussian ordination to CCA are:

$$\lambda u_k = \sum_{i=1}^{n} \frac{y_{ik}\, x_{ii}}{y_{+k}} \tag{5.3}$$

$$x_i^* = \sum_{i=1}^{m} \frac{y_{ik}\, u_k}{y_{i+}} \tag{5.4}$$

$$\boldsymbol{b} = (\boldsymbol{V}'\boldsymbol{R}\boldsymbol{V})^{-1}\boldsymbol{V}'\boldsymbol{R}\boldsymbol{x}^* \tag{5.5}$$

$$\boldsymbol{x} = \boldsymbol{V}\boldsymbol{b} \tag{5.6}$$

where y_{+k} and y_{i+} are attribute and site totals, respectively; $\boldsymbol{R}$ is a diagonal $n \times n$ matrix with y_{i+} as the $(i,i)^{th}$ element; $\boldsymbol{V} = \{v_{ij}\}$ is an $n \times (q+1)$ matrix of environmental data and a column of ones; and $\boldsymbol{b}$, $\boldsymbol{x}$ and $\boldsymbol{x}^*$ are column vectors: $\boldsymbol{b}=(b_0, b_1, \ldots, b_q)'$: $\boldsymbol{x}=(x_1, \ldots$

$x_n)'$ and $x^*=(x^*_1, \ldots, x^*_n)'$. The transition formulae show the link between COR and CCA with λ being the eigen value (Ter Braak, 1986).

5.3 Algorithms

5.3.1 Weighted averaging method (CCA)

The algorithm of CCA is akin to the procedure of reciprocal averaging used for CA developed by Hill (1979), but modified to include a step to constrain site scores to linear combinations of environmental attributes. The following is summary of the iterative algorithm to solve the transition formulae from the detailed algorithm given by Ter Braak (1987; 1988):

[1] Initialize arbitrary but unequal site scores.

[2] Compute the scores of the variable of interest by weighted averaging of the site scores using equation (5.3) with $\lambda=1$.

[3] Compute new site scores by weighted averaging of the variable scores using equation (5.4).

[4] Calculate regression coefficients by weighted multiple regression of the site scores on the environmental attributes, the weights being the site totals , y_{i+} , using equation (5.5).

[5] Obtain new site scores using equation (5.6); thus the new site scores are the fitted values of the regression of step [4].

[6] Standardize the site scores for each environmental attribute such that

$$\sum_{i=1}^{n} y_{i+} x_i = 0 \quad \text{and} \qquad \sum_{i=1}^{n} y_{i+} x_i^2 = 1$$

[7] Stop on convergence when the new site scores are sufficiently close to the site scores of the previous iteration; if not go to step [2].

Usually, two or more axes are required for the analysis to be meaningful . To obtain additional axes requires an additional step after step [5] to make the trial scores uncorrelated with the previous axes. In the case of CA, steps [4] and [5] are omitted but with the option that site scores may be regressed on environmental attributes. Alternatively, the transitional formulae can be solved by methods of eigen analysis (Ter Braak, 1987).

5.3.2 Weighted summation method (PCA and RDA)

The iterative algorithm for linear methods, such as RDA, is essentially the same as CCA except that the weighted averaging in steps [2] and [3] is replaced by weighted summation using equations (1) and (2) respectively . The algorithms for RDA and COR are also very similar, although RDA is designed to resolve certain limitations in the application of COR in ecological research (Ter Braak, 1987). In COR the variable scores are estimated by multiple regression of the site scores on the variables, whereas in RDA the variable scores are the weighted sum of site scores. Thus in COR, the number of variables must be smaller than the number of sites plus the number of environmental attributes, i.e. $m < n+q$. Even though these limitations may not be of practical consequence in pedological research where sampling sites are often more numerous than the soil variables under investigation, it is important to add that the multicollinearities among soil variables and among environmental attributes pose a problem in COR which makes it less attractive than either RDA or CCA. COR will therefore not be applied in our subsequent analysis.

The difference between RDA and PCA is analogous to the difference between CCA and CA. Whereas in RDA the iterative algorithm includes a step for multiple regression of the site scores on environmental attributes, in PCA such a step is omitted. RDA is therefore the canonical form of PCA in which the site scores are linear combinations of environmental attributes.

5.4 Material and Methods

5.4.1 Landform analysis

There are various quantitative methods for describing landform features. However, specific geomorphometry (Evans, 1980), in which point attributes of landform are determined, was required for this study. Specific geomorphometry is the measurement and analysis of specific land-surface features which are defined according to clearly defined

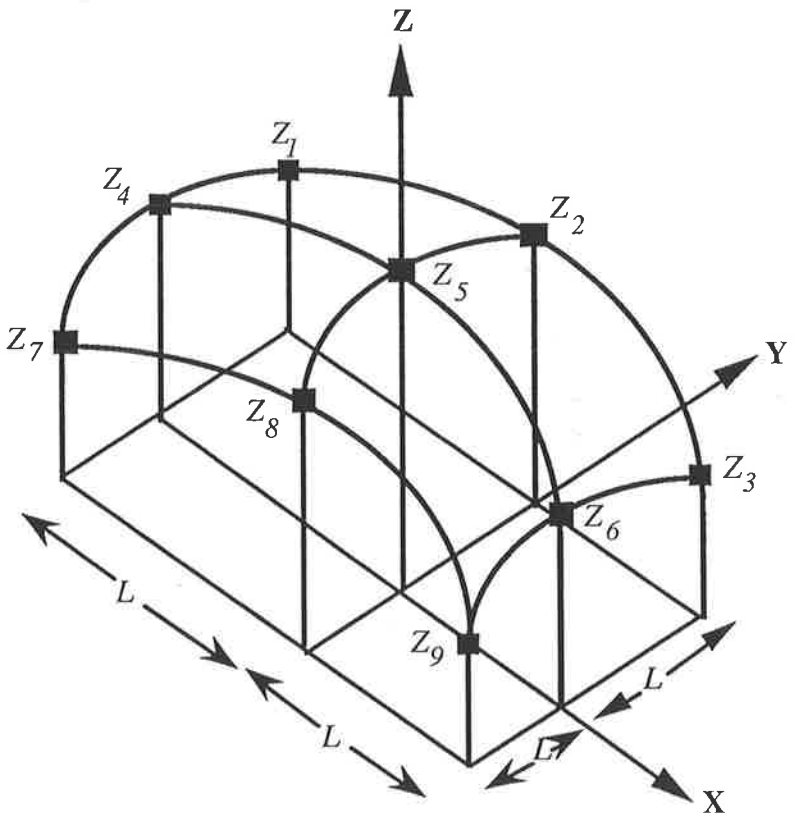

Fig. 5.3 A 3 x 3 submatrix of elevations.

criteria. The landform features determined for this study were gradient, aspect, plan and profile curvatures, upslope area and upslope distance. Gradient is the maximum rate of change of elevation, and it influences the rate of water and sediment flows. Aspect is the direction of the gradient using North as the reference. Aspect therefore defines the direction

of flow and determines what upslope area contributes to the flow at any point within a catchment. Profile curvature, which is the rate of change of gradient, affects flow acceleration and deacceleration and hence influences soil aggradation or degradation. Plan curvature is defined as the rate of change of aspect and affects flow convergence or divergence. As Hall (1983) has indicated, water movement and distribution on slopes are the principal cause of soil variation. It is the influence of landform attributes on water movement and distribution processes that determines the type of soil occurring at any point on the landscape, given that the slopes are relatively stable and that there has been no recent geomorphologically catastrophic event.

An elevation matrix at a grid mesh of 10 m covering the study area was obtained from controlled pairs of aerial photographs using a Zeiss Planicomp Analytical Stereo Plotter (South Australian Department of Lands). The landform attributes of gradient, aspect, plan curvature and profile curvature were derived in accordance with the procedure of Zevenbergen and Thorne (1987). The attributes were calculated for every point of the elevation matrix, except the peripheral points, by derivation from the partial quartic equation:

$$Z = Ax^2y^2 + Bx^2y + Cxy^2 + Dx^2 + Ey^2 + Fxy + Gx + Hy + I, \qquad (5.7)$$

where Z is the elevation at the centre of the submatrix (Z_5 in Fig. 5.3); A, B ,....and I are the nine parameters calculated from the nine 3 x 3 submatrix of elevations around the central point (Fig. 5.3); x and y are the spatial co-ordinates. Given that L represents grid length of the submatrix, the nine parameters are related to equation (5.7) and the nine submatrix elevations in Fig. 5.3 as follows:

$$A = \{[(Z_1 + Z_3 + Z_7 + Z_9)\,4^{-1}] - [(Z_2 + Z_4 + Z_6 + Z_8)\,2^{-1}] + Z_5\}\,L^{-4}$$

$$B = \{[(Z_1 + Z_3 - Z_7 - Z_9)\,4^{-1}] - [(Z_2 - Z_8)\,2^{-1}]\}\,L^{-3}$$

$$C = \{[(-Z_1 + Z_3 - Z_7 + Z_9)\,4^{-1}] + [(Z_4 - Z_6)\,2^{-1}]\}\,L^{-3}$$

$$D = \{[(Z_4 + Z_6)\,2^{-1}] - Z_5\}\,L^{-2}$$

$$E = \{[(Z_2 + Z_8)\,2^{-1}] - Z_5\}\,L^{-2}$$

$$F = (-Z_1 + Z_3 + Z_7 - Z_9)/4L^2$$

$$G = (-Z_4 + Z_6)/2L$$

$$H = (Z_2 - Z_8)/2L$$

$$I = Z_5.$$

By setting $x = y = 0$, the gradient, S, in the aspect direction, θ, is derived as

$$S = \delta Z/\delta T$$

$$= G \cos\theta + H \sin\theta, \tag{5.8}$$

where T is the horizontal dimension in the θ direction.

At the origin,

$$\cos\theta = -G/(G^2 + H^2)^{0.5}$$

$$\sin\theta = -H/(G^2 + H^2)^{0.5}$$

implying that

$$S = -(G^2 + H^2)^{0.5}, \tag{5.9}$$

with negative sign indicating that the direction, θ, is down-slope. Aspect, θ, is derived by minimization of equation (5.8):

$$\delta S/\delta\theta = -G \sin\theta + H \cos\theta = 0$$

$$\theta = \arctan(-H/-G).$$

The curvature, ρ, for any direction ϕ, is the second derivative of Z with respect to T :

$$\rho = \delta S^2/\delta T^2 = 2(D \cos^2\phi + E \sin^2\phi + F \cos\phi \sin\phi). \tag{5.10}$$

The profile curvature, $\rho(r)$, is in the aspect direction ($\phi = \theta$) and is derived as follows:

$$\rho(r) = -2(D \cos^2\theta + E \sin^2\theta + F \cos\theta \sin\theta)$$

$$= [-2(DG^2 + EH^2 + FGH)] (G^2 + H^2)^{-1}. \tag{5.11}$$

The plan curvature, $\rho(l)$, which is orthogonal to θ (*i.e.*, $\phi = \theta + \pi/2$), is given as

$$\rho(l) = 2(D \sin^2\theta + E \cos^2\theta - F \sin\theta \cos\theta)$$

$$= [2(DH^2 + EG^2 - FGH)] (G^2 + H^2)^{-1}. \tag{5.12}$$

Equations (5.10), (5.11) and (5.12) give curvatures as directional derivatives. Because gradient is derived in dimensionless term, *(L/L)*, it is also appropriate to derive the curvatures as per unit length *(L^{-1})*:

$$\rho = \frac{\delta^2 Z / \delta T^2}{[1 + (\delta Z / \delta T)^2]^{1.5}},$$

where *T* is in the appropriate directions as described for profile curvature and plan curvature respectively. Aspect values in degrees were also transformed into two variables, sin θ and cos θ as recommended by Mardia (1972) and Batschelet (1981).

Upslope area *(a)* and upslope distance *(d)* were estimated on the assumption that each point of the altitude matrix represents one grid square area or upslope grid length respectively. A point receives upslope area (L^2) or upslope distance (*L*) from any of its eight adjacent points if their slopes face the central point.

Grid scale

The choice of an appropriate grid size is clearly of fundamental importance. Anderson and Burt (1980) have discussed the appropriateness of a grid mesh for defining land-surface forms. They noted that the appropriateness of a grid mesh is dependent on 1) the physical processes involved with the landform attributes; 2) the other variables being studied; 3) the scale of variation of slope and aspect. Also the precision of elevation data is important (Zevenbergen and Thorne, 1987). However, the precise grid mesh selected is probably of little consequence, provided that the the mesh is not too large as to miss the topographic features of a land-surface, or not too small that will require excessive, precise data giving only microscale land features. Strictly speaking there is no "correct" grid size (Burt and Butcher, 1985). The choice here of a 10 m altitude grid for the study area reflects the author's judgement of spatial scale of landform influence on soil distribution patterns.

5.4.2 *The soil data*

Of the entire data points (pedons) sampled along the two transects as explained in chapter 3, one in every two coincided with altitude points for which landform attributes were calculated as described in subsection 5.4.1 above. Recalling that the directions of the transects were chosen to traverse the most apparent variability in the landscape and hence soil spatial variation, it was considered that the selected pedons were, to a considerable degree, representative of the possible pedons existing in the subcatchment. The data for selected pedons were used for the following analyses

5.4.3 *Ordination analyses*

A FORTRAN program (CANOCO), written by Ter Braak (1988), was used for all ordination analyses. As described in chapter 2, the study area is a relatively stable, low-order subcatchment without an extensive depositional low-slope area except for narrow bands of colluvio-alluvial deposits adjacent to the creeks. The landscape consists mainly of hill-side slopes (termed here as hillslopes for short) adjacent to shoulders and ridges. From some studies of soil-landform relationships (Ruhe and Walker, 1968; Furley, 1971) it is known that regression-based empirical models may conflict with continuous and discontinuous soil-landform associations when used to describe the whole soilscape in a catchment. The relationships between some soil variables and landform attributes are continuous only within partial landscape units. This is of particular importance inasmuch as areas that fall outside the continuous land units may distort the distributional relationships assumed for soil variation along environmental gradients. Ordination analyses were, therefore, carried out using only the predominantly hillslope pedons, totalling 125.

In addition to the landform attributes, parent material-related attributes of solum depth and depth to bedrock were correlated with other soil variables. This was to enhance, from a pedogenetic point of view, our understanding of soil development especially as it was

Table 5.1

a) Comparison of R(soil, environment), eigenvalues and variance accounted for by the first two axes resulting from CCA with those from CA/regression, using untransformed soil data; Total eigenvalue for either method = 0.5103

Analysis	Eigenvalue (λ)		% of total λ		Cumulative %		R(soil, env.)	
	Axis							
	1	2	1	2	1	2	1	2
CA/regression	0.21	0.08	41.2	15.4	41.2	56.6	0.44	0.39
CCA	0.04	0.02	8.7	3.8	8.7	12.5	0.48	0.56

b) Comparison of intra-set correlations of the first two CCA axes with inter-set correlations of the first two CA/regression axes.

Environmental attribute	CCA (intra-set)		CA/regression (inter-set)	
	Axis			
	1	2	1	2
Solum depth	-0.45	0.23	-0.05	-0.06
Depth to bedrock	-0.49	0.52	0.25	-0.39
Gradient	0.11	-0.81	-0.07	0.18
Profile convexity	0.32	-0.22	-0.19	-0.16
Plan convexity	-0.25	0.35	-0.02	-0.03
Upslope area (a)	-0.23	0.14	0.41	0.44
Square root of a	-0.22	0.23	0.49	0.42
Upslope distance	-0.30	0.31	0.58	0.48
Sin θ	-0.63	-0.12	0.22	0.41
Cos θ	0.44	0.26	0.16	-0.39

Table 5.2 The soil variables and environmental attributes used and their symbols as shown on ordination diagrams

Variable	[#1] Symbol	Variable	Symbol	Env. attribute	Symbol
Topsoil colour L	*alc*	topsoil structure (grade)	*agrd*	solum depth	SLDEP
Topsoil colour a	*aac*	topsoil structure (horizontality)	*ahon*	depth to bedrock	RKDEP
Topsoil colour b	*abc*	topsoil structure (verticality)	*aver*	slope gradient	GRAD
Subsoil colour L	*blc*	topsoil structure (flatness of face)	*afla*	profile convexity	PROFC
Subsoil colour a	*bba*	topsoil structure (accommodation)	*acom*	plan convexity	PLANC
Subsoil colour b	*bbc*	subsoil structure (grade)	*bgrd*	upslope distance	UPDIS
Subsoil mottle colour L	*bml*	subsoil structure (horizontality)	*bhon*	upslope area *(a)*	UPA
Subsoil mottle colour a	*bma*	subsoil structure (verticality)	*bver*	square root of *a*	UPSQ
Subsoil mottle colour b	*bmb*	subsoil structure (flatness of face)	*bfla*	sine aspect in deg *(θ)*	SIN Θ
Parent material mottle colour L	*cml*	subsoil structure (accommodation)	*bcom*	cosine aspect in deg *(θ)*	COS Θ
Parent material mottle colour a	*cma*	topsoil gravel	*grav*		
Parent material mottle colour b	*cmb*	topsoil %-sand	*asan*		
Topsoil consistence-strength	*astr*	topsoil %-silt	*asil*		
Topsoil consistence-plasticity	*apla*	topsoil %-clay	*acla*		
Topsoil consistence-stickiness	*asti*	subsoil %-sand	*bsan*		
Subsoil consistence-strength	*bstr*	subsoil %-silt	*bsil*		
Subsoil consistence-plasticity	*bpla*	subsoil %-clay	*bcla*		
Subsoil consistence-stickiness	*bsti*	topsoil %-organic carbon	*aoc(aom)*		
Subsoil cutan abundance	*bcab*	subsoil %-organic carbon	*boc(bom)*		
Parent material cutan abundance	*ccab*	topsoil Ec	*aec*		
Topsoil pH	*aph*	subsoil Ec	*bec*		
Subsoil pH	*bph*				

[#1] The abbreviated symbols for the untransformed Munsell variables are: hue- *hu*, chroma- *cr*, and value- *va;* each of these symbols is preceded by *a* or *b* indicating topsoil or subsoil respectively; also *bm* or *cm* preceding the symbols are indicative of subsoil or parent material mottle colour respectively.

suspected that the depth attributes influenced the contemporary pedogenetic processes. This contrasts the other view that understanding the correlation of landform with soil variables would improve our methods of soil spatial prediction. In all of the analyses where environmental attributes were used, the attribute values were standardized to zero mean and unit variance prior to analysis. This removed any arbitrariness in the units of measurement of the attributes thus making the results comparable without affecting other aspect of the analysis.

5.5 Results and Discussion

5.5.1 Weighted averaging based on unimodal models

As unimodal models are more general than monotonic ones (Ter Braak and Prentice, 1988), it is appropriate to start by analyzing the data using CA with regression (termed here as CA/regression) and its canonical counterpart, CCA. These initial analyses were undertaken to indicate how unimodal are the relationships among soil variables with environmental attributes. A good indicator of unimodality of a data set is the length of an ordination (or canonical) axis (Ter Braak, 1987). If the lengths of ordination axes are less than 3 units of standard deviation, then most of the response curves are linear, otherwise they are mostly non-linear. The significance of CCA axes can also be tested.

The initial analysis using CA/regression and CCA indicated that the lengths of ordination and canonical axes are mostly less than 3 units of standard deviation. Nevertheless the results are shown in Table 5.1. As Table 5.1-a indicates, eigenvalues of the first two axes of CCA are much less than those for CA/regression, a fact due to restriction imposed on the site scores by CCA. However, the restriction did not improve the soil-environment correlations when compared with the multiple correlations resulting from regression of CA axes with the environmental attributes. The R(soil, env.) of the first two CCA axes are just significant at 0.05 level (Monte Carlo permutation test). Log-

transformation of soil data did not improve the results either. These indicate that soil-

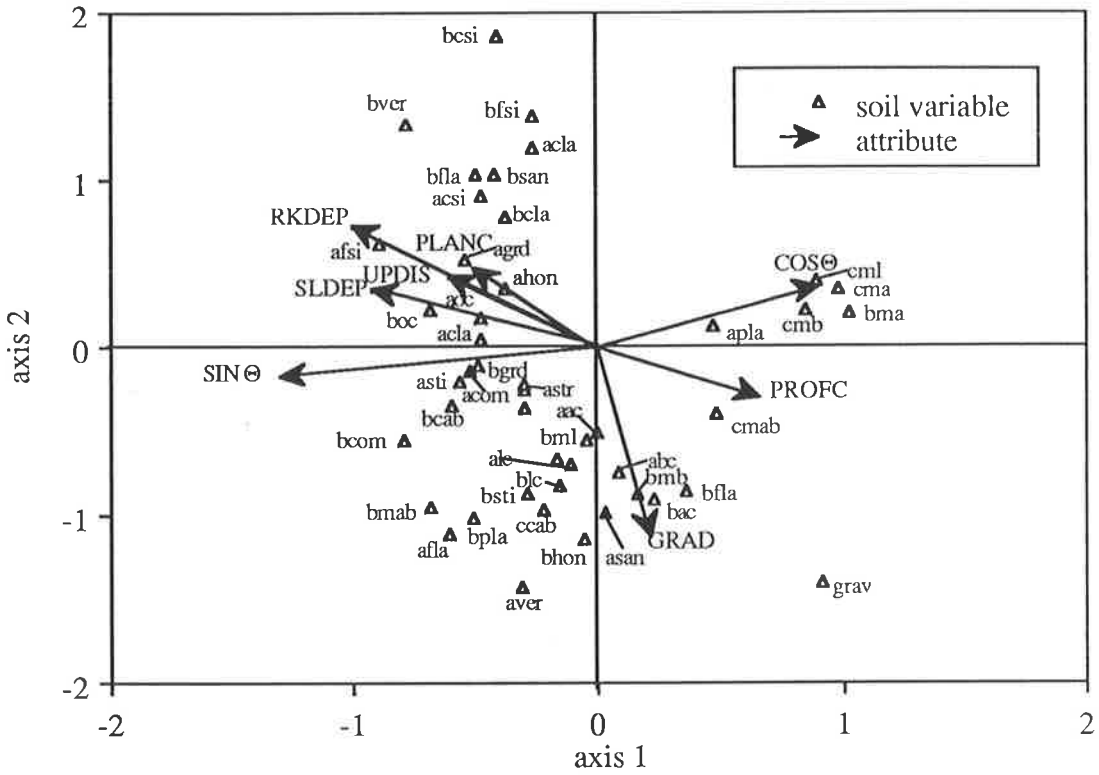

Fig. 5.4 Ordination diagram resulting from CCA on untransformed soil variables with environmental attributes; abbreviated symbols for the soil variables and environmental attributes are as shown in Table 5.2; site scores are not shown.

environment interrelationships in the study area are more complex than unimodal.

The useful parts of ordination results for interpretation of the axes are the canonical coefficients and intra-set correlations in the case of canonical methods, and inter-set correlations. Whereas intra-set correlations are due to regression of restricted site scores (which are linear combinations of environmental attributes) on environmental attributes, inter-set correlations are those due to site scores derived from soil data only, i.e., x_i in equations (5.2) and (5.4). Canonical coefficients, analogous to coefficients of multiple regression, are sensitive to multicollinearities among environmental attributes (Ter Braak, 1987). Insofar as this investigation indicated that some of the environmental attributes used

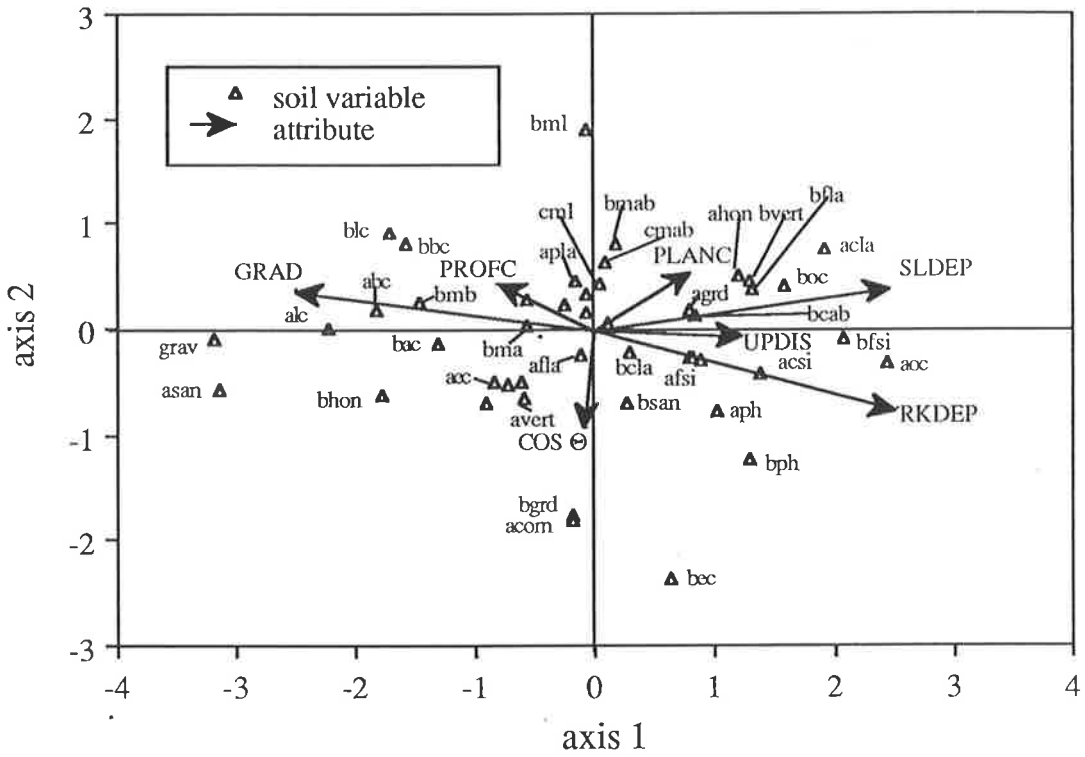

Fig. 5.5 Ordination diagram resulting from standard RDA on untransformed soil variables with environmental attributes; abbreviated symbols for the soil variables and environmental attributes are as shown in Table 5.2; site scores are not shown.

here are mutually correlated, it is inappropriate to interpret the canonical coefficients.

Table 5.1-b gives the intra-set correlations of the first two CCA axes and inter-set correlations of the first two CA axes with environmental attributes. The intra-set correlations resulting from CCA are generally higher than the inter-set correlations from CA/regression especially with respect to the first axis. While the first CCA axis shows a negative trend with sin θ, solum depth and depth to bedrock, and positive trend with cos θ, the second axis has a very high negative correlation with gradient (-0.81) and a smaller positive correlation with depth to bedrock (0.52). In contrast, inter-set correlations of CA are comparatively very low, only upslope distance showing a fairly high positive correlation (0.58) with the first axis.

Table 5.3

a) Comparison of R(soil, environment), eigenvalues and variance accounted for by the first two axes resulting from linear methods, using untransformed soil data (Note: the PCA axes are regressed on the environmental attributes, hence their R(soil, env.) are actually multiple correlations)

Analysis	Eigenvalue (λ)		% of total λ		Cumulative (%)		R(soil, env.)	
	Axis							
	1	2	1	2	1	2	1	2
PCA (ordinary)	0.38	0.28	38.0	27.5	38.0	65.8	0.27	0.18
PCA (standard)	0.14	0.12	14.2	12.1	14.2	26.3	0.49	0.26
RDA (ordinary)	0.05	0.03	5.3	2.9	5.3	8.2	0.52	0.30
RDA (standard)	0.07	0.02	6.6	2.2	6.6	8.8	0.76	0.61

b) Intra-set correlations (of environmental attributes with the first two axes) resulting from standard RDA and ordinary RDA on untransformed soil data

Environmental attribute	Standard RDA		Ordinary RDA	
	Axis			
	1	2	1	2
Solum depth	0.82	0.12	0.21	0.29
Depth to bedrock	0.84	-0.26	0.51	0.21
Gradient	-0.84	0.12	-0.30	0.08
Profile convexity	-0.27	0.14	-0.38	-0.11
Plan convexity	0.25	0.18	0.02	0.31
Upslope area (a)	0.34	0.02	0.07	0.16
Square root of a	0.35	-0.03	0.13	0.10
Upslope distance	0.40	-0.02	0.12	0.20
Sin θ	-0.04	-0.31	0.32	0.54
Cos θ	-0.15	-0.03	0.02	-0.47

CCA ordination diagram

The results of CCA, and indeed any ordination analysis, can be displayed in an ordination diagram in which scores of sites and of (soil) variables are represented by points. In CCA, scores for the environmental attributes are indicated as arrows (Fig. 5.4). To avoid overcrowding, site scores are omitted in all of the ordination diagrams.

In interpreting the ordination diagram, each of the arrows representing an environmental attribute gives a direction or axis of variation in relation to the two canonical ordination axes (usually the first two axes that are extracted from soil variables as linear combinations of environmental attributes) . The arrows can be extended in both directions and perpendicular lines drawn (or by imagined projection) onto it from the points of the soil variables. The order in which the projected points relate to the environmental axis indicates the relative importance or ranking of the weighted means of the soil variables with respect to the attribute. The weighted mean of a soil variable shows approximately its optimum along the environmental attribute gradient.

The arrow length for each environmental attribute quantifies the rate of change in the weighted means of soil variables as indicated in the ordination diagram. The length, therefore, indicates how variations in measured variables differ along the environmental gradients. This also means that environmental attributes that are highly correlated with an ordination axis are represented by longer arrows which are closer to the axis than those for the less important environmental attributes.

The CCA ordination diagram (Fig. 5.4) illustrates, in an exploratory manner, the relationships between the soil variables and the environmental attributes. The first canonical axis is mainly the aspect (θ) trend, with sin θ and cos θ complementing each other. Structural and mottle-colour features, and cutan abundance are closely related to aspect. Slope gradient accounts for significantly high variation in the second axis with particle-size fractions contributing much to the variation. This is not surprising. The fact that the points of the fine particle-size fractions (silt and clay) are at the opposite end of the slope gradient arrow and that the coarse fractions (topsoil sand and gravel) are close to the arrow head implies that particle-sizes become coarser with increase in slope gradient. This is particularly

true for the topsoil. Subsoil and topsoil organic carbon, and topsoil clay, structural grade and horizontality are positively correlated with depth, upslope attributes and plan convexity.

5.5.2 Linear methods

The PCA (with the same implications for its canonical counterpart, RDA) as treated in statistical textbooks is the variable-centered PCA which is termed 'ordinary' PCA by Ter Braak (1987). The other is the standardized PCA which is referred to here as standard PCA for simplicity. In centering by variables, the value of each variable is weighted by its variance. Thus the variables with high variance dominate the results of PCA whereas the variables with low variance have negligible influence on the PCA solution. In standard PCA, the value of each variable is divided by its standard deviation. In this case, the variables that do not vary substantially, unduly influence the results.

In addition to standardization by variables, which is required for variables measured in different units, standardization by sample totals is necessary for proportional data (e.g. percentage data) that sum to unity (Ter Braak, 1988). Standardization by sample total is, therefore, not required for the soil data. But whether to standardize by variables in addition to centering depends on the variances of the variables concerned. Table 5.3 compares the results of ordinary PCA with those of standard PCA in addition to the results of their canonical counterparts, used on the untransformed soil data. The eigenvalues and variance accounted for by the first two axes (Table 5.3-a) are much higher in the PCA/regression than in their corresponding RDAs. The reason for this is as previously explained for CA versus CCA, that the canonical methods restrict the site scores. Unlike in the non-linear methods, however, the restriction considerably improved the R(soil, env.) in the RDA methods in comparison with the multiple correlations (R^2) resulting from PCA axes that were correlated with the environmental attributes. Whereas the R(soil, env.) of the first and second standard RDA axes are significant at 0.01 and 0.05 confidence limits respectively, it is only the R(soil, env.) of the first ordinary RDA axis that is significant at 0.05 level. Log-transformation of soil data did not alter the results significantly even though the standard

RDA appears to be more appropriate for our data sets.

Table 5.3-b shows the intra-set correlations resulting from standard RDA and ordinary RDA on the soil data. Because all the soil variables receive more or less equal weights in the standard RDA, the variables with small variance, particularly the nominal and ordinal variables, unduly influence the results. This explains why the first axis is highly correlated with some of the environmental attributes (solum depth, depth to bedrock and gradient) and not the second axis. In the ordinary RDA, the variables with high variance dominate the solution and thus completely alter the multidimensional relationships of the soil variables with environmental attributes. More equitable distribution of eigenvalues among the ordinary RDA axes gives a probable explanation for low correlations of the first and second axes with most of the environmental attributes. However, relatively high correlations of sin θ and cos θ with the second canonical axis are somewhat similar to CCA results .

RDA ordination diagram

The standard RDA ordination diagram in Fig. 5.5 shows the relationships of soil variables with the environmental attributes. The interpretation of the RDA ordination diagram (Ter Braak, 1987) is quite similar to that of the CCA diagram. In the RDA diagram, the variable points and environmental arrows jointly approximate the covariance of soil variables with environmental attributes. If one imagines a projected arrow from the origin to variable points, the cosine of an angle between the the arrow of a soil variable and that of an environmental attribute approximately quantifies the correlation between the soil variable and environmental attribute. This means that arrows pointing roughly in the same direction indicate high positive correlation, that arrows pointing in the opposite directions imply high negative correlation and that arrows crossing at right angles indicate zero correlation. For example, the particle-sizes are highly correlated with slope gradient. While the topsoil gravel and sand have acute angles (imagine arrows projected from the origin to their points on the diagram) with the gradient arrow indicating positive correlation, silt and clay fractions are roughly in the opposite directions of the gradient arrow implying their

negative correlation with slope. As for CCA, the steeper the gradient the coarser the particle-sizes of the soil.

However, in view of low but significant R(soil, env) of RDA (also of CCA) on untransformed soil data, an investigation of the appropriateness of a further data transformation prior to ordination by RDA was carried out.

5.5.3 Data Transformation

The soil data were determined in different units of measurement, i.e., in fuzzy codes, and ordinal and numeric scales (see Tables 3.1 and 3.2 in chapter 3). That is why standardization by variables was required in the first place. However, such standardization overemphasizes the influence of variables with low variances, particularly the nominal and

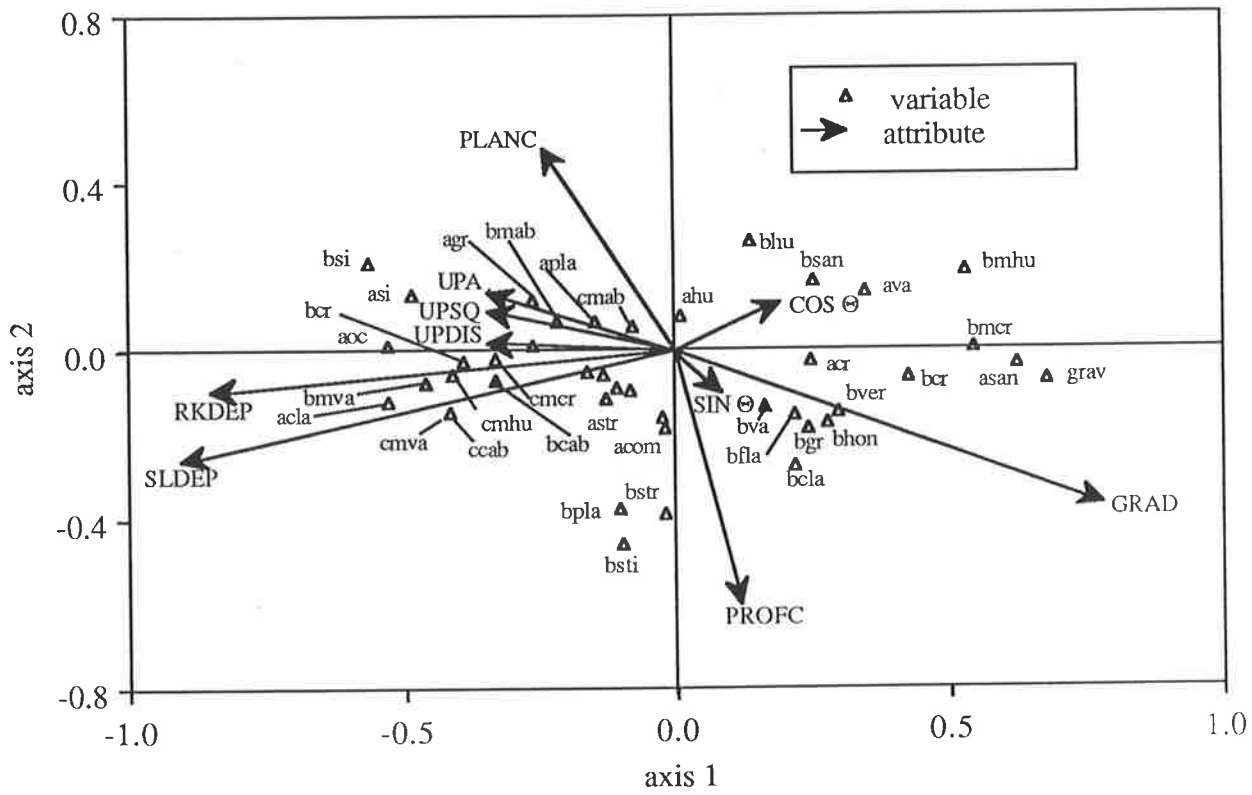

Fig. 5.6 Ordination diagram resulting from standard RDA on transformed soil variables with environmental attributes; abbreviated symbols for the soil variables and environmental attributes are as shown in Table 5.2; site scores are not shown.

ordinal variables. In order to alleviate this problem, transformation of soil data prior to ordination analysis was carried out. The first was to even up the variances of both the ordinal and numeric variables with fuzzy-coded structural variables. The soil colour CIE-coordinates were first re-transformed to their hue, value and chroma. Since the soil hue for the study area ranges from 5Y to 10R, the hue is categorized as indicator of the degree of soil redness which is zero for 5Y and 6 for 10R. Both the chroma (relative purity of the dominant wavelength) and value (lightness associated with grayness) range from zero to a maximum of 8. Thus the colour variables in semi-numeric form of CIE-coordinates were converted into ordinal form.

To even up the variances of soil variables, all the ordinal variables were divided by their respective maximum values to reflect their relative magnitude rather than their absolute values. Percentage data of particle-size fractions and that of organic carbon (first converted to % organic matter because of low values of Oc) were transformed into decimals. For the pure numeric data of electrical conductivity and pH, each of the variable values was divided by its respective maximum. Thus all the transformed variables have values between and including 0 and 1 which brings them on a par with the fuzzily coded structural features in Table 3.2 in chapter 3. The soil data consisted of a mixture of fuzzy codes, proportional, and coded- ordinal and numeric variables. They do not have the characteristic of sample values summing to unity as for pure fuzzy or proportional or dummy variables.

5.5.4 Canonical ordination of transformed soil data

Beginning with CCA on the transformed soil data to investigate how unimodal the data were, the eigenvalues for the first four CCA axes were very low (each has 0.01 or less), accounting for less than 5% of the total. Moreover, the axes lengths were even less than 2 units of standard deviation, a fact which suggest that the results were very poor indeed. Log-transformation did not improve the results either.

Table 5.4

a) Variance accounted for by the first four canonical axes obtained by standard RDA on (log-) transformed soil variables (sum of all canonical eigenvalues (trace) = 0.321)

Axis	Eigenvalue (λ)	% of total λ	Cumulative %	R(soil, env.)
1	0.17	53.1	52.5	0.83
2	0.10	31.2	84.3	0.59
3	0.03	9.4	93.7	0.55
4	0.01	3.1	96.8	0.58

b) Intra-set correlations of environmental attributes with the first four canonical axes obtained as in (a)

Environmental attribute	Axis			
	1	2	3	4
Solum depth	-0.91	-0.26	0.01	0.25
Depth to bedrock	-0.86	-0.09	-0.34	-0.11
Gradient	0.78	-0.37	0.15	-0.09
Profile convexity	0.12	-0.81	0.11	-0.48
Plan convexity	-0.24	0.74	0.12	-0.53
Upslope area (*a*)	-0.34	0.14	-0.20	-0.05
Square root of *a*	-0.35	0.10	-0.25	-0.11
Upslope distance	-0.35	0.02	-0.33	-0.08
Sin θ	0.08	-0.10	-0.24	0.07
Cos θ	0.19	0.12	-0.03	0.09

Table 5.5

a) Variance accounted for by the first four canonical axes obtained by standard RDA on particle-size fractions (log-transformed); sum of all canonical eigenvalues (trace) = 0.325

Axis	Eigenvalue	% of total	Cumulative %	R(soil, env.)
1	0.21	65.4	65.4	0.79
2	0.08	25.0	89.4	0.43
3	0.02	6.4	95.8	0.38
4	0.01	2.1	97.9	0.26

b) Intra-set correlations of environmental attributes with the first four canonical axes obtained as in (a)

Environmental attribute	Axis			
	1	2	3	4
Solum depth	-0.85	-0.46	-0.05	-0.06
Depth to bedrock	-0.81	-0.18	0.25	-0.39
Gradient	0.85	-0.23	-0.07	0.18
Profile convexity	0.13	-0.23	-0.19	-0.16
Plan convexity	-0.27	0.65	-0.02	-0.03
Upslope area (a)	-0.40	0.18	0.41	0.44
Square root of a	-0.44	0.13	0.49	0.42
Upslope distance	-0.40	0.08	0.58	0.48
Sin θ	0.04	0.05	0.22	0.41
Cos θ	0.28	0.01	0.16	-0.39

Table 5.6

a) Variance accounted for by the first four canonical axes obtained by standard RDA on morphological variables (log-transformed); sum of all canonical eigenvalues (trace) = 0.152

Axis	Eigenvalue	% of total	Cumulative %	R(soil, env.)
1	0.08	52.5	52.5	0.77
2	0.04	26.3	78.8	0.64
3	0.02	13.2	92.0	0.64
4	0.01	6.6	98.6	0.46

b) Intra-set correlations of environmental attributes with the first four canonical axes obtained as above

Environmental attribute	Axis			
	1	2	3	4
Solum depth	-0.90	-0.04	0.25	-0.23
Depth to bedrock	-0.84	-0.16	0.23	0.30
Gradient	0.68	-0.35	-0.24	-0.25
Profile convexity	0.01	-0.65	-0.46	-0.11
Plan convexity	-0.23	0.36	-0.45	0.50
Upslope area (a)	-0.35	0.14	0.11	0.27
Square root of a	-0.35	0.06	0.09	0.34
Upslope distance	-0.37	-0.04	0.16	0.33
Sin θ	0.07	-0.19	0.22	0.05
Cos θ	0.23	0.08	0.09	0.01

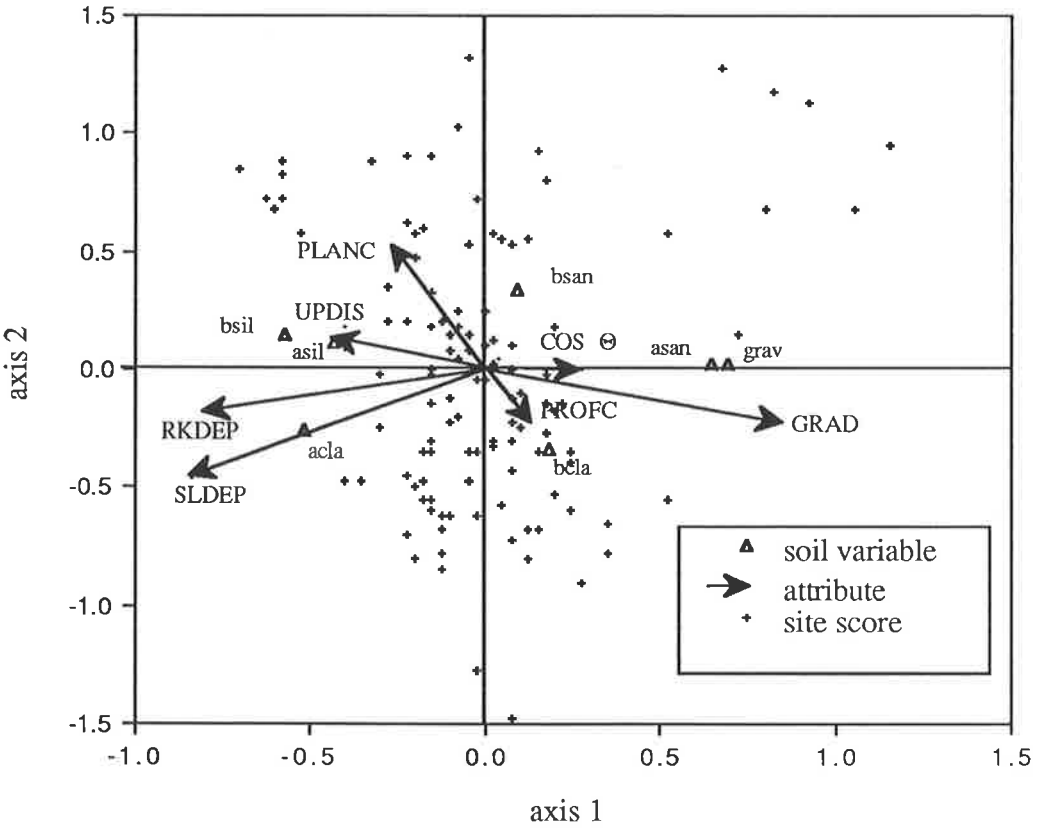

Fig. 5.7 Ordination diagram resulting from standard RDA on transformed particle-size fractions with environmental attributes; abbreviated symbols for the soil variables and environmental attributes are as shown in Table 5.2.

Because the transformed data consisted of a mixture of fuzzy codes, proportional, and coded-, ordinal and numeric variables, it was considered inappropriate to use variable-centered RDA only. The site values do not necessarily sum up to a unity, therefore centering by site totals was not necessary. Standardization and centering by variables were used, and this time, with log-transformation. Table 5.4-a shows the canonical eigenvalues, variance accounted for by the first four RDA axes and the R(soil, env.) resulting from such analysis. The first four canonical axes explain 96.8 % of the total variance. A comparison of the eigenvalues (due to soil variables) of the first two axes (total = 0.27) with those for corresponding standard RDA axes from untransformed data (total eigenvalues for the first

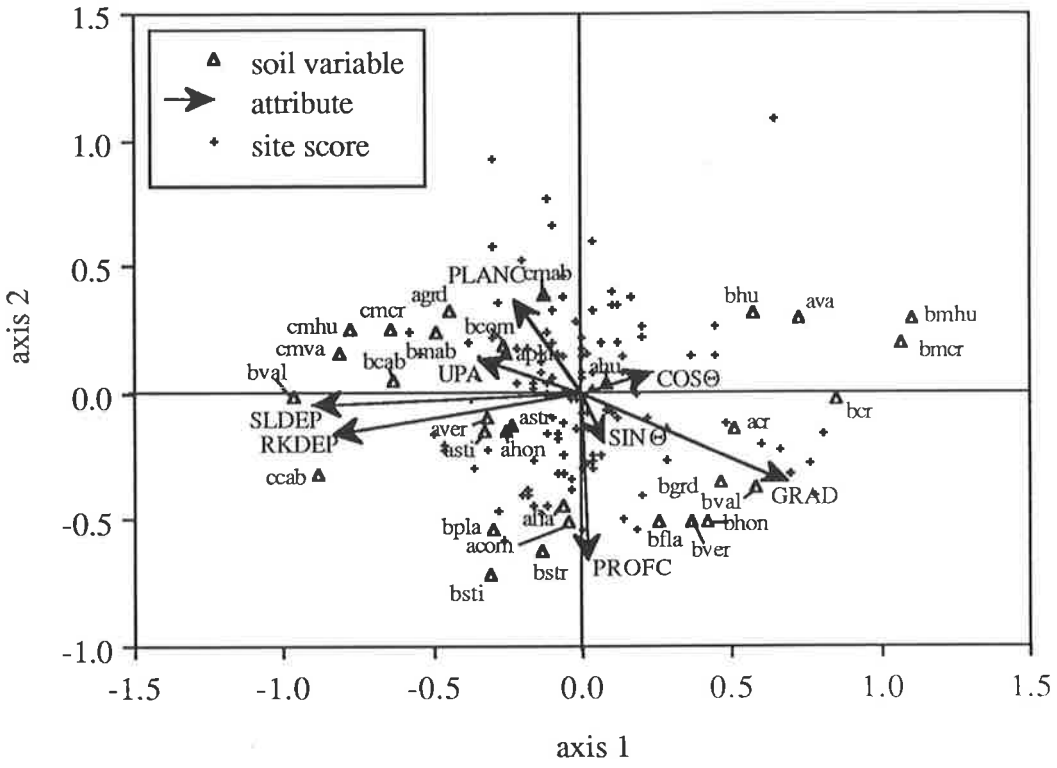

Fig. 5.8 Ordination diagram resulting from standard RDA on transformed morphological variableswith environmental attributes; abbreviated symbols for the soil variables and environmental attributes are as shown in Table 5.2.

two axes = 0.09), as shown in Table 5.3, indicates a considerable improvement.. The soil-environment correlation for the first axis also improves from 0.76 for untransformed data to 0.83 for transformed data. The correlation is slightly lower for the second axis, i.e., 0.61 compared with 0.59.

The intra-set correlations for the transformed data are given in Table 5.4-b. It shows that the first axis has a high negative trend with solum depth (-0.91) and depth to bedrock (-0.86), and a positive trend with slope gradient (0.78). The second RDA axis is negatively correlated with profile convexity (-0.81) and positively correlated with plan convexity (0.74). The RDA ordination diagram in Fig. 5.6, which accounts for 84.3 % of the total

canonical variance, illustrates the relationships of soil variables with environmental attributes for the transformed soil data. Figs. 5.7 and 5.8 are the RDA ordination diagrams for soil particle-size fractions and morphological variables respectively. While Fig. 5.7 represents 89.4 % of the total variance, Fig. 5.8 accounts for 78.8 % (see Tables 5.5 and 5.6). The same interpretation of the ordination diagram given for RDA above applies to these diagrams.

5.5.5 Physical Interpretation

An important aspect of this study was to give physically meaningful explanations of the results of canonical ordination analyses of soil variables in relation to the environmental attributes. The question is: why are some environmental attributes more highly correlated with soil (canonical) axes, and hence with related soil variables, than others? An answer to this question is central to the importance of this approach to quantitative pedology.

An interesting feature of all the methods, whether unimodal or linear, is the trend of the topsoil particle-size fractions with the slope gradient (see Figs. 5.4, 5.5 and 5.6, and also Table 5.5). However, it is more difficult to interpret the results of CCA in terms of the optimum values of the environmental attributes at which there is maximum or minimum value of the soil variable in question. This is because only few of the soil variables show unimodal relationships among themselves and with the environmental attributes.

Whereas the topsoil gravel and sand fractions show a positive trend with the gradient angle, silt and clay fractions decrease with increase in steepness of slopes. There appear to be geomorphological processes involved in the selective removal of the fine materials from the topsoil such that, as the steepness of slope increases, fine particles are mobilized and redeposited downslope as the gradient decreases. This is illustrated in Figs. 5.6 and 5.7 which indicate that there is an increase in topsoil clay and silt, and decrease in topsoil gravel and sand, as the upslope distance and area increase. The CCA ordination diagram (Fig. 5.4) also shows that subsoil silt and clay decrease with increase in slope gradient and with decrease in upslope attribute values. This is not the case with the RDA diagram shown in

Fig. 5.6 which indicates that the soil variables are more unimodal in their relations with some of the environmental attributes than with others. However, the relationships of finer particle fractions with gradient, as indicated by the CCA ordination diagram, are probably the result of a combination of *in situ* weathering processes and translocation/deposition processes. Weathering is moisture-limited on steep slopes because of relatively low moisture in the weathering environment as runoff water is not sufficiently delayed for infiltration to take place. Thus the coarse particles occurring on steep slopes, in contrast to fine silt and clay on gentle slopes, may partially be due to reduced weathering caused by local drought in subsoil environment. This may have been complicated by somewhat imperceptible depositional processes in the downstream side as sideslope soils merge into the narrow bands of colluvio-alluvial soils adjacent to the creeks.

Void argillans or cutans provide evidence of translocation of clay in the soil profile (Soil Survey Staff, 1975). In Figs. 5.6 and 5.8, cutan abundance *(bcab and ccab)* in the deep layers, i.e. the subsoil and the upper part of the parent material, show positive correlation with the depth attributes, and upslope distance and area. Deep soils tend to contain more of the finer materials in their upper horizons as evidenced by the high correlation of topsoil clay with depth attributes (Figs. 5.6 and 5.7). This condition is more conducive for eluvio-illuvial processes. But the fact that the subsoil clay does not increase with increase in depth of solum suggests that there is more than eluvio-illuvial processes accounting for the quantity of clay in the subsoil, especially of the shallower profiles. If eluvio-illuvial processes were to account for much of the clay in the subsoil, particularly of the shallow profiles, then the absence of cutans requires explanation. Cutans may have been destroyed by the shrink-swell activity due to seasonal moisture changes (Chittleborough and Oades, 1980). Seasonal moisture variation is well marked in the study area (note that the climate is xeric). Differential weathering in the lateral and vertical dimension, influenced by land-surface form and pre-existing local soil conditions and parent material, may have accounted for much of the variation in subsoil clay particularly in the shallow pedons, i.e. the distribution of cutans may be an inherited feature. Another explanation for the high amounts of cutans in the subsoil of soils on the lower slopes is lateral translocation of

colloid. Chittleborough *et al.* (1990) have observed that, within a similar soil type, considerable amounts of clay are translocated downslope from A to lower B horizons, by macropore flows.

Subsoil clay is negatively correlated with plan convexity, i.e. the clay content increases with increase in plan concavity. Two possible hypotheses to explain this relationship are proposed . First, there is flux of fine material due to convergence of subsurface flows, and second, there is an increase in weathering rate as a consequence of a more optimal moisture condition i.e. the gentler concave slopes sufficiently delay runoff for water to infiltrate into the soil. The amount of clay in the topsoil does not show such a distinct relationship with plan convexity as subsoil clay probably because of the ready dispersal and removal of surface and subsurface clay into the main drainage system: water discharge increases downslope due to convergence of flows.

Soil colour variations may be indicative of differences in drainage condition of soil, which is influenced by land-surface configuration (Gerrard, 1981). Colour *hue* is a measure of redness or yellowness or in the more extreme cases, blueness of soil colours. *Chromaticity* of soil colours reflects the relative purity of the dominant wavelength, represented by hue. The colour *value* is indicative of lightness of the soil colour. The three components of soil colour are sensitive to the concentrations of particular minerals (especially iron oxides of clay size) and organic matter. The accumulation is more of less dependent on redox conditions which in turn are dependent on drainage conditions.

The RDA ordination diagrams in Figs. 5.6 and 5.8 show the relationships of soil colour variables and the environmental attributes. Topsoil and subsoil *hue*, and subsoil mottle *hue* and their *chroma* values are negatively correlated with solum depth and upslope area (and distance) respectively. Subsoil *chroma* and *value*, and topsoil *chroma* are, however, more highly influenced by gradient angle than are the other soil colour variables (Fig. 5.8). The parent material colour variables of *hue*, *chroma* and *value* are negatively influenced by gradient and positively correlated with depth attributes and upslope area and distance.

Thus, three factors are responsible for soil colour variation in the study area. The

first is the slope gradient which determines the soil hydrological condition through its influence on the balance between runoff and infiltration. The second, which is related to the first, constitutes the upslope attributes of distance and area. The third, which is related to parent material, consists of depth of solum and depth to the bedrock. Thus the upper-slope soils are well-drained, reddish to reddish-brown podzolics, the colour indicative of the presence of non-hydrated iron oxides. These soils are shallow and occur mainly on steep slopes. On the mid-slope reddish-brown to yellow podzolics are juxtaposed. The drainage is slower in the yellowish soils due to localized areas of low gradient. The lower-slope soils, formed as a narrow band of brown and brownish-yellow podzolics at the fringe of creeks and on the gentler slopes, are more imperfectly drained than the podzolics of the mid and upper slopes. They are the moderately deep to very deep pedons. Their colours are indicative of the presence of hydrated iron oxides, probably limonite and goethite, caused by seasonal waterlogging which is accentuated by the presence of a textural B-horizon. Deeper layers, particularly the lower part of the B horizon and the upper part of the C horizon are moderately gleyed. The dark colour (low colour *value* and *chroma*) of the topsoil is caused by relatively high amounts of organic matter (up to 15 % in the lower-slope soils).

The amount of organic carbon (matter) in both topsoil and subsoil increases with increase in solum depth, and upslope distance and area (Fig. 5.6). But organic carbon content is negatively correlated with slope gradient. Deep soils, occurring mainly on the lower-slopes, are subject to seasonal waterlogging, a condition which promotes accumulation of organic material, particularly in the topsoil. Electrical conductivity and pH do not vary systematically with the landform attributes nor with the depth attributes because the ionic concentrations in the study area are not sufficiently high to influence their variation.

There are also relationships between some of the soil properties . Two examples will be considered. Topsoil structural grade (which indicates the degree of distinctness of soil aggregates) has a positive correlation with topsoil organic matter (Fig. 5.6). This is not surprising given our understanding of the role of organic matter in aggregate development. Subsoil structural grade is also positively correlated with clay concentration which in turn has positive relationships with landform (as discussed earlier) and with consistence variables

of strength, plasticity and stickiness (Figs. 5.6 and 5.6).

5.6 Conclusions

For the Forreston catchment data it was concluded that:

1) CA and CCA were less attractive than their linear counterparts, PCA and RDA, because few of the soil variables determined had unimodal relationships among themselves or with the environmental attributes used.
2) Standard RDA, following transformation of soil data, was found to be most robust of the linear methods.
3) The environmental attributes gradient angle, solum depth, depth to bedrock, plan and profile convexity, and to a lesser extent, upslope distance and area, account for most of soil variation in the study area.
4) The results of any canonical ordination analysis can be displayed in an ordination diagram in which the relationships among soil variables and/or soil with environmental attributes can be viewed simultaneously, thus highlighting their pedogenetic implications.

As has already been pointed out, soil-environment correlations resulting from COR in the manner used by Webster (1977a) are usually affected by multicollinearities among soil variables (Ter Braak, 1987). This is because, in COR, estimates of the variable scores are obtained by multiple regression of the site scores on the soil variables. Moreover, using COR normally involves entering the soil and environmental data into the analysis in a symmetrical way which makes the results difficult to interpret, particularly with respect to site scores. These problems are not found with RDA.

The significance of this study is that it has been shown, in a quantitative manner, the extent to which certain landform attributes affect soil development and distribution patterns. Land unit delineation to define sampling pattern should prove to be a useful first step, prior to soil survey by improving sampling efficiency and reducing boundary interpolation and soil classification errors. The results confirms expectations contained in chapters 3 and 4.

CHAPTER 6

SPATIAL MODELLING OF FUZZY (SOIL) CLASS MEMBERSHIP VALUES

6.1 Introduction

In the preceding chapters 4 and 5, it was concluded that landform (and to a lesser extent lithology) influence spatial variation of soil in the study area. The interactions of individual soil variables with landform attributes were discussed in chapter 5. However, it was confirmed in chapter 4 that there are systematic relationships between soil classification units and landform and lithologic features. The optimal density of field sampling envisaged was that which took into consideration these relationships (see chapter 4, subsection 4.3.3). It is the aim of this chapter to report and discuss the implementation of the sampling scheme thus designed, the resulting isarithmic maps of the dominant soil classes optimally generated by FCME and the relationships of these classes with the physical features in the study area. The spatial modelling that yielded isarithmic maps was achieved by application of the geostatistical interpolation methods of kriging, which is reviewed briefly.

6.2 Optimal Interpolation- Kriging

As explained in chapter 1 and in chapter 3, the regionalized variable theory developed by Matheron (1965) provides the basis for calculation of semivariogram of a given soil property, and subsequent use of the semivariogram for optimal estimation- kriging, and for planning rational sampling schemes for mapping soil properties. The basic principle of the theory was treated briefly in chapter 3, but repeated here in more detail because of the relevance of the theory to the method of interpolation used in this chapter. The account

given here is based on the publications of Burgess and Webster (1980a and b), McBratney *et al.* (1981), Trangmar *et al.* (1985) and Webster (1985).

Recall the kriging equation 3.8 in subsection 3.2.5 of chapter 3:

$$z^*(x_0) = \sum_{i=1}^{n} \lambda_i \, z\,(x_i)$$

where $z^*(x_0)$ is the value of a given property or attribute at unsampled location, $z\,(x_i)$ are the values z at n sampling locations and λ_i are the weights associated with the sampling locations. The weights are chosen such that the estimates $z^*(x_0)$ are unbiased, i.e.,:

$$E[z(x_0) - z^*(x_0)] = 0,$$

where $z(x_0)$ is the true value. The unbiased condition is assured as λ_i sum to unity:

$$\sum_{i=1}^{n} \lambda_i = 1.$$

The estimation variance, σ^2, defined by equations 3.9 and 3.10 for punctual kriging and equation 3.11 for block kriging is minimized such that

$$\sigma^2 = \text{var}[z(x_0) - z^*(x_0)] = \text{minimum.}$$

The minimum is obtained by introducing the Lagrangian multiplier such that the estimation variance is defined by

$$\sigma_e^{\,2} = \sum_{i=1}^{n} \lambda_i \, \gamma(x_i, x_0) + \psi \qquad (6.1)$$

for punctual kriging, and

$$\sigma_B{}^2 = \sum_{i=1}^{n} \lambda_i \gamma(x_i, B) + \psi_B - \sigma^2(B), \tag{6.2}$$

for block kriging.

Equations (6.1) and (6.2) indicate that, for a given estimation procedure, there are n equations in n unknowns and a set of unbiased conditions required for ψ to be determined. For punctual kriging, the matrix equations are represented as follows:

$$\boldsymbol{b} = \boldsymbol{A} \begin{bmatrix} \lambda \\ \\ \psi \end{bmatrix}, \tag{6.3}$$

where

$$\boldsymbol{A} = \begin{bmatrix} \gamma(x_1, x_1) & \gamma(x_2, x_1) & \cdots & \gamma(x_n, x_1) & 1 \\ \gamma(x_1, x_2) & \gamma(x_2, x_2) & \cdots & \gamma(x_n, x_2) & 1 \\ \vdots & \vdots & & \vdots & \vdots \\ \gamma(x_1, x_n) & \gamma(x_2, x_n) & \cdots & \gamma(x_n, x_n) & 1 \\ 1 & 1 & \cdots & 1 & 0 \end{bmatrix},$$

$$\begin{bmatrix} \lambda \\ \\ \psi \end{bmatrix} = \begin{bmatrix} \lambda_1 \\ \lambda_2 \\ \vdots \\ \lambda_n \\ \\ \psi \end{bmatrix} \quad \text{and} \quad \boldsymbol{b} = \begin{bmatrix} \gamma(x_1, x_0) \\ \gamma(x_2, x_0) \\ \vdots \\ \gamma(x_n, x_0) \\ 1 \end{bmatrix}. \tag{6.4}$$

Equation (6.3) is solved to obtain the weights, λ_i, so that the estimation variance is obtained by

$$\sigma_e^2 = b^T \begin{bmatrix} \lambda \\ \\ \psi \end{bmatrix} \tag{6.5}$$

For block kriging, the semivariance between sample points and unobserved point in equation (6.4), i.e., $\gamma(x_i, x_0)$, is replaced by $\gamma(x_i, B)$, the average semivariance between observation points and block B. Also the right-hand terms in equation (6.5) is less $\sigma^2(B)$, the within block semivariance.

Using the matrix method as outlined above is the most efficient as noted by Burgess and Webster (1980a). The estimated value at any unsampled location is the most accurate given the available data and one that can be used with known confidence. The kriging variance depends only on the semivariogram and sampling grid configuration (Burgess and Webster, 1980a; McBratney *et al.*, 1981). Thus it is the local error term that determines more the precision of estimation than the global error terms of other interpolation methods (Trangmar *et al.*, 1985). For this reason, only sample locations that fall within the area of spatial dependence are used for kriging.

Applications in soil spatial studies indicate that the semivariograms are usually linear to within the lag of spatial dependence in which case there must be sufficient number of data locations or points within the range of the semivariogram, if it is transitive. In view of the local nature of kriging, no more than 16 observations are needed for kriging one estimate (Webster, 1985), although Trangmar *et al.* (1985) gave higher conservative estimates of between 20 and 25 observations. The choice of number of observations for reliable estimation depends not only on the configuration of the sampled and kriged locations but

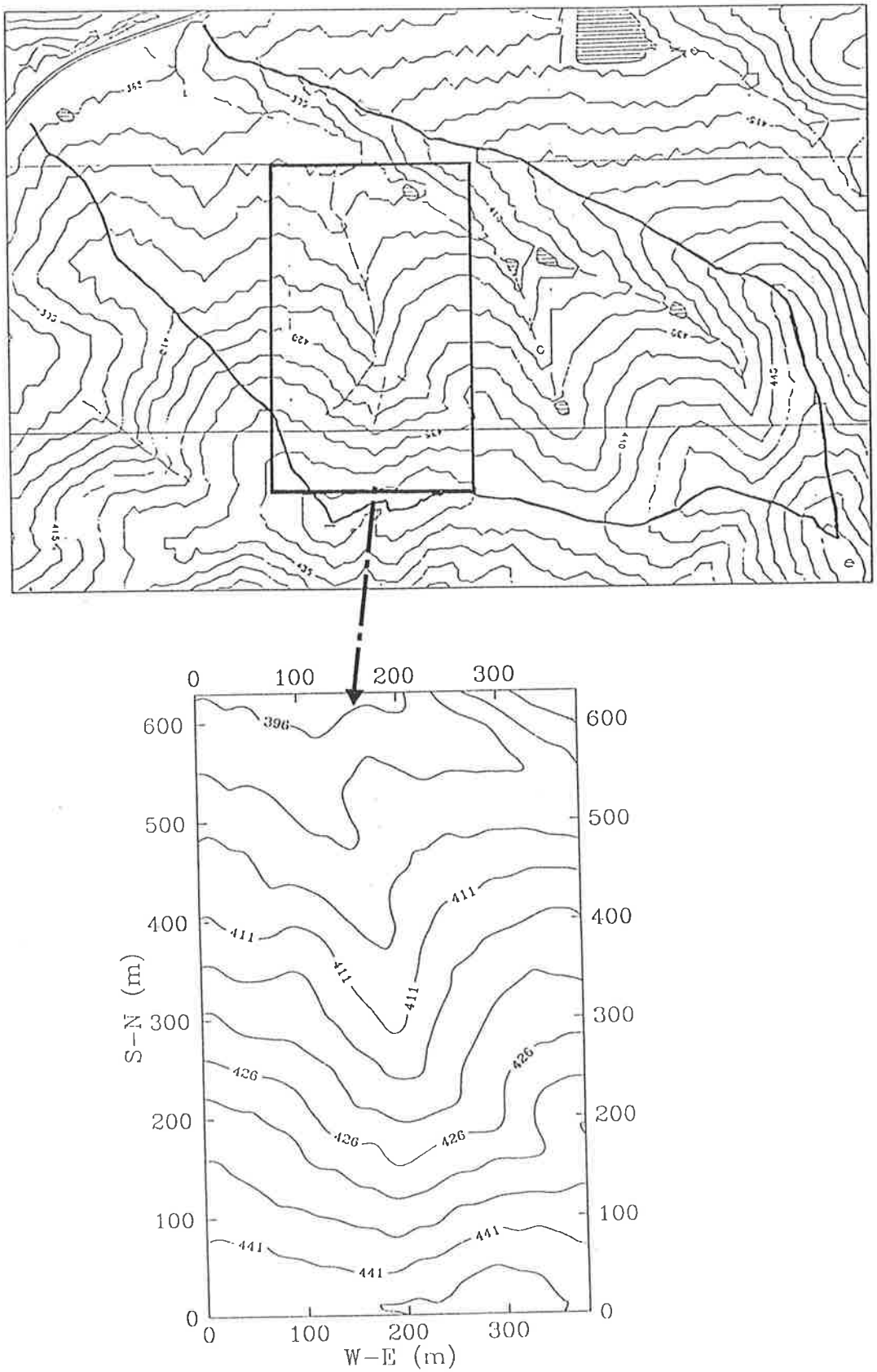

Fig. 6.1 Part of the subcatchment sampled for isarithmic mapping.

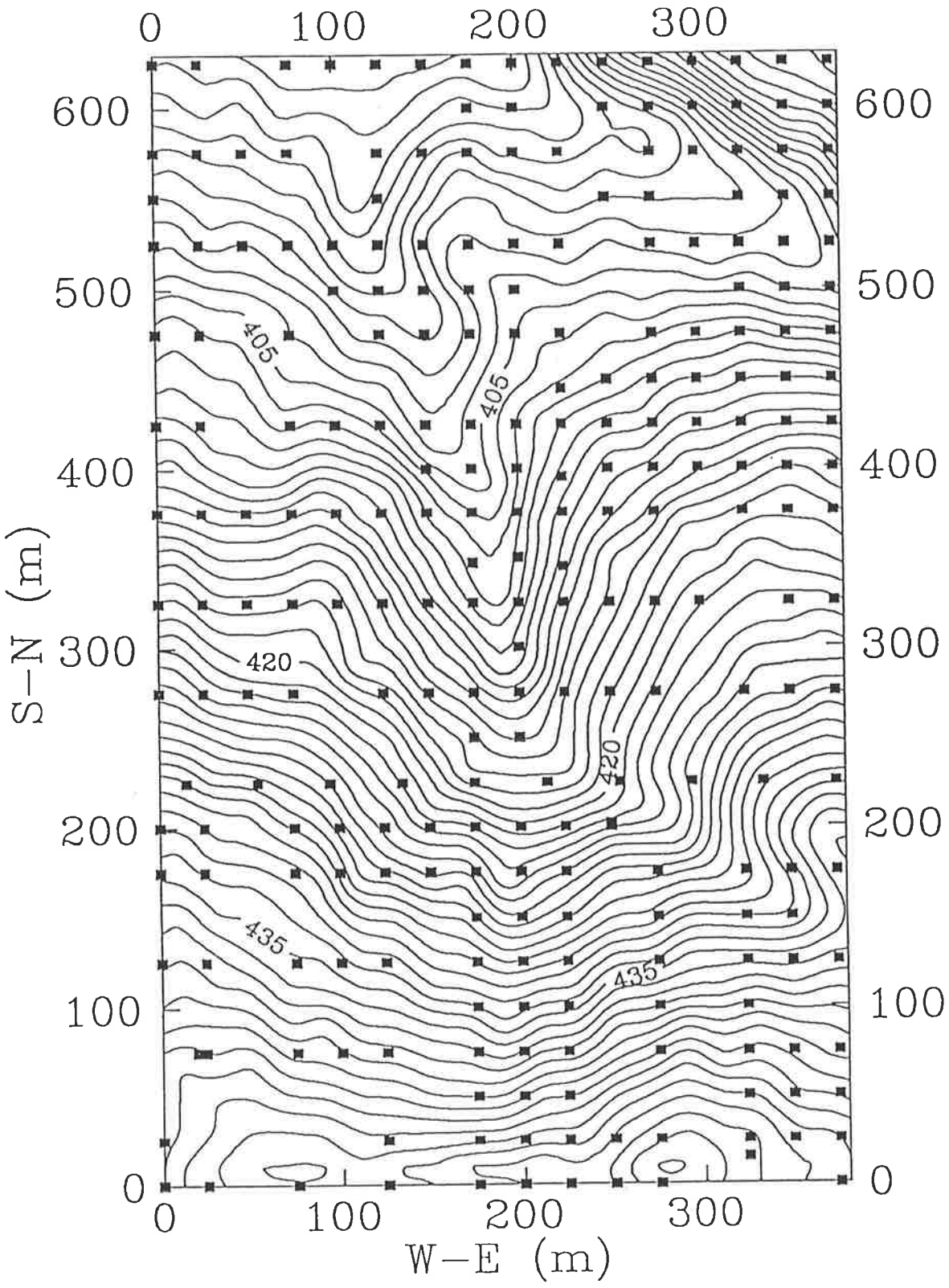

Fig. 6.2 Spatial layout of field sampling with solid squares denoting the observation points. Contour interval is 1 m and the closeness of the contours highlights the steepness of slopes. Some of the observations on relatively steep slopes are from paired samples with off-point sample at a distance of 2 m in the direction of the steepest slope.

also on whether variation is anisotropic or not. The choice of 50 nearest points for determination of optimal sampling schemes in chapter 3, subsection 3.2.5 was due to the fact that estimates were based on samples which were taken at close intervals along the transects (the closest sampling interval was 2 m).

6.3 Field Sampling and Laboratory Procedures

For the purpose of mapping the soil of the study area in two spatial dimensions, part of the subcatchment (Fig. 6.1) covering an area of 625 x 375 m was selected. The sampling strategy and laboratory procedures adopted are described.

6.3.1 Stratified sampling based on a predetermined sampling design

In chapter 4 (subsections 4.3.2 and 4.3.3), an optimal density of sampling for mapping the soil of the study area was recommended. In subsection 4.3.3, the soil segment boundaries along the transects, determined by a digital segmentation procedure, were found to be within the range of semivariograms computed from fuzzy (soil) class membership values. The coincidence of most of the boundaries along the transects with landform and lithologic features lead to the recommendation that sampling for two-dimensional mapping of soil of the study area be at a close intervals where these features are prominent. Among these features, slope gradient was the most important.

Fig. 6.2 shows the spatial layout of field sampling, following the recommendation. The contours, which are at an interval of 1 m, illustrate the steepness of slope gradients. Sampling interval was 10 m in some areas where there are lithologic discontinuities, evidenced by preponderance of quartz stone and gravel, and sharp differences in texture. In some other areas, sampling interval was much wider; 25 m in areas where slopes are relatively steep (> 15 %), 50 to 75 m where there is no obvious variation in landform and lithology. Some of the observations from locations where lithologic variation and slope

gradient were the determining criteria of sampling intervals were from paired samples with the off-point sample taken at a distance (commensurate with the degree of variation) in the direction of maximum variation. It was envisaged that the sampling strategy thus adopted would compensate for higher error of estimation at the spatial interpolation stage. Each of the 269 undisturbed soil cores to bedrock (diameter = 50 mm) were taken from accurately located points as illustrated in Fig. 6.2.

6.3.2 Morphology description and laboratory analysis

The soil cores were subsampled, and the morphological characteristics described and quantified following the procedures contained in chapter 3, subsection 3.2.3. In the laboratory, particle-size analysis was carried out on the subsamples, using the hydrometer method as described in chapter 3, subsection 3.2.4. Organic carbon (Oc), electrical conductivity and pH were not determined because, as it was found during the transect survey, their variations were shown not to be of agronomic significance, although variation of Oc was pedologically significant (chapter 5).

6.4 Fuzzy Analysis

Experience gained during the application of FCME to the transect data in chapter 4 made it comparatively simple to choose the parameters required for fuzzy classification of soil data obtained at this stage of survey. As was carried out with the transect data, three sets of soil data were analysed. Applying the FCME algorithm to the data, ϕ value of 1.15 was tried on the whole soil data, 1.13 on morphological data (whole soil data minus particle-size data) and, 1.25, 1.35 and 1.40 (these ϕ values are close to or equal to 1.35, the value validated for particle-size data in chapter 4) were tried on particle-size data. Three ϕ values were tried on particle-size data because, as observed in chapter 4, the particle-size variables are all of purely numeric type and therefore did not pose a convergence problem for the

FCME algorithm. For this reason, there were several plausible combinations of number of classes, c, and degree of fuzziness manifested by ϕ values.

As for the whole soil data and the morphological data, the ϕ chosen (i.e.,ϕ equals 1.15 for whole soil data and ϕ equals 1.13 for morphological data) were considered appropriate. To further validate the fuzzy classification of the two data sets, the F' and H' criteria described in chapter 4, subsection 4.2.3, were used to obtain the optimal number of classes, c. Both criteria indicated that c equals 7 and c equals 5 for the morphological data. The resulting membership matrices were accepted for further analysis.

Having used three values of ϕ for the textural data, it was considered appropriate to carefully examine the results of fuzzy analysis relative to the raw data. This was approached by comparing the class centroids resulting from fuzzy classification of the data, using each of the ϕ values, with the variable (particle-size) values for individuals (pedons) having given memberships, m_i. For a given ϕ value, individuals (pedons) with high membership values ($m_i \geq 0.5$) or low membership values ($m_i < 0.5$), that have variable values that do not deviate proportionately (in terms of membership values) from the class centroids, are less acceptable. Such careful examination indicated that ϕ equals 1.40 was most appropriate which is not much different from 1.35 used in chapter 4 for particle-size data. However, the optimal number of classes, c, equals 5, which is less than 6 as determined for the particle-size data in chapter 4. The probable reason for this is that the transects used in chapter 4, especially the W-E transect, traversed a wider geographical area and therefore incorporated more taxonomic individuals than the sampled area shown in Figs. 6.1 and 6.2 (compare Fig. 3.1 in chapter 3 with Fig. 6.1).

The membership matrix, $\boldsymbol{M}$, optimally produced by fuzzy classification of each of the data sets were used for kriging and subsequent isarithmic mapping.

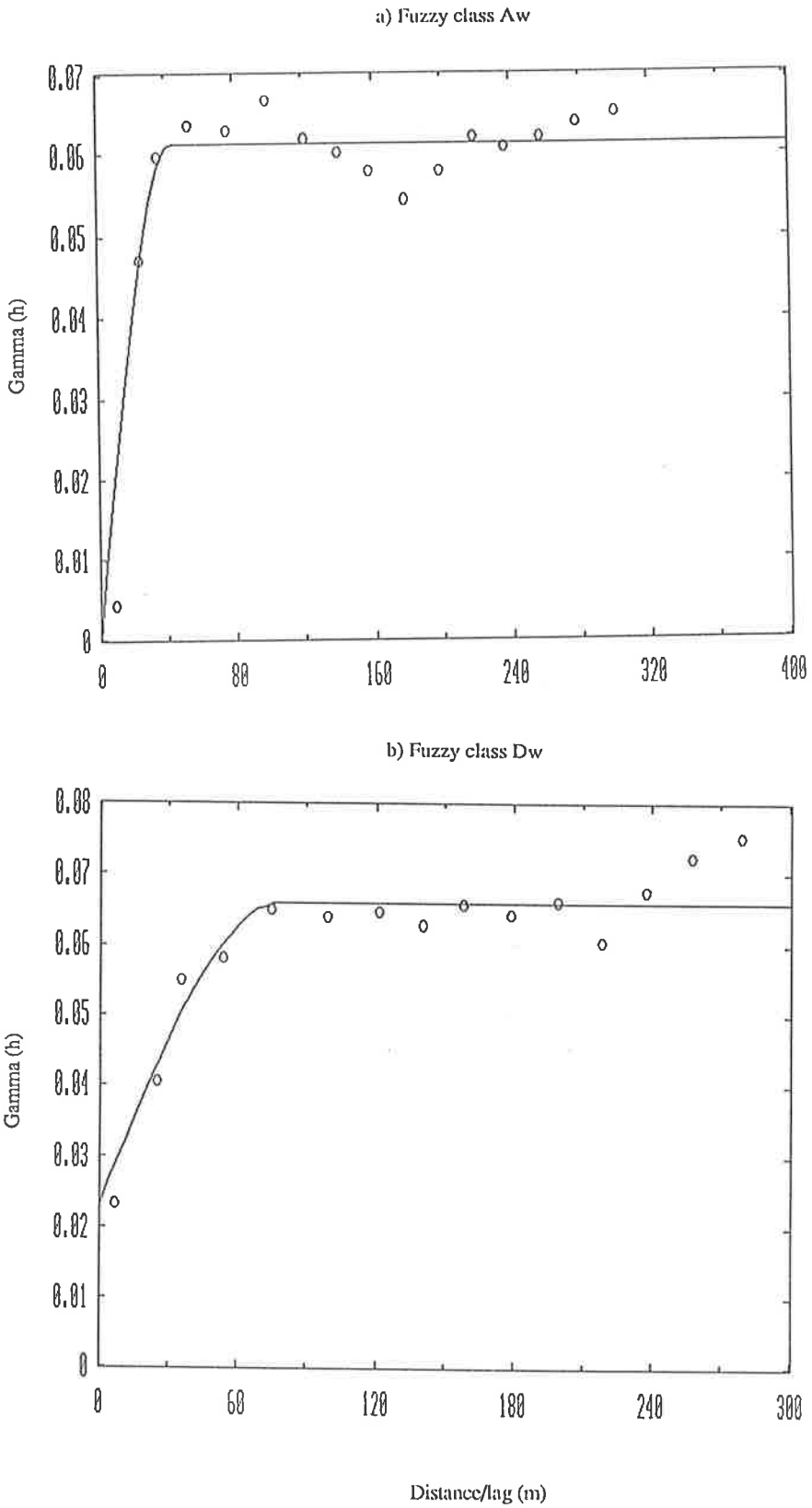

Fig. 6.3 Isotropic semivariograms of fuzzy class membership coefficients resulting from fuzzy classification of whole soil data: (a) fuzzy class Aw, (b) fuzzy class Dw and (c) fuzzy class Ew (next page); note that the gamma (h) is in membership coefficient squared.

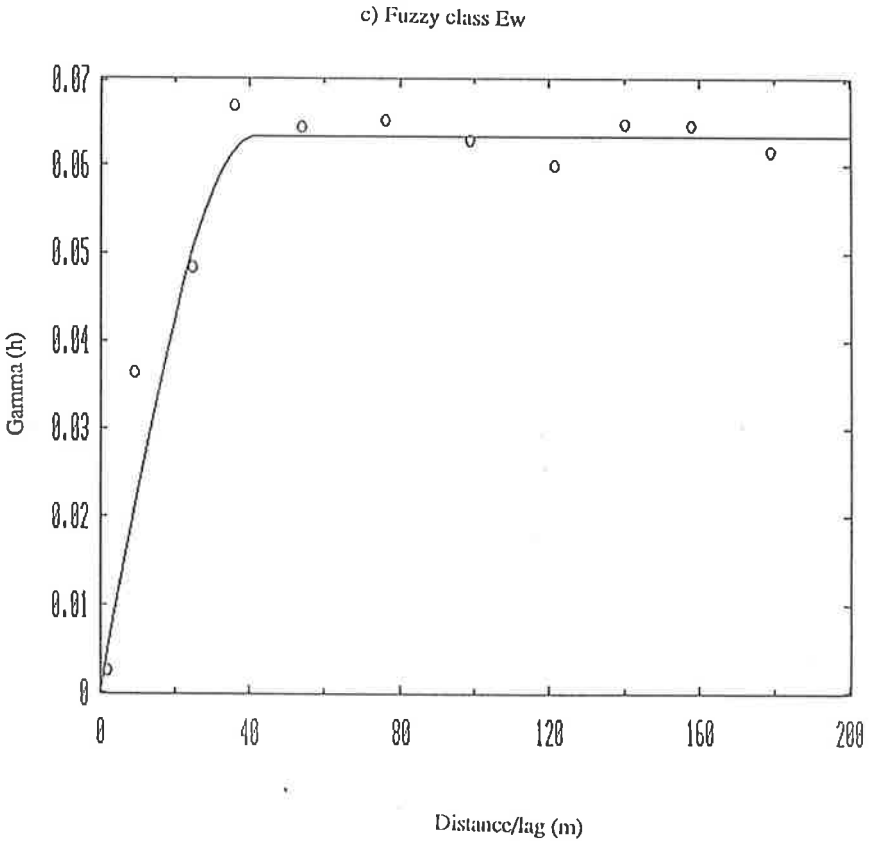

Fig. 6.3 (continued)

Isotropic semivariogram of (c) fuzzy class Ew; note that the gamma (h) is in membership coefficient squared.

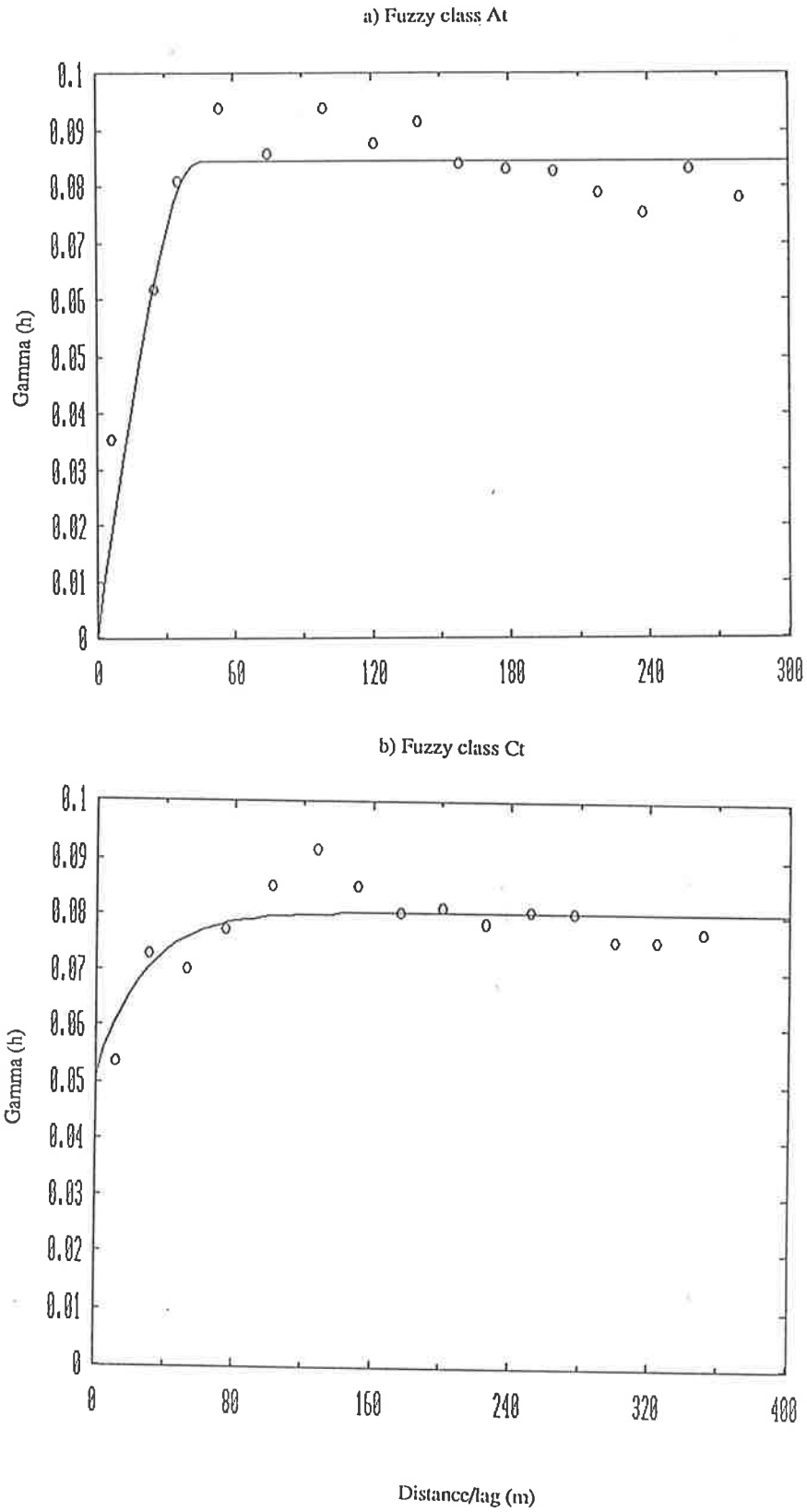

Fig 6.4 Isotropic semivariograms of fuzzy class membership coefficients resulting from fuzzy classification of particle-size data: (a) fuzzy class At, (b) fuzzy class Ct.and (c) extragrade class (next page); note that the gamma (h) is in membership coefficient squared.

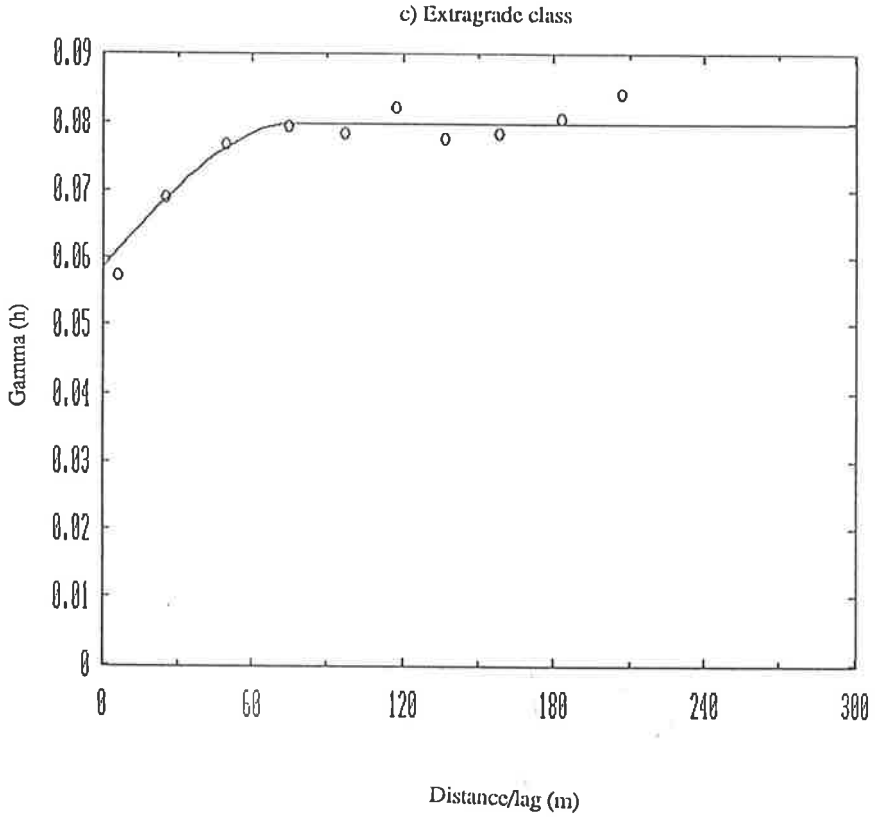

Fig. 6.4 (continued)

Isotropic semivariogram of (c) extragrade class; note that the gamma (h) is in membership coefficient squared.

Table 6.1 Parameter values of isotropic semivariograms for the soil classes resulting from whole soil data; note that the semivariances of soil classes are in membership coefficient squared.

Soil class	[1@] $\gamma(h)$	C_0	C	a (m)	Model
Aw	0.0613	0.0011	0.0602	44	spherical
Bw	0.0728	0.0513	0.0215	32	spherical
Cw	0.0682	0.0021	0.0661	54	spherical
Dw	0.0660	0.0229	0.0431	79	spherical
Ew	0.0654	0.0022	0.0632	43	spherical
Fw	0.0645	0.0035	0.0610	49	spherical
Gw	0.0722	0.0037	0.0685	58	spherical
Extragrade	0.0608	0.0035	0.0573	47	exponential

Table 6.2 Parameter values of isotropic semivariograms for the soil classes resulting from particle-size variables; note that the semivariances of soil classes are in membership coefficient squared.

Soil class	[1@] $\gamma(h)$	C_0	C	a (m)	Model
At	0.0845	0.0011	0.0834	45	exponential
Bt	0.0624	0.0259	0.0365	84	spherical
Ct	0.0759	0.0509	0.0250	32	exponential
Dt	0.0724	0.0031	0.0693	43	spherical
Et	0.0610	0.0008	0.0602	43	spherical
Extragrade	0.0832	0.0571	0.0261	76	spherical

[1@] The semivariogram parameters symbols have the same meanings as given in equation 3.2 in chapter 3

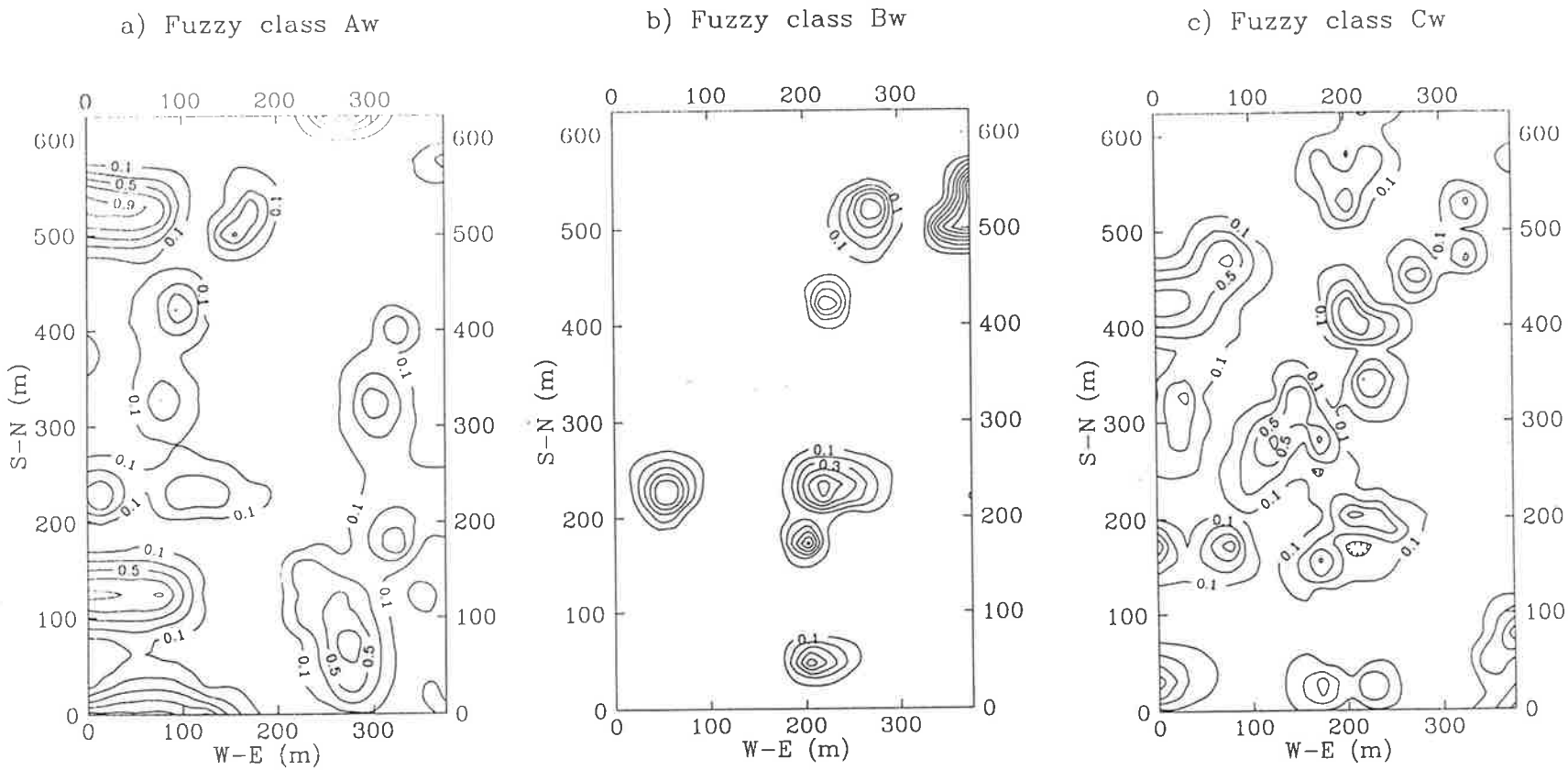

Fig. 6.5 Isarithmic maps of membership values of classes resulting from fuzzy classification of whole soil data.

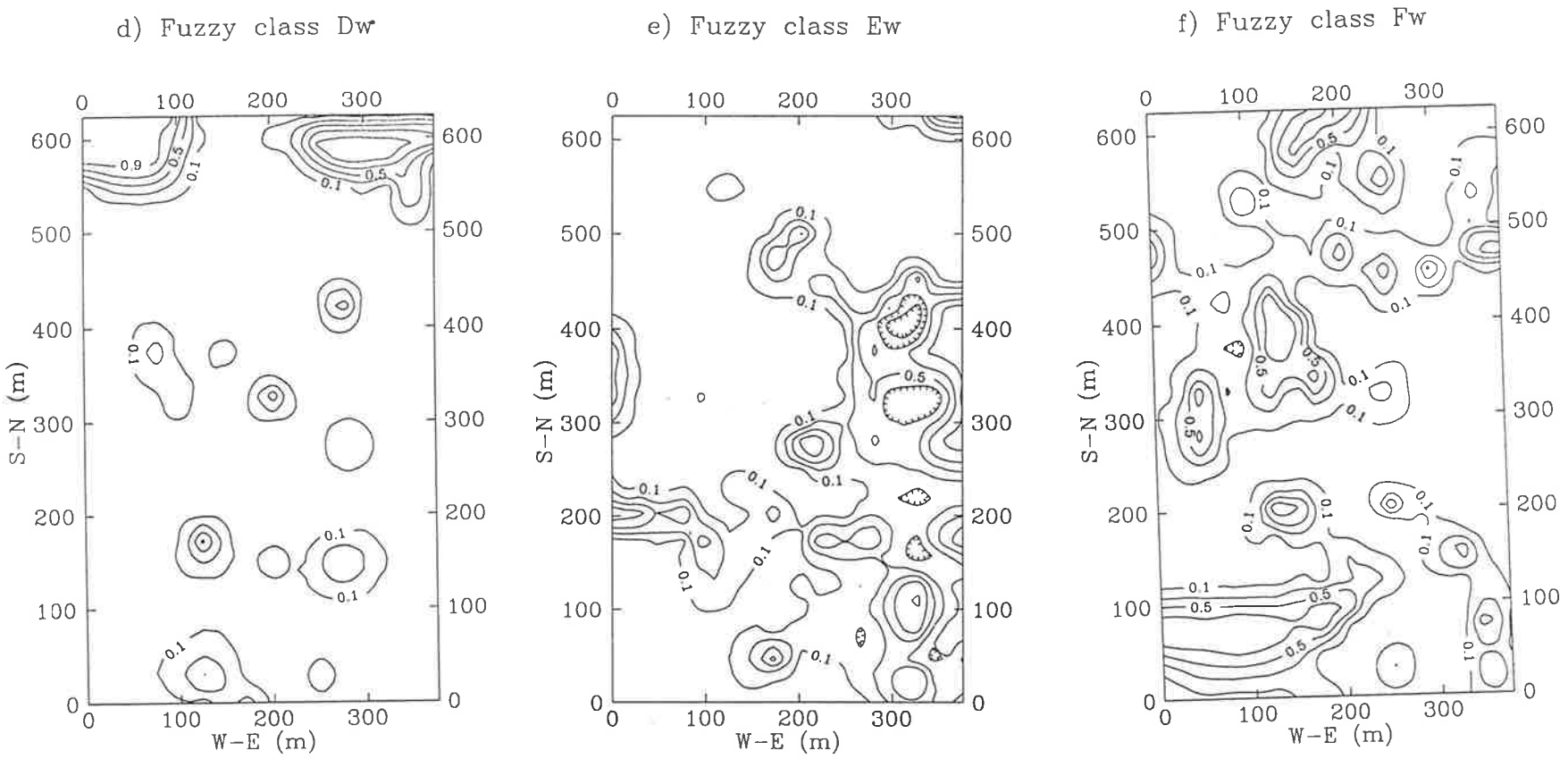

Fig. 6.5 (continued) Isarithmic maps of membership values of classes resulting from fuzzy classification of whole soil data.

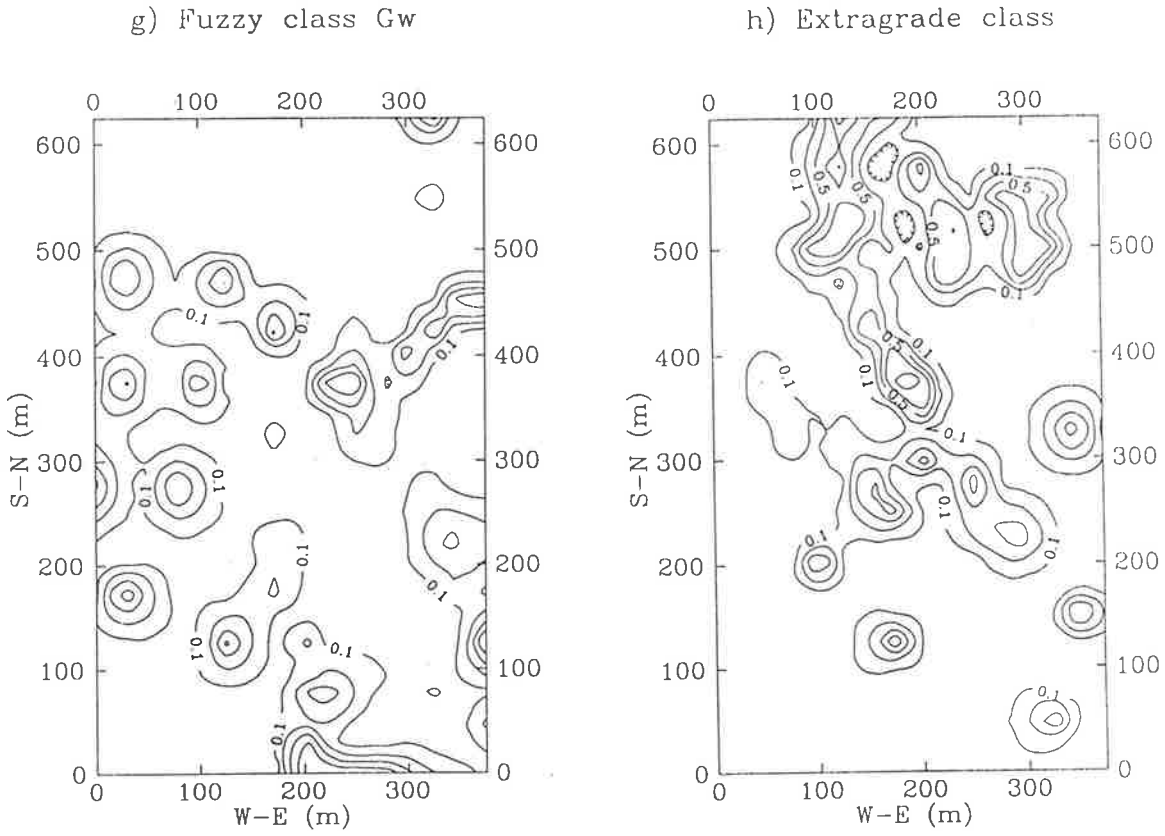

Fig. 6.5 (continued) Isarithmic maps of membership values of classes resulting from fuzzy classification of whole soil data.

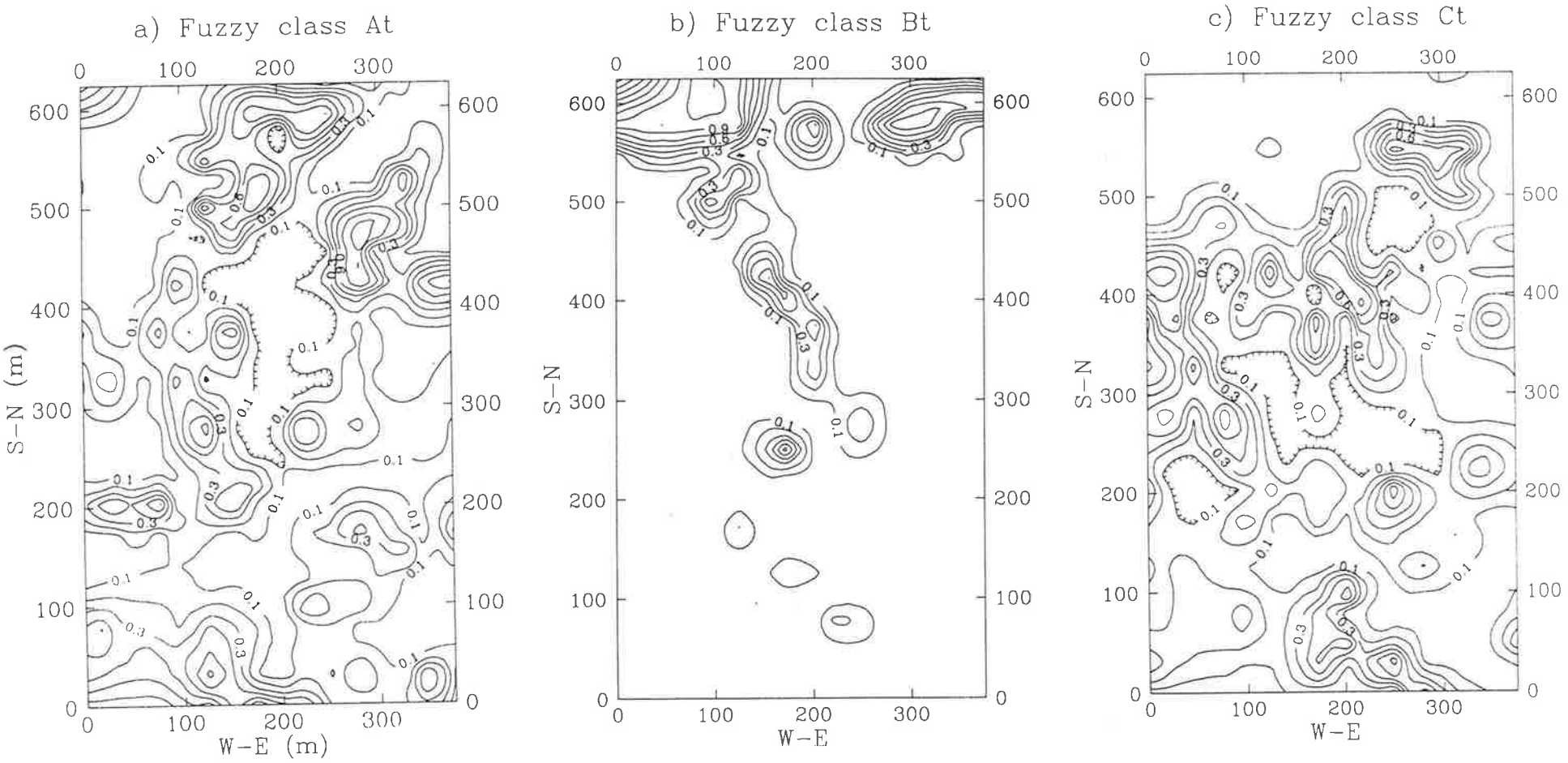

Fig. 6.6 Isarithmic maps of membership values of classes resulting from fuzzy classification of particle-size data.

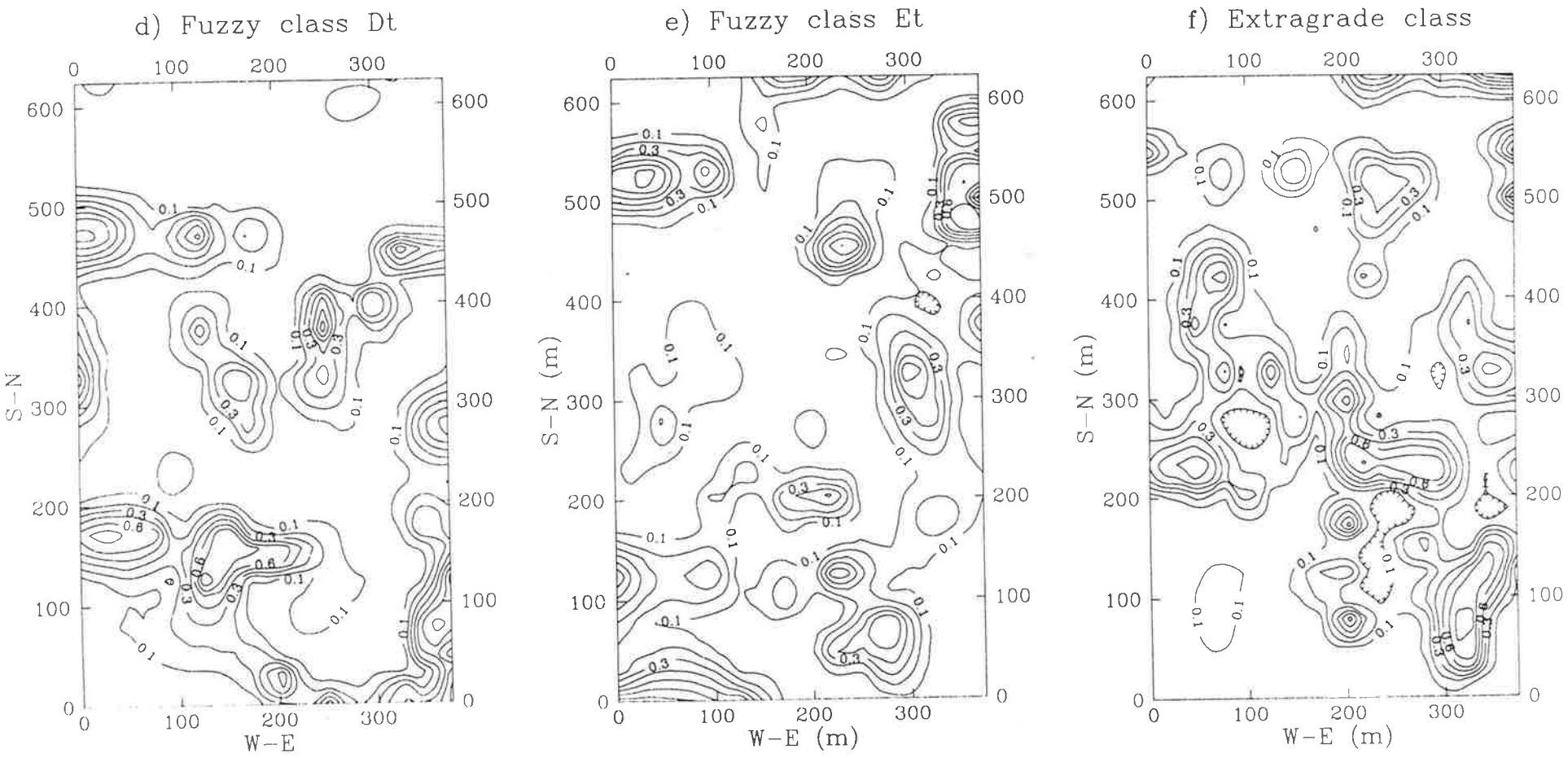

Fig. 6.6 (continued) Isarithmic maps of membership values of classes resulting from fuzzy classification of particle-size data.

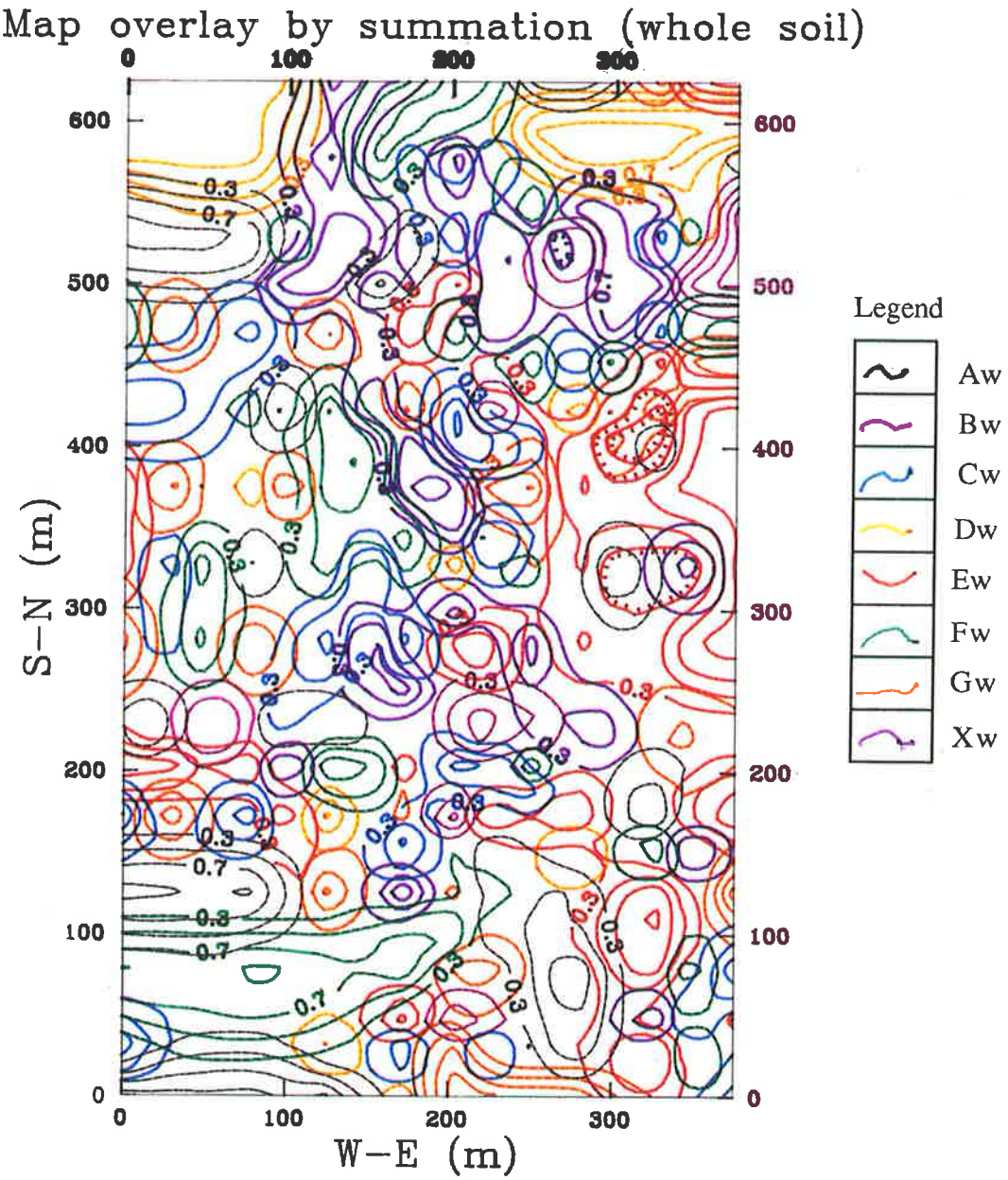

Fig. 6.7 Map overlay by summation (whole soil classes)

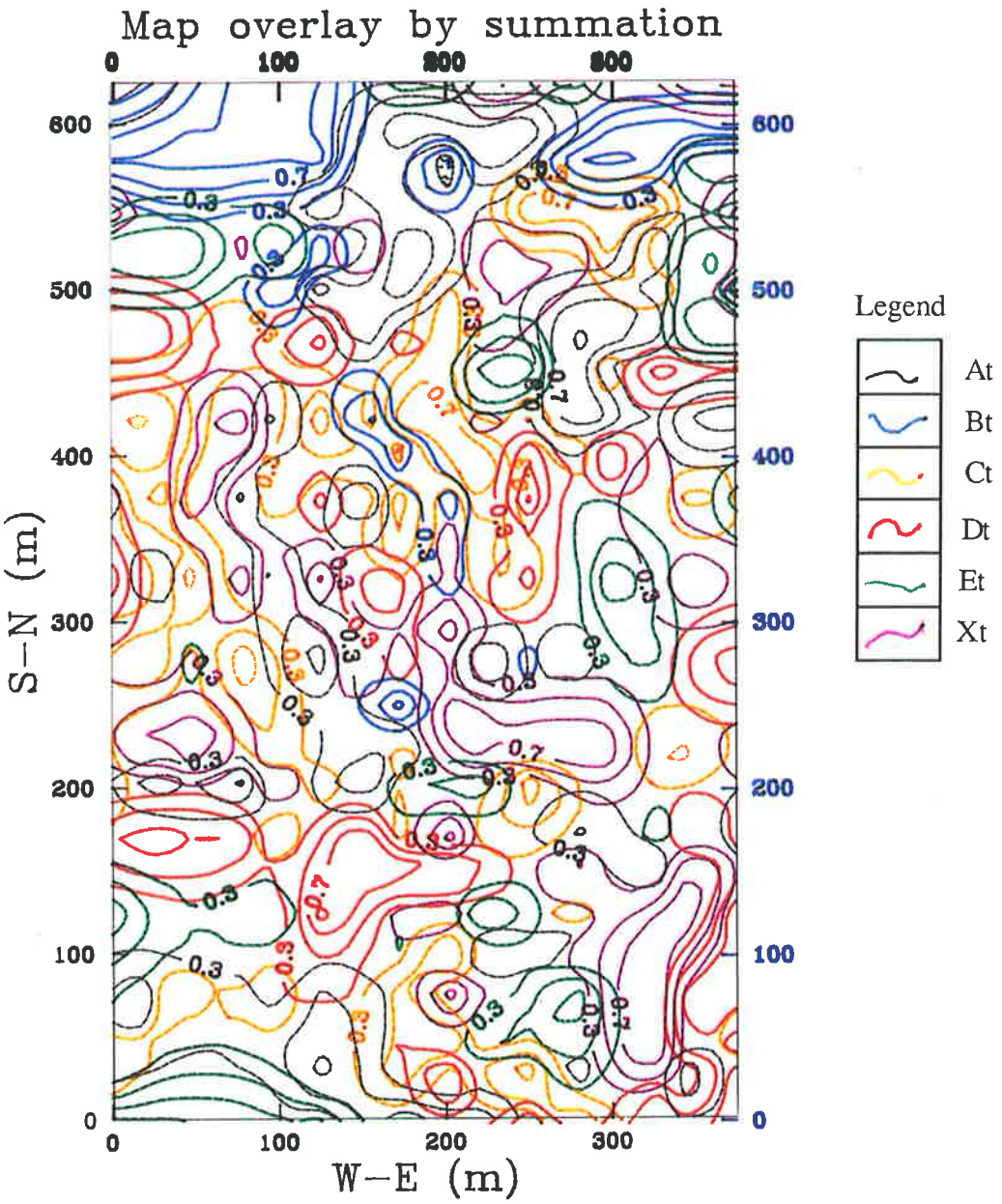

Fig. 6.8 Map overlay by summation (particle-size classes)

6.5 Kriging Analysis and Results

6.5.1 Kriging analysis

Taking a vector of membership values for each fuzzy class, c_j, of each of the membership matrices optimally produced by FCME for the data sets, semivariances were computed, using equation 3.1 in subsection 3.2.1 of chapter 3. This was done initially in four directions, $3\pi/4$, $\pi/2$, $\pi/4$ and 0, to determine whether there was anisotropic variation of any of the fuzzy class membership vectors, as found with transect survey in chapter 4. Surprisingly, there was no evidence of anisotropic variation for any of the fuzzy classes. A probable explanation for this is that in the transect survey, the density of sampling was sufficiently close to include more of the local variations than was the case with sample spacings shown in Fig. 6.2. The local variation thus included must have contributed to the anisotropy. However, it is to the author's satisfaction that sample spacings as shown in Fig. 6.2 adequately represent the general variation of the soil continuum.

The results obtained for morphological data indicated that semivariograms were of pure nugget type for all of the fuzzy classes, thus confirming the findings in chapter 4, subsection 4.4.4, that variation in soil morphology is erratic and represents short-range spatial changes.

The class membership semivariograms for the other two data sets: whole soil data and particle-size data, were fitted with both the spherical and exponential models and some of them are illustrated in Fig. 6.3 for the whole soil classes and Fig. 6.4 for the particle-size classes. The semivariogram parameters thus determined are shown in Table 6.1 for the whole soil data and in Table 6.2 for the particle-size data. These parameters were used for kriging as described below.

Results shown in Tables 6.1 and 6.2 indicate that membership values for the classes show spatial coherence as evidenced by the membership semivariograms. It is, therefore, appropriate to map these classes by kriging. Isarithmic maps resulting from point kriging are shown in Figs 6.5 and 6.6.

The figure fields from kriging were smoothed with cubic splines to remove spikes and pits on the contour lines to produce the maps in Figs. 6.5 and 6.6.

6.5.2 Composite maps- map overlays

All the maps resulting from a given set of data can be combined into a single map having $c + 1$ layers, where the sum of the memberships is 1 for a given point. This is map overlay by summation operator. The maps resulting from summation of memberships of fuzzy classes are shown in Fig. 6.7 for the whole data and in Fig. 6.8 for the particle-size data. These maps illustrate the very complex nature of the soil continuum with classes overlapping. A procedure to simplify the complex situation was , therefore, adopted.

One of the set-theoretic operations that is applicable to fuzzy sets is the "union" operation. For example, given two fuzzy subsets, A and B, the union of the two subsets is defined by:

$$\begin{aligned} m_A \cup m_B &= m_A \vee m_B \\ &= \max(m_A, m_B). \end{aligned} \tag{6.6}$$

This is an "OR" operation based on point attributes (Burrough, 1986), the locus of which is the point or pedon with vertical vectors of attribute values or fuzzy class memberships.

Recall the three conditions defining fuzzy classes in chapter 4, section 4.2:

(1) $\sum_{j=1}^{c} m_{ij} = 1 \qquad 1 \le i \le n$

(2) $\sum_{i=1}^{n} m_{ij} > 0 \qquad 1 \le j \le c$

(3) $m_{ij} \in [0,1]; \qquad 1 \le i \le n; \quad 1 \le j \le c$

condition (1) ensure that no two objects (pedons) should have the maximum membership of the same class, unless the two have equal memberships ($m_i = 0.5$) of a given fuzzy class; condition (2) rules out a non-empty class; and condition (3) allows for partial memberships of objects in the same class, thus ensuring overlapping of at least one pair of fuzzy classes. The significance of these conditions is that whereas some pedons may have high affinities for certain classes, others may have features that demand partial memberships in most or all of the fuzzy classes. This is a reflection of an intuitive idea of the real relationship between individuals of the data. Such a realistic relationship should be exploited to produce a single (composite) map highlighting all the optimally generated fuzzy classes from a data set, as they exist in the field. This is the ultimate aim of any soil surveyor.

Applying equation (6.6) to the fuzzy classes resulting from whole data and textural data revealed an interesting outcome of this operation. Given that the fuzzy classes generated from whole soil data are denoted by Aw, Bw,..., Gw and Xw, the last being the extragrade class, the union of the memberships of seven normal classes and the extragrade class to produce a composite map is defined by:

$$m_{Aw} \cup m_{Bw} \cup \ldots \cup m_{Xw} = \max(m_{Aw} > z, m_{Bw} > z, \ldots, m_{Xw} > z); z = 0.5, \qquad (6.7)$$

and the union of the textural classes, At, Bt, ..., Xt, is defined by:

$$m_{At} \cup m_{Bt} \cup \ldots \cup m_{Xt} = \max(m_{At} > z, m_{Bt} > z, \ldots, m_{Xt} > z); z = 0.5. \qquad (6.8)$$

In using equations (6.7) and (6.8), a lower limit of maximum membership was set to 0.5. because there were many fuzzy classes (not just a couple of them); the intragrade pedons that do not have high affinity for any of the fuzzy classes (i.e., those situations where pedons have low membership values of all the classes that are even or nearly so) were left out of the union operation. This is important as only pedons with maximum memberships of any class ($m_{ij} \geq 0.5$) would appear on the composite map, although, a couple of pedons that have equal memberships in a pair of fuzzy classes may still pose an overlapping

Table 6.3 The main features of the centroids for seven classes derived by FCME algorithm ($\phi = 1.15$) on whole soil data (italicized clauses describe the relative landscape location and the parent material, if transported)

Class	Main features of centroid
Aw	very shallow (14 cm) topsoil of dark brown, slightly gravelly (11 %) sandy loam, weak pedality (2.4) of granular structure; overlying yellowish red light medium clay with common (19 %) olive brown mottles, strong pedality (4.1) of subangular blocky structure; depth of solum = 72 cm; *occurs on gentle upper slopes and on crests, lower slope positions adjacent to low knolls*
Bw	very shallow (14 cm) topsoil of dark brown, moderately gravelly (27%) sandy loam, moderate pedality (2.7) of subangular blocky structure; overlying yellowish red light clay with few (9 %) yellowish brown mottles, strong pedality (3.7) of subangular blocky structure; depth of solum = 58 cm; *occurs in mid- to lower slopes (1-10 %).*
Cw	moderately deep (22 cm) topsoil of very dark brown, loamy sand, moderate pedality (3.2) of granular structure; overlying brown sandy clay loam with common-few (8-13 %) dark yellowish brown mottles, moderate pedality (3.4) of subangular blocky structure; depth of solum = 65 cm; *developed on colluvial material near slope breaks and on mini-depressions on sideslopes (5-10 %).*
Dw	shallow (18 cm) topsoil of olive brown, sandy clay loam, moderate pedality (3.0) of granular structure; overlying brown heavy clay with common (18 %) , moderate pedality (3.4) of angular blocky structure; depth of solum = 81 cm; *well developed pedons on alluvial material close to the major creek*
Ew	shallow (17 cm) topsoil of brown, very gravelly (30 %) loam, moderate pedality (23.3) of granular structure; overlying yellowish red light clay with few (8 %) yellowish brown mottles, strong pedality (3.8) of angular blocky structure; depth of solum = 52 cm; *occurs on crests and spurs.*
Fw	moderately deep (24 cm) topsoil of very dark brown, very slightly gravelly (6 %) sandy clay loam, moderate pedality (3.0) of granular structure; overlying dark light olive brown loam with few (8 %) yellowish brown mottles, moderate pedality (3.4) of subangular blocky structure; depth of solum = 83 cm; *on gentle slopes (1-5%) adjacent to the creeks and near the crests*
Gw	shallow (16 cm) topsoil of dark brown, slightly gravelly (12 %) sandy loam, moderate pedality (3.0) of subangular blocky structure; overlying dark yellowish brown heavy clay with few (9 %) olive brown mottles, strong pedality (3.6) of angular blocky structure; depth of solum = 76 cm; *occurs mainly on moderately steep upper to lower slopes; not extensive*

Table 6.4 Centroids of five fuzzy classes derived by FCME algorithm ($\phi = 1.40$) on particle-size fractions (italicised clauses describe the relative landscape location)

Class	Topsoil (%)				Subsoil (%)			Remark
	sand	silt	clay	gravel	sand	silt	clay	
At	57.18	29.78	13.03	7.35	28.75	27.58	43.67	sandy loam over clay loam *-mainly on relatively gentle lower and upper slopes (5-10 %)*
Bt	69.73	20.23	10.04	2.04	61.84	17.91	20.25	-sandy loam over sandy clay loam, most texturally uniform *-on gentle slopes (1-5 %) adjacent to the major creeks*
Ct	45.44	35.75	18.81	5.54	18.42	20.32	61.26	-loam over heavy clay *-on gentle slopes (1-10 %) at colluvio-alluvial junctions*
Dt	68.09	18.60	13.88	17.10	22.55	20.28	57.17	-slightly gravelly sandy loam over heavy clay, relatively coarse-textured *-mainly on steep slopes (> 15 %) and on or near slope breaks*
Et	51.73	29.19	19.08	29.80	33.20	24.05	42.75	-moderately gravelly sandy loam over sandy clay loam, also coarse-textured *-mainly on crest and spurs slopes (5-15%)*

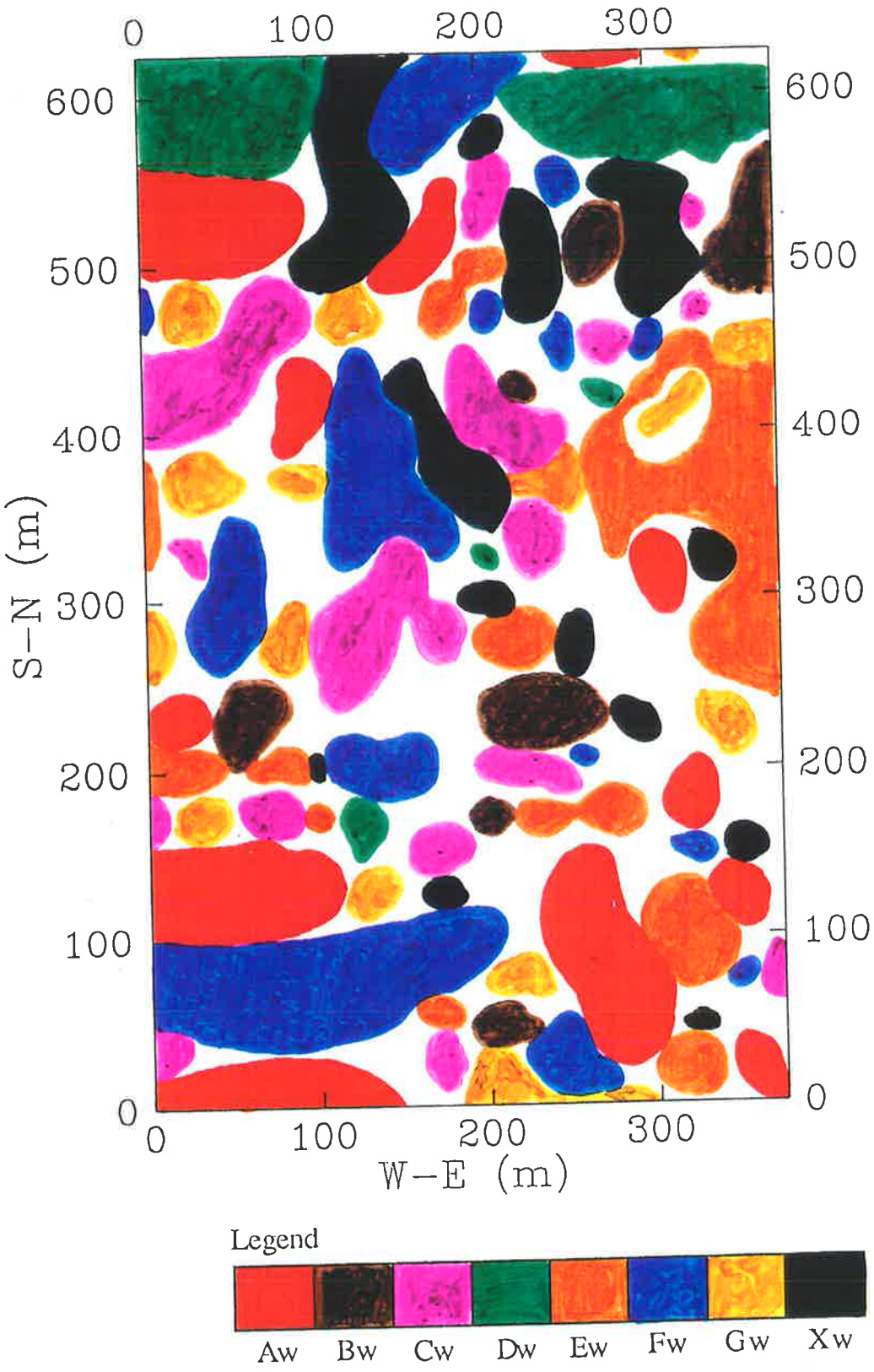

Fig. 6.9 Composite map showing the core areas of fuzzy classes resulting from the whole soil data; the main centroid characteristics of classes shown on the legend are described in Table 6.3

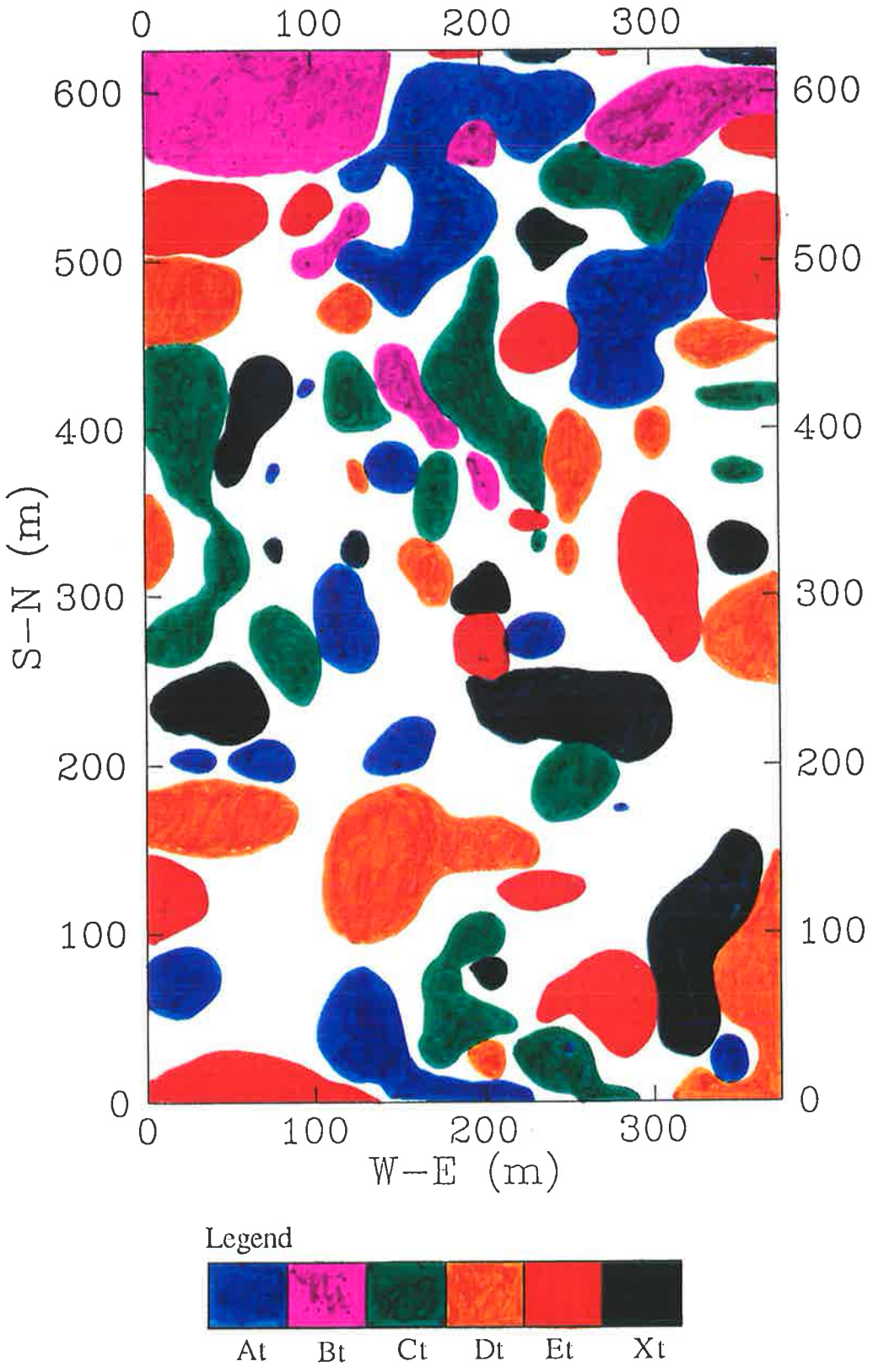

Fig. 6.10 Composite map showing the core areas of fuzzy classes resulting from the particle-size data; the centroids of classes shown on the legend are given in Table 6.4

problem. However, such a situation did not arise in the examples described here because of the many fuzzy classes optimally generated by FCME and the fact that most pedons have some degree of affinity for more than a couple of fuzzy classes. The composite map in Fig. 6.9 for the fuzzy classes resulting from whole soil data and the one in Fig 6.10 for the fuzzy textural classes show the core areas of various fuzzy classes. They were produced by overlay of the isarithmic maps shown in Fig 6.3 (whole soil classes) and in Fig. 6.4 (textural classes). The blank spaces between the core areas constitute the intragrades that represent the transitional pedons, i.e., the pedons belonging to several fuzzy classes with membership value less than 0.5 for any of the classes.

6.5.3 The class centroids

The class centroids described in Tables 6.3 (for the whole soil data) and 6.4 (for the textural data) give the main characteristics of the pedons in the core areas of their respective composite maps. Comparison of the typical features given in Table 6.3 with those in Table 4.4 (chapter 4), and those in Table 6.4 with Table 4.5 indicates similarities between fuzzy classes generated from the same soil features. However, some differences occur because the soil chemical properties that were among the soil features analyzed in the whole soil data were left out here, and because the geographical tracts covered were different- transects in chapter 4 and a 625 x 375 m area for the study reported here.

The centroids describe the feature characteristics of the typical pedons of fuzzy classes represented in the legends (Figs. 6.9 and 10.).

6.5.4 The extragrade units

The composite maps (Figs. 6.9 and 6.10) show the extragrade core areas (geographical units) that have spatial correlations with certain landscape positions and slopes (Table 6.3 and 6.4). As explained in chapter 4, subsection 4.4.4, the extragrade members (pedons that

have memberships of extragrade class, $m_{ij} \geq 0.5$) are atypical and are considered as part of the "impurities" interspersed with or within the typical classes. They are the pedons that have either very low or very high values of one or more of the variables used for classification. Surprisingly, the extragrade classes for the two data sets exhibit spatial coherence as their semivariograms (Tables 6.1 and 6.2), isarithmic maps (Figs. 6.5-g and 6.6-f) and the composite maps (Figs 6.9 and 6.10) indicate.

The extragrade units on the composite maps could be regarded as complexes (Hole and Campbell, 1985), defined as the "assemblage of contrasting" soil units "occurring in patterns that changes so frequently that detailed mapping of them would be of no practical value". Their inclusion here is to illustrate their presence and to show the efficiency of the FCME algorithm in extracting the plausible groups in a data set while excluding the atypical members.

6.5.5 Physical interpretation- relationships of soil patterns with landform

In chapter 4, subsection 4.4.4, it was shown that some of the fuzzy classes (and the extragrade classes as discussed above) occur in association with certain landscape positions and slopes along the transects. Figs 6.5 and 6.6 show this association in two-dimensional area. The relative landscape positions and the slopes of the various fuzzy classes are presented in Tables 6.3 for the whole soil data and 6.4 for particle-size data. This association has confirmed the hypothesis raised in chapter 4 that the nature of soil variation is related to the complexity of landscape processes of which slope gradient exerts the dominant influence. However, the degree of influence varies from one group of soil features to others. Thus the spatial continuity (and contiguity) of fuzzy classes is much influenced by the soil features used for classification. Figs 6.9 and 6.10 attest to this premise.

6.5.6 Relevance to geographical information systems (GIS)

In Chapter 5, it was shown how remotely sensed elevation data can be utilized to study the soil-landform interactions. The digital elevation data obtained photogrammetrically, were re-analysed to produce the landform parameters which in turn were correlated with the ground-acquired data, the soil variables. The collective approach from remote sensing through aerial photo analysis to earthbound survey for acquisition of soil data, is an integral part of geographical information systems, or GIS. On the other hand,the results of fuzzy classification in Chapter 4, and the discussion contained in subsection 6.5.5, above have demonstrated the importance of landform and lithology to field sampling for spatial interpolation. In fact, the actual field-sampling layout (Fig. 6.2) was in response to the recommended sampling design in Chapter 4 - progressive increase in sampling density as the spatial changes in the landform and lithologic features increase. In this sense, the mapping tools that are essentially of GIS have been utilized to sample the soil for fuzzy classification. The questions then are: how do we integrate the resulting fuzzy (soil) class membership values into GIS? or could the fuzzy sets theory be applied to analyse other GIS information? If the answers to these questions are in the affirmative, then what are the benefits?

The answer to the first question is certainly positive. It has been demonstrated already, in this Chapter, how point (or pedon) memberships in various classes can be utilized for map overlay by the set-theoretic operations, summation and "OR/max". Whether this has some beneficial outcomes is still unanswered, but any system or output that represents a set or subsets of objects as they exist in the real world can be regarded as most accurate. The map overlays represent the soil as a continuum as it is in the real world. Thus the fuzzy classification techniques allow for more accurate information transfer. A soil parameter value could be estimated for any geographical location within the mapped area, if its membership of fuzzy classes are known. This could be achieved by weighted means of all the class centroids, the weights being the class membership coefficients. In contrast, the conventionally produced maps are shown to have discrete units representing the supposedly

"uniform" soil classes. Thus, if the within unit variance is high, the predictor, which is the class mean, cannot be transferred to other unsampled locations with any reasonable confidence.

Application of fuzzy sets to analyse GIS data other than or in addition to soil is yet to be tested. Considerable benefits could be accrued from such application possibly with FCME algorithm integrated into the GIS with the option of retrieving and analysing those variables that are desired.

After all is said and done, the results of interpolation for isarithmic mapping of fuzzy class membership values and the subsequent map overlay discussed here has illustrated that the fuzzy classification approach has a significant role to play in GIS.

6.6 General Remarks and Conclusions

The combined use of the theory of regionalized variables and fuzzy sets has enabled the mapping of soil as a continuous entity. Whereas the fuzzy set calculus was used to generate the continuous soil classes (quantified by the class membership coefficients), kriging which is based on the regionalized variable theory, was used for optimal interpolation of the membership coefficients. Isarithmic maps resulting from kriging techniques show the loci of the pedons of the fuzzy classes and the extragrades. However, the main motive for using fuzzy sets here (and indeed elsewhere in the thesis) was not to deal in any way with the concept of "vagueness", a term used for inexact description of objects or vague language. Recently, Burrough (1989) reported a number of examples of soil surveys in which fuzzy sets were applied in the context of "vagueness".

In a similar manner to the method used here, Burrough (1989) used point kriging to isarithmically map the fuzzy membership grades resulting from "AND" or "OR" operations that answered certain land evaluation questions.

The composite maps (Figs 6.9 and 6.10) produced from the "OR" operation indicate variable width of transitional areas between the core areas of optimally generated fuzzy classes. Close contacts between the core areas are a manifestation of sharp changes between

the core areas, although the maximum value of the digital gradient, g, as defined in chapter 4, subsection 4.3.3, is 0.5 (note that the lower limit of maximum operator as used in the "OR" operation was set to 0.5). This implies that transition between core areas is more gradual than the close contacts appear to indicate. If there were to be absolutely sharp boundaries between two areas (i.e., $g = 1.0$), fuzzy sets would take care of such a situation provided that all the three conditions defining fuzzy sets are met. The "hard" set is a special case of fuzzy sets (Bezdek, 1981) as one of the conditions defining fuzzy sets, $m_{ij} \in [0,1]$, allows membership values between and including 0 and 1. Such abrupt changes were not encountered in the examples described here.

A definite problem with the fuzzy sets approach is the difficulty associated with wrong perception of the soil as a continuous entity. This is because we are drawn to make sense out of a complex situation by imposing sharp cut-offs within the universe of an entity. If a real cut-off is absent, spurious ones are created. This invariably impairs our ability to appreciate the extra information about the entity we are trying to perceive (McBratney and Moore, 1985). The colouring of the core areas of the composite maps was to enhance our perception of the continuous nature of soil variation although this needs to be improved upon. Perhaps, improvement could be achieved by better colour graphics with variable colour combinations in the transition areas between the core areas. This is not an insurmountable problem.

CHAPTER 7

GENERAL SUMMARY AND CONCLUSIONS

7.1 Summary

Three quantitative approaches to pedological studies are dealt with in this work which is based on investigations carried out in a subcatchment near Forreston in the Mt. Lofty Ranges of South Australia.

First, is the geostatistical approach which offers the possibility of quantifying the spatial variation of a soil property and its range of spatial dependence, and thus facilitates the design of an optimal sampling scheme at the initial stage of the soil survey. To this end, Chapter 3 describes and discusses the first stage of field sampling which was carried out along two transects laid across the length and breadth of the subcatchment. These transects traversed the most apparent variability in the landscape. Semivariogram estimates, determined for a number of spatially dependent soil properties, were used to devise optimal sampling schemes. The results highlighted the difficulty in selecting a sampling scheme that provides a satisfactory compromise for all the properties used. The complexity of the soilscape is such that spatial changes in soil properties do not coincide. In addition, there are soil variables that showed discrete variations that need to be included. In order to alleviate this problem, a suitable means of reducing the number of soil variables to a manageable number, that still show spatial coherence of soil as a whole, has to be adopted.

The second quantitative approach attempted to redress the limitations posed by the geostatistical approach. This is contained in Chapter 4. This approach recognizes that soil variation is more continuous than discrete, and thus should be incorporated into soil classification and mapping. Fuzzy set theory provides such an approach that quantitatively assigns individuals into geographically and taxonomically continuous classes. It was hypothesized that the fuzzy-c-means algorithm, based on a fuzzy objective functional, could

be used to quantify pedons into intragrade and extragrade classes, and that minimization of the functional would allow for the most "precise" classification which could be validated by mathematically heuristic methods. These methods assume that local extrema (or abrupt changes) in the value of the objective functional or its derivatives indicate optimal grouping.

The fuzzy approach was applied on the data obtained for the two transects. The resulting fuzzy classes, which could be regarded as continuous, were found to have reasonable spatial continuity and contiguity which were associated with local variation in slope features and lithology. Thus the spatially dependent and spatially discrete soil variables (the latter are mostly morphological properties) were incorporated into a matrix of class membership coefficients. From this matrix, semivariograms were estimated from the membership values of each class. The semivariograms were used to devise a more realistic (in terms of soil as it exists in the field) sampling strategy for isarithmic mapping of class membership values. Soil boundaries along the transects, detected by the method of digital gradient segmentation, further confirmed the association of soil changes with local variation in landform and lithology. The optimal density of field sampling was devised in relation to slope and lithologic features.

The problems of extragrades and how to determine the appropriate degree of fuzziness for an optimal number of classes, were also addressed using the FCME algorithm. Whereas the (mostly) discrete data posed some problems of convergence in the FCME algorithm and, therefore, there were fewer options from which an optimal number of classes could be obtained, the continuously variable set of data, e.g. particle-size fractions, showed a wide range of "good" combination of c, the optimal number of classes and ϕ, the degree of fuzziness. In choosing the optimal number of classes for the first type of data the F' and H' criteria were used. However, choosing an appropriate degree of fuzziness was guided by intuitive notions. In the latter type of data, a derivative of the objective functional was used to gauge for the degree of fuzziness after using the F' and H' criteria to select few options of the possible number of classes.

The results obtained by FCME algorithm are quite similar to the ones obtained by the FCM algorithm for optimal sampling design, in terms of spatial continuity and contiguity of

classes in relation to landform and lithologic features. The atypical pedons were, however, assigned into the extragrade class. These atypical members could be regarded as part of the "impurity" that is interspersed with or within the map unit delineation or soil complexes, as used in the traditional methods. The importance of the assignment into extragrade class (and indeed into typical classes) depends on whether the differences in the definitive features call for different management. However, it shows the effectiveness of the FCME algorithm in assigning pedons into plausible classes and differentiating the atypical pedons.

In Chapter 5, the need to elucidate the cause of soil variation in the study area was examined. Thus, the third approach involved the application of commonly used multivariate methods in ecological studies to elucidate the causes of soil variation. It was hypothesized that landform, especially slope gradient, was the major factor influencing soil distribution patterns in the subcatchment. Therefore landform attributes of gradient, profile and plan convexity, aspect, upslope area and upslope distance were estimated, using a nine-parameters quartic equation, for points coinciding with sampling locations along the transects. The landform attributes were correlated with soil variables using canonical ordination methods assuming different models. Standard redundancy analysis (RDA), following data transformation, gave a clearer insight into pedogenetic implications of soil-landform interactions than canonical correspondence analysis (CCA). This was because interactions among soil variables and/or between soil variables and landform attributes were either more linear than unimodal or, if non-linear, were not unimodal.

Of all the landform attributes used in the analysis, gradient angle, plan convexity, profile convexity and to a lesser extent, upslope area and distance, were shown to have accounted for much of the spatial changes in soil properties in the study area. The slope gradient influences the distribution of surficial particles indicating selective removal of fine materials from the steep slopes and their subsequent deposition on the gentler slopes. That higher subsoil clay percentages were associated with concave slopes may be ascribed to either increased weathering and/or influx of material due to convergence of water flows. Depth of sola and depth to bedrock, which are dependent on the nature of parent material, also appeared to have controlled processes which are more pronounced in the relatively deep

lower-slope pedons. This is evidenced by cutans in their subsoil layers. Soil drainage conditions seemed to have been influenced by soil depth attributes as these in turn were influenced by slope, upslope distance and area. This was manifested in the manner of spatial changes in both topsoil and subsoil colours. Thus the results of the multivariate analysis confirmed the relation of segments boundaries along transects with landform and lithology, thereby considerably improving the detailed understanding of soil genesis in the study area. The significance of this is that land unit delineation to define sampling pattern should prove to be a useful first step, prior to soil survey, by improving sampling efficiency and reducing classification errors.

Finally, the ultimate product of spatial modelling of distribution pattern of soil is the soil map. In Chapter 6, methods and analyses involved in the making of soil maps that reflect the continuous nature of soil are discussed. By implementation of an optimal sampling scheme envisaged in Chapter 4, i.e., one which took into consideration the relationships of soil with conspicuous changes in landform and lithology, isarithmic maps of the fuzzy classes were produced. This was achieved by combined use of the theory of regionalized variables and fuzzy sets. Whereas the fuzzy set calculus was used to generate the continuous soil classes, kriging, which is based on the regionalized variable theory, was used for optimal interpolation of the membership coefficients. The maps resulting from kriging techniques show the loci of pedons in the fuzzy classes and the extragrade classes. Composite maps were produced by "OR" set-theoretic operation. The maps indicate variable width of transitional areas between the core areas of optimally generated fuzzy classes. Close contacts between the core (coloured) areas are a manifestation of sharp changes between the fuzzy classes dominant in the core areas, although the maximum value of digital gradient , g (as defined in Chapter 4) is 0.5. Thus, transition between core areas is more gradual than the close contacts appear to indicate. Had there been absolutely sharp boundaries between two areas, i.e. $g = 1.0$, fuzzy sets would have taken care of such situations as the "hard" set is a special case of fuzzy sets.

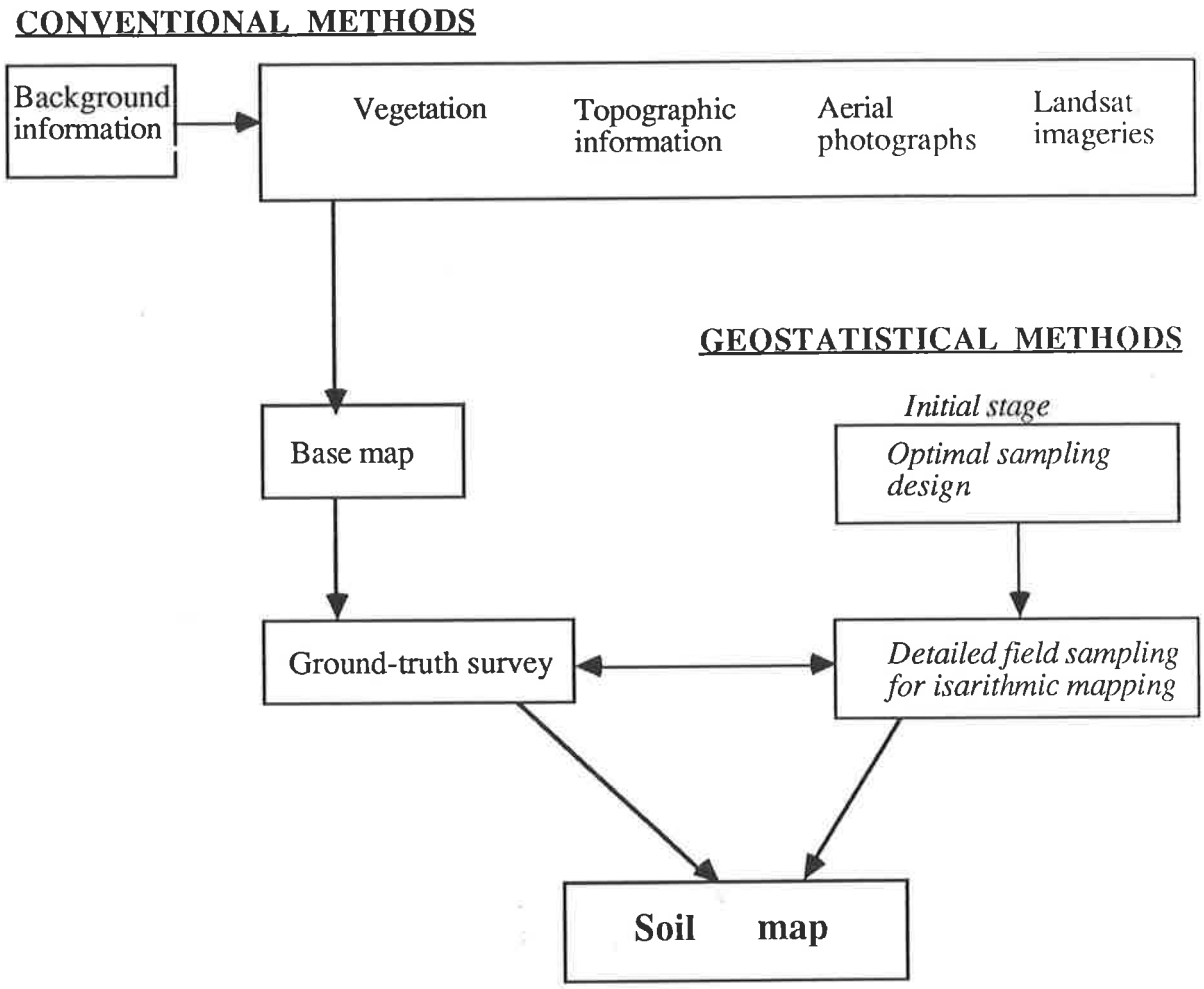

Fig. 7.1 The possible pathways to spatial modelling of soil

Fig. 7.1 shows some of the current methods used for spatial modelling of soil. The conventional approach makes use of the environmental information that has some correlations with soil to produce the basic map. This is followed by some ground-truth survey from which the final soil map evolved. However, the geostatistical methods involved an initial work for an optimal sampling design at the final stage of the survey. Kriged estimates from data obtained during the detailed field sampling are used for isarithmic mapping of the measured soil properties. Thus the purely geostatistical approach involves direct field survey and sampling right from the initial stage of the survey.

The spatial modelling techniques used in this work constitute a hybrid of the two approaches described above, in which an optimal sampling scheme was established to be linked with the slope and lithologic features. These features, in conjunction with the geostatistical sampling scheme for mapping the soil as a whole, were used to design the sampling pattern for isarithmic mapping of the fuzzy soil classes. Thus the hybrid approach involving the use of slope features, lithologic variation, data transformation (fuzzy classification) and geostatistical techniques in addition to cartography, constitutes some of the major tools of the GIS.

7.2 General Conclusions

The three quantitative approaches have demonstrably been used to elucidate soil patterns in the subcatchment. From this work, therefore, the following general conclusions are drawn:

(1) Whereas the theory of regionalized variables has successfully been used to spatially model individual soil properties of an area, it has been shown here to be difficult where the soil as a whole is to be modelled. The soil is a multivariate entity with its parameters showing spatial variation at different scales, i.e., the complexity of the soilscape is such that spatial changes in soil properties hardly coincide.

(2) Soil has long been recognised as a continuous system in both a geographical and taxonomic context. The application of fuzzy sets to soil classification and mapping takes this into account. Thus the approach is more realistic than the conventional approach as the former reflects the (usually) gradual variation and fuzzy boundaries of soil in the field.

(3) The fuzzy classification approach is more flexible than the conventional methods. The latter method involved assignment of pedons into predetermined

classes or existing classification. Most existing general classification schemes produce classes that do not correspond to local soil conditions (McKenzie and Austin, 1989). Whereas, FCM and FCME allow for any number of classes within the fuzzy-c-partition space $1 < c < n$ (if the soil is homogeneous or there is no plausible groupings in the area being surveyed, then classification would not be necessary) from which an optimal number of classes could be chosen by mathematically heuristic methods. An optimal number of classes thus chosen could be regarded as a realization of some structural organization due to some physical processes.

(4) Redundancy analysis (RDA) following data transformation (which was found to be better than other canonical ordination methods) gave a clear insight into pedogenetic implications of soil-landform interactions. The significance of this is that it has been shown quantitatively, the extent to which certain landform attributes affect soil development and distribution patterns.

(5) Segmentation of soil along transects by means of a digital gradient procedure revealed the correlation of soil (boundaries) with environmental markers which were predominantly landform and lithologic features. Thus field-sampling in the main survey was enhanced by progressively increasing sampling intensity in the locations where changes in these features are conspicuous.

(6) The application of spatial analysis as used in geostatistical survey, combined with fuzzy classification techniques, enabled the interpolation of membership values of soil profile data which yielded isarithmic maps, and therefore provided better information transfer.

(7) In comparison with the conventional methods of soil survey and classification, where values of the typical pedon of a mapping unit are transferred to

any geographical location within the unit, the fuzzy set approach allows for more accurate information transfer. Thus the soil variable values could be estimated for any geographical location within the mapped area, if its memberships of fuzzy classes are known, by weighted means of all the class centroids, the weights being the class membership coefficients.

Table 7.1 Comparison of conventional, geostatistical-conventional and geostatistical soil surveys

Characteristic	Conventional survey	Geostatistical-conventional survey	Geostatistical survey
Scale	1000-1 km small-medium	100 km-10 m medium-large	100 km- 10 m medium-large
Prediction/ information transfer	soil class (mean)	soil class (membership) semivariogram	soil attribute semivariogram/ cross-semivariogram
Assumed continuity	discontinuous	semi-continuous	continuous
Number of properties	may be many or few diagnostic	few-many	few
Precision	unknown-low	medium-high	medium-high

7.3 General Remarks and Suggestions for Future Research

7.3.1 Remarks

As stated in chapter 6, philosophical objections may be raised by the logical implications of building a mathematical structure on the premise of soil continuity, epitomized by fuzziness. This is because of the aesthetic attractiveness of the orthodox approach to the mapping of soil which requires that an object either belong to a class or not

at all. However, uncertainty is associated not only with randomness and measurement errors, but also with vague description and the continuum nature of soil variability. This shows that fuzzy sets have an intuitively plausible philosophical basis worth pursuing and is the basis for using fuzzy sets to model the soil continuum in this work.

The field sampling design used in Chapter 6 is somewhat comparable with conventional approach to field survey in that it takes into account the strong relation between soil and the environment, in this case slope and lithologic features. As Dudal (1986) put it, "the use of modern and quantitative methods should not detract from the experience of co-variance between the soil and the various elements of landscape. They should blend with each other". This novel approach which involved stratified field sampling and the subsequent geostatistical interpolation of class membership values represents the hybrid of the conventional approach and the geostatistical approach termed here as "geostatistical-conventional survey method". It is a method that embraces the good traits of both the classical and geostatistical methods as summarised in Table 7.1.

7.3.2 Future Research

Research such as this, which presents a number of novel approaches to soil pattern recognition, no doubt, raises more questions than answers. This is all the more so when the work is carried out within the time-limit of the scholarship and also because of the practical constraints imposed by available technology and manpower. As Bezdek (1981) noted, choosing a model or construction of a new one depends on the type, availability, and means for processing data; technical support; economic constraints and time; among other factors. Certainly one or more of these factors, in some way, have played a role on the author's inability to exhaustively analyse the data and discuss the results as humanly possible. In view of this fact, here-under are some suggestions for further research. The list is by no means exhaustive.

(1) The criteria used to determine the balance between structure in the data and continuity of the resulting classes is heuristic in nature. Certainly, a comparison of results of fuzzy classification with those of other methods e.g. numerical (hard) classification, will make the judgement easier.

(2) Results of fuzzy analysis in Chapter 4 show the weak link between the class membership values and the raw data. More work needs to be done to enhance the predictability of fuzzy classification as suggested in the concluding section.

(3) The application of class membership semivariograms is fraught with some problems; the assumption of stationarity of means and variances was not tested. Thus the use of the average semivariograms over the entire study area may have lead to some hidden errors. Nevertheless, kriging was the most reliable predictor among the available alternatives.

(4) Validation of fuzzy analysis and (cross-)validation of kriging were not carried out. Validation for either of these methods, in the author's opinion, will require carefully planned experiments which, at this stage of the novel approach, will require the acquisition of much data including separate independent data that were not used for the original analysis (Voltz and Webster, 1990).

(5) The technicalities involved in the making of map overlays that reflect soil as a continuous system need to be improved upon. The colour overlays in Chapter 6 were prepared manually. Perhaps, improvement can be achieved by better graphics with variable colour mix to reflect the continuum nature of soil, especially in the transition areas between the core areas. Work will continue in this regard.

(6) Other potential applications of fuzzy classification are in the areas of soil and/or land evaluation, crop-soil interactions and pedological classification.

Recently, Burrough (1989) presented examples of the application of fuzzy sets to soil survey and land evaluation, although using "the semantic import models" instead of constructing continuous classes. Also recently, McBratney and DeGruijter (1990) applied FCME algorithm to horizon classification. Work is still continuing in this direction.

(7) Fuzzy classes can be constructed based on the "central concepts" of classes that are defined *a priori,* using the conventionally defined classes such as in Soil Taxonomy and other classification systems. In that case, Picard iteration is not needed to calculate the membership values. This area needs to be examined.

(8) Finally, this work has shown how some of the GIS methods such as landform parametric analysis from DEM, can be utilised for soil-landform interaction study. Research into the integration of soil class membership coefficients into GIS, or even into application of fuzzy objective functionals to analyse GIS information, will be very useful.

APPENDIX: PUBLISHED AND SUBMITTED PAPERS

Published papers

Odeh, I. O. A., McBratney, A. B. and Chittleborough, D. J. 1990. Design of optimal sampling spacings for mapping soil using fuzzy-k-means and regionalized variable theory. Geoderma, 47: 93-122. ***(Reprint attached).***

Odeh, I. O. A., Chittleborough, D. J. and McBratney, A. B. 1990. Elucidation of soil-landform interrelationships by cannonical ordination analysis. Geoderma (in press).

Abstract paper

Odeh, I. O. A. and Chittleborough, D. J. 1988. Quantitative evaluation of soil-landscape relationships. A paper presented at the National Soils Conference held at ANU, Canberra, Australia- 9-12 May 1988. Aust. Soc. Soil Sci. Inc.

Submitted paper

Odeh, I. O. A., McBratney, A. B. and Chittleborough, D. J. 1990. Soil pattern recognition with fuzzy-c-means: Classification and pedogenesis. Soil Science Society of America Journal (submitted).

Geoderma, 47 (1990) 93–122
Elsevier Science Publishers B.V., Amsterdam

Design of optimal sample spacings for mapping soil using fuzzy-k-means and regionalized variable theory

I.O.A. Odeh[1], A.B. McBratney[2] and D.J. Chittleborough[1]
[1]*Department of Soil Science, Waite Agricultural Institute, The University of Adelaide, Glen Osmond, S.A. 5064 (Australia)*
[2]*Soil Science, School of Crop Sciences, University of Sydney, Sydney, N.S.W. 2006 (Australia)*

(Received March 7, 1989; accepted after revision September 6, 1989)

ABSTRACT

Odeh, I.O.A., McBratney, A.B. and Chittleborough, D.J., 1990. Design of optimal sample spacings for mapping soil using fuzzy-k-means and regionalized variable theory. Geoderma, 47: 93–122.

This paper examines the application of fuzzy grouping and geostatistical methods to the design of optimal sampling schemes for mapping soil types on a small subcatchment near Forreston in the Mount Lofty Ranges of South Australia. Optimal sampling strategies (devised from semivariogram estimates for a number of spatially dependent soil attributes) highlighted the difficulty involved in selecting a sampling scheme that provides a satisfactory compromise for all the soil attributes used. A fuzzy classification approach was first used to incorporate both the continuously variable and categorical soil attributes into a matrix of membership coefficients, a reduced data set for the determination of membership semivariograms. From these semivariograms, an optimal sampling strategy for isarithmic mapping of the class membership coefficients was devised.

Inter-boundary distances determined by digital gradient segmentation, a method devised for detecting soil boundaries along transects, were found to be within the spatial range of class membership semivariograms and were also associated with landform and geologic features. This suggested that the sampling intervals to achieve the desired level of precision were, to some extent, dependent on these features. The optimal density of sampling for interpolation of class membership coefficients was, therefore, devised in relation to the landform and geologic features. This approach termed the geostatistical-conventional survey method, will thus provide a more efficient means of soil information transfer than would either geostatistical or conventional methods.

INTRODUCTION

Traditionally, soil survey and soil classification have been the most practical approaches to separation and grouping of different soil types within the landscape. They rely on the surveyors' intuition to create classes and locate soil boundaries on the assumption that there are strong relations between soil type and the environment. These subjective methods have attracted the crit-

ical interest of a number of authors (Beckett and Webster, 1971; Burgess et al., 1981; McBratney et al., 1981; Burgess and Webster, 1984). The classical method (as traditional or conventional soil survey is called: e.g. Burgess et al., 1981; Trangmar et al., 1985; Webster, 1985) also implies that soil classes are discrete with abrupt boundaries. Thus the predicted value of a soil attribute at any unsampled location is the value for the typical pedon or mean value for the mapping unit. The precision of any prediction is therefore dependent on the homogeneity of the mapping units and hence on the within-unit variance (Trangmar et al., 1985). Usually there is no independent quality control or verification of precision other than the assumption of strong relations between soil type and the environment. The classical approach does not account for the spatially dependent component of the variability within the mapping unit (Burgess and Webster, 1980; McBratney and Webster, 1981a), especially for intensive surveys of small areas and featureless areas with no obvious changes in soil boundaries.

The classical method usually involves incorporation of some exotic classification system (Butler, 1980) which may not be relevant to the objective of the survey or the area being surveyed. Moreover, many classification systems make use of only few diagnostic properties, especially those that can easily be measured. As Dudal (1986) noted, these properties may not necessarily be the most important from the viewpoint of land utilization.

Because of the uncertainty inherent in the classical method, a number of workers have proposed new approaches aimed at providing known precision for, and improving the quality of, soil maps. Burgess and Webster (1984) used the gamma function to describe the probability distribution of soil boundary spacings in order to improve the siting of soil boundaries in the field. However, most classifications for specific purposes may require more information than the field-observed soil attributes that this method suggests. In addition, the mathematics involved may not be attractive to pedologists, most of whom are not familiar with the intricate computations that are needed to be done quickly in the field, although this could be programmed for field computers. The geostatistical approach developed by McBratney et al. (1981) and Burgess et al. (1981) involves a prior knowledge of the semivariogram determined by transect sampling during the initial stage of survey. The semivariogram is needed to estimate the error variance of interpolation for any sampling scheme to be used in the main stage of survey. This approach is optimal because the sparsest sampling intensity that can achieve a desired precision could be derived for a given soil attribute. The question remains, 'how do we apply the results of optimal sampling schemes derived for different soil attributes to satisfy a given or required classification?' To confound this problem, some soil attributes that are used for soil classification may be nominal, ordinal or even binary, and therefore do not show as much spatial dependence as the continuous variables. Should these soil properties be ig-

nored? If not what alternative should be pursued to enable their inclusion so that their somewhat semi-continuous contribution to the soil variability can be assessed?

Some authors have transformed their data by principal component analysis (McBratney and Webster, 1981a) before embarking on spatial analysis. But this assumes linear relationships between soil variables, a condition which is not often the case with soil properties (DeGruijter and McBratney, 1988). Classification rather than ordination is therefore preferred for data reduction. However, soil variation is generally gradual instead of abrupt. Therefore discrete classes, as used in conventional classification, do not realistically fit the situation being described. Fuzzy classification techniques (Bezdek, 1981) which allows for partial membership of individuals (e.g. soil pedons) in each class depending on the deviation of their attributes from the class centriods, seems more appropriate. The resulting membership coefficients of individuals in each class can easily be related spatially.

Another problem associated with geostatistical methods is that sampling schemes are based on predetermined regular grids of various configurations which do not take into account the geologic and geomorphological differences that form the basis for soil-map delineation in the conventional methods. In recognising this restriction Stein et al. (1988a, b) used existing soil-map delineations in conjunction with geostatistical techniques of (co-)kriging to devise a procedure that improved considerably the accuracy of prediction of some land qualities at minimal effort and cost. This shows that land stratification based on the assumption of correlation of soil with major landform and geologic features before embarking on sampling for geostatistical predictions should give more precise results compared to either conventional survey or regular grid sampling common to geostatistical methods.

The main objectives of this paper are therefore: (1) to highlight the difficulties involved in the use of geostatistical approach to design of optimal sampling schemes when many soil attributes are involved; (2) to evaluate the potentials of using the fuzzy-k-means to improve the geostatistical methodology to soil survey; (3) to examine the spatial relationships between soil types and the major landform and geologic features as an aid to delineating soil class boundaries and thus to enable a more effective sampling strategy that will improve geostatistical prediction at the main stage of survey.

TRANSECT SURVEY

Study area

The area is located in a subcatchment near Forreston in the Mt. Lofty Ranges, about 60 km northeast of Adelaide in South Australia (Fig. 1). The subcatchment is close to the eastern fringe of Adelaide Geosyncline, the sub-

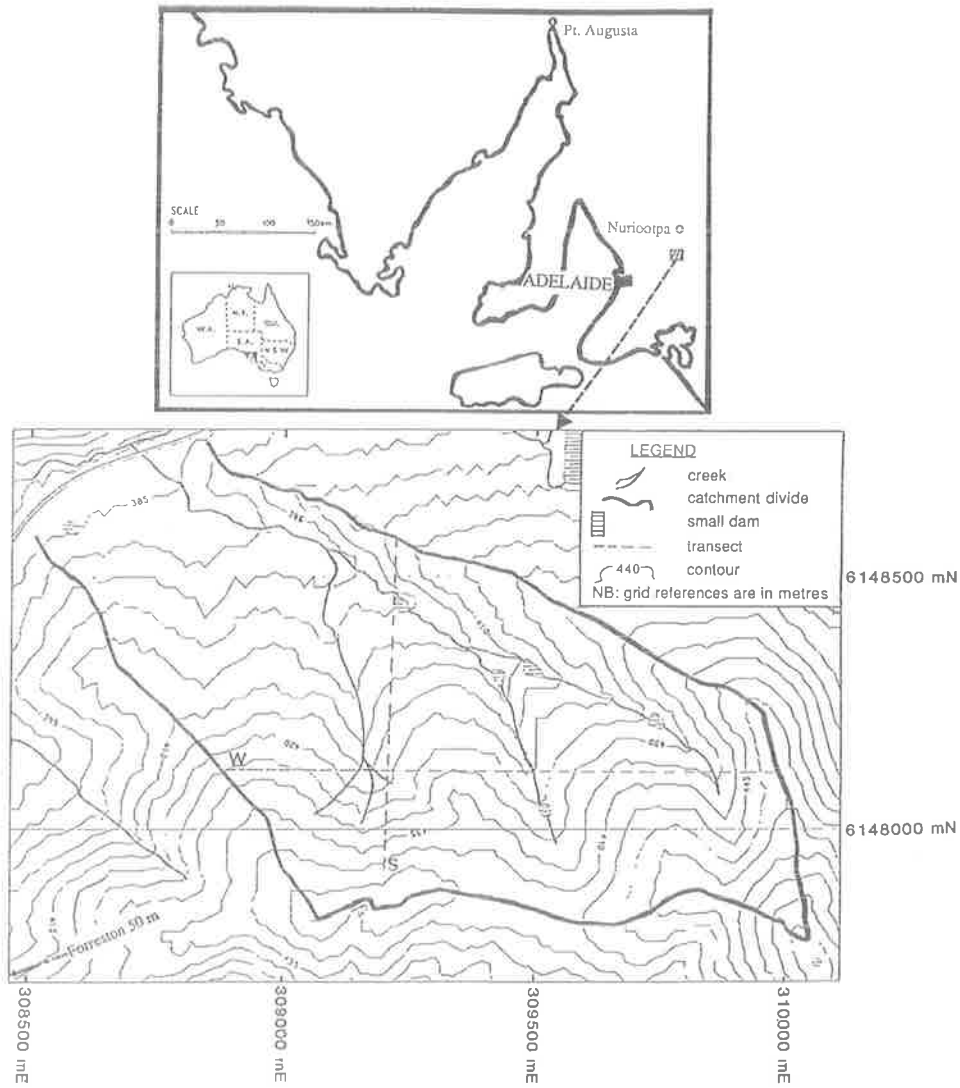

Fig. 1. Location of study area.

parallel ridges and valleys of which are largely controlled by lithology (Northcote, 1983). Geodetically the area is at approximately 34°48′N and 138°54′E which is equivalent to the Australian National Grid Reference of 6148800 mN, 308500 mE and 6147800 mN, 310100 mE. The soil parent material consists mainly of grey to dark grey phyllites, siltstones and fine sandstones of the Woolshed Flat Formation (Forbes and Preiss, 1987). Landform appears to be the dominant factor affecting soil development. The terrain comprises

predominantly round hills and spurs with slopes ranging from less than 1% on the lower slopes up to 20% on the middle to upper slopes. There is no conspicuous rock outcrop. The dominant soil pedons as mapped at the scale of 1:50,000 (Maschmedt, 1987) are shallow to moderately deep Xeralfs (Soil Survey Staff, 1975) or yellow-brown and brown podzolics (Stace et al., 1968). Land use is mainly sheep grazing, although part of the site has been used in the past for vegetable production.

Field sampling

For the purpose of this study, the line-transect technique was used as it was considered more suitable for the study of spatial variation of soil in a small area (McBratney and Webster, 1981a). To ensure an accurate geodetic reference, a laser theodolite was used to lay two transects, orthogonal to each other, in the west–east and north–south directions. The directions were chosen to transect the most obvious variability in the landscape and hence reveal any related soil anisotropy. In order to ensure that sampling reflected both the local and general soil variation, paired sampling was adopted, with each pair containing points 2 m apart and adjacent pairs 8 m apart. The laser theodolite was also used to locate sampling points with reference to some neighbouring spot heights to ensure geodetic accuracy of about 0.3 m. Undisturbed 50 mm soil cores to bedrock were taken at each point for the determination of some key physical, chemical and morphological properties. Throughout this paper the west–east and north–south transects are referred to as transect-W and transect-S, respectively. A total of 247 cores were taken with 100 on transect-S and 147 on transect-W. All symbols that include W or S or their lower case subscripts describe conditions or quantities associated with transect-W or transect-S.

Soil morphology

The samples were taken to the laboratory and key morphological characteristics (see Table I) of the major horizons, topsoil (0–20 cm) and subsoil (40–60 cm), were determined in accordance with the system of McDonald et al. (1984). The main and mottle colours were obtained by comparing with Munsell colour chart under standard illumination (Pendleton and Nickerson, 1951; Melville and Atkinson, 1985). The Munsell notations were transformed into CIELAB coordinates (CIE, 1978) to give some uniformity of scale.

Laboratory work

The subsamples were air-dried, ground with a rubber pestle, and the gravel fraction obtained by sieving with a 2 mm sieve. The main particle-size frac-

TABLE I

The soil attributes

Attribute	Type	Attribute	Type
Depth of organic stained layer	continuous	topsoil structure (grade)	ordinal
Depth to mottles	continuous	topsoil structure (horizontality)	nominal
Depth to maximum clay	continuous	topsoil structure (verticality)	nominal
Depth of solum	continuous	topsoil structure (flatness of face)	nominal
Depth to bedrock	continuous	topsoil structure (accommodation)	nominal
Topsoil colour L	semi-continuous	subsoil structure (grade)	ordinal
Topsoil colour a	semi-continuous	subsoil structure (horizontality)	nominal
Topsoil colour b	semi-continuous	subsoil structure (verticality)	nominal
Subsoil colour L	semi-continuous	subsoil structure (flatness of face)	nominal
Subsoil colour a	semi-continuous	subsoil structure (accommodation)	nominal
Subsoil colour b	semi-continuous	topsoil gravel	continuous
Parent material colour L	semi-continuous	topsoil %-sand	continuous
Parent material colour a	semi-continuous	topsoil %-silt	continuous
Parent material colour b	semi-continuous	topsoil %-clay	continuous
Subsoil mottle colour L	semi-continuous	subsoil %-sand	continuous
Subsoil mottle colour a	semi-continuous	subsoil %-silt	continuous
Subsoil mottle colour b	semi-continuous	subsoil %-clay	continuous
Subsoil mottle colour b	semi-continuous	topsoil %-organic carbon	continuous
Topsoil consistence-moist	ordinal	subsoil %-organic carbon	continuous
Topsoil consistence-plasticity	ordinal	topsoil Ec	continuous
Topsoil consistence-stickiness	ordinal	subsoil Ec	continuous
Subsoil consistence-moist	ordinal	topsoil pH	continuous
Subsoil consistence-plasticity	ordinal	subsoil pH	continuous
Subsoil consistence-stickiness	ordinal		
Subsoil cutan abundance	ordinal		

tions were determined using the hydrometer method of Gee and Bauder (1986). In addition, the following chemical determinations were carried out: pH in 1:5 soil–water suspension (McLean, 1982), electrical conductivity in 1:5 soil–water suspension (Rhoades, 1982), and organic carbon content by the dry-combustion method using a Leco CR-12 resistance furnace (Merry and Spouncer, 1988).

SPATIAL ANALYSIS AND OPTIMAL SAMPLING STRATEGIES

Soil attribute semivariogram

The theory of regionalized variables introduced by Matheron (1971) provides the basis for estimating semivariogram of a soil property. The theory is also the basis for interpolation of soil properties by kriging and also to planning of a rational soil sampling scheme for mapping soil types (Oliver, 1987). Theoretically, it is defined as follows: given that $Z(x)$ denotes the value of a

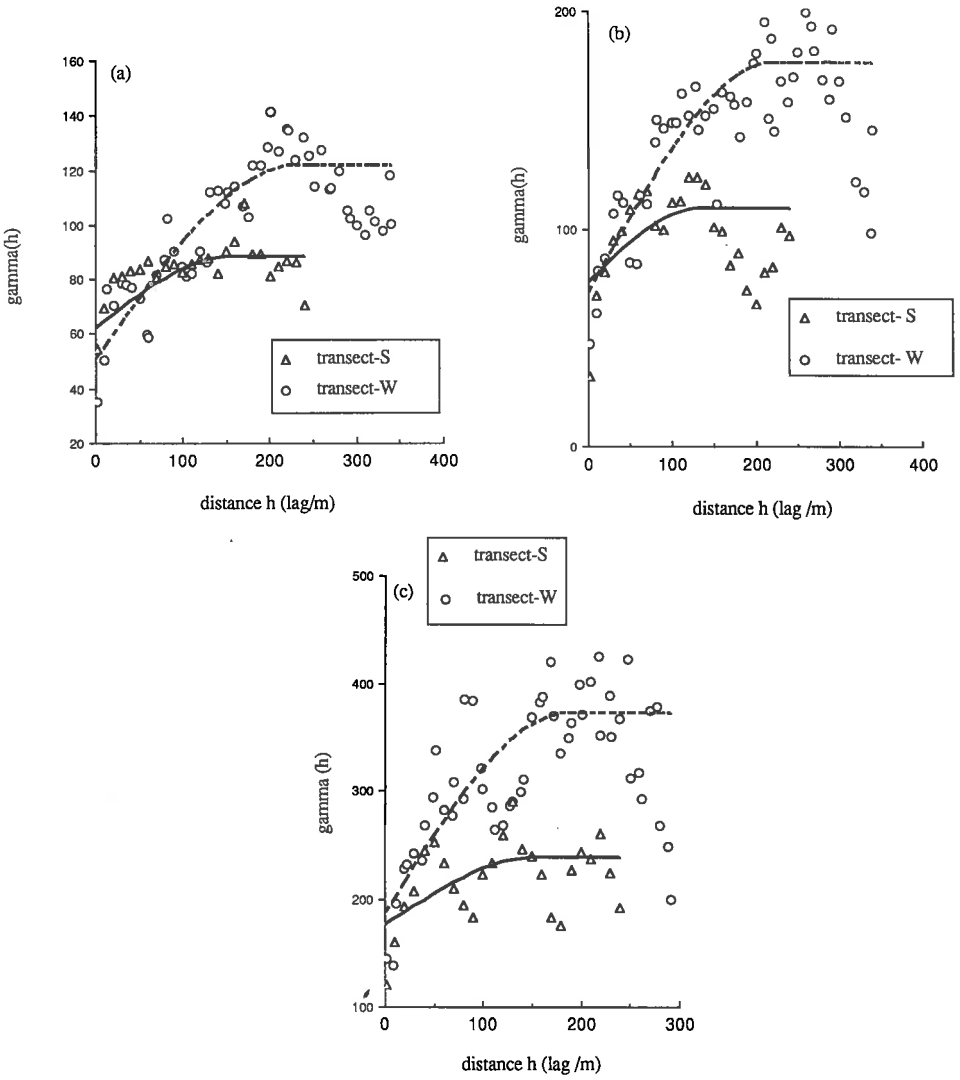

Fig. 2. Sample and model semivariograms showing anisotropic variation in (a) topsoil sand, (b) topsoil gravel and (c) subsoil clay. the gamma (h) is in $(\%)^2$.

soil property at a point x, and $Z(x)$ is modelled by a random function that satisfies the conditions for the intrinsic hypothesis (McBratney and Webster, 1981a), then the semivariogram is given by:

$$\gamma(h)/\alpha/ = (1/2)\mathrm{Var}Z[(x)-Z(x+h)] = (1/2)E\{[Z(x)-Z)x+h)]^2\} \quad (1)$$

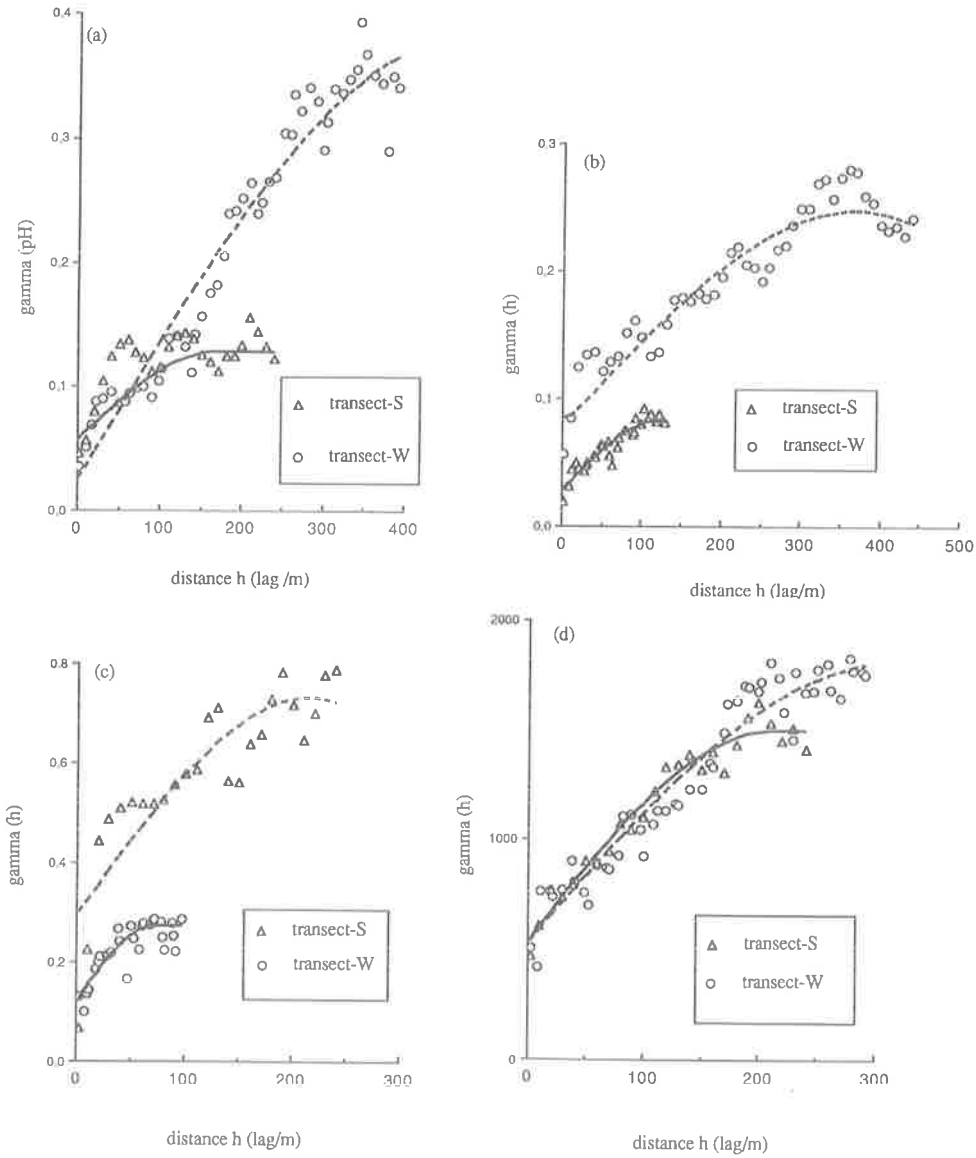

Fig. 3. Sample and model semivariograms showing anisotropic variation in (a) topsoil pH, (b) subsoil pH, (c) subsoil organic carbon content (%) and (d) subsoil electrical conductivity (S m^{-1}). The gamma (h) for the soil attributes is in units of measurements squared.

where h is any integral multiple of the interval between points and α is the direction.

Based on the expression in eq. 1, sample semivariograms for the continu-

ously variable soil properties were estimated by:

$$\gamma(h)=\frac{1}{2(n-h)}\sum_{i=1}^{n-h}[z(x_i)-z(x_i+h)]^2 \quad (2)$$

where $(x_1, x_2, ..., x_n)$ constitute n sampling locations along the transect. To make the sample semivariogram more meaningful and useful for kriging, some form of model that satisfies the positive definite condition (Journel and Huijbregts, 1978) needs to be fitted. We used the spherical model that has served very well for soil properties (Burgess et al., 1981; Webster, 1985). The spherical model is described by:

$$\begin{aligned}&\gamma(h)=C_0+C(3h/2a-h^3/2a^3) && \text{for } 0<h<a\\ &\gamma(h)=C_0+C && \text{for } h>a\\ &\gamma(h)=0\end{aligned} \quad (3)$$

where a is the range, C_0 is the nugget variance, and C_0+C constitutes the sill. The C denotes the spatially dependent component of the semivariance. Figs. 2 and 3 show the sample semivariograms for selected soil attributes in the two orthogonal directions.

Soil anisotropy

The sample semivariogram model for a soil attribute in a given direction describes isotropic variation. As shown in Figs. 2 and 3, variation is not the same in the two directions, that is, the soil variation is anisotropic. This is less so for the sample semivariogram of subsoil electrical conductivity (Fig. 2a). A number of anisotropic features is apparent. Firstly, each of the soil attributes has different nugget variance in the two directions. Secondly, the gradient of the first few lags of a sample semivariogram is also variable with the direction. Thirdly, all the soil attributes depict different sills in the two directions, a feature normally referred to as zonal anisotropy (Trangmar et al., 1985). It was therefore necessary that a model of anisotropy be enunciated that took account of all the above features. Taking the original sample semivariograms as

$$\begin{aligned}&\gamma_w(h)=C_{0w}+C_w && \text{for transect-W and}\\ &\gamma_s(h)=C_{0s}+C_s && \text{for transect-S}\end{aligned} \quad (4)$$

the following transformations were carried out:
the nugget variances for a given attribute were averaged as

$$\hat{C}_0=\frac{C_{0w}+C_{0s}}{2} \quad (5)$$

then the spatially dependent component was derived as

$$C'_w = \gamma_w(h) - \hat{C}_0 \text{ and}$$
$$C'_s = \gamma_s(h) - \hat{C}_0 \quad (6)$$

and the gradients of the first few lags of the semivariograms were calculated as

$$b_w = 3C'_w/2a_w \quad \text{for transect-W}$$
$$b_s = 3C'_s/2a_s \quad \text{for transect-S} \quad (7)$$

(see McBratney and Webster, 1986).
The anisotropic ratios for the soil attributes were then derived by

$$R = b_w/b_s \quad (8)$$

The results of the transformations for some of the particle-size fractions are shown in Table II. Some of these particle-size fractions depict pure nugget variances in the S-direction, a feature which is interpreted as absence of any spatial dependence in the data at the scale of sampling (Oliver, 1987). Anisotropic variation is in evidence for some other soil attributes (e.g. topsoil sand, topsoil gravel, subsoil clay, etc.). The anisotropic ratios indicate higher variation in the W-direction than S-direction except for the topsoil clay fraction and subsoil organic carbon. The former has an anisotropic ratio of 5.5 which is considered large for soil properties (Trangmar et al., 1985; McBratney and Webster, 1986).

Design of optimal sampling schemes

We followed the procedure described in McBratney et al. (1981) and Burgess et al. (1981) to derive optimal sampling schemes for the study area. This involves the theory of kriging, a method of interpolating a given soil property, z, at an unsampled location x_0 by the equation:

$$z^*(x_0) = \sum_{i=1}^{n} \lambda_i z(x_i)$$

where λ_i are the weights associated with the sampling points. The weights sum to unity, a condition which indicates unbiased estimation. The kriging variance which is a measure of deviation of the estimated values from the actual values, is defined by:

$$\sigma_e^2 = E\{[z(x_0) - z^*(x_0)]^2\}$$
$$= 2\sum_{i=1}^{n} \lambda_i(x_i, x_0) - \sum_{i=1}^{n}\sum_{j=1}^{n} \lambda_i \lambda_j \gamma(x_i, x_j)$$

TABLE II

Parameter values of isotropic and anisotropic semivariograms for some soil attributes (N denotes pure nugget variation, a is in m and o.c. denotes organic carbon; the semivariances are in the units of measurement squared)

Soil attribute	$\gamma_w(h)$	$\gamma_s(h)$	C_{0w}	C_{0s}	$\hat{C}_0$	C'_w	C'_s	a_w	a_s	R in W:S
Topsoil sand (%)	121.9	88.3	50.4	68.9	60.1	61.9	28.3	233	157	1.5:1
Topsoil grav. (%)	176.8	109.1	70.1	75.2	72.4	104.8	37.1	224	134	1.7:1
Topsoil silt (%)	38.8	22.1	28.5	22.1	25	13.8	N	220	N	–
Topsoil clay (%)	34.3	38.1	24.9	19.18	22	12.3	16.1	306	73	1:5.5
Topsoil o.c. (%)	0.87	0.19	0.43	0.19	0.31	0.56	N	171	N	–
Topsoil E_c (S m^{-1})	2748	1403	1408	1403	1406	1345	N	65	N	–
Topsoil pH	0.36	0.14	0.02	0.04	0.03	0.33	0.11	407	170	1.2:1
Subsoil sand (%)	211.8	68.3	87.3	68.3	77	134.8	N	178	N	–
Subsoil silt (%)	46.1	26.8	32.5	26.8	30	13.6	N	277	N	–
Subsoil clay (%)	392.0	239.1	185.9	175.7	180	212.0	59.1	190	156	3:1
Subsoil o.c. (%)	0.27	0.63	0.12	0.25	0.18	0.09	0.45	73	116	1:3.2
Subsoil E_c (S m^{-1})	1705	1500	525	529	527	1178	973	277	213	1:1.1
Subsoil pH	0.25	0.08	0.08	0.03	0.06	0.19	0.03	360	129	2.7:1

where $\gamma(x_0,x_i)$ is the semivariance between x_0 and x_i and $\gamma(x_i,x_j)$ is the semivariance between x_i and x_j. To minimize kriging variance, the Lagrange multiplier, ψ, is introduced so that the σ_e^2 which is for punctual kriging, becomes:

$$\sigma_e^2 = \sum_{i=1}^{n} \lambda_i \gamma(x_i,x_0) + \psi \tag{9}$$

and the variance for block kriging is estimated by:

$$\sigma_B^2 = \sum_{i=1}^{n} \lambda_i \gamma(x_i,B) + \psi_B - \sigma^2(B) \tag{10}$$

where $\gamma(x_i,B)$ is the mean semivariance between the point, x_i and the block B, and σ_B^2 is the within block semivariance. The semivariogram parameter values in Table III are based on the linear section of the spherical models fitted to the sample semivariograms, so that the model used for estimating the kriging variances is in the form:

$$\gamma(h) = \hat{C}_0 + bh \tag{11}$$

b being the gradient of the first few lags of the isotropic sample semivariogram, fitted by the spherical model, up to the sill at $h=a$. It was derived as in eq. 7.

Burgess et al. (1981) and McBratney et al. (1981) have emphasized the merits of using regular grids in isarithmic mapping so that we based the design of sampling strategy in this work on terms of rectangular grids. Using the

TABLE III

Grid spacings in transect-W and transect-S directions obtained for some soil particle-size data at an estimation error of 5% (equivalent to 25 $(\%)^2$ error variance) for 10×10 m and 100×100 m blocks

Soil attribute	Block-size (m)	Grid spacing (m)	
		transect-W	transect-S
Topsoil sand	10×10	8	12
	100×100	23	35
Topsoil gravel	10×10	5	9
	100×100	20	32
Topsoil silt	10×10	20	N
	100×100	40	N
Subsoil clay	10×10	4	12
	100×100	16	48
Subsoil sand	10×10	5	N
	100×100	17	N

semivariogram parameter values for particle-size fractions in Table II, kriging variances were computed for points and block sizes of 10×10 m and 100×100 m, respectively, by the OSSFIM program developed by McBratney and Webster (1981b). This was done by solving eqs. 9 and 10 using the model in eq. 11 and a search radius of 2.00 and 50 nearest points.

We restricted the computation of kriging variances to the particle-size variables only for ease of comparison. The results for some of the particle-size data that depict variation in transect-W direction only are illustrated in Figs. 4 and 5. We chose 5% (equivalent to error variance of 25 $(\%)^2$ of particle-size fraction) as reasonable because, as Burrough (1986, pp. 158–159) re-

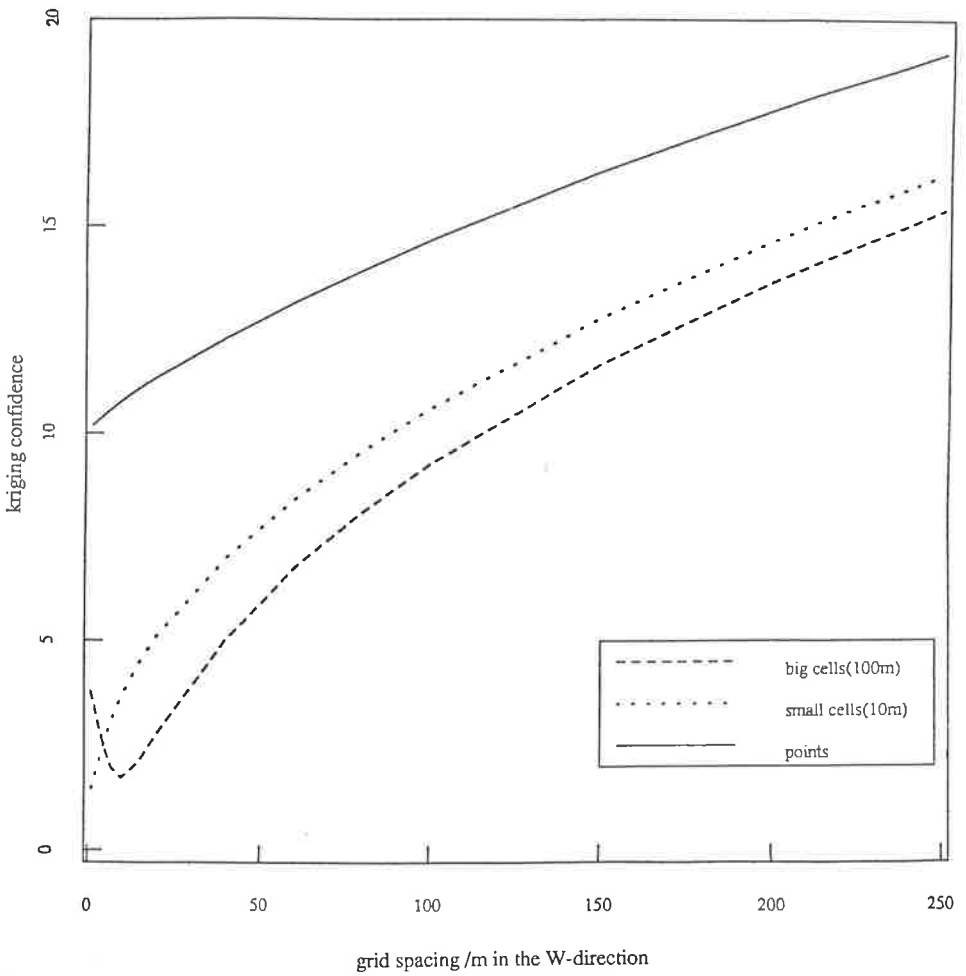

Fig. 4. Kriging confidence for punctual and block estimation of topsoil silt (%) as a function of grid spacing in transect-W direction.

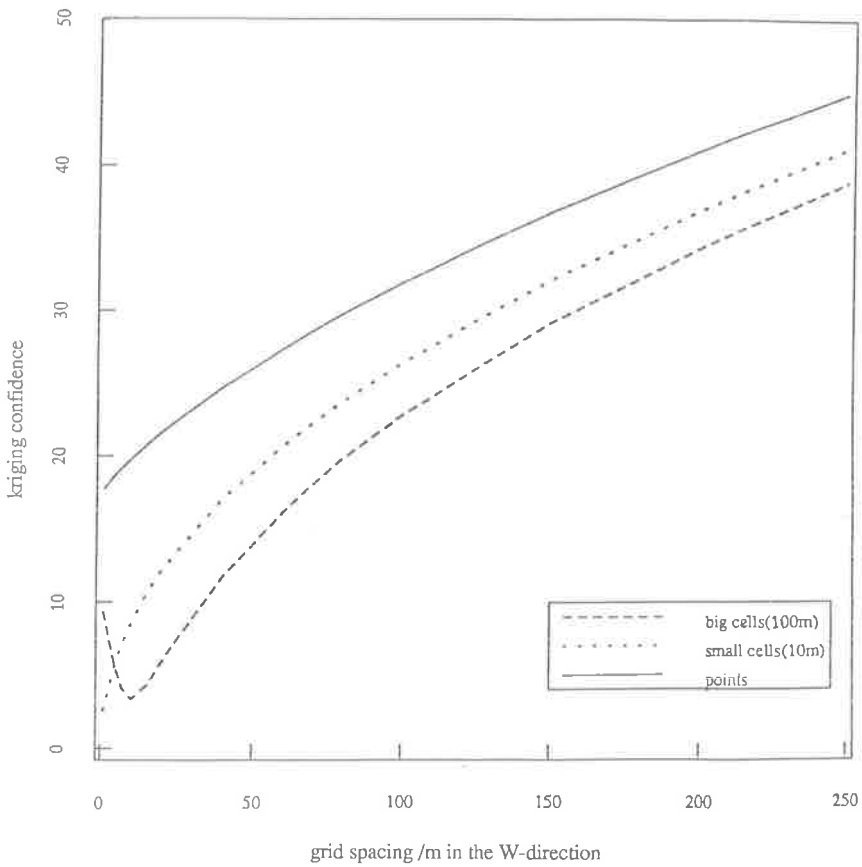

Fig. 5. Kriging confidence for punctual and block estimation of subsoil sand (%) as a function of grid spacing in transect-W direction.

ported, most conventional soil surveys at 1:25,000 scale have within-class variances of between 10.62 and 41.86 $(\%)^2$ clay with an average variance of 39.92 $(\%)^2$. These estimates are unreliable; variances may be much higher, as estimates were based on few samples. Table IV also gives the grid spacings in W-direction obtained for 10×10 m and 100×100 m cells at kriging error of 5% for some particle-size fractions that show variation in W-direction only. A grid spacing at this error margin could not be obtained for point estimates, because the error due to nugget variance is much higher than 5%. Soil variation in the S-direction is pure nugget for these attributes as sampling was too sparse to gain any insight into the form of autocorrelation. One option is to sample at closer intervals to incorporate more of the local variation into the spatial autocorrelation. There may be no end to this. Another option is to ignore the spatially independent attributes and determine the optimal density

TABLE IV

Brief description of soil class centroids

Soil class	Main features of centroid
A	Shallow (19 cm) topsoil of brown, slightly gravely (15%) loam, moderately weak pedality (2.5) of granular structure, pH = 7.0, overlying reddish brown heavy clay with common (15%) light olive brown mottles, moderate pedality (4) of angular blocky structure, pH = 6.3; depth of solum = 60 cm.
B	Shallow (17 cm) topsoil of dark reddish brown, very gravelly (24%) loam, moderate pedality (3.5) of granular structure, pH = 7.1, overlying yellowish red heavy clay with few (10%) reddish brown mottles, strong pedality (4) of angular blocky structure, pH = 6.5; depth of solum = 65 cm.
C	Moderately deep (25 cm) topsoil of dark brown, slightly gravelly (15%) loam, moderate pedality (3.4) of granular structure, pH = 6.9, overlying brown light medium clay with common (17%) dark reddish brown mottles, moderate pedality (3.1) of subangular blocky structure, pH = 6.2; depth of solum = 58 cm.
D	Moderately deep (24 cm) topsoil of dark brown, slightly gravelly (17%) loam of moderate pedality (3.2) of subangular blocky structure, pH = 7.1, overlying brown medium clay with few (5%) faint mottles, very weak pedality and massive, pH = 6.2; depth of solum = 57 cm.
E	Shallow (18 cm) topsoil of dark reddish brown, very gravelly (30%) loamy sand, very weak pedality loose and single-grained, pH = 6.8, overlying reddish brown light medium clay with few (7%) yellowish brown mottles, moderately weak pedality (2) of subangular blocky structure, pH = 6.2; depth of solum = 48 cm.
F	Shallow (19 cm) topsoil of dark brown, very slightly gravelly (9%) sandy loam, moderate pedality (2.7) of subangular blocky structure, pH = 6.5, overlying yellowish brown heavy clay with common (16%) light olive brown mottles, moderate pedality (3.1) of subangular blocky structure, pH = 6.2; depth of solum = 58 cm.
G	Very deep (35 cm) topsoil of very dark brown, very slightly gravelly (8%) loam, moderate pedality (3.2) of granular structure, pH = 7.2, overlying dark brown loam with few (6%) yellowish brown mottles, moderate pedality (2.1) of subangular blocky structure, pH = 6.5; depth of solum = 86 cm.

of sampling for those that are anisotropically variable with the spatial component in both directions. The unidirectional optimal density of sampling for those that show variation in one direction only can be incorporated later. The latter option was followed.

We have previously discussed the form of anisotropy exhibited by some of the soil attributes, the results of which are given in Table II. To obtain the optimal density of sampling for a given soil property, e.g. one of the particle-size fractions for the topsoil, the kriging variances were computed against the corresponding grid spacings using the isotropic semivariogram derived for the direction of maximum variation, in this case W-direction. The grid spacing in the S-direction was then obtained as the grid interval in the W-direction times R, the anisotropic ratio as derived in eq. 8. Figs. 6 and 7 illustrate the

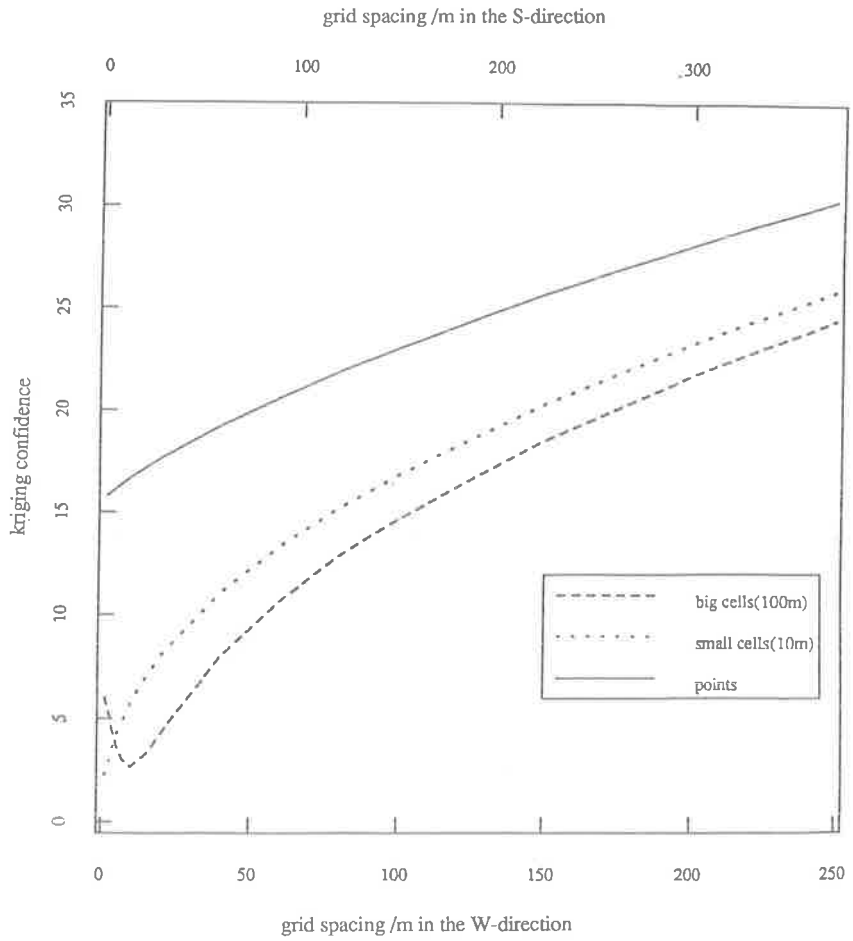

Fig. 6. Kriging confidence for punctual and block estimation of topsoil sand (%) as a function of grid spacing in transect-W and transect-S directions.

kriging error (square root of variance) plotted against grid intervals in both directions for some particle-size fractions. Again, choosing 5% of the particle-size fraction as a reasonable maximum, we also obtained optimal sampling intervals for some of the particle-size attributes that show anisotropic variation as shown in Table III. Once again the kriging errors are much higher for point estimates than for either 10×10 m or 100×100 m cells due to the large nugget variances. Table III also shows that optimal grid spacings are quite variable for different soil particle-size fractions, even without considering other spatially variable soil attributes. The problem is how to choose a grid spacing at a given error variance to satisfy the spatial variation of several soil attributes. One solution is to obtain the optimal density for all the soil attri-

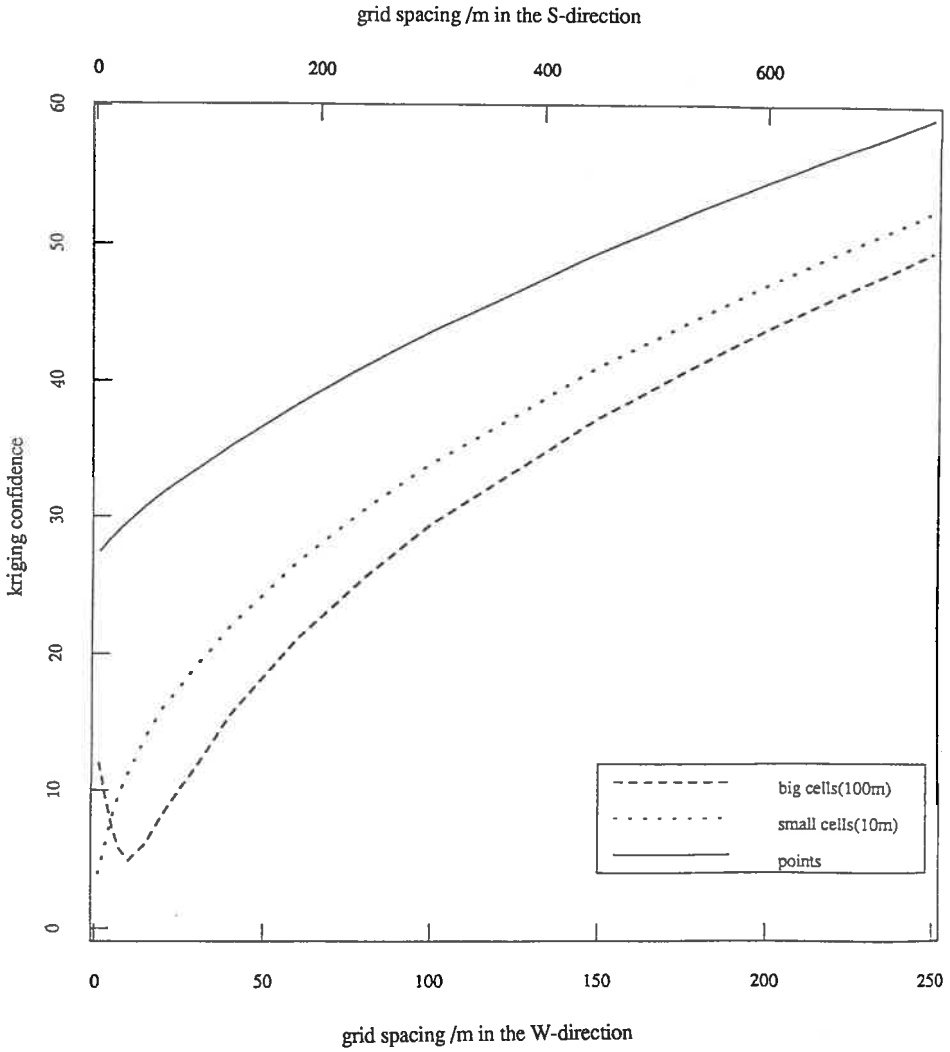

Fig. 7. Kriging confidence for punctual and block estimation of subsoil clay (%) as a function of grid spacing in transect-W and transect-S directions.

butes required for a given classification and select the sampling scheme for the attribute that shows the least spatial variation. In this case sampling at 4×12 m or 16×48 m to estimate means of subsoil clay over blocks of 10×10 or 100×100 m, respectively, would be close enough to map most of the soil particle-size attributes to achieve an error of $\leq 5\%$.

This approach is by no means easy, especially if all the other attributes are considered. In this work there are 48 soil attributes (Table I) of which 18 are

continuously variable types that show spatial variation. To obtain error variances with the corresponding grid spacings for all 18 attributes before deciding on the optimal sampling scheme will be computationally very involved, expensive, and probably not worth the effort. Even if this is attainable there is the problem of how to combine all the isarithmic maps resulting from such an exercise to serve the purpose of mapping the soil types. Moreover, the spatially independent attributes should be considered when mapping soil types because they are also important from the viewpoint of soil management.

To alleviate this problem, a suitable means of reducing the number of soil attributes to a manageable number has to be adopted. Multivariate methods of linear transformation such as principal component analysis (McBratney and Webster, 1981a) have been used. These methods assume linear relationships between the attributes, a condition which is not often the case with soil properties (De Gruijter and McBratney, 1988). We therefore opted for classification rather than ordination for the purpose of reducing all the soil attributes to a manageable number of new variables or classes.

In a situation where soil spatial variation is continuous rather than abrupt, hard classification as used in traditional soil survey and classification is inappropriate. This is the case with the soil type studied in this work. The parent material (fine-grained phyllites and schists with occasional minor intrusions of quartz or quartzite) is essentially uniform across the landscape. The most apparent causes of soil spatial variation are lateral and vertical pedogenetic processes differentially caused by the effect of landform. Thus the traditional or hierarchical classification system is unsuitable for our purpose. A more flexible and realistic approach was therefore more appropriate. We therefore applied the fuzzy-k-means as described below.

FUZZY CLASSIFICATION FOR OPTIMAL SAMPLING SCHEMES

The concept of fuzzy classes

The concept of fuzzy classes is the generalization of "hard" or discrete classes. Given a data set matrix, $\mathbf{X}$, of which there are $n \times p$ values, n being the number of objects (e.g. pedons) and p the number of attributes, the hard partitioning of the data set into c classes produces an $n \times c$ matrix, $\mathbf{M}$, of memberships. Let $\mathbf{M} = m_{ij}$; $m_{ij} = 1$ if individual i belongs to class j and $m_{ij} = 0$ otherwise. There are three conditions that ensure that classes are exclusive, jointly exhaustive:

$$(1) \sum_{j=1}^{c} m_{ij} = 1 \quad i = 1,...,n$$

$$(2) \sum_{i=1}^{n} m_{ij} > 0 \quad j = 1,...,c$$

$$(3)\ m_{ij} \in \{0,1\} \quad i = 1,...,n; j = 1,...,c$$

Condition (3) indicates that individual i either belongs to a class or does not at all. However, in fuzzy classes, condition (3) is relaxed so that class memberships are allowed to be partial and thus can take any value between and including 0 and 1. Condition (3) therefore becomes:

(4) $m_{ij} \in [0,1] \quad i=1,...n; j=1,...,c$

Fuzzy classification techniques involve operations that satisfy conditions (10) (2) and (4) and therefore are generalization of hard classifications. The best known fuzzy classification is variously known as the fuzzy-k-means of fuzzy-c-means (Bezdeck, 1981). It is described by the objective functional:

$$J(M,C) = \sum_{i=1}^{n} \sum_{j=1}^{c} m_{icj}^{\phi} d^2(x_i, c_{je}) \tag{12}$$

where $J(M,C)$ is the sum of square error as a function of each individual by the centre of its class, c_{je}; c is the number of fuzzy continuous classes; x_i is the vector representing individual i; m_{icj} is membership of an individual, i, in the class c_j; ϕ is the exponent that determines the degree of fuzziness of the solution and it can take the value between 1 and ∞; and d^2 (x_j, c_{je}) is the square of the distance between individuals, x_i and c_{je} according to the chosen distance.

The distance frequently used in numerical classification is the Euclidean distance which gives equal weights to all the attributes. However, attributes that have much larger variance will weigh more heavily on the solution. In our example, we therefore used the Mahalanobis distance defined as:

$$d^2_{(xi,cje)} = (x_i - c_{je})' \sum -1_{(xi-cje)}$$

where $\sum$ is the sample covariance matrix of $\mathbf{X}$. It has an advantage over Euclidean distance in that it takes account of correlation between attributes (Bezdek, 1981).

In obtaining the optimal fuzzy-k-partition of the dataset $\mathbf{X}$, the objective functional, $J(M,C)$, is minimized for the case $\phi > 1$ using the fuzzy-k-means algorithm (see Bezdek, 1981 pp. 65–70).

Fuzzy classification of soil

In applying the fuzzy-k-means classification algorithm to our example, ϕ values of 1.11, 1.15 and 1.50 were tried, each for a series of 2 to 10 fuzzy classes using all the soil data. The results for $\phi = 1.11$ were not fuzzy enough to warrant using the fuzzy-k-means classification techniques, and those for $\phi = 1.50$ were too fuzzy for the data set. The results for $\phi = 1.15$ were more appropriate and therefore accepted for further analysis. Before further analysis, however, the problem of "cluster validity" had to be solved. The ques-

tion is how many classes existed in the data set? In other words, how well has the algorithm identified the structure that is present in the data? In the case of soil data, it is unlikely to find a wholly satisfactory answer because it is not known if the samples are representative of all the possible entia in either geographical or taxonomic context. However, many authors have proposed validity functionals as a means of solving the clustering validity problem.

Two of these functionals are the fuzziness performance index (FPI) and normalized classification entropy (NCE) which were found to be most useful when applied to artificial data by Roubens (1982). McBratney and Moore (1985) also used these criteria to evaluate the varying number of fuzzy climatic classes. The FPI is a measure of the degree of fuzziness while NCE indicates the degree of disorganization. The least fuzzy or disorganized number of classes is considered optimal. This is paradoxical because here are we eschewing hard classification due to presumable real fuzziness in the data set and then measuring the amount of fuzziness in **M**, and presume that the least fuzzy partitions to be most valid. Accepting this, however, Fig. 8 shows that both FPI and NCE are minimal when number of classes, c, equals 7, even though the actual minimum for FPI is c equals 2. Commonsense criteria indicate that we choose c equals 7 for further analysis. The seven soil classes are arbitrarily labelled as class A, B, ..., G, respectively. Table IV gives a brief description of some soil class centroids.

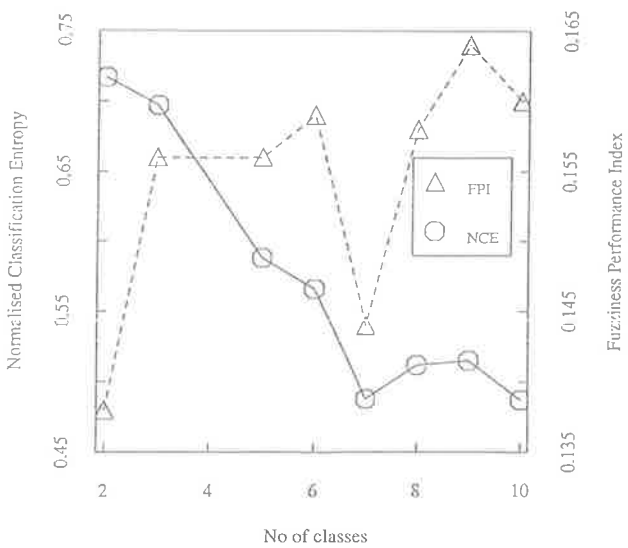

Fig. 8. Normalized classification entropy and fuzziness performance index against number of classes.

Soil class membership semivariograms and optimal sampling strategy

The results of fuzzy-k-means classification as described above were in the form of a $n \times c$ class membership coefficients matrix, $\mathbb{M}$, n being the total number of soil individuals (in this case pedons). There are 247 pedons sampled in this study with 100 on transect-S and 147 on transect-W. Taking a vector of membership coefficients of each fuzzy class, c_j, semivariances were estimated for each of the transect directions as described for the continuously variable soil attributes (see eq. 2). The sample semivariograms for some of the class membership coefficients were also fitted with the spherical model as per eq. 3. Some are illustrated in Figs. 9 and 10.

The class membership semivariograms of some classes show the same anisotropic features as for some of the soil attributes. Using the same reasoning and calculations contained in eqs. 4–8, we arrived at the semivariogram parameter values as presented in Table V. Like some of the particle-size variables, membership of a number of soil classes (classes A, B, and D) exhibit

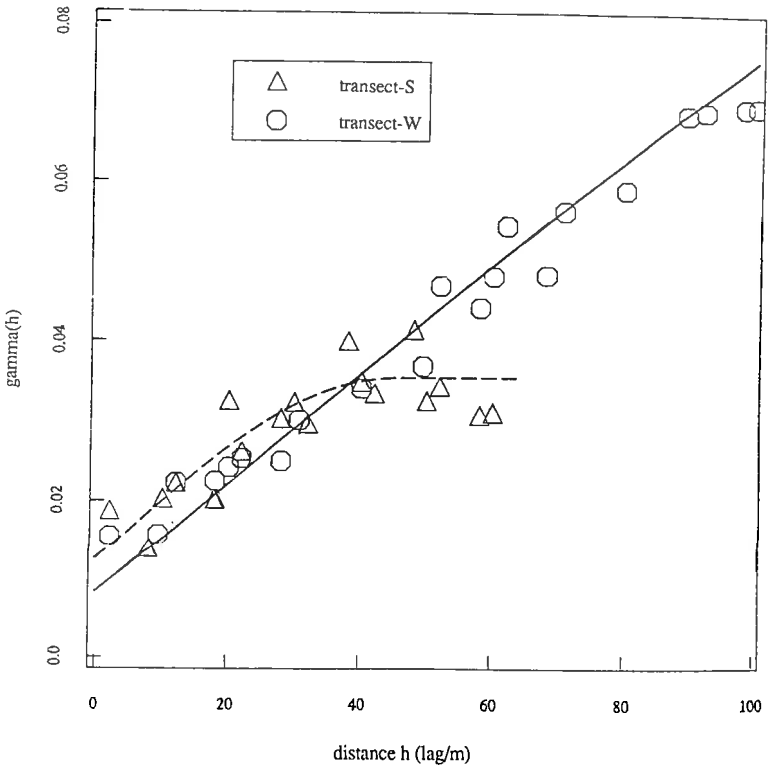

Fig. 9. Anisotropic semivariograms of fuzzy-class membership coefficients for soil class B. The gamma(h) is in membership coefficient squared.

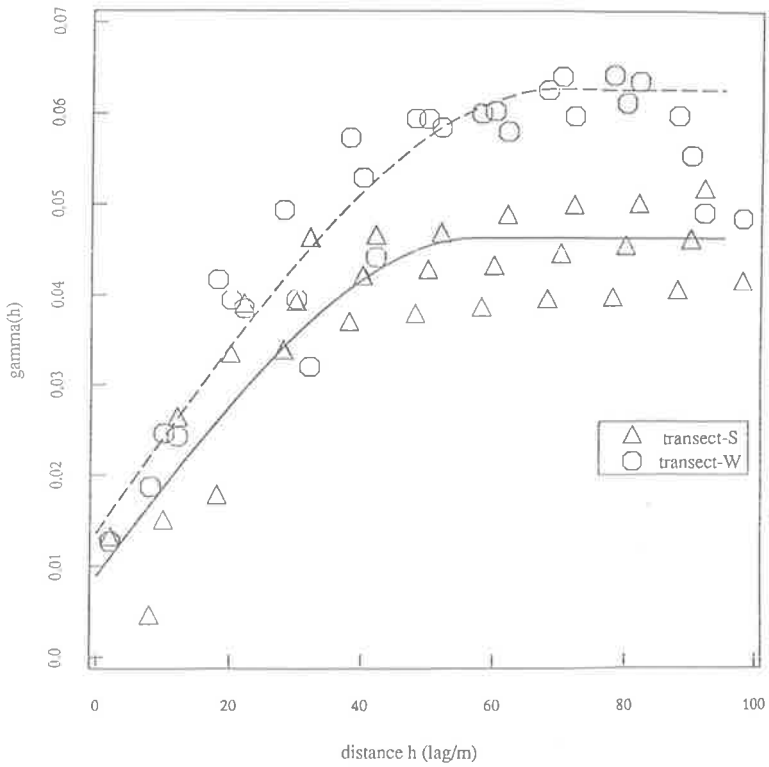

Fig. 10. Anisotropic semivariograms of fuzzy class membership coefficients for soil class G. The gamma(h) is in membership coefficient squared.

TABLE V

Parameter values of isotropic and anisotropic semivariograms for the soil classes (N denotes pure nugget variation and a is in m, the semivariances of soil classes are in membership coefficient squared)

Soil class	$\gamma_w(h)$	$\gamma_s(h)$	C_{0w}	C_{0s}	$\hat{C}_0$	C'_w	C'_s	a_w	a_s	R in W:S
A	0.0350	0.0575	0.0215	0.0335	0.0275	0.0075	0.0300	30	35	1:3.4
B	0.1314	0.0354	0.0083	0.0126	0.0105	0.1209	0.0249	309	45	1:1.4
C	0.0496	0.0353	0.0242	0.0228	0.0235	0.0236	0.0120	40	48	2.4:1
D	N	0.1154	0.0417	0.0573	0.0495	N	0.0659	–	30	–
E	N	N	0.0609	0.0286	0.0443	N	N	–	–	–
F	0.0686	N	0.0148	0.0101	0.0124	0.0562	N	50	–	–
G	0.0563	0.0463	0.0127	0.0090	0.0109	0.0454	0.0354	67	57	1.1:1

anisotropic variation with the maximum occurring instead in the S-direction. Variation of membership of class E is pure nugget in both directions indicating erratic occurrence across the landscape. This class is the shallow (solum

depth is about 50cm) variety described in Table IV. It occurs mainly on relatively steep slopes and slope breaks. Soil classes D and F appear to complement each other with the former predominantly occurring on transect-S and the latter on transect-W.

Using the form of model in eq. 11 in the OSSFIM program, the kriging variances and errors were also determined for estimates on points and over blocks of 10×10 m and 100×100 m, with the corresponding grid spacings for all but soil class E. Some of the results are illustrated in Figs. 11 and 12. We consider a kriging error of 0.1 of class membership as a reasonable maximum for estimates over 1 ha (100×100 m block) and obtained grid spacings for mapping the soil classes. The results are presented in Table VI.

As Table VI shows, we were left with six possible ways of optimally map-

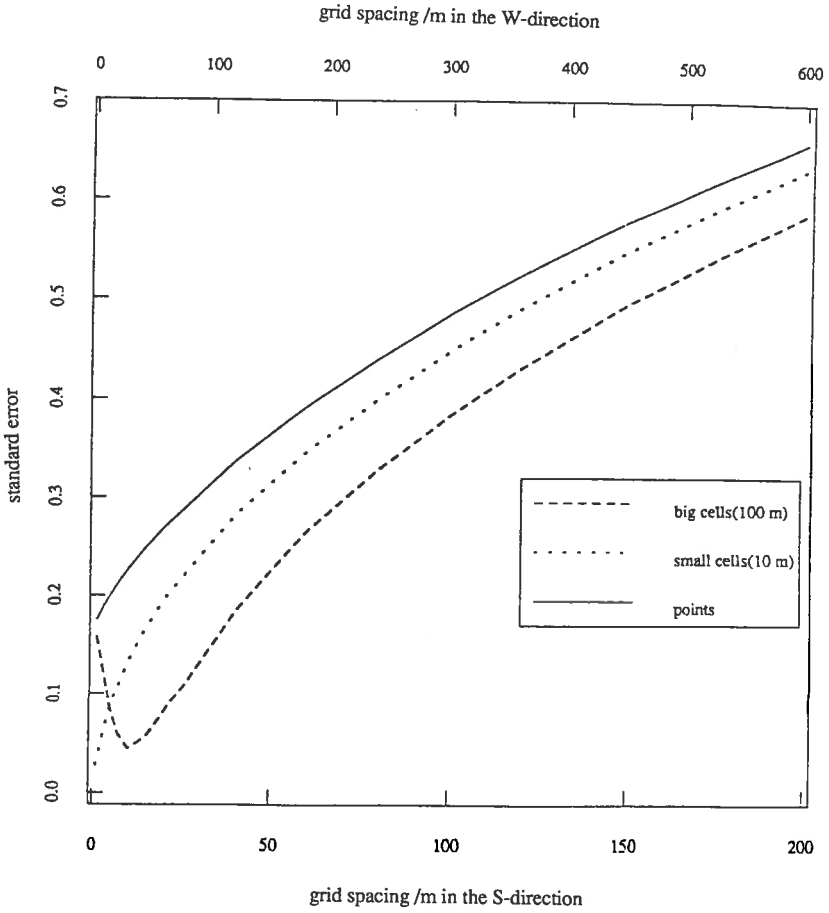

Fig. 11. Kriging error for punctual and block kriging of fuzzy class membership coefficients for soil class A as a function of grid spacings in transect-W and transect-S directions.

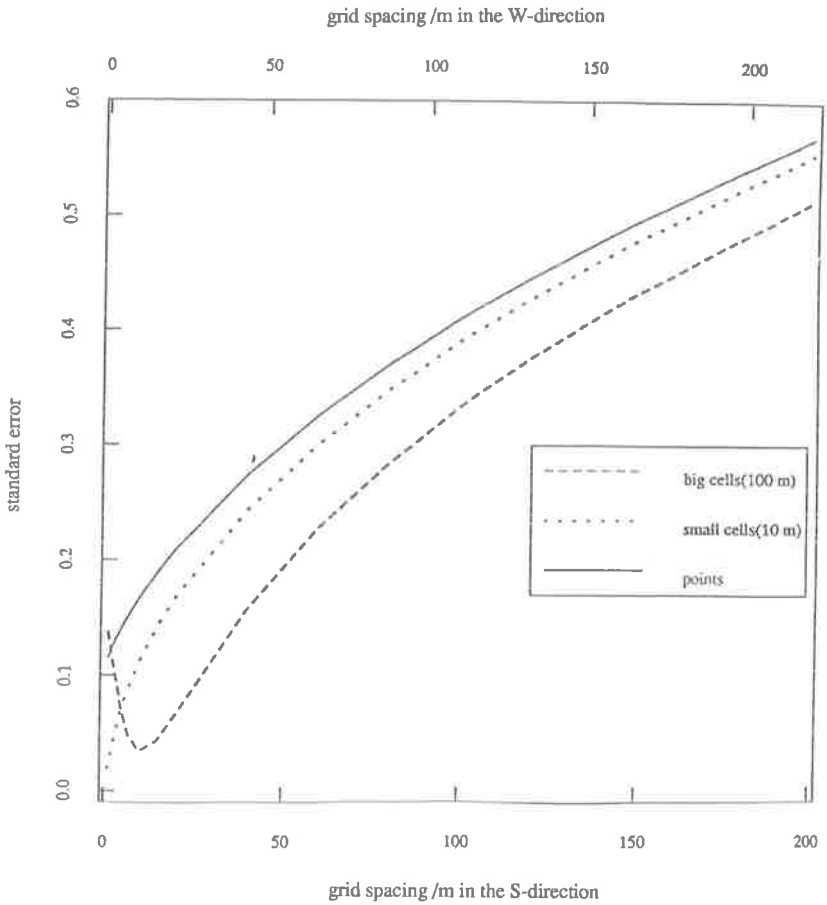

Fig. 12. Kriging error for punctual and block kriging of fuzzy-class membership coefficients for soil class G as a function of grid spacings in transect-W and transect-S directions.

TABLE VI

Grid spacings in transect-W and transect-S directions obtained for some soil classes at an estimation error of 0.1 of membership coefficient for 100 × 100 m block

Sub class	Grid spacing (m)	
	transect-W	transect-S
A	47	23
B	42	29
C	27	66
D	N	21
F	23	N
G	31	33
Mean	34	34

ping the soil type in the study site. For example, if sampling was done at the interval of 23 m along transect-W and 21 m along transect-S as obtained for soil classes D and F, respectively, it would suffice to block "krige" over 1 ha with an error margin of ≤ 0.1 of membership of all the classes listed in Table VI. There was room for modification, however. The sampling density can be optimised by relating soil occurrences to geologic and landform features as is done in the traditional survey method. This required some form of segmentation along the transects to elucidate boundary locations and spacings. This can be performed easily using the matrix of class membership coefficients and the method is described in the next section.

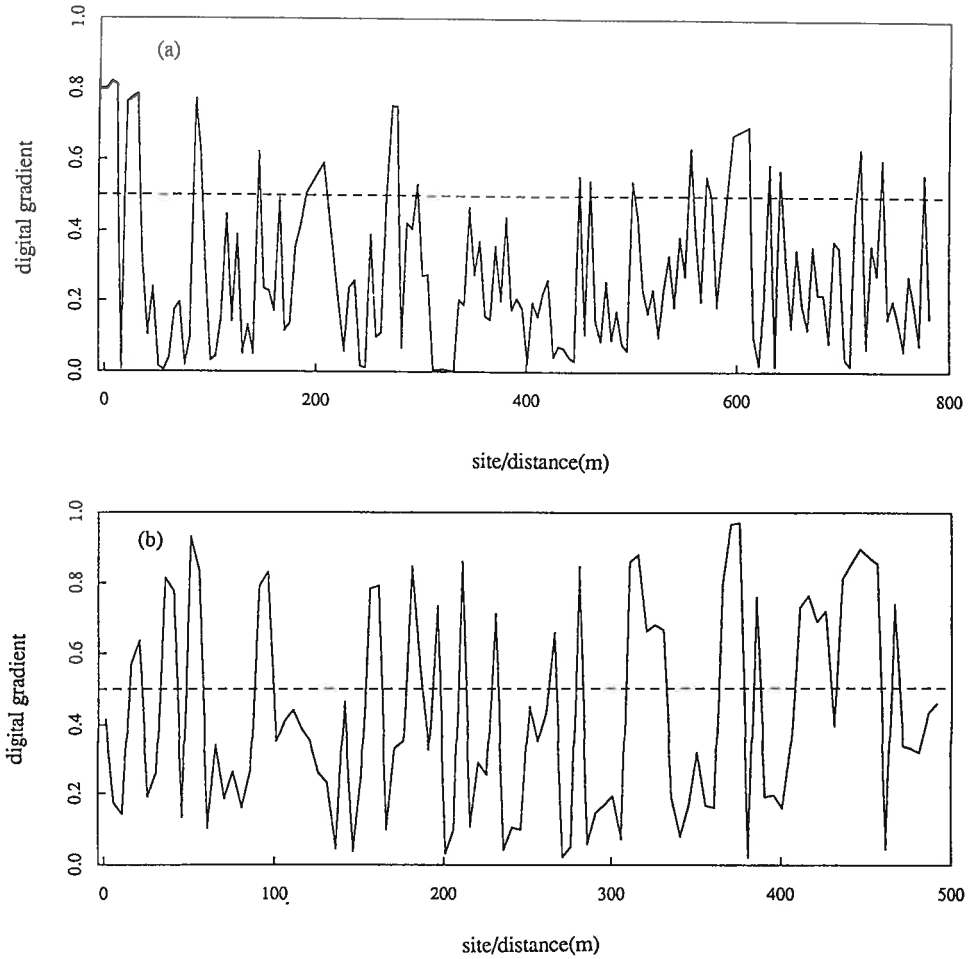

Fig. 13. Digital gradient g of soil classes along (a) transect-W and (b) transect-S as an indicator of segment boundaries.

TABLE VII

Comparison of conventional, geostatistical-conventional and geostatistical soil surveys

Characteristic	Conventional survey	Geostatistical-conventional survey	Geostatistical survey
Scale	1000–1 km small-medium	100 km–10 m medium-large	100 km–10 m medium-large
Prediction/ information transfer	soil class (mean)	soil class (membership) semivariogram	soil attribute semivariogram/ cross-semivariogram
Assumed continuity	discontinuous	semi-continuous	continuous
Number of properties	may be many or few diagnostic	few-many	few
Precision	unknown–low	medium–high	medium–high

Segmentation along transects

The sample semivariogram of membership of a given class merely indicates the spatial dependence and the range of variation along the transect. It does not indicate the physical locations of soil class boundaries and where each class predominates. Similarly, the sampling scheme obtained using the sample semivariogram only suggests optimal intensity of sampling and does not give information pertaining to boundary locations at this stage of survey. One approach is to proceed anyway and sample at the intervals suggested by the optimal sampling design using the sample semivariograms, and interpolate to produce isarithmic maps of soil class memberships. Boundaries can then be sought by overlaying of various isarithmic maps of membership of soil classes with boundary locations at certain cross-over values of membership coefficients (e.g. > 0.5 difference) between two points or areas. An alternative is further optimization of sampling density at the initial stage of survey. This can be achieved by some form of segmentation along transects and relating segment boundaries to some physical features that are predominant in the survey area. We preferred the latter option as this would further enhance sparser sampling intensity for the same level of precision.

With this in mind, we applied the digital gradient segmentation procedure, an extension of the method described by Rosenfeld and Kak (1982) which has been used for soil study by Powell et al. (1990). The digital gradient is a

measure of rate of change of membership between two sites on the transect. It is defined as:

$$g_{x+0.5} = \left[\frac{\sum_{j=1}^{c} (u_{j,x} - u_{j,x+1})^2}{2} \right]^{0.5}$$

where $u_{j,x}$ and $u_{j,x+1}$ are the memberships of class j at sites x and $x+1$, respectively, on the transect. Large values of g suggest points of sharp change and hence the soil (segment) boundaries and small values indicate points of stasis. Fig. 13 illustrates the digital gradient along the two transects. There are 15 and 17 prominent peaks above a value of $g=0.5$ for transect-W and transect-S, respectively. The inter-peak distances were determined as an indication of segment lengths on each transect. Transect-W showed segment length in the range of 10–154 m with a mean of 44 m; while transect-S had a range of 10–65 m and a mean of 28 m. This was in agreement with the findings of the spatial analysis (see Table V) which showed the spatial range varying from 30 to 309 m for transect-W and 30 to 57 m for transect-S.

To be useful for further optimization of the sampling strategy, we sought the coincidence or otherwise of segment boundaries along the two transects with any conspicuous landform and geologic features in the field. Up to 65% of the segment boundaries coincided with either slope breaks, ridge or spur crests, colluvio-alluvial contacts and some minor formation of quartz enrichment or quartzite within the main geologic formation of fine-grained phyllites and siltstones. Guided by these geomorphological and geologic features, it was envisaged that sampling would have to be at the intervals of 10 m, where these features are prominent, and 50 m where these features are virtually absent. These spacings are within the range of grid intervals given in Table VI and have been adopted in the detailed sampling for interpolation of membership coefficients of the soil classes.

GENERAL DISCUSSION AND CONCLUSIONS

Geostatistics offers the possibility of quantifying the spatial variation of a soil property within the mapping units and thus facilitates the design of an optimal sampling scheme at the initial stage of the soil survey. However, it is a difficult task to reach an optimal density of sampling when several soil attributes are involved. A suitable means of data reduction, which should also include the spatially independent soil attributes, is therefore required. The fuzzy-k-means classification techniques offer such a possibility.

Fuzzy-k-means classification allowes for partial membership of an individual of each of the classes, therefore yielding membership coefficients that can readily be related spatially. Class-membership semivariograms obtained for the soil classes can be used to derive the estimation error at any given grid interval for subsequent isarithmic mapping of the class-membership coefficients.

Digital gradient segmentation of soil types along the transects also allows for correlation of soil boundaries with landform features in the field. This can further enhance optimization of sampling intensity at any given precision. In this way, the assumption that there is a strong relation between the soil type and the environment, which is usual with the traditional soil survey method, is blended with the geostatistical soil survey to advantage. As Dudal (1986) put it, the use of modern and quantitative methods should not detract from the experience of co-variance between soil types and the various elements of landscape. They should blend with each other. This novel approach which uses geostatistics, fuzzy sets, and geomorphological and geologic information is hereby termed the geostatistical-conventional survey method (Table VII). It is a method that embraces the good traits of both the classical and geostatistical methods in the following ways:

(1) In contrast to classical methods of soil survey and classification where values of the typical pedon of a mapping unit are transferred to any geographical location within the unit, fuzzy classification techniques allow for more accurate information transfer. Thus the soil attribute values could be estimated for any geographical location within the mapped area, if its memberships of fuzzy classes are known, by weighted means of all the class centroids. The weights, in this case, are the class membership coefficients.

(2) The application of spatial analysis as used in geostatistical survey combined with fuzzy-classification techniques would enable the interpolation of membership coefficients of soil profile data, yielding isarithmic maps and therefore providing better information transfer.

(3) The continuous nature of soil is taken into account. Soil spatial variation is usually gradual, and where boundaries exists, are fuzzy. Fuzzy classification, in this sense, is more realistic than conventional methods.

(4) The fuzzy-classification approach is more flexible than the conventional methods. In the latter, soil pedons are assigned to predetermined classes or existing classification, whereas fuzzy-k-means allow for any number of classes within the fuzzy-k-partition space $1<c<n$ (if the soil is uniform or the number of classes is equal to the total number of pedons in the area being surveyed, then classification would not be necessary) from which an optimal number of classes could be chosen by means of cluster validity functionals. An optimal number of classes thus chosen could be regarded as a realization of some structural organization due to some physical processes.

(5) Segmentation of soil along transects by means of a digital gradient pro-

cedure allows for correlation of soil boundaries with environmental markers (e.g. landform and geologic features) such as is done in the traditional methods. When done at the initial stage of survey, considerable reduction of sampling intensity in the main survey can be achieved for the same level of precision.

ACKNOWLEDGEMENTS

We should like to thank Australian International Development Assistance Bureau for providing financial support to the first author and the Agricultural University, Makurdi, Nigeria, for granting him study leave. The CSIRO Division of Soils is gratefully acknowledged for providing the resources for carrying out the analysis of the data.

REFERENCES

Beckett, P.H.T. and Webster, R., 1971. Soil variability: a review. Soils Fert., 34: 1–15.
Bezdek, P.A., 1981. Pattern Recognition with Fuzzy Objective Function Algorithms. Plenum Press, New York, N.Y., 256 pp.
Burgess, T.M. and Webster, R., 1980. Optimal interpolation and isarithmic mapping of soil properties, I. The semivariogram and punctual kriging. J. Soil Sci., 31: 315–331.
Burgess, T.M. and Webster, R., 1984. Optimal sampling strategies for mapping soil types, I Distribution of boundary spacings. J. Soil Sci., 35: 641–654.
Burgess, T.M., Webster, R. and McBratney, A.B., 1981. Optimal interpolation and isarithmic mapping, IV. Sampling strategies. J. Soil Sci., 32: 643–659.
Burrough, P.A., 1986. Principles of Geographical Information Systems for Land Resources Assessment. Clarendon Press, Oxford, 193 pp.
Butler, B.E., 1980. Soil Classification for Soil Survey. Oxford University Press, Oxford, 129 pp.
CIE, 1978. Recommendations on uniform colour spaces, colour difference and psychometric colour terms. Suppl. No. 2 to Publ. No. 15, Colorimetric (E-1.3.1) 1971/TC1.3, CIE, Paris.
De Gruijter, J.J. and McBratney, A.B., 1988. A modified fuzzy k-means method for predictive classification. In: H.H. Bock (Editor), Classification and Related Methods of Data Analysis. Elsevier, Amsterdam, pp. 97–104.
Dudal, R., 1986. The role of pedology in meeting the increasing demands on soils. Trans. XIII Congr. ISSS, Hamburg, Vol I (plenary papers), pp. 80–96.
Forbes, B.G. and Preiss, W.V., 1987. Stratigraphy of the Burra Group. In: W.V. Preiss (Compiler), The Adelaide Geosyncline–Late Proterozoic Stratigraphy, Sedimentation, Palaeontology and Tectonics. Bull. Geol. Surv. S. Aust., 53: 97–109.
Gee, G.W. and Bauder, J.W., 1986. Particle-size analysis. In: A. Klute (Editor), Method of Soil Analysis, Part 1. Am. Soc. Agron., pp. 383–411.
Journel, A.G. and Huijbregts, C.J., 1978. Mining Geostatistics. Academic Press, London, 600 pp.
Maschmedt, D.J., 1987. Soil and Land Use Potential, Onkaparinga, South Australia. 1:50,000 Map sheet, Dept. of Agric. S. Aust. Tech. Pap., 16, 78 pp.
Matheron, G., 1971. The theory of regionalized variables and its applications. Cah., Cent. Morphol. Math. Fontainebleau, 5, 211 pp.

McBratney, A.B. and Moore, A.W., 1985. Application of fuzzy sets to climatic classification. Agric. For. Meteorol., 35: 165–185.
McBratney, A.B. and Webster, R., 1981a. Spatial dependence and classification of soil along a transect in northeast Scotland. Geoderma, 26: 63–82.
McBratney, A.B. and Webster, R., 1981b. The design of optimal schemes for local estimation and mapping of regionalized variables, II. Program and examples. Comput. Geosci., 7: 335–365.
McBratney, A.B. and Webster, R., 1986. Choosing functions for semivariograms of soil properties and fitting them to sampling estimates. J. Soil Sci., 37: 617–639.
McBratney, A.B., Webster, R. and Burgess, T.M., 1981. The design of optimal schemes for local estimation and mapping of regionalized variables, I. Theory and method. Comput. Geosci., 7: 331–334.
McDonald, R.C., Isbell, R.F., Speight, J.G., Walker, J. and Hopkins, M.S., 1984. Australian Soil and Land Survey Field Handbook. Inkata Press, Melbourne, 160 pp.
McLean, E.O., 1982. Soil pH and lime requirement. In: A.L. Page et al. (Editors), Methods of Soil Analysis, 2. Am. Soc. Agron., pp. 199–224.
Melville, M.D. and Atkinson, G., 1985. Soil colour: its measurements and its designation in models of uniform colour space. J. Soil Sci., 495–512.
Merry, R.H. and Spouncer, L.R., 1988. The measurement of carbon in soils using a microprocessor-controlled resistance furnace. Commun. Soil Sci. Plant Anal., 19: 707–720.
Northcote, K.H., 1983. Central Southern Region (V). In: Soils: An Australian Viewpoint. Division of Soils, CSIRO, pp. 211–217 (CSIRO, Melbourne/Academic Press, London).
Oliver, M.A., 1987. Geostatistics and its application to soil science. Soil Use Manage., 3: 8–20.
Pendleton, R.L. and Nickerson, D., 1951. Soil colours and special Munsell soil colour charts. Soil Sci., 36: 495–512.
Powell, B., McBratney, A.B. and MacLeod, D.A., 1990. The application of ordination and fuzzy classification techniques to field pedology and soil stratigraphy in the Lockyer Valley, Queensland. Submitted to: Catena.
Rhoades, J.R., 1982. Soluble salts. In: A.L. Page et al. (Editors), Methods of Soil Analysis, 2. Am. Soc. Agron., pp. 167–180.
Rosenfeld, A. and Kak, A.C., 1982. Digital Picture Processing, 2. Academic Press, New York, N.Y., 349 pp.
Roubens, M., 1982. Fuzzy clustering algorithms and their cluster validity. Eur. J. Opt. Res., 10: 294–301.
Soil Survey Staff, 1975. Soil Taxonomy. A Basic System of Soil Classification for Making and Interpretating Soil Surveys. USDA-SCS Agric. Handb. 436, Washington, D.C., 754 pp.
Stace, H.T.C., Hubble, G.D., Brewer, R., Northcote, K.H., Sleeman, J.R., Mulcahy, M.J. and Hallsworth, E.G., 1968. A Handbook of Australian Soils. Rellim, Glenside, S.A., 435 pp.
Stein, A., van Dooremolen, W., Bouma, J. and Bregt, A.K., 1988a. Co-kriging point data on moisture deficit. Soil Sci. Soc. Am. J., 52: 1418–1423.
Stein, A., Hoogerwerf, M. and Bouma, J., 1988b. Use of soil-map delineations to improve (co-)kriging of point data. Geoderma, 43: 163–177.
Trangmar, B.B., Yost, R.S. and Uehara, G., 1985. Applications of geostatistics to spatial studies of soil properties. Adv. Agron., 38: 45–94.
Webster, R., 1984. Quantitative spatial analysis of soil in the field. Adv. Soil Sci., 3: 1–70.

REFERENCES

Aandahl, A. R. 1948. The characterization of slope positions and their influence on the total nitrogen content of a few virgin soils of western Iowa. Soil Science Society of American Proceedings, 13: 449-454.

Anderson, M. G. and Burt, T. P. 1978. The role of topography in controlling throughflow generation. Earth Surface Processes, 3: 331-334.

Anderson, M. G. and Burt, T. P. 1980. Towards more detailed field monitoring of variable source areas. Water Resources Research, 14: 1123-1131.

Arabie, P., Carroll, J. D., DeSarbo, W. and Wind, J. 1981. Overlapping clustering: a new method for product positioning. Journal of Marketing Research, 18: 310-317.

Barker, S. 1986. The evolution of the South Australian environment. In: Nance, C. and Speight, D. L. (Editors): A Land Transformed: environmental changes in South Australia. Longman Cheshire Pty. Ltd. Melbourne.

Batschelet, E. 1981. Circular Statistics in Biology. Academic Press. London.

Beckett, P. H. T., and Webster, R. 1971. Soil variability: a review. Soils and Fertilizers, 34: 1-15

Beckmann, G. G., 1983. Evolution of Australian landscapes. In: 'Soils: an Australian viewpoint', Division of Soils, CSIRO, pp. 211-217 (CSIRO, Melbourne/Academic Press, London).

Bezdek, J. C. 1981. Pattern Recognition with Fuzzy Objective Function Algorithms. Plenum Press, New York.

Bezdek, J. C. 1974. Numerical taxonomy with fuzzy sets. Journal of Mathematical Biology, 1: 57-71

Bezdek, J. C., Trivedi, M., Ehrlich, R. and Full, W. 1981. Fuzzy clustering: a new approach for geostatistical analysis. International Journal of Systems, Measurements and Decisions, 2: 13-23

Breewer, R. 1955. Mineralogical examination of a yellow podzolic soil formed on granodiorite. CSIRO (Australia) Soil Publication No. 5.

Buol, S. W., Hole, F. D. and McCracken, R. J. 1973. Soil Genesis and Classification. Iowa State University Press, Ames Iowa.

Bureau of Meteorology. 1971. Climatic Survey, Adelaide, Region 1, South Australia. Australian Government Publishing Service.

Burgess, T. M. and Webster, R. 1980a. Optimal interpolation and isarithmic mapping of soil properties. I. The semivariogram and punctual kriging. Journal of Soil Science, 31: 315-331.

Burgess, T. M. and Webster, R. 1980b. Optimal interpolation and isarithmic mapping of soil properties. II. Block kriging. Journal of Soil Science, 31: 333-341.

Burgess, T. M. and Webster, R. 1984. Optimal sampling strategies for mapping soil types. I Distribution of boundary spacings. Journal of Soil Science, 35: 641-654.

Burgess, T. M., Webster, R. and McBratney, A. B. 1981. Optimal interpolation and isarithmic mapping. IV. Sampling strategies. Journal of Soil Science, 32: 643-659.

Burrough, P. A. 1986. Principles of Geographical Information Systems for Land Resources Assessment. Clarendon Press, Oxford.

Burrough, P. A. 1987. Mapping and mapping analysis: new tools for land evaluation. Soil Use and Management, 3: 20-25

Burrough, P. A. and Webster, R. 1976. Improving a reconnaissance soil classification by multivariate methods. Journal of Soil Science, 27: 554-571.

Burrough, P. A., Brown, L. and Morris, E. C. 1977. Variations in vegetation and soil pattern across the Hawkesbury Sandstone Plateau from Barren Grounds to Fitzroy Falls, New South Wales. Australian. Journal of Ecolology, 2: 137-159.

Burt, T. P. and Butcher, D. P. 1985. Topographic control of soil moisture distributions. Journal of Soil Science, 36: 469-486

Butler, B. E. 1980. Soil Classification for Soil Survey. Oxford University Press, Oxford.

Chamberlin, T. C. 1883. Geology of Wisconsin. Madison: Commissioners of Public Printing, 4 Volumes.

Chittleborough, D. J. and Oades, J. M. 1980. The development of red-brown earth. III The degree of weathering and translocation of clay. Australian Journal of Soil Research, 18: 383-393.

Chittleborough, D.J., Smettem, K.R.J., Cotsaris, E. and Leaney, F.W. 1990. Seasonal changes in pathways of dissolved organic carbon through a hillslope soil (Xeralf) with contrasting texture. Geoderma (submitted).

Chittleborough, D. J. Oades, J. M. and Walker, P. H. 1984. Textural differentiation in chronosequences from eastern Australia. Geoderma, 32: 206-226.

CIE. 1978. Recommendations on uniform colour spaces, colour difference and psychometric colour terms. Suppl. No. 2 to Publ. No. 15, Colorimetric (E-1.3.1) 1971/TC1.3, CIE, Paris.

Cipra, J. E., Bidwell, O. W. and Rohlf, F. J. 1970. Numerical taxonomy of soils from nine orders by cluster and centroid-component analyses. Soil Science Society of America Proceedings, 34: 281-287.

Crocker, R. L. 1952. Soil genesis and the pedogenic factors. Quarterly Review of Biology, 27: 139-168

Crowther, E. M. 1953. The skeptical soil chemist. Journal of Soil Science, 4: 107-122.

Daily, B., Firman, J. B., Forbes, B. G. and Lindsay, J. M. 1976. Geology. pp 5-42 In: Twidale C. R., Tyler, M. J. and Webb, B. P. (Editors), Natural History of the Adelaide Region, Adelaide, Australia. pp 5-42. Royal Society of South Australia Inc.

Dale M. B., McBratney, A. B. and Rusell, J. S. 1989. On the role of expert systems and numerical taxonomy in soil classification. Journal of Soil Science, 40: 223-234.

DeGruijter, J. J. 1977. Numerical Classification of Soils and its Application in Survey. Agricultural Research Report No. 855. Pudoc, Wageningen.

DeGruijter J. J. and McBratney, A. B. 1988. A modified fuzzy k-means method for predictive classification. In: H. H. Bock (Editor), Classification and Related Methods of Data Analysis. Elsevier, Amsterdam, pp. 97-104.

Dudal, R. 1986. The role of pedology in meeting the increasing demands on soils. Transactions XIII Congr. ISSS. Hamburg. Vol I (plenary papers): 80-96.

Dunn, J. C. 1974. A fuzzy relative of the isodata process and its use in detecting compact, well-separated clusters. Journal of Cybernetics, 3: 22-57.

Evans, I. S. 1980. An integrated system of terrain analysis and slope mapping Zeitschrift fur Geomorphologie, N. F. Supplementband, 36: 274-295.

Fisher, R. A. 1954. Statistical Methods for Research Workers. Oliver and Boyd, Edinburgh.

FitzPatrick, E. A. 1980. Soils: their Formation, Classification and Distribution. Longman, London

Food and Agricultural Organization (FAO). 1974. "Soil Map of the World. Vol. 1 Legend". UNESCO. Paris.

Forbes, B. G. and Preiss, W. V. 1987. Stratigraphy of the Burra Group. In: Preiss, W. V. (Compiler) The Adelaide Geosyncline- late Proterozoic stratigraphy, sedimentation, palaeontology and tectonics. Bulletin of Geological Survey, South Australia, 53., pp 97-109.

Fridland, V. M. 1974. Structure of the soil mantle. Geoderma, 12: 35-41

Furley, P. A. 1971. Relationships between slope form and soil properties developed over chalk parent materials. In: Brusden D. (Editors), Institute of British Geographers special publ., 3: 141-164.

Gee, G. W. and Bauder, J. W. 1986. Particle-size analysis. In: A. Klute (Editor), Method of Soil Analysis, Part 1. American Society of Agronomy, pp. 383-411.

Gerrard, A. J. 1981. Soil and Landforms: an Integration of Geomorphology and Pedology. George Allen and Unwin, London.

Gordon, A. D. 1987. Classification and assignment in soil science. Soil Use and Management, 3: 3-8.

Hall, G. F. 1983. Pedology and geomorphology. In: Wilding L. P., Smeck, N. E. and Hall, G. F. (Editors), Pedogenesis and Soil Taxonomy I. Concepts and Interactions. Elsevier, Amsterdam pp. 117-140.

Hartigan, J. 1975. Clustering Algorithms. Wiley, New York.

Hill, M. O. 1979. DECORANA: A FORTRAN program for detrended correspondence analysis and reciprocal averaging. Section of Ecology and Sytematics, Cornell University, Ithaca, New York.

Hole, D. F. and Campbell, J. B. 1985. Soil Landscape Analysis. Rowman and Allanheld, Totowa, New Jersey.

Huggett, R. J. 1975. Soil landscape systems: a model of soil genesis. Geoderma, 13: 1-22.

Jenny, H. 1941. Factors of Soil Formation, a System of Quantitative Pedology. McGraw-Hill, New York, 281pp.

Jones, K. S., and Jackson, D. 1967. Current approaches to classification and clump finding at the Cambridge Language Research Unit. Computer Journal, 10: 29-37.

Journel, A. G. and Huijbregts, C. J. 1978. Mining Geostatistics. Academic Press, London.

Kandel, A. 1986. Fuzzy Mathematical Techniques with Applications. Addison-Wesley, Massachusetts.

Laslett, G. M., McBratney, A. B., Pahl., P. J. and Hutchinson, M. F. 1987. Comparison of several spatial prediction methods for soil pH. Journal of Soil Science, 38: 325-341.

Laut, P. *et al.* 1977. (Compilers). Environment of South Australia, Province 3, Mt. Lofty Block CSIRO. (Australia) Division of Land Use Research.

Lyford, W. H. 1974. Narrow soils and intricate soil patterns in South New England. Geoderma, 11: 195-208.

Mardia, K. V. 1972. Statistics of Directional Data. Academic Press, London.

Maschmedt, D. J. 1987. Soil and Land Use Potential, Onkaparinga, South Australia. 1:50,000 Map sheet. Dept. of Agric. South Australia Technical Paper No. 16.

Matheron, G. 1965. Les Variables Regionalisées et leur Estimation. Masson, Paris.

Matheron, G. 1971. The Theory of Regionalized Variables and its Applications. Cah., Centre Morphol. Mathem. Fontainebleau, No. 5.

Maud, R. R. 1972. Geology, geomorphology and soils of Central Country Hindmarsh (Mt. Compass-Milang), S. Australia. CSIRO (Australia) Soil Publ. 29.

McBratney, A. B. and DeGruijter, 1990. A continuum approach to soil classification and mapping: classification by modified fuzzy k-means with extragrades. (submitted to Journal of Soil Science).

McBratney, A. B. and Moore, A. W. 1985. Application of fuzzy sets to climatic classification. Agricultural and Forest Meteorology, 35: 165-185.

McBratney, A. B. and Webster, R. 1981a. Spatial dependence and classification of soil along a transect in north-east Scotland. Geoderma, 26: 63-82.

McBratney, A. B. and Webster, R. 1981b. The design of optimal schemes for local estimation and mapping of regionalized variables. II. Program and examples. Computers and Geosciences, 7: 335-365.

McBratney, A. B. and Webster, R. 1983. Optimal interpolation and isarithmic mapping of soil properties. V. Co-regionalization and multiple sampling strategy. Journal of Soil Science, 34: 137-162.

McBratney, A. B. and Webster, R. 1986. Choosing functions for semivariograms of soil properties and fitting them to sampling estimates. Journal of Soil Science, 37: 617-639.

McBratney, A. B., Webster, R. and Burgess, T. M. 1981. The design of optimal schemes for local estimation and mapping of regionalized variables. I. Theory and method. Computers and Geosciences, 7: 331-334.

McDonald, R. C., Isbell, R. F. , Speight, J. G. , Walker, J. and Hopkins, M. S. 1984. Australian Soil and Land Survey Field Handbook. Inkata Press, Melbourne, 160 pp.

McKenzie, N. J. and Austin, M. P. 1989. Utility of the Northcote Key and Soil Taxonomy in the lower Macquarie valley, N. S. W. Australian Journal of Soil Research, 27: 286-311

McKenzie, N. J. and MacLeod, D. A. 1989. Relationships between soil morphology and soil properties relevant to irrigated and dryland agriculture. Australian Journal of Soil Research, 27: 235-258

McLean, E. O. 1982. Soil pH and lime requirement. In: Page, A. L. et al. (Editors), Methods of Soil Analysis, Part 2. American Society Agronomy, pp.199-224.

Melville, M. D. and Atkinson, G. 1985. Soil colour: its measurement and its designation in models of uniform colour space. Journal of Soil Science, 495-512.

Merry, R. H. and Spouncer, L. R. 1988. The measurement of carbon in soils using a microprocessor -controlled resistance furnace. Communications in Soil Science and Plant Analysis, 19: 707-720.

Montgomery, D. C. and Peck, E. A. 1982. Introduction to Linear Regression Analysis. John Wiley, New York.

Moore, A. W., Isbell, R. F. and Northcote, K. H. 1983. Classification of Australian soils In: 'Soils: an Australian viewpoint', Division of Soils, CSIRO, pp. 211-217 (CSIRO, Melbourne/Academic Press, London).

Moore, A. W. and Russell, J. S. 1976. Problems in numerical classification of soil data. In: Williams W. T. (Edits.), Pattern Analysis in Agricultural Science. pp. 215-223. Elsevier, New York.

Nielsen, D. R. 1987. Emerging frontiers in soil science. Geoderma, 40: 267-273.

Norris, J. M. 1970. Multivariate methods in the study of soil. Soils and Fertilizers, 33: 313-318.

Northcote, K. H. 1960. A Factual Key for the Recognition of Australian Soils. CSIRO Division of Soils, Rellim, Adelaide S. Australia

Northcote, K. H. 1976. Soils. In: Twidale C. R., Tyler, M. J. and Webb, B. P. (Edits.), Natural History of the Adelaide Region, Adelaide, Australia. pp 61-73. Roy. Soc. S. Austr. Inc.

Northcote, K. H. 1983. Central Southern Region (V). In: 'Soils: an Australian Viewpoint', Division of Soils, CSIRO, pp. 211-217 (CSIRO, Melbourne/Academic Press, London).

Oertel, A. C. 1974. The development of a typical Red-brown earth. Australian Journal of Soil Research, 12: 97-105.

Ohashi, Y. 1984. Fuzzy clustering and robust estimation. 9th. Meeting of SAS users Group International, Hollywood Beach, Florida.

Oliver, M. A. 1987. Geostatistics and its application to soil science. Soil Use and Management, 3: 8-20.

O'Loughlin, E. M. 1981. Saturation regions in catchments and their relationships to soil and topographic properties. Journal of Hydrology, 53: 229-246.

Pendleton, R. L. and Nickerson, D. 1951. Soil colours and special Munsell soil colour charts. Soil Science, 36: 495-512.

Powell, B., McBratney, A. B. and MacLeod, D. A. 1991 The application of fuzzy classification to soil pH profiles in the Lockyer Valley, Queensland, Australia. Catena (in press).

Preiss, W. V. 1987. (Compiler): The Adelaide Geosyncline- late Proterozoic stratigraphy, sedimentation, palaeontology and tectonics. Bulletin of Geological Survey, South Australia, 53, pp 97-109.

Prescott, J. A. 1931. The soils of Australia in relation to vegetation and climate. Council for Science and Industrial Research, Australia, Bulletin. No. 52.

Prescott, J. A. 1944. A soil map of Australia. Council for Science and Industrial Research, Australia, Bulletin. No. 177.

Rhoades, J. R. 1982. Soluble salts. In: Page, A. L. et al.. (Editors), Methods of Soil Analysis, Part 2 American Society of Agronomy, pp.167-180.

Rosenfeld, A and Kak, A. C. 1982. Digital Picture Processing. Vol. 2. Academic Press, New York.

Ross, D. J., Spier, T. W., Giltrap, D. J., McNeilly, B. A. and Molloy, L. F. 1975. A principal component analysis of some biochemical activities in a climosequence of soils. Soil Biology and Biochemistry, 7: 349-355.

Roubens, M. 1982. Fuzzy clustering algorithms and their cluster validity. European Journal of Operational Research, 10: 294-301.

Ruhe, R. V. and Walker, P. H. 1968. Hillslope models and soil formation: I. Open systems. Transactions of the 9th Congress, International Soil Science Society, Adelaide 4: 551-560.

Ruspini, E. H. 1969. A new approach to clustering. Information Control, 15: 22-32.

Shannon, C. E. 1948. A mathematical theory of communication. Bell System Technology, 27: 379-423.

Simonson, R. W. 1959. Outline of a generalized theory of soil genesis. Soil Science Society of America Proceedings, 23: 152-156.

Sleeman, J. R. 1975. Micromorphology and mineralogy of red-brown earth profiles. Australian Journal of Soil Research, 13: 101-117

Soil Survey Staff, 1975. Soil Taxonomy. A Basic System of Soil Classification for Making and Interpretating Soil Surveys. USDA-SCS Agric. Handbook 436, Washington D.C.

Sondheim, M. W., Singleton, G. A. and Lavkulich, L. M. 1981. Numerical analysis of a chronosequence, including the development of chronofunction. Soil Science Society of America Journal, 45: 558-563.

Stace, H. T. C., Hubble, G. D., Brewer, R., Northcote, K. H., Sleeman, J. R., Mulcahy, M. J. and Hallsworth, E. G. 1968. A Handbook of Australian Soils. Rellim, Glenside S. Australia.

Stein, A., van Dooremolen, W., Bouma, J. and Bregt, A. K. 1988a. Co-kriging point data on moisture deficit. Soil Science Society of America Journal, 52: 1418-1423.

Stein, A., Hoogerwerf, M. and Bouma, J. 1988b. Use of soil-map delineations to improve (co-)kriging of point data. Geoderma, 43: 163-177.

Stephen, C. G. 1946. Pedogenesis following the dissection of lateritic region in southern Australia. Council for Science and Industrial Research, Australia, Bulletin. No. 206.

Stephen, C. G. 1947. Functional synthesis in pedogenesis. Transactions, Royal Society of Australia, 71: 168-181.

Stephen, C. G. 1961. The soil landscapes of Australia. CSIRO Soil Publication No. 18.

Stoer, J. and Bulirsh, R. 1980. Introduction to Numerical Analysis. Springer-Verlag New York.

Ter Braak, C. J. F. 1985. Correspondence analysis of incidence and abundance data: properties in terms of unimodal response model. Biometrika., 41: 859-873.

Ter Braak, C. J. F. 1986. Canonical correspondence analysis: a new eigenvector technique for multivariate direct gradient analysis. Ecology, 67: 1167-1179.

Ter Braak, C. J. F. 1987. Ordination. In: R. H. J. Jongman, C. J. F. Ter Braak and O. F. R. Van Tongeren (Editors), Data Analysis in Community and Landscape Ecology. pp 91-173. Pudoc, Wageningen.

Ter Braak, C. J. F. 1988. CANOCO: A FORTRAN Program for Canonical Community Ordination by [partial] [detrended] [canonical] Correspondence Analysis and Redundancy Analysis (version 2.1). Agricultural Mathematics Group, Wageningen, The Netherlands.

Ter Braak, C. J. F. and Prentice I. C. 1988. A theory of gradient analysis. Advances in Ecological Research, 18: 271-317

Trangmar, B. B., Yost, R. S. and Uehara, G. 1985. Application of geostatistics to spatial studies of soil properties. Advances in Agronomy, 38: 45-94.

Troeh, F. R. 1964. Landform parameters correlated to soil drainage. Soil Science Society of America Proceedings, 28: 808-812.

Twidale, C. R. 1976. Geomorphological evolution. pp 43-59. In: Twidale C. R., Tyler, M. J. and Webb, B. P. (Editors), Natural History of the Adelaide Region, Adelaide, Australia. pp5-42.Royal Society of South Australia Inc.

Voltz, M. and Webster, R. 1990. A comparison of kriging, cubic splines and classification for predicting soil properties from sample information. Journal of Soil Science, 41: 473-490.

Ward, A. W, Ward W. T., McBratney, A. B and DeGruijter, J. J. 1990. *Mac*Fuzzy, a program for generalized fuzzy k-means. CSIRO Division of Soils, Divisional Report 999, Glen Osmond South Australia.

Webb, D. A. 1954. Is classification of plant communities either possible or desirable? Saertrysk Af Botanisk Tidsskrift, 51: 361-370.

Webster, R. 1977a. Canonical correlation in Pedology: how useful? Journal of Soil Science, 28: 196-221.

Webster, R. 1977b. Quantitative and Numerical Methods in Soil Classification and Survey. Oxford University Press, Oxford.

Webster, R. 1985. Quantitative spatial analysis of soil in the field. Advances in Soil Sciience, 3: 1-70.

Webster, R. and Burrough, P. A. 1974. Multiple discriminant analysis in soil survey. Journal of Soil Science, 25: 120-134.

Webster, R. and Butler, B. E. 1976. Soil survey and classification studies at Ginninderra. Australian Journal of Soil Research, 14, 1-24.

Williams, W. T. and Dale, M. B. 1965. Fundamental problems in numerical taxonomy. Advances in Botanical Research, 2: 35-68.

Wilson, A. F. 1952. The Adelaide System as developed in the Riverton-Clare region, northern Mt. Lofty Ranges. S. Australia Transaction of Royal Society Australia, 75: 131-149.

Yost, R. S., Uehara, G. and Fox, R. L. 1982. Geostatistical analysis of soil chemical properties of large land areas. I. Semivariograms. Soil Science Society of America Journal, 46: 1028-1032.

Yaalon, D. H. 1975. Conceptual models in pedogenesis: can soil-forming functions be solved? Geoderma, 14: 189-205.

Zadeh, L. A. 1965. Fuzzy sets. Information Control, 8: 338-353.

Zevenbergen, L. W. and Thorne, C. R. 1987. Quantitative analysis of land surface topography. Earth Surface Processes and Landforms, 12: 47-56.